PROPERTIES AND INTERACTIONS OF THE MEDIAL AND THE LATERAL PERFORANT PATHWAYS IN RAT DENTATE GYRUS

by

HSIEN-YI SABRINA WANG

A thesis submitted in conformity with the requirements
for the Degree of Doctor of Philosophy
Graduate Department of Physiology
University of Toronto.

Properties and interactions of the medial and the lateral perforant pathways in rat dentate gyrus.

Abstract

The hippocampal formation is a crucial brain structure for spatial memory and associative learning in rats. In order to understand the neurophysiological mechanisms underlying these high cognitive functions, we have to explore the synaptic properties, connections, plasticities, and interactions in the hippocampal formation. The medial and lateral perforant pathways are the major external inputs to the hippocampal formation. Thus, knowledge of the properties and interactions of the medial and lateral perforant pathway inputs to the hippocampus is the foundation for understanding the mechanism of complex cognitive functions of hippocampal formation. The medial perforant pathway originates from medial entorhinal cortex and terminates in the middle one third of the dentate gyrus molecular layer, whereas the lateral pathway originates from lateral entorhinal cortex and terminates on the outer one third of dentate molecular layer. This anatomical organization provides an easy access to activation of the functionally different medial and lateral perforant pathways. I used extracellular field potential recordings and whole-cell patch recordings in the hippocampal slice preparation to study the two perforant pathways *in vitro*.

In particular, I have addressed the hypothesis that by studying the synaptic properties and the LTP mechanisms in the perforant pathways, we can identify the cellular mechanism of associative learning. A number of important differences in the synaptic properties of the medial and lateral pathways were identified. The synaptic

responses of medial pathway depress readily during high frequency stimulation. The medial pathway is characterised by fewer presynaptic L-AP4 sensitive receptors and weak $GABA_B$ inhibition. However, it possesses high capacity for long-term potentiation (LTP) which can be further facilitated by lateral pathway during co-activation. In contrast, the synaptic responses of lateral pathway are more resistant to high frequency depression. The lateral pathway is characterised by strong $GABA_B$ inhibition which can be potentiated by tetanic stimulation and thereby limit the LTP capacity of this pathway. LTP induced by medial pathway stimulation involves selective enhancement of AMPA current, but not NMDA current. This observation, with the assistance of quantal analysis, suggests recruitment of "silent" synapses as one mechanism for LTP expression. Two new roles for $GABA_B$ receptors have been identified. In the lateral pathway, it was found that postsynaptic $GABA_B$ inhibition plays an important role in controlling LTP capacity. The heterosynaptic depression of the medial pathway by the lateral pathway is partially mediated by presynaptic $GABA_B$ receptors. Co-activation of both pathways with high frequency stimulation leads to significantly larger LTP in the medial pathway than activation of this pathway alone; whereas in the lateral pathway the co-activation has no additional effect. The synaptic properties, inhibitory inputs, and interactions of the two perforant pathways suggest that the system design favours signal transmission in the medial perforant pathway. The interactions between the two pathways are organized to maximize associative LTP in the medial pathway; this may be important for types of learning and memory attributed to the hippocampal formation.

Acknowledgements

I would like to use this opportunity to express my deep gratitude to all the people who helped me during my study. First of all, I have to thank my supervisor Dr. Wojtowicz, who patiently guided me not only on my research, but also on many other grounds. He gave me the freedom to explore my project and listened to my wild theories (sometimes based only on my imagination). I have to say I had a wonderful time in his laboratory, doing the research I thoroughly enjoyed. I cannot thank him enough for all the things he did for me. He is the best mentor one could ever hope for. Secondly, I would like to thank my committee members, Dr. Atwood and Dr. Dostrovsky, who gave me good advice (as Dr. Atwood said, "reality check") on my research and helped me extensively in my thesis writing. Thirdly, I have to thank my parents for their endless supports (both emotionally and financially). They initiated my interest in life science early on in my education and encouraged me to pursuit it. Without them, none of this would have been possible. I have to thank my brother Hsien-Dee for his "tolerance". Although I have been far away from home during my study, my aunt Jolie and uncle David Chou provided me an instant family here in Toronto. I am grateful for their help and companionship. I also would like to thank my best friends Irene Han and Connie Wang, for keeping me connected to the "real world" and for their moral support. Finally, how can I forget my "lab-mates". I would like to thank Mrs. Marianne Hegström Wojtowicz for her help with laboratory supplies and mystery book supplies. She makes the life in the laboratory more interesting. Dr. Robin Cooper taught me how to use confocal microscope. Dr. Leo Marin taught me how to use electron microscope. I have to thank Kathryn Kennedy and Una Cheung for the workout sections in Heart House; and Brian Scott for the discussions of granule cells and serial killers.

TABLE OF CONTENTS

List of Figures

List of Tables

List of Abbreviations

Ab	angular bundle
AChE	acetylcholinesterase
AChR	acetylcholine receptor
1S, 3R-ACPD	aminocyclopentane-1S, 3R-dicarboxylate
ACSF	artificial cerebrospinal filuid
AIC	Akaike information criterion
AMPA	alpha-amino-3-hydroxy-5-methyl-4-isoxazole-proprionic acid
AP5	D-2-amino-5-phosphonopentanoate acid
CaMKII	Ca^{2+}/calmodulin-dependent protein kinase II
CCK	cholecystokinin
CCK-8	cholecystokinin-octapeptide
CCK-L	cholecystokinin-like
ChAT	choline acetyltransferase
CNQX	6-cyano-7-nitroquinoxaline-2,3-dione
Com/assoc	commissural associational fibers
CREB	cAMP-responsive element-binding protein
D-APV	D-2-amino-5-phosphonovaleric acid
DG	dentate gyrus
DMSO	dimethyl sulphoxide
Enk	enkephalin
EPSC	excitatory postsynaptic current

EPSCs	excitatory postsynaptic currents
EPSP	excitatory postsynaptic potential
EPSPs	excitatory postsynaptic potentials
F	fimbria
GAD	glutamate decarboxylase
HICAP	hilar cells with axon terminals in the commissural and associational pathway
HIPP	hilar cells with axon terminals distributed in conjuction with the perforant pathway termination field
L-AP4	L(+)-2-amino-4-phosphonobutyric acid
LPP	lateral perforant pathway
LTP	long-term potentiation
m	mean quantal content
MCPG	(RS)-α-methyl-4-carboxyphenylglycine
MOPP	the cells with soma in the molecular layer has axons associated with the perforant pathway termination field
MPP	medial perforant pathway
n	number of contributing quantal units
NMDA	N-methyl-D-aspartate
p	probability of release
$\hat{p}$	average probability of release
PaS	parasubiculum
PKA	protein kinase A

PKC	protein kinase C
Prs	Presubiculum
RSA	rhythmic slow activity
S	subiculum
t-ACPD	1-aminocyclopentane-1SR,3RS-carboxylic acid
TEA	tetraethyl ammonium

Chapter 1 General Introduction

The ultimate challenge for the neuroscientist is to understand how learning and memory and other cognitive functions are achieved by the brain. Advances in neurobiology have yielded some important clues for our understanding of learning and memory. The most crucial finding is that neurons show many kinds of plasticities. The plasticities of the nervous system are evident in such diverse phenomena as drug tolerance, enzyme induction, sprouting of axon terminals after a brain lesion, and strictly synaptic events such as facilitation and depression. It is the latter, synaptic facilitation and depression, that draw most of the attention from students of learning and memory. The discovery of the mechanisms underlying these and other types of plasticity would likely provide important clues for understanding how the nervous system accomplishes complex cognitive functions such as learning and memory.

In 1949 Donald Hebb published his synaptic modification theory: "When an axon of cell A is near enough to excite cell B and repeatedly or persistently take part in firing it, some growth process or metabolic change takes place in one or both cells such that A's efficiency, as one of the cells firing B, is increased." This theory had profound impact on neuroscientists' way of thinking about the mechanisms underlying learning and memory in the brain. However, the direct evidence came much later. An abstract by Terje Lømo (1966) and the subsequent full report by Bliss, Lømo, and Gardner-Medwin (1973) showed that brief high-frequency electrical stimulation of the perforant path input to the dentate gyrus of the hippocampal formation could elicit an enhancement of

synaptic transmission in this pathway that persisted for days or weeks. The physiological characteristics of this phenomenon, termed long-term potentiation (LTP), fit Hebb's theory and made it an attractive candidate for the mechanism of learning and memory. The physiological characteristics include:

1. Persistence: LTP can last for days and even weeks, while the inducing stimulation is very brief (hundreds of milliseconds). Although Hebb did not clearly state that the change in cell A's efficiency is a long lasting one, he suggested that "some growth process or metabolic change takes place in one or both cells", which could very well last longer than the action potentials evoked in cell B by cell A's activation. For a memory to last, this long-term change is certainly a necessary feature. However, we do not know yet what is the maximum duration of LTP or whether LTP is only the initial part of a memory consolidation process which is responsible for real long-term memory storage (years).

2. Input specificity: LTP is confined to those synapses that are active during the time of high-frequency stimulation or during the period of postsynaptic depolarization. Thus, only events associated with high activity at synapses will be preserved. In Hebb's theory, only when cell A is near enough to excite cell B and repeatedly or persistently take part in firing it, will the efficiency of transmission between cell A and B change.

3. Cooperativity/Associativity: LTP induction needs both presynaptic activation and postsynaptic depolarization. The cooperation between pre-and postsynaptic cells is like the cell A and cell B in Hebb's hypothesis. Furthermore, stimulation to multiple pathways will produce stronger LTP than the summation produced by stimulating a single pathway.

A weak input can be potentiated if it is paired with a strong input (Levy and Steward, 1979; Lee, 1983). Usually, learning and memory involve multimodal sensory inputs and their complex interactions; the cooperativity/associativity feature of LTP can further strengthen the activated inputs.

1.1 Long-term Potentiation

Following the discovery of LTP in rabbit perforant pathway, LTP has since been reported in other areas in the hippocampal formation (CA1: Schwartzkroin and Wester, 1975; Dunwiddie and Lynch, 1979; Bliss et al., 1983; CA3: Alger and Teyler, 1976 Higashima and Yamamoto, 1985; Harris and Cotman, 1986) and in many other brain regions, including neocortex (Baranyi and Szente, 1987; Bindman et al., 1987), the limbic forebrain (Racine et al., 1986); and motor (Sakamotor, 1987), somatosensory (Rasmusson and Dykes, 1988), visual (Aroniadou and Teyler, 1992; Perkins and Teyler, 1988; Artola and Singer, 1987), pyriform (olfactory) (Kanter and Haberly, 1990; Stripling et al., 1988), and entorhinal (Alonso et al., 1990) cortices. Furthermore, several different forms, and methods of induction of LTP have been described. The most commonly used method is electrical stimulation, which includes brief high frequency stimulation originally used by Bliss and coworkers (Bliss et al., 1973) and various other high frequency stimulation patterns that have been found to efficiently induce LTP. Among these methods, the "theta burst stimulation", which resembles a naturally occurring hippocampal activity - the theta rhythm, is worth mentioning. The theta rhythm is 4-5 Hz

synchronized hippocampal activity recorded during exploratory behaviour or during a particular phase of sleep in the rats (Otto et al., 1991; Capocchi et al., 1992). The theta burst stimulation, optimal for LTP induction, consists of several short high frequency (100 Hz) bursts of a few pulses delivered at an inter-burst interval of 200 ms, similar to the theta rhythm frequency (Larson et al., 1986; Capocchi et al., 1992).

There are also non-electrical methods of inducing long-lasting potentiation of synaptic transmission, which can seem very similar to LTP, for example, application of the K^+ channel blocker tetraethyl ammonium (TEA) (Aniksztejn and Ben-Ari, 1991; Huang and Malenka, 1993), high extracellular Ca^{2+} (Turner et al., 1982), 1-oleoyl-2-acetyl glycerol (a diacylglycerol derivative) in a low Mg^{2+} solution (Kato et al., 1991), norepinephrine (Stanton et al., 1989; Stanton and Sarvry, 1985), the metabotropic glutamate receptor agonist aminocyclopentane-1S, 3R-dicarboxylate (1S,3R-ACPD) (Bashir et al., 1993; Bortolotto and Collingridge, 1993; Zheng and Gallagher, 1992), and even anoxia (Crepel et al., 1993).

1.1.1 Classifications and mechanisms of LTP

Various forms of LTP can be classified by their induction mechanism. A broad division is based on whether or not the induction requires activation of N-methyl-D-aspartate (NMDA) subtype of glutamate receptor (Bliss and Collingridge, 1993; Zalutsky and Nicoll, 1990; Nicoll and Malenka, 1995). The NMDA receptor-ion channel complex is one of three classes of glutamate receptors which are involved in excitatory synaptic transmission; AMPA (alpha-amino-3-hydroxy-5-methyl-4-isoxazole proprionic acid), and

metabotropic being the other two. NMDA and AMPA receptors are receptor-channel complexes whereas the metabotropic receptor is G-protein linked and triggers a second-messenger cascade. The NMDA receptor directly gates a glutamate-activated channel permeable to Ca^{2+}, K^{+}, and Na^{+} and has several regulatory binding sites for glycine, Zn^{2+}, MK-801 (a noncompetitive blocker), and Mg^{2+}. The channel is normally blocked by Mg^{2+} and becomes unblocked only when the postsynaptic cell is adequately depolarized through the activation of many non-NMDA glutamate receptors in close proximity on the same postsynaptic dendritic membrane. Thus, the NMDA receptor is unique in being gated by both a chemical agonist and a voltage sensor.

1.1.2 Mechanism of NMDA-dependent LTP

The induction mechanism of NMDA-dependent LTP was first proposed by Collingridge at 1985. The clues came from the discovery of Mg^{2+} as a potent NMDA antagonist (Evans et al., 1977), and that the antagonism was due to the blocking of the NMDA receptor channel by Mg^{2+}; the blockade occurred in a highly voltage-dependent manner, decreasing with depolarization (Nowak et al., 1984). It was postulated that Mg^{2+} prevented the synaptic activation of NMDA receptor-channels during low-frequency transmission, and during high-frequency stimulation the postsynaptic neuron became depolarized sufficiently for an adequate length of time to enable the NMDA receptor-channel to be activated. This idea was tested experimentally (Herron et al., 1986) and confirmation of the NMDA receptor hypothesis was obtained independently by three groups (Kelso et al., 1986; Wigström et al., 1986; Sastry et al., 1986). It had been shown

that when single stimuli were applied to afferent fibers either in phase or out of phase with strong depolarizing pulses applied to the postsynaptic cell; LTP occurred only when the two events were in phase. The NMDA hypothesis provides an explanation of input specificity, cooperativity, and associativity properties of LTP (Gustafsson and Wigström, 1988).

When Collingridge proposed the NMDA hypothesis of LTP induction in 1985, he already suspected that the Ca^{2+} influx, via the NMDA receptor, plays a central role in LTP induction. It has been subsequently demonstrated using imaging techniques, that Ca^{2+} can permeate synaptically activated NMDA receptor and increase concentrations of Ca^{2+} transiently within spines (Bliss and Collingridge, 1993; Malinow et al., 1994). Furthermore, it has been shown by Lynch et al. (1983) that intracellular injections of EGTA, a Ca^{2+} chelator, and that lowering extracellular Ca^{2+} prevents the induction of LTP (Dunwiddie and Lynch, 1979). Thus, postsynaptic Ca^{2+} influx is necessary for LTP induction. However, the sequence of events that occurs following the Ca^{2+} influx remains controversial. Especially, whether LTP expression is mediated by presynaptic or postsynaptic sites is under constant debate. It is known that Ca^{2+}- dependent protein kinases are involved, which include protein kinase C (PKC) (Akers et al., 1986; Linden and Routtenberg, 1989; Malinow et al., 1989; Klann et al., 1991) and Ca^{2+}/calmodulin-dependent protein kinase II (CaMKII) (Malenka et al., 1989; Ito et al., 1991; Silva et al., 1992). Although the LTP induction requires postsynaptic Ca^{2+} surge there is also evidence indicating that presynaptic transmitter release is increased (Dolphin et al., 1982). Therefore, a retrograde messenger has been proposed. The candidates include

arachidonic acid (Williams and Bliss, 1989; Williams et al., 1989); nitric oxide (O'Dell et al., 1991; Böhme et al., 1991; Schuman and Madison, 1991); and carbon monoxide (Marks et al., 1991; Verma et al., 1993).

1.1.2.1 Protein kinase C

PKC is the first kinase to be implicated in the induction of LTP. Inhibitors of PKC applied in a certain time window have been reported to block both the induction and persistence of LTP (Malenka et al., 1989). Extracellular application of activators of PKC such as phorbol esters induce synaptic transmission potentiation (Malenka et al., 1986) as does the intracellular injection of the catalytic subunit of PKC (Hu et al., 1987). The cellular events following PKC activation are less clear. It has been suggested that PKC can phosphorylate and modulate (increase) postsynaptic AMPA receptor conductance (Reymann et al., 1988; Blackstone et al., 1994). In addition, there is evidence that NMDA channel conductance can be enhanced by the activation of PKC (Kelso et al., 1992; Ben-Ari et al., 1992). Furthermore, in the trigeminal neurons, activation of PKC increases NMDA channel conductance via phosphorylation of NMDA channels that causes a reduction of Mg^{2+} blockade of the channel (Chen and Huang, 1992). However, this modulation mechanism has not been demonstrated in hippocampal neurons. PKC and two other protein kinases (PKA and CaMK II) have been shown to phosphorylate nitric oxide synthase, the enzyme producing the putative retrograde messenger nitric oxide (Bredt et al., 1992); this could affect the presynaptic transmitter release by nitric oxide.

1.1.2.2 Ca^{2+}/calmodulin-dependent protein kinase II

CaMKII is heavily enriched in postsynaptic densities (Kelly et al., 1984; Kennedy et al., 1983). It has been demonstrated that inhibitors of CaMKII can block LTP (Malenka et al., 1989; Ito et al., 1991). In addition, transgenic mice lacking the α-subunit of CaMKII have severely impaired LTP (Silva et al., 1992). The events following CaMKII activation to trigger LTP expression are believed to be the phosphorylation of AMPA receptors. It has been reported that activated CaMKII can phosphorylate AMPA receptors, located also in the postsynaptic densities, and resulting in the upregulation of the receptor function (McGlade-McCulloh et al., 1993; Tan, et al., 1994; Nicoll and Malenka, 1995). The upregulation of AMPA receptor function by phosphorylation could involve changes in single-channel properties or in the insertion and/or unmasking of clusters of functional AMPA receptors. The exact mechanism is currently unknown; however, there is evidence supporting the latter mechanisms (see Chapter 5).

1.1.2.3 Protein Kinase A

A cyclic adenosine monophosphate (cAMP) dependent protein kinase, protein kinase A (PKA), is involved in LTP induction. It has been shown that the level of cAMP is elevated in an NMDA receptor-dependent manner during LTP (Chetkovich et al., 1991). The cAMP subsequently activates PKA which, as mentioned above, could phosphorylate nitric oxide synthase (Bredt et al., 1992). Alternatively, it has been shown that cAMP itself, by activating cAMP-responsive element-binding protein (CREB), could initiate gene transcription and protein synthesis and is important for a late phase of LTP

(Frey et al., 1993; Nguyen et al., 1994; Bourtchuladze et al., 1994).

1.1.3 Mechanism of NMDA-independent LTP

NMDA-independent LTP is found in the mossy fiber synapses, the synapses between dentate gyrus and CA3 pyramidal cells. Previous results suggest that the site for both the induction and expression of this form of LTP is presynaptic, whereas postsynaptic activation of NMDA receptors and Ca^{2+} elevation are not required (Zalutsky and Nicoll, 1990; Weisskopf et al., 1994; Nicoll and Malenka, 1995). It has been shown that the transient rise in Ca^{2+} in the presynaptic terminal during tetanic stimulation is necessary for the induction of LTP (Ito and Sugiyama, 1991; Castillo et al., 1994). It is proposed that the Ca^{2+} may activate Ca^{2+}/calmodulin-sensitive adenylyl cyclase I which increases the concentration of cAMP (Weisskopf et al., 1994). PKA is subsequently activated by cAMP and causes a persistent enhancement of evoked glutamate release (Weisskopf et al., 1994; Nicoll and Malenka, 1995). However, how PKA enhances transmitter release remains obscure due to our incomplete understanding of transmitter release machinery.

1.1.4 The connections between LTP and learning and memory

LTP is currently the most favoured candidate of the cellular mechanisms for learning and memory. However, to date, there is no conclusive evidence supporting the hypothesis that LTP is the basis of learning and memory. In a recent review on the history of advances in this field, Eichenbaum (1996) pointed out that the failure to find

conclusive evidence supporting a connection between LTP and learning is rooted in the limitations of experimental strategies taken so far. There are three general approaches: demonstrations of changes in synaptic physiology as a consequence of learning experience; attempts to prevent learning by "saturation" of hippocampal LTP; and attempts to alter learning performance by pharmacological or genetic manipulation of LTP induction.

The first approach, trying to find changes in synaptic physiology consequent to learning and memory, is, in Eichenbaum's words, like finding "the needle in a haystack". The magnitude of synaptic changes following any normal learning experience would be very small and unlikely to be detected by gross electrophysiological recordings from a population of neurons (extracellular field potential recording). In addition, most computational neuroscientists believe that learning involves changes in synaptic efficacy in both the positive and negative directions. Thus, there might be a re-distribution of potentiated and depressed or depotentiated synapses, and no overall shift in the evoked field potential profile.

The second approach, consisting of blocking learning by saturating LTP of all of the excitatory synapses in the hippocampus before training, has also been plagued by methodological problems since it is difficult to be certain that all the synapses in the hippocampus are saturated, even in a single stage of the hippocampal circuit. In addition, the stimulation used to produce "saturation" is very intense and we don't know if the information processing (as contrasted with plasticity) within the hippocampal network remains fully normal after such treatments. Even ignoring the potential complications

mentioned above, the experimental results obtained by this approach are far from conclusive. The earlier studies indicated that saturation of the perforant pathway synapses resulted in severely impaired new learning and spared learning accomplished previously in the normal state (McNaughton et al., 1986). In addition, succeeding experiments showed that learning capacity returned when synaptic efficacy levels dropped back to baseline (Castro et al., 1989). However, more recent experiments found no effect of saturation across a variety of experimental protocols examining learning and memory (Cain et al., 1993; Jeffery and Morris, 1993; McNamara et al., 1993; Sutherland et al., 1993); even the authors who succeeded in earlier experiments cannot reproduce their initial findings (Korol et al., 1993) (review on saturation experiments, see Bliss and Richter-Levin, 1993).

The third approach, attempting to alter learning performance by pharmacological or genetic manipulation of LTP induction is, thus far, the most compelling and promising method. However, this method is not flawless either. We have to assume that the drugs used are selective for plasticity; that they do not affect normal information processing in the brain; and that they affect only one critical kind of plasticity which underlies the particular learning and memory function tested experimentally. The earlier experiments using the specific NMDA receptor blocker D-2-amino-5-phosphonopentanoate acid (AP5) which is selective for plasticity (blocks the NMDA-dependent LTP), showed that the blockade of NMDA receptors prevented new learning in a spatial memory test (Morris et al., 1986). Later, NMDA receptor block has been shown to be effective in blocking acquisition of fear conditioning memory (Kim et al., 1991). Targeted genetic

manipulations have shown that blocking the cascade of the molecular triggers for LTP also results in severe memory impairments (Grant et al., 1992; Silva et al., 1992a,b).

However, some experiments showed that a function of learning survived even a total block of capacity for LTP (Davis et al., 1992). In addition, two recent studies provided evidence of intact hippocampal-dependent learning (see below) even when the capacity for hippocampal LTP is fully blocked (Bannerman et al., 1995; Saucier and Cain, 1995).

However, knowing that there are multiple forms of LTP, some of which are not dependent on the NMDA receptors, we probably should not be too surprised to find negative results. These results may suggest that there are parallel mechanisms underlying learning and memory. Furthermore, it has become clear that there are different forms of memory mediated by distinct brain circuits, and these memory systems have different associational and temporal properties (MacDonald and White, 1993; Eichenbaum, 1996). We have to know where in the brain LTP was affected by the pharmacological or genetic manipulations and whether the brain systems affected support the kind of memory examined in behaviour tests, to make these kind of tests meaningful. Although the conclusive evidence of a connection between LTP and memory still awaits further research, there is no doubt that the brain structure in which LTP was discovered, the hippocampal formation, is a crucial one for learning and memory, especially for new memory formation.

1.2 Hippocampus

In the 1950s, the standard procedure to cure uncontrollable seizures in patients was to perform bilateral or unilateral temporal lobectomy. This operation alleviated the patient's seizure activity; however, some patients who had bilateral temporal lobectomy developed the amnesic syndrome (Scoville and Milner, 1957). It was found that in these patients (including the famous patient H.M.), the excisions extended sufficiently posterior to include a large portion of the hippocampal formation and parahippocampal gyrus in addition to the amygdala region. The other patients who were free of amnesic syndrome had excisions that either excluded the hippocampal formation entirely or damaged it only slightly. From these data, a supposition arose that severe anterograde amnesia in man was due to hippocampal damage. This supposition was further strengthened by evidence from a second series of cases reported by Penfield and Milner (1958). In this series, 2 of 90 patients unexpectedly developed an amnesic syndrome after a temporal lobectomy that, while extending sufficiently posterior to cause damage to a large portion of the hippocampal formation and parahippocampal gyrus, was only unilateral. In one of these patients, autopsy findings later indicated (Penfield and Mathieson, 1974) that the hippocampal formation in the unoperated temporal lobe was severely shrunken and necrotic, while the amygdala seemed intact. It was concluded that human amnesia was entirely ascribable to bilateral damage to the hippocampal formation. Furthermore, it was found that hippocampal lesions especially affected the patients' declarative memory and left the procedural memory intact (Milner et al., 1968; Cohen and Squire, 1980; Squire and Zola-Morgan, 1991; Squire, 1992). Declarative memory involves associations among

items or events that can be accessed flexibly to guide memory expression in various situations (Squire, 1992).

Although the above evidence showed a strong connection of hippocampal formation with memory formation, we have to realize that in these cases, the lesions were rarely confined within the hippocampal formation (except patient R.B. who had confined bilateral lesions in CA1 regions due to global ischemia; (Zola-Morgan et al., 1986). Thus, the contribution of medial temporal lobe components other than hippocampal formation to declarative memory has to be considered (Jaffard and Meunier, 1993).

From ablation studies carried out in monkeys, it was suggested that all medial temporal-lobe components are likely to participate in normal memory function (review, see Jaffard and Meunier, 1993). However, hippocampal formation lesions alone could cause severe memory impairment (Parkinson et al., 1988; Zola-Morgan et al., 1992). Especially, the spatial memory is hampered by hippocampal damage. For example, the memory of where in the environment a particular visual stimulus has been seen is one of the types of memory specifically impaired by hippocampal damage in primates including man (Cahusac et al., 1989; Rolls et al., 1989).

O'Keefe and Dostrovsky (1971) discovered hippocampal "place cells" in rats. The place cells were named after their property of firing rapidly only when a freely moving rat is in a limited region of the space (firing field) accessible to the rat (O'Keefe and Dostrovsky, 1971; O'Keefe, 1976; Muller et al., 1987; Muller and Kubie, 1987). Subsequently, O'Keefe and Nadel (1978) proposed the cognitive mapping theory for

hippocampal function in rats. Indeed, rats that had lesions in hippocampal formation showed distinct spatial memory impairment (Morris et al., 1982; Jarrard, 1986; Jarrard et al., 1987; Morris et al., 1990; Jarrard, 1993). However, apparently spatial memory is not the only memory system affected by hippocampal lesions. Non-spatial declarative memory processing in rat was also affected by hippocampal lesions (Staubli et al., 1984; Eichenbaum et al., 1986; Eichenbaum et al., 1989; Otto et al., 1992; Eichenbaum, 1994; Bunsey and Eichenbaum,1996).

There are many different theories about the roles of hippocampus in learning and memory. For example, there is a cognitive mapping theory (O'Keefe and Nadel, 1978); configural theory (Sutherland and Rudy, 1989); contextual encoding theory (Hirsh, 1974); declarative memory theory (Cohen and Squire, 1980; Squire, 1987); working memory theory (Olton et al., 1979; Olton, 1986); and relational representation theory (Eichenbaum, Cohen et al., 1992, Eichenbaum, Otto et al., 1992; Cohen and Eichenbaum, 1993). Every theory stresses some properties of hippocampal functions, derived from animal lesion experiments and/or from observations of amnesic human subjects, in learning and memory. At first glance, most of the theories seem to have little in common. After careful analysis, some common features among these theories emerge. In particular, hippocampal formation is necessary for processing comparisons among items in memory and for encoding essential relations among items presented either simultaneously or sequentially (Eichenbaum, 1994). To test just how, at the cellular level, the hippocampal formation performs the "comparison among items" and "encoding the relationship among items", I will use the two major input pathways to the hippocampal

formation, the medial and the lateral perforant pathways, to study the possible mechanisms in terms of spatial and temporal integration of two different inputs.

1.3 Anatomy of the Dentate Gyrus and Perforant Pathways

1.3.1 The dentate gyrus

The dentate gyrus is one of the cortical regions which constitute the hippocampal formation (Fig.1-1). In the literature, there is some dispute about which areas should be included in the hippocampal formation. According to Amaral and Witter (1995) the hippocampal formation is composed of six cytoarchitectonically distinct regions which include the dentate gyrus, hippocampus proper, which is subdivided into three fields (CA3, CA2, and CA1); subiculum; presubiculum; parasubiculum; and entorhinal cortex. Some authors include only the allocortical (cortical regions having fewer than six layers) or three-layered regions as parts of the hippocampal formation. By this definition, the hippocampal formation would comprise only the dentate gyrus, hippocampus proper, and subiculum; the other regions which include presubiculum, parasubiculum and entorhinal cortex would be called parahippocampal cortex. In this dissertation I will use the latter definition for simplicity.

The dentate gyrus comprises three layers, the molecular layer (*stratum moleculare*), granule cell layer (*stratum granulosum*), and hilus (Fig.1-1). The molecular layer is adjacent to the hippocampal fissure and is a relatively cell-free area, containing the apical dendrite arborization of the dentate granule neurons and afferent fibers from

Figure 1-1 Anatomical organization of hippocampal formation -- Schematic drawings. **A**. Localization of hippocampal formation in the rat brain. **B**. Two section plans "a" (coronal section) and "b" (ventral horizontal section) of hippocampal formation. **C**. Schematic drawing of cellular arrangement at section plan "a". **D**. The horizontal section showing the relationship of hippocampal formation and entorhinal cortex. Medial and lateral entorhinal cortex are indicated. Ab, angular bundle; Com/assoc, commissural associational fibers; F, fimbria; LPP; lateral perforant pathway; MPP, medial perforant pathway, PaS, parasubiculum; PrS, Presubiculum; S, subiculum.

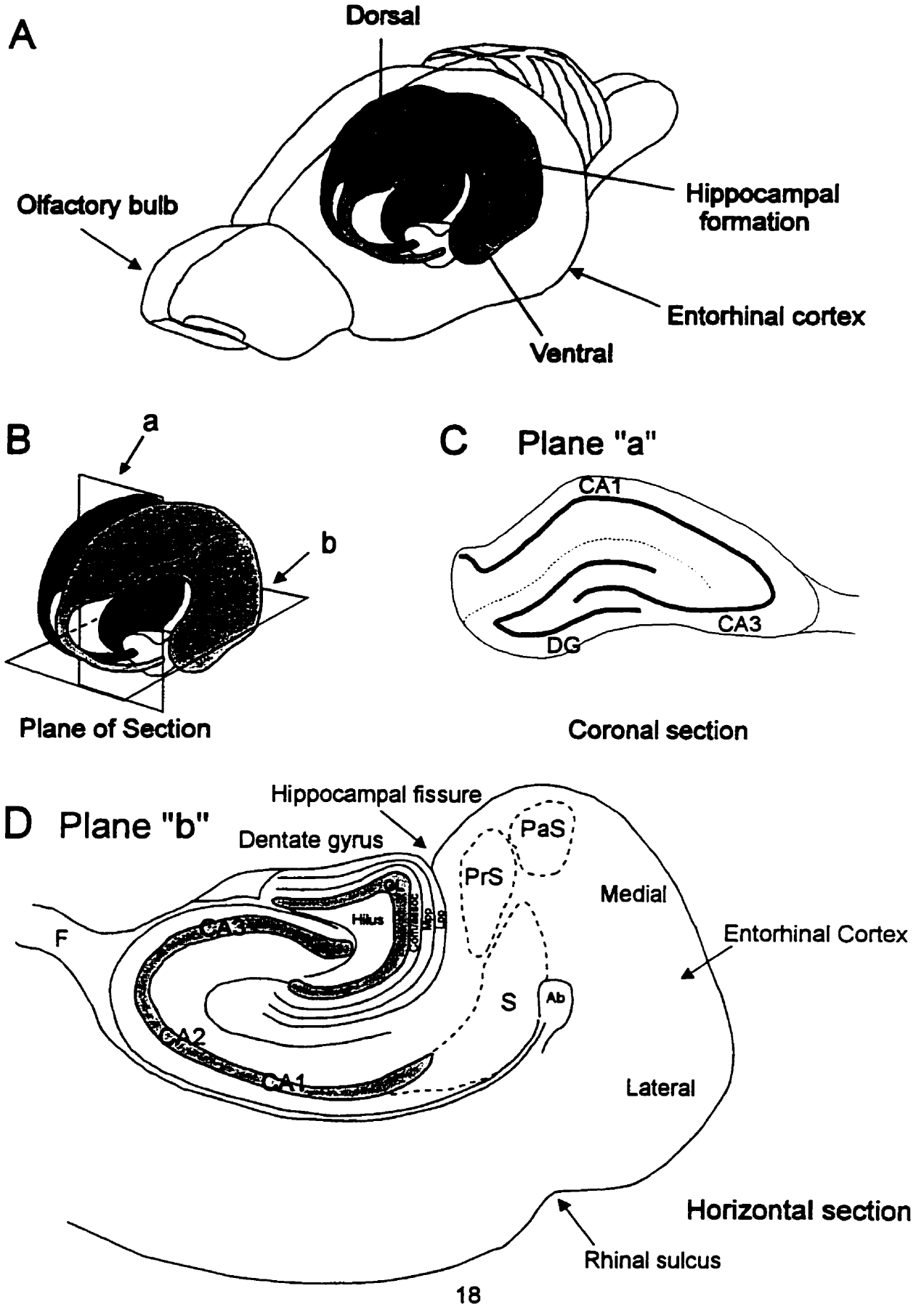
A
Dorsal
Olfactory bulb
Hippocampal formation
Entorhinal cortex
Ventral
B
a
b
Plane of Section
C Plane "a"
CA1
CA3
DG
Coronal section
D Plane "b"
Hippocampal fissure
Dentate gyrus
PaS
PrS
Medial
Entorhinal Cortex
F
CA3
Hilus
S
Ab
CA2
CA1
Lateral
Horizontal section
Rhinal sulcus

other cortical and subcortical regions. The perforant pathway is the major afferent system occupying this area.

The granule cell layer contains dentate granule neuron somas, and along with the molecular layer forms a V- or U-shaped structure (depending on the dorsal-ventral position). This structure encloses a cellular region called the hilus which constitutes the third layer of the dentate gyrus (Fig.1-1). The granule cell is the principal cell in the dentate gyrus. In the rat, the total number of granule cells in one dentate gyrus is estimated to range from 0.6×10^6 to 2.2×10^6 (Amaral et al., 1990; Boss et al., 1985; Gaarskjaer, 1978; Seress and Pokorny, 1981), and the number depends on the age (Bayer, 1982; Bayer et al., 1982) and strain of the animal. In part, the variability in cell counts is due to the fact that proliferation of granule cells continues at a slow rate well into adult life (Bayer, 1982; Bayer et al., 1982).

1.3.1.1 Local interneurons in the dentate gyrus

There is a large variety of interneuron cell types in the dentate gyrus. They can be divided into excitatory and inhibitory interneurons. The excitatory interneurons are the unique "mossy cells" in the hilus area of dentate gyrus (Fig. 1-1D). Mossy cells are named after their appearance: the extremely dense coating of spines and thorny excrescences that covers their proximal dendrites gives the cell a "covered with moss" image (Amaral, 1978). These mossy cells constitute the most numerous of the hilar cell types (Amaral, 1978; Ribak et al., 1985). They have large cell bodies, and an extremely large dendritic tree that spans the hilus and can extend into the dentate molecular layer

(Amaral, 1978). Their axon collaterals ramify within the inner molecular layer of the dentate and their target cells are granule neurons (Schwartzkroin et al., 1990). Mossy cells receive excitatory synaptic inputs from the axon collaterals of the granule cells, which produce large EPSPs (Schwartzkroin et al., 1990). When mossy cells are stimulated with superthreshold stimulation, they discharge in a burst pattern which makes them distinguishable from granule cells (Schwartzkroin et al., 1990). The neurotransmitter system of the mossy cells appears to be glutamatergic (Storm-Mathisen et al., 1983), although definitive evidence is still lacking. This observation suggests the mossy cells could generate feedback excitation to granule cells.

There are many different types of inhibitory interneurons in the dentate gyrus. Halasy and Somogyi (1993) reported five types of inhibitory interneurons in the dentate gyrus based on their soma location, dendritic arborization, and axonal distribution. Most, if not all, of these neurons identified by Halasy and Somogyi (1993) are GABA-immunopositive and form symmetrical synapses with other cells (many of which are identified as dentate granule cells).

(1) HICAP cells: These cell are named so because they are hilar cells with axon terminals in the commissural and associational pathway termination field. The HICAP cell is a multipolar neuron with soma beneath the granule cell layer (the polymorphic layer of hilus), axon in the inner one-third of the molecular layer (as mentioned above, the terminal field of commissural and associational pathway), and dendrites distributed in both the molecular layer and the hilar region (Han et al., 1993). One interesting feature of this cell is that although most of the dendrites are either smooth or sparsely spinous,

one main branch gives rise to spines on its segment in the central one-third of the molecular layer (where medial perforant pathway terminates). The dendritic arborization of this cell type suggests that it may receive the whole range of available inputs (perforant pathway, associational, commissural granule cell inputs). However, it would be of interest to determine whether the presence of numerous dendritic spines in the middle of the molecular layer is correlated with disproportionally stronger input from the medial perforant pathway.

(2) HIPP cells: The hilar cell with axon terminals distributed in conjunction with the perforant path termination field. The soma of the HIPP cell is located just below the granule cell layer as is that of the HICAP cell. However, their axons, after reaching the outer third of the molecular layer (where perforant pathway terminates), branch repeatedly and form an elaborate meshwork of thin, varicose fibers (Han et al., 1993). The dendrites of the HIPP cell are strictly confined to the hilar region (Han et al., 1993). Thus, this cell type is predisposed to receive hilar afferents, such as associational, commissural granule cell inputs, but virtually none of the perforant pathway projection in the molecular layer (Han et al., 1993).

(3) MOPP cells: The cell with soma in the molecular layer has axons associated with the perforant pathway termination field. In contrast to the previous cells, this MOPP cell has its soma located in the inner third of the dentate molecular layer (Han et al, 1993). Both the axons and dendrites remain confined to the outer two-third of the molecular layer (Han 1993). It is reasonable to predict that MOPP cells are mainly activated by perforant pathway input. The electron microscopic examination of the

synaptic terminals on the dendrites supports this suggestion since the synaptic boutons found on the dendrites of the MOPP cell in the molecular layer were similar to those supplying the granule cells (Halasy and Somogyi, 1993). The location of the cell makes it virtually impossible to be contacted by recurrent granule cell collaterals, which are strictly confined to the hilus and granule cell layer (Claiborne et al., 1986; Ribak and Peterson, 1986). Thus, it is very likely that the MOPP cells mediate feed-forward inhibition in the dentate gyrus.

(4) Basket cells: These are large neurons located within or adjacent to the granule cell layer, with major dendritic trees that extend parallel to the dendrites of the granule cell into the molecular layer (Amaral, 1978). The dendrites are aspinous or sparsely spinous, and receive a high density of synaptic contacts (Ribak and Anderson, 1980). The extensive axonal arborization of the basket cell terminates mainly on somata and proximal dendrites in the granule cell layer (Halasy and Somogyi, 1993). The basket cells have been shown to be activated by perforant pathway stimulation; thus, this particular cell type may be involved in feed-forward inhibitory circuits in the dentate gyrus (Han et al., 1993).

(5) Axon-axonic cells (or chandelier cells): This cell type is characterized by its chandelier-like rows of boutons following the direction of the axon initial segments of granule cells, or of other neurons in the hilar region (Halasy and Somogyi, 1993). These cells are located in the hilus and they synapse exclusively on the axon initial segments of granule cells in the granule cell layer, and on initial segments of presumed mossy cells in the hilus (Halasy and Somogyi, 1993). The dendritic arborization of axon-axonic cell

is not well described by Han et al. (1993), due to the loss of labelling material (biocytin) from the soma and dendrites during post-filling incubation period. However, they detected several labelled dendrites in the molecular layer, which could be followed through the granule cell layer pointing towards the recording site in the hilus (Han et al., 1993).

These interneurons are in a position to receive direct excitatory input, not only via axon collaterals of the granule cell population (as would be required to mediate feedback inhibition), but also directly from the perforant pathway. The latter could provide the feed-forward inhibition to granule cells (Buzsáki, 1984; Sloviter, 1991). Some of these interneurons make synapses on the distal dendrites of granule cells, for example the HIPP, and MOPP cells; some make synapses on the proximal dendrites and the soma (HICAP cells and basket cells); while the axon-axonic cell contacts the initial segment of the granule cell axon (Halasy and Somogyi, 1993). Unfortunately, little is known about each cell type's physiological function and its relationships with afferents to the dentate gyrus, with dentate granule cells, and with each other. The local circuitry of the dentate gyrus requires further investigation.

1.3.2 The perforant pathway

The perforant pathway terminates on dentate granule neurons in the molecular layer where the perforant pathway synapses make up more than 85% of the synaptic population (Nafstad, 1967). The origin of the perforant pathway is the layer II and III cells of the entorhinal cortex (Zimmer, 1971; Steward, 1976; Steward and Scoville, 1976;

Wyss, 1981; Schartz and Coleman, 1981; Witter, 1993). Cells in layer II send their axons almost exclusively to the dentate gyrus and collaterals to the subiculum (Lingenhöhl and Finch, 1991; Tamamaki and Nojyo, 1993), whereas cells in layer III send their axons exclusively to field CA1 and to the subiculum (Witter, 1993).

Differences have been observed in the terminal distribution of the fibers in the molecular layer of the dentate gyrus, depending on their origin in lateral entorhinal cortex versus medial entorhinal cortex. Fibers from lateral entorhinal cortex compose the lateral perforant pathway and terminate in the outer one-third of the molecular layer, whereas fibers from the medial entorhinal cortex which compose the medial perforant pathway preferentially distribute to the middle one-third of the molecular layer (Hjorth-Simonsen,1972; Hjorth-Simonsen and Jeune, 1972; Steward, 1976; Witter, 1989; Wyss, 1981). The lateral and medial divisions of the perforant pathway not only have different anatomical origins, but also are functionally different, as indicated by the functional intrinsic and extrinsic neuronal circuitry in the entorhinal cortex (Witter et al., 1989). The inner third of the molecular layer receives a projection that originates predominantly from cells in the hilus (Blackstad, 1956; Laurberg, 1979; Laurberg and Sorensen, 1981; Swanson et al., 1981). Because this projection originates from both the ipsilateral and the contralateral sides, it has been called the commissural/associational projection. The projection from the medial septal nucleus to the dentate gyrus also terminates in the inner third of the molecular layer and in the hilus.

1.3.3 The entorhinal cortex

The entorhinal cortex can be divided into medial and lateral parts. This division is based on cytoarchitecture, on the projection of the entorhinal cortex to the hippocampal formation, and on its intrinsic and extra-hippocampal projections (Köhler, 1985, 1986, 1988; Witter et al., 1989)(Fig.1-2). There are three major cortical inputs that terminate in the superficial layers I-III of the entorhinal cortex where the perforant pathways originate. First, the superficial layers receive prominant inputs from olfactory structures, such as the olfactory bulb, anterior olfactory nucleus, and prepiriform cortex (Heimer, 1968; Haberly and Price, 1978; Kosel et al., 1981; Room et al., 1984; Witter, 1989). Olfactory input terminates throughout most of the rostrocaudal extent of both lateral and medial entorhinal cortex. Only the most caudal part of the medial entorhinal cortex does not receive olfactory inputs. Furthermore, Wilson and Steward (1978) demonstrated that olfactory responses recorded from the hippocampal formation are probably relayed selectively through lateral entorhinal cortex since destruction of this area abolishes the responses in the hippocampal formation. The second prominant input comes from the laterally adjacent perirhinal cortex (Fig.1-2). This projection distributes to a restricted lateral part of both lateral and medial entorhinal cortex. Since perirhinal cortex is connected with the temporal cortex (auditory, visual, and polymodal association cortex) as well as with the insular cortex (autonomic and limbic association cortex) and the medial prefrontal cortex (frontal eye field and supplementary motor cortex), various sensory inputs could be relayed to the hippocampal formation via the perirhinal and entorhinal cortex (Witter et al., 1989). However, this conclusion is based on anatomical

findings; more detailed electrophysiological examination of the various sensory connections with the entorhinal cortex is still lacking. The third major input to the superficial layers of the entorhinal cortex originates in the presubiculum and parasubiculum (Fig.1-2). The parasubiculum projection is unilateral and reaches both lateral entorhinal cortex and medial entorhinal cortex. The presubiculum projection is bilateral and distributes exclusively to the medial entorhinal cortex. In the rat, it has been observed that the dorsal part of the presubiculum receives a well-defined input from the primary visual fields 17 and 18 (Vogt and Miller, 1983; Vogt et al., 1986) and input from retrosplenial cortex. The claustrum is another visually related (possible visualmotor integration, Witter et al., 1989) area which projects densely to the presubiculum. Thus, there is a strong visual component in the projection from presubiculum to the medial entorhinal cortex.

Projections from the subiculum to the entorhinal cortex have been described in the rat (Beckstead, 1978; Finch et al., 1983, 1986; Köhler, 1985; Swanson and Cowan, 1977). This projection terminates mainly in the deeper layers but also in the superficial layers of the caudal part of the medial entorhinal cortex (Köhler, 1985; Witter et al., 1989).

There is also a projection from the medial septal nucleus which primarily terminates in medial entorhinal cortex (Alonso and Köhler, 1984)(Fig.1-2). The septal region is considered to act as a pacemaker for Rhythmic Slow Activity (RSA). The dentate gyrus and field CA1 may generate RSA (with a phase difference of approximately 180°; Lopes da Silva et al., 1989). Mitchell and Ranck (1980) suggested

that two neuronal populations in the entorhinal cortex are responsible for the generation of the RSA of this cortical area. The cells of layer II generate a RSA that is in phase with that found in the dentate gyrus, whereas cells in layer III generate a RSA that approximates closely that in CA1. This is of interest since layer II cells are the major source of the projection to the dentate gyrus, whereas cells in layer III give rise to the projection to CA1.

The entorhinal cortex also gives rise to a projection to the contralateral hippocampal formation (Blackstad, 1956,1958; Goldowitz et al., 1975). The largest component of this projection is directed towards the dentate gyrus. In the dorsal pole of the dentate gyrus, there is a marked crossed projection to the dentate gyrus that is almost as dense as the ipsilateral one. While ipsilaterally the strongest labelling shifts to more ventral levels, the density of the crossed projection sharply declines with the result that no crossing fibers terminate ventral to the dorsal one-third of the contralateral dentate gyrus. (Only the dorsal part of the dentate gyrus receives the crossed projection from contralateral entorhinal cortex, and the crossed projection becomes weaker along the dorsal-ventral axis of the dentate gyrus). The origin of the crossed entorhinal-dentate pathway is restricted to lateral and caudal parts of the lateral and medial entorhinal cortex. With respect to its laminar origin, Steward and Scoville (1976) showed that in the rat the commissural projections arise exclusively from cells of layer III of the entorhinal cortex.

The projection between entorhinal cortex and hippocampal formation is topographically organized. The lateral parts of lateral and medial entorhinal cortex are

Figure 1-2 Major input and output connections of entorhinal cortex layer II and III cells. The olfactory bulb, olfactory nucleus, and prepiriform cortex project to both the medial and lateral entorhinal cortices however, the projection to the lateral entorhinal cortex is stronger than the one to the medial entorhinal cortex as indicated by thick and thin arrows. The light and dark grey filled arrows indicate the medial and lateral perforant pathways respectively. Note that there is a strong visual input to the presubiculum and that the projection from the presubiculum to medial entorhinal cortex layer II cells is emphasized by a thick arrow. The projections from the subiculum to the entorhinal cortex terminate in deeper cell layers (layer III, IV, and V) and include both medial and lateral entorhinal cortices. Com/assoc, commissural associational fibers; DG, dentate gyrus.

Major Input and Output Connections of Entorhinal Cortex
Layer II and III Cells

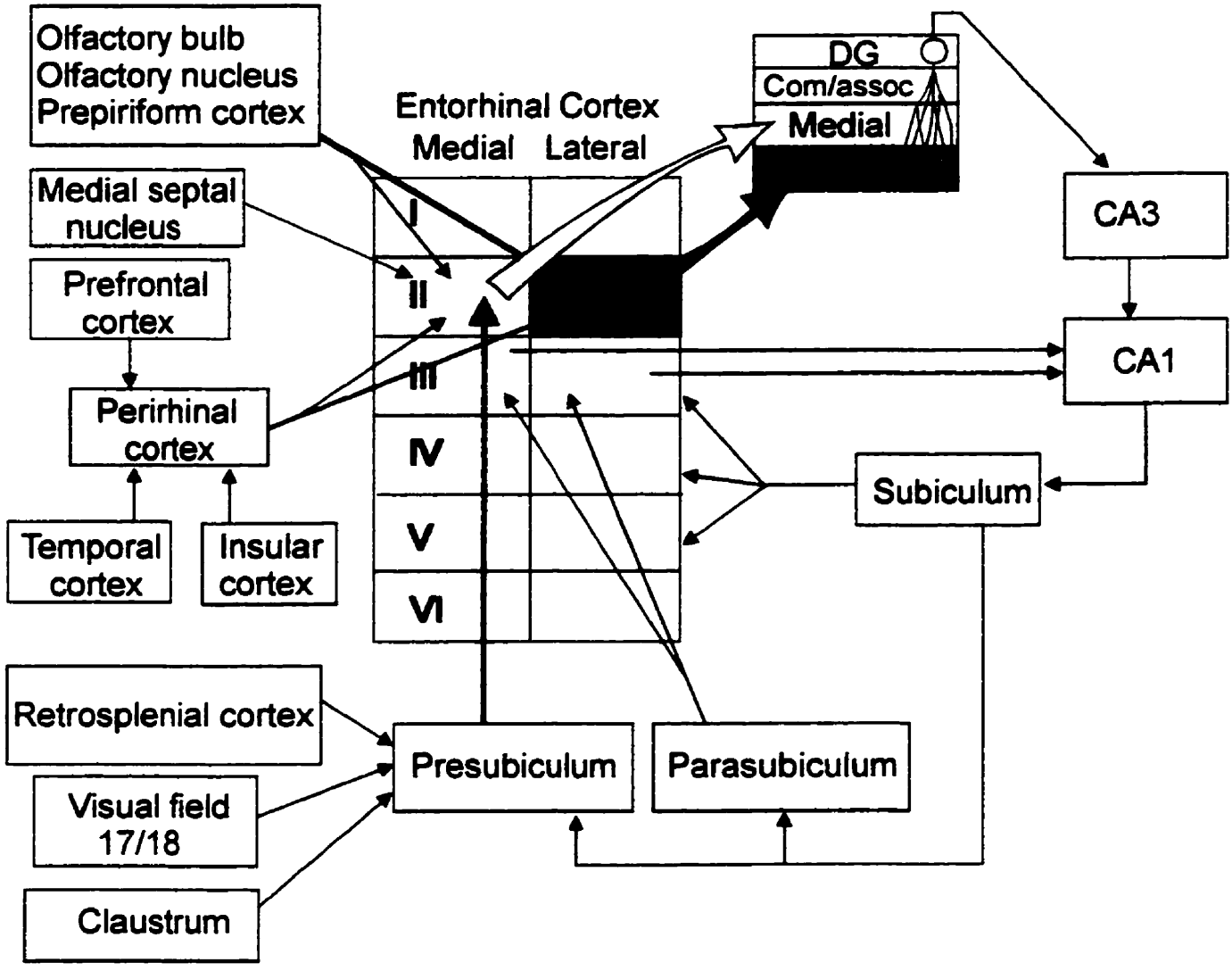

related to the dorsal part of the hippocampal formation, and more medial parts of lateral and medial entorhinal cortex are related to the ventral part of the hippocampal formation (Ruth et al., 1982,1988; Witter and Groenewegen, 1984; Witter et al., 1989, Witter, 1993).

The hippocampal formation projects back to the parahippocampal region. The origin of this projection is mainly from the subiculum and CA1. The fibers predominately distribute to medial entorhinal cortex and the pre-and parasubiculum. In medial entorhinal cortex, they appear to interact with cells in the deeper layers of the cortex, whereas the termination in the pre- and parasubiculum is mainly in the superficial layers. The major projections to the medial and lateral entorhinal cortices are summarized in Figure 1-2. Note that dentate gyrus granule cells do not have reciprocal connections with the entorhinal cortex.

1.4 Physiology of the Perforant Pathway

1.4.1 Neurotransmitters

Nadler et al. (1976), White et al. (1977), Di Lauro et al. (1981) proposed that the neurotransmitter used by the perforant pathway was amino acid. Nadler et al. (1976) made the first attempt to identify this amino acid and more importantly its release from perforant pathway fibers. They found that aspartate and glutamate were released by superfused hippocampal slices in a Ca^{2+}-dependent manner when slices were depolarized by high K^+ solution and that their efflux was associated in part with

commissural fibers and perforant path fibers. Subsequently, it was further demonstrated that direct electrical stimulation of the perforant pathway could elevate glutamate release as determined by measuring glutamate content in the superfuse fractions. Furthermore, superfusion with a Ca^{2+} -free medium drastically reduced glutamate output in response to stimulation, demonstrating that the release of glutamate occurred in a Ca^{2+}-dependent manner. Thus, glutamate was identified as the transmitter in the perforant pathway (Strom-Mathisen, 1977; White et al., 1977).

In Alzheimer's disease, cells in the entorhinal cortex, the source of perforant pathway are destroyed. When tissues of the perforant pathway terminal zone were microdissected out and assayed for glutamate, it was found that there was an 83% decrease in the level of free glutamate in subjects with Alzheimer's disease as compared to control (Hyman et al., 1987). Thus, glutamate is the putative neurotransmitter of the perforant pathway for both human and rat.

1.4.2 Other neurotransmitters which modulate perforant pathway responses

1.4.2.1 Acetylcholine

The medial septal nucleus and the nucleus of the diagonal band of Broca project to the dentate gyrus through the fimbria and dorsal fornix (Witter, 1989, Amaral, 1995). These projections were shown to be cholinergic (Lewis and Shute, 1967; Alonso and Köhler, 1984; Rye et al., 1984; Woolf et al., 1984; Amaral and Kurz, 1985) and GABAergic (Köhler et al., 1984). The termination zones of this projection are in the hilus area and the inner third of the molecular layer (Frotscher and Léránth, 1985; Amaral and

Witter, 1995b). However, acetylcholinesterase (AChE) staining, choline acetyltransferase (ChAT) immunolocalization, and acetylcholine receptor (AChR) autoradiography showed positive labelling in the perforant pathway terminal zone as well (Storm-Mathisen, 1970; Steward, 1976; Frotscher and Léránth, 1986).

Kahle and Cotman (1989) reported that bath application of a cholinergic agonist carbachol (10-20 μM) depresses synaptic responses in the medial but not the lateral perforant pathway in the guinea pig hippocampal slice. In the rat medial perforant pathway, bath application of muscarine at a concentration (1 μM), which has no effect on evoked response, showed a facilitatory effect on LTP induction (Burgard and Sarvey, 1990). However, at higher concentration (10 μM), muscarine depressed evoked responses and has no effect on LTP induction (Burgard and Sarvey, 1990; Bugard et al, 1993). With whole-cell recordings, Wang and Wojtowicz (1996) showed that 10 μM carbachol reduces synaptic transmission while increasing the excitability of granule cells. Furthermore, LTP induced during carbachol (10 μM) application had a larger magnitude than LTP induced in controls (Wang and Wojtowicz, 1996).

1.4.2.2 Serotonin

The serotonergic fibers in the dentate gyrus originate from several subdivisions of the raphe nuclei (Amaral and Witter, 1995). This projection terminates most heavily in the hilus polymorphic layer, but the projection tends to be limited to an immediately subgranular portion of the layer (Conard et al., 1974; Moore and Halaris 1975). Halasy et al. (1992) have shown that the raphe serotonergic fibers preferentially terminate on

a class of interneurons (basket cells) in the dentate gyrus that primarily influence the proximal dendrites of the granule cells. Thus, the serotonergic input could potentially modulate the excitability of the granule cell. However, depletion of serotonin had no effect on either the occurrence of LTP, the population spike or the dendritic EPSP-LTP in the dentate gyrus (Stanton and Sarvey, 1987,1985).

1.4.2.3 Cholecystokinin

The cholecystokinin-like (CCK-L) immunoreactive cells are located in the polymorphic zone of the dentate hilus (Greenwood et al., 1981; Somogyi et al., 1984). Almost all of the CCK-L immunoreactive cells are also glutamate decarboxylase (GAD) immunoreactive positive, which indicates CCK is localized in GABAergic interneurons (Somogyi et al., 1984; Kosaka et al., 1985). Han et al. (1993) suggest that it is likely that the CCK-L immunoreactive cells are the HICAP cells identified by them (mentioned above in section 1.3.1.1). However, some basket cells terminating on the somata of granule cells are also immunopositive for CCK (Hendry and Jones, 1985), therefore this peptide may be present in a functionally heterogeneous group of interneurons in the dentate gyrus (Han et al., 1993). CCK-L immunoreactive fibers extend among granule cells and inner third of molecular layer of the dentate gyrus (Greenwood et al., 1981; Han et al., 1993). When cholecystokinin-octapeptide (CCK-8) was administered systemically, the amplitude of the recorded action potential in the dentate gyrus evoked by stimulation of the medial entorhinal cortex was increased (Dahl, 1987). Intraventricularly applied CCK-8 had no consistent effect on the perforant pathway evoked action potential in the

granule cell layer of dentate gyrus, but when CCK-8 was iontophoretically applied in the granule cell layer, a reduction in the slope of the evoked response recorded in the dentate molecular layer was observed (Sinton, 1988a). Later, the same author reported that iontophoretically applied CCK-8 in the granule cell layer increases the cell excitability as indicated by a shift of the input/output curve to the left (Sinton, 1988b). Thus, exogeneously applied CCK-8 seemed to reduce the threshold for synaptic excitation (Sinton, 1988b). However, the mechanism underlying this excitability change is still unclear.

1.4.2.4 Norepinephrine

The dentate gyrus receives a particularly prominent noradrenergic input primarily from the pontine nucleus locus coeruleus (Haring and Davis, 1983; Haring and Davis, 1985a,b; Koda et al., 1987a,b; Moore et al, 1978; Pickel et al., 1974; Swanson and Hartman, 1975). The noradrenergic fibers terminate mainly in the hilus polymorphic layer of the dentate gyrus.

Neuman and Harley (1983) first reported that norepinephrine, iontophoretically applied to dentate granule cell layer in the anesthetized rat, produced a significant potentiation of the perforant pathway evoked population spike that lasted for many minutes. Later, using the brain slice preparation, Lacaille and Harley (1985) identified the β-adrenergic receptor as the receptor responsible for norepinephrine's potentiation effects observed in the *in vivo* preparation. Stanton and Sarvey (1987) demonstrated that both the population spike and field EPSP recorded from dentate molecular layer were

potentiated by norepinephrine in the brain slice preparation. Furthermore, this enhancement has been shown to be pathway specific. The β-adrenergic agonist isoproterenol induced a long-lasting potentiation of responses evoked by medial perforant pathway stimulation. In contrast, the same agonist reduced the responses evoked by lateral perforant pathway stimulation (Dahl and Sarvey, 1989).

1.4.3 Electrophysiology

McNaughton and Barnes (1977) showed that activating the dorsomedial (medial) and ventrolateral (lateral) perforant pathways in the anesthetized rats could result in quantitatively different extracellularly recorded EPSPs in the dentate gyrus. They found that EPSPs evoked by dorsomedial pathway activation had a shorter latency to peak than the EPSPs evoked by ventrolateral pathway activation. Also, the ventrolateral EPSP's half-width (defined as the width of the EPSP at one half its height above baseline) was larger than the dorsomedial EPSP. Furthermore, when they plotted the peak latencies and half-widths as a function of stimulus depth (as stimulation electrode advanced from dorsomedial pathway towards ventrolateral pathway), the curve showed a sharp increase of both peak latency and half-width when the stimulation electrode was at the junction of dorsomedial and ventrolateral pathways, indicating there are two distinct bundles of fibers instead of a continuously ordered fiber system. Moreover, when they used paired-pulse stimulation with interpulse interval of 35 ms, both the dorsomedial and ventrolateral pathway responses showed facilitation for the second pulse. However, when they stimulated one pathway and followed 35 ms later by stimulation of the other

pathway, they saw no heterosynaptic facilitation. Thus, they concluded that the stimulating electrodes were activating non-overlapping pathways.

One of the criteria used for identifying a monosynaptic EPSP was the ability of the response to follow stimulus trains of high frequency (Lømo, 1971; McNaughton and Barnes, 1977). Although both pathways can follow 100 Hz stimulation, indicating monosynaptic connections, the dorsomedial pathway responses follow less well, i.e., show greater attenuation than the ventrolateral pathway responses (McNaughton and Barnes, 1977). This difference in high frequency responses in the medial and lateral pathway was further examined by McNaughton (1980). He found a distinct difference in the responses of lateral and medial perforant path even at 2 Hz stimulation. The medial pathway response depressed rapidly with repeated stimulation while the lateral pathway responses showed little depression at 2 Hz. Furthermore, the ratio of EPSP to presynaptic fiber volley was found to be greater in the medial pathway; thus, the author concluded that the medial pathway releases a larger fraction of its available transmitter per impulse than the lateral pathway.

1.4.3.1 Contralateral and ipsilateral inputs

The entorhinal cortex projects not only to the ipsilateral dentate gyrus but also to the contralateral dentate gyrus (section 1.3.3). The contralateral projection is a weak one because in the anesthetized rat, tetanic stimulation to one entorhinal cortex reliably elicits LTP at the ipsilateral dentate gyrus synapses, while the synapses of the collateral, crossed pathway to the contralateral dentate gyrus do not exhibit LTP (Levy and

Steward, 1979). Furthermore, in the dentate gyrus ipsilateral to the stimulated entorhinal cortex the convergent crossed pathway from the contralateral side, which itself had not been stimulated, failed to exhibit heterosynaptic LTP (Levy and Steward, 1979). While the crossed entorhinal-dentate gyrus projection never exhibited LTP when tetanized alone, the crossed input could be potentiated by paired, near-simultaneous (1 ms interval) tetanic stimulation of ipsi-and contralateral inputs. This type of cooperative LTP is proposed to be related to associative learning (Levy and Steward, 1979).

White et al. (1988,1990) demonstrated cooperative LTP and LTD between the overlapping ipsilateral and contralateral projection of the perforant pathway. In anesthetized rats, stimulation electrodes were placed bilaterally in the lateral and the medial division of entorhinal cortex (nonoverlap condition) or in the medial and the intermediate division of the entorhinal cortex bilaterally (overlap condition), while a recording electrode was placed in the hilus of the dentate gyrus. They found that the extent of associative LTP or LTD depended on the extent of overlap between the terminal fields of the pathways. Co-activation of two pathways that overlapped by 51-100% led to LTP; co-activation of pathways that overlapped 0-50% between the terminal fields did not. LTD was induced in a crossed pathway when an ipsilateral pathway that overlapped by 51-100% was activated, but not when a non-overlapping (0-50% overlap) ipsilateral pathway was activated. Interactions are maximal between inputs that converge on the same portion of the dendrite, whereas interactions are limited between spatially segregated inputs.

1.4.3.2 Interaction of medial and lateral pathways

Interactions between lateral and medial pathways have been examined *in situ*. McNaughton et al. (1978) were first to propose cooperative interactions between perforant afferents. In their experiments, performed on anesthetized animals, LTP induced by concurrent activation of medial and lateral pathways was larger than during activation of either pathway alone.

Harris et al. (1979) examined the homosynaptic depression by recording population EPSPs and population spikes from dentate gyrus while stimulating either medial entorhinal cortex or lateral entorhinal cortex in anesthetized rats. They found that repeated low frequency stimulation (1 Hz) of either medial or lateral entorhinal cortex resulted in habituation-like response decrements. However, habituating stimulation of one subdivision of the entorhinal cortex did not result in decreased responsiveness to stimulation of the other. Repetitive low-frequency stimulation or even a single pulse delivered to either subdivision did, however, result in a potentiation of granule cell discharge in response to stimulation of the other subdivision (a form of heterosynaptic potentiation). This heterosynaptic potentiation of granule cell discharge was not accompanied by any increase in the extracellularly recorded EPSP. Thus, they concluded that repetitive activation of the perforant pathways has two effects on granule cell output. One effect is a habituation-like decrement in synaptic activation, and the other one is a potentiation of granule cell discharge as a consequence of prior activation.

Abraham and Goddard (1983) found that LTP of either the lateral or medial components of the perforant path afferent is associated with only short-lasting reciprocal

heterosynaptic depression. However, using more detailed measurement of stimulus intensity curves, they found that tetanization of either the lateral perforant pathway or the medial perforant pathway reliably depresses synaptic transmission in the other pathway for at least 3 hours. This heterosynaptic depression, considerably smaller than the usual magnitude of LTP, was obtained regardless of whether LTP had been produced in the tetanized homosynaptic pathway. However, heterosynaptic long-term depression was not observed if the test pathway had been previously tetanized. Thus, the interactions between medial and lateral perforant pathways are related to the temporal and spatial relationships between the inputs and the past history of the inputs.

1.5 Summary and rationale of the project

On the basis of the evidence provided by previous studies, we know that the hippocampal formation is crucial for some forms of memory. In rats, hippocampal formation is especially important for spatial memory and associational learning (section 1.1). We still don't know how the hippocampal formation integrates various sensory cues to create a cognitive map or how it performs associational learning. Furthermore, LTP might play a role in spatial memory (section 1.1.4), but we don't know what is potentiated and how the potentiation underlies spatial memory or associational learning. In order to understand how the hippocampal formation performs the various tasks, we should start by defining the properties of the inputs to the hippocampal formation.

Anatomical data indicate that the perforant pathway is the major external input to

the hippocampal formation and have delineated the connections between the hippocampal formation and various sensory cortices (section 1.3.2). Furthermore, the perforant pathway can be divided into medial and lateral subdivisions according to the origin and terminal field of each pathway. Clearly, the anatomical connections of medial and lateral entorhinal cortices (section 1.3.3) indicated that, the medial and lateral perforant pathways relay different information to dentate gyrus. Both pathways converge onto dentate granule cells, one terminating on distal dendrites and the other on more proximal dendrites. Thus, the anatomical organization of the perforant pathway provides an ideal preparation to examine the integration of different inputs by dentate granule cells. Previous *in vivo* studies have shown that the interactions of medial and lateral pathways produce heterosynaptic depression or heterosynaptic potentiation, and depend on the stimulation pattern and temporal relationship (section 1.4.3.2). However, *in vivo* studies are limited to extracellular recordings and the mechanisms underlying various interactions cannot be easily deciphered by this crude measurement. Furthermore, the experiments are performed under conditions in which the whole brain circuitry is more or less intact (under the influence of anesthetics). Thus, although *in vivo* experiments are closer to natural condition than *in vitro* experiments, there are metabolic and hormonal influences which are hard to control and might affect neuronal responses.

In this project, I will use the *in vitro* hippocampal slice preparation. In this much reduced circuitry, interference from other brain regions is greatly reduced and the external environment can be manipulated and kept under strict control. Using this simplified preparation, we can learn the basic properties of perforant pathways as the

first step to understanding more complex circuitry. The hypothesis to be tested is that medial and lateral pathways are different physiologically, either through differentiation of the intrinsic properties of each pathway or as a result of differences in external modulation, or both; and that these differences may reflect the function of each pathway. Since LTP is a characteristic feature of hippocampal formation, LTP of medial and lateral pathways will be examined in detail. In order to examine how dentate granule cells integrate multiple inputs, co-activation of lateral and medial pathways will be used to mimic multiple sensory inputs arriving at dentate granule cells with short (milliseconds) inter-pathway intervals.

2.1 Animals

Wistar rats of either sex from sixteen to thirty days old were used in experiments presented in this dissertation. Young animals were chosen in this study for two reasons. First, it was believed that it is easier to do whole-cell patch clamp recordings in young slices, presumbly due to less connective tissues in young animals. Secondly, the animals at this age are still undergoing extensive development in establishing the adult neuronal network; thus, are more "plastic" than adult animals.

The rats were supplied by Charles River Canada Ltd. Upon arriving in the Medical Sciences Building animal facility, the rats were kept in a light/dark controlled room with litter-mates and lactating mother. The rats were weaned when 21 days old and then male and female rats were separated.

2.2 Brain Slice Preparation

The rats were anaesthetized with halothane and decapitated by a guillotine. Hippocampi were quickly removed from the brain and sliced by a tissue chopper into 400 μm transverse slices. Slices were kept in a moist and oxygenated holding chamber for over 1 hour at room temperature, before being transferred to a recording chamber for experimentation. In the recording chamber, the slice was continuously superfused with artificial cerebrospinal fluid (ACSF) (2ml/min) that had been saturated with 95% O_2-5%

CO_2. The composition of the ACSF was (in mM): 124 NaCl, 3 KCl, 1.25 NaH_2PO_4, 1 $MgCl_2$, 2 $CaCl_2$, 26 $NaHCO_3$, 10 dextrose, and 0.01 bicuculline methiodide. The temperature of the medium was kept at 30-32°C.

2.3 Equipment

All recordings were performed using Axopatch-1D patch-clamp amplifier (Axon Instruments). The signals from the amplifier were monitored by an oscilloscope (Hameg 20MHz storage scope, model HM 205-3) and were further amplified by a signal conditioner (Intronix technologies corporation, model 2004-F). After the second amplification the signals, monitored by another oscilloscope (Nicolet Explorer I Oscilloscope), were forwarded into a digital recorder (Neuro Data Instruments Corp., model DR-384) and stored on VCR tapes for additional off line analysis. The same signals were digitized by a analog/digital converter (modified Labmaster board) and displayed by a PC 486/66 MHz computer for on line analysis and signal storage.

2.4 Stimulation and Recording Techniques

2.4.1 Electrodes and stimulator

Two bipolar tungsten electrodes (Frederick Haer & Co. Inc., medium size) were placed at the outer and middle thirds of the dentate gyrus molecular layer to stimulate the lateral and medial perforant pathways, respectively (Fig. 2-1). The distance between the

Figure 2-1 Schematic drawing of brain slice preparation. Stimulation electrodes S1 and S2 were positioned in the termination fields of medial and lateral perforant pathways respectively. The whole-cell recording electrode recorded from single granule cells from dentate granule cell layer. MPP, medial perforant pathway; LPP, lateral perforant pathway; DG, dentate gyrus. A representative dentate gyrus granule neuron filled with Lucifer Yellow is shown below.

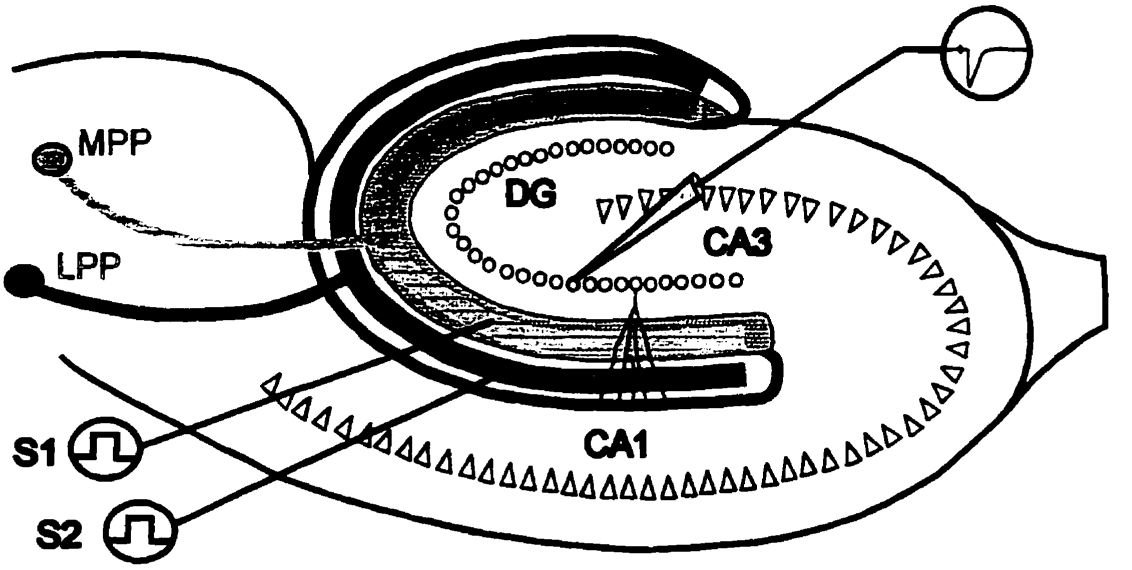
MPP
LPP
S1
S2
DG
CA3
CA1

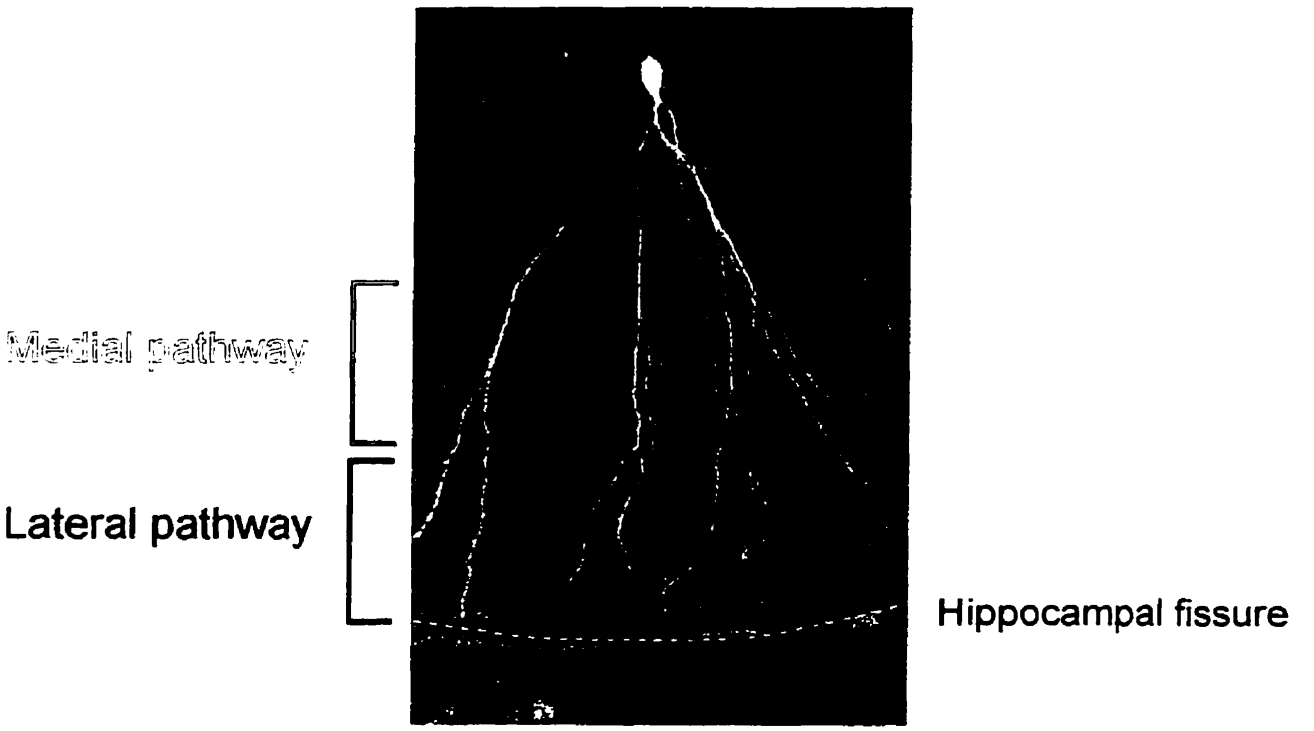
Medial pathway
Lateral pathway
Hippocampal fissure

two stimulating electrodes was 80-100 μm. Stimulation pulses (0.01 ms) were generated by a Grass 800 stimulator and passed through the signal isolation unit to convert into constant current. The stimulating current ranged from 0.1-1.0 mA. In most of the experiments the stimulating current was kept under 0.5 mA unless particularly large responses were required. Whole-cell patch electrodes were made from borosilicate glass capillaries containing an inner filament (o.d. 1.5 mm x 1.12 mm i.d., Frederick Haer & Co. Inc.). The glass capillaries were pulled in 2-3 steps by Flaming-Brown micropipette puller (model P-87, Sutter Instrument Co.). The electrodes had 1-2 μm outside tip diameter and a resistance of 5-8 MΩ when filled with K^+-salt intracellular solution. The composition of intracellular solution was (in mM) : 142.5 potassium gluconate, 17.5 $KMeSO_4$, 8 NaCl, 10 HEPES, 0.1 EGTA, 2 MgATP, 0.2 GTP, pH=7.3, osmolality=290-300 mOsm.

Extracellular field electrodes were made from the same glass capillaries described above and were pulled in 3 steps by the same micropipette puller. The electrodes had 5 μm outside tip diameter and were filled with ACSF.

2.4.2 Extracellular field potential recordings

A single extracellular field potential electrode was placed in the terminal field of the medial pathway about 400 μm away from stimulation electrodes. Medial perforant pathway stimulation created a current sink near the recording electrode whereas lateral pathway stimulation created a current source which were readily distinguishable in the recorded trace. The distinct wave form generated by the different pathways was one criterion to verify the separation of the two stimulated pathways. The slices which failed

to show distinct current sinks and sources for the different pathways were rejected. In the accepted slices, the stimulating electrodes were kept at the same place throughout the experiment. Usually the stimulation intensity was further reduced to avoid the possible overlap of the stimulation fields of the two pathways. Stimulation was applied at 0.1 Hz and the delay between the pulses activating medial and lateral perforant pathways was 50-200 ms. It was determined that this procedure produced no mutual facilitation or depression between synapses of the two pathways.

Field potential EPSPs were quantified by measuring the initial slope of the responses to avoid possible error produced by population action potential. Slope measurement is a valid approximation of synaptic responses because extracellular current recorded in the vicinity of the synapses represent, to first approximation, intracellular synaptic current. In all cases when field potential responses were recorded I measured the initial slope. In all whole-cell recordings (EPSPs or EPSCs) response peak amplitude was measured.

2.4.3 Patch recordings

Before starting whole-cell patch recordings, an extracellular field potential electrode was used to verify the separation of the medial and lateral pathways by the current sink and source method mentioned above. In the accepted slices, the stimulating electrodes were kept at the same place throughout the experiment, while the intensity of the stimulation was further reduced during whole-cell recordings to obtain "minimal" stimulation, with occasional failures of synaptic transmission (in some experiments, larger

stimulation strengths were used). "Blind" whole-cell patch-clamp recordings, were made from dentate granule cells with patch electrodes (Fig. 2-1). During voltage-clamp recordings cells were held at a constant membrane potential ranging from -55 to -75 mV. All membrane potentials presented in this dissertation refer to the potential recorded at the soma.

Excitatory synaptic currents (EPSCs) were elicited by test pulses applied once every 2-5 seconds to the medial and the lateral perforant pathway with 50 -200 ms delay between the two pathways. It is not certain how many axons were recruited by the stimulation, nor whether stimulation always reached threshold at the participating axons, but I made sure that stimulation produces constant EPSCs and that the response was not changed during LTP. Experiments that had unstable baseline or non-stationary responses after LTP induction were discarded.

The EPSCs were quantified by measuring the peak amplitude of the responses. In some quantal analysis experiments the charge (pA × ms) of the response was measured. The charge was measured by integrating the current trace. These two methods (peak and charge) gave similar results in quantal analysis.

2.5 LTP induction paradigms

Three methods were employed to induce LTP in lateral and medial pathways. Induction of LTP was considered successful when the mean of evoked responses 15-20 minutes after tetanization reached a level statistically different (paired t-test, $P < 0.05$)

from control. The first induction method was to release the cell from voltage-clamp during tetanic stimulation. This stimulation consisted of two 100 Hz trains (1 s duration) at test pulse intensity, applied 10 s apart. This method proved not to be very effective in inducing LTP. The second and more effective method was to voltage-clamp the cell to -20 mV while applying tetanic stimulation consisting of two 100 Hz trains (1 s duration) at test pulse intensity applied at 10 second intervals. The third and most effective method was to voltage-clamp the cell to -20 mV while applying four 100 Hz trains (0.5 s duration) at test pulse intensity (10 sec intervals). The success rates for these procedures among the cells analyzed is shown in Table 4 -1 and Table 4 - 2. Under voltage-clamp configuration, the first method induced successful medial pathway LTP in 10% of the cells tested whereas in the lateral pathway 14% of the cells showed LTP. The second method induced medial pathway LTP in 25% of the cells tested and lateral pathway LTP in 14% of the cells tested. The third, and the most effective method, induced medial pathway LTP in 50% of the cells tested and lateral pathway LTP in 35% of the cells.

In extracellular field recording recordings, LTP was induced by tetanic stimulation composed of four trains of 100 Hz pulses at the test pulse intensity. Each train was 0.5 s long and applied at 10 s intervals.

2.6 Data analysis

Records illustrated in this dissertation were digitized at 100-200 μs intervals (5-10 kHz). The averaged traces, which included 6-500 individual sweeps depending on the demands of the experiment, were stored in the computer. Occasionally, several hundred

consecutive single sweeps were collected and stored for quantal analysis. The digitization and data analysis software "AveragePlot" was developed by Mr. Steve Jones in The Medical Computing Division of The University of Toronto.

2.6.1 Exponential curve fitting

To evaluate the rates of decay of the evoked synaptic currents, we fitted double exponentials to the decay phases of averaged traces of EPSCs using the curve fitter in Sigma Plot, Jandel Scientific (1993). Only traces giving two clear exponentials fitted with standard errors of less than 5% of the estimated values of parameters were accepted for analysis. Out of the 25 current traces fitted with double exponential curves, 5 did not pass the test and were rejected.

2.6.2 Quantal analysis

The analysis of statistical fluctuations of the evoked synaptic responses was performed on four representative data sets obtained from the medial perforant pathway. The observed LTP in these data sets ranged from 16-450%. In three other data sets the analysis was attempted, but results did not satisfy the criteria for stationarity of the responses and reliability of the procedure. Thus, these latter data are not included.

The observed distributions of peak amplitudes or areas (charge transfer, the time integral of current) of a large number of evoked EPSCs (usually 400-500) were matched to an unconstrained quantal model using a maximal likelihood estimate (modified from Akaike information criterion: Smith et al., 1991,1993) as a criterion of the goodness of fit.

Because the baseline noise from the instrument and from the preparation was included in the measurement of evoked EPSCs, the simulated (fitted) response frequency distribution should include the variance of the noise. I measured the noise variance from a section of baseline free of spontaneous miniature EPSCs. Gaussian (normal) distributions of noise and quantal components were assumed. Furthermore, since maximum likelihood always increases with the number of estimated parameters, a penalty factor was introduced for each added quantal component. Thus, I compared models with different numbers of quantal components using this modified maximum likelihood estimate, also known as the Akaike information criterion, or AIC (Smith et al., 1991; Smith, 1993).

The estimated parameters were: noise variance, mean quantal size, quantal variance, number of Gaussian components (number of peaks) and relative weighting of each component (height of each peak). The procedure was tested on prefabricated data sets and found to be reliable with a small (up to five) number of Gaussian components. Higher numbers resulted in different predicted fits to the simulated data each time the program was executed. Thus, this procedure became unreliable. Consequently, in cases where the fitted distributions demanded a relatively high number of Gaussian components to match the data, I have estimated quantal parameters according to a simple (uniform) binomial distribution using analytical equations as described by others (Robinson,1976; Wojtowicz and Atwood, 1986; Voronin, 1993).

To narrow down the range of possible parameter values, the fitting procedure used the starting values of the noise variance measured as described above and the mean and

variance of quanta based on spontaneous EPSCs observed in the data.

The reliability of the fitted estimates was confirmed by dividing data sets in half and performing the fitting procedure on both segments. Only data sets in which each half yielded an estimated number of Gaussian components within ± 1 of those for the complete data set have been used.

The weights of the Gaussian components estimated from the above procedure give the deconvolved discrete distributions of quantal units in the data sets. We analyzed these distributions using the previously established method to estimate parameters *n* (number of contributing quantal units), *p* (average probability of release) and variance of *p* (Wojtowicz et al., 1991). The fitted distributions were found not to differ significantly from the observed distributions (Kolmogorov-Smirnov test at $P < 0.05$). Further confirmation of the reliability of the estimates was obtained by analyzing distributions of either peak amplitudes or areas of EPSPs. Both measures gave virtually identical results.

2.6.3 The coefficient of variation analysis of LTP

Following studies of Bekkers and Stevens (1990), Malinow and Tsien, (1990) and Xiang et al. (1994) we calculated the ratio of the mean of the evoked responses squared, to their variance (M^2/var). This ratio is equal to the inverted and squared coefficient of variation. As shown originally by del Castillo and Katz (1954), the coefficient of variation varies in a predictable way with quantal content of synaptic transmission but is independent of the quantal size. However, the relationship between the variance and quantal content depends on the characteristics of the release process. Thus it will be

different for Poisson and binomial distributions. The calculated change in the M^2/var ratio associated with a five-fold increase in quantal content for a simple binomial distribution is larger than five. For a Poisson distribution the ratio should be much larger than five. In the above cases the slope of the vectors on the graphical variance analysis plot should be greater than 45°. Lower slopes indicate a larger change in variance than expected from the simple binomial or Poisson distributions. It can be shown that for a non-uniform binomial distribution, characterized by variable probability (p) of release among synapses, the variance of EPSCs is strongly (inversely) dependent on the variance of p (del Castillo and Katz, 1954). This dependence can produce low (<45°) slopes on the graphical variance plots under certain conditions when, for example, the variance of p is reduced as the amplitude of responses is increased (quantal content is increased). However, changes of the mean responses caused by increases in quantal size would not be expected to alter M^2/var ratios (Malinow and Tsien 1990).

Faber and Korn (1991) pointed out certain caveats in the coefficient of variation method when probabilities among the quantal units are non-uniform. Given many hypothetical factors which can alter the coefficient of variation of evoked EPSCs, one should use it carefully. For example, I have addressed a hypothetical situation given by Faber and Korn with an experiment in which additional axons are recruited during an experimental manipulation and found a predicted change in the M^2/var ratio.

2.7 Chemicals

The chemicals used to make ACSF and the intracellular solution were purchased from BDH Inc. (Canada), J.T. Baker Inc. (Canada) and Sigma Chemical Co. (USA). Bicuculline methiodide, D-2-amino-5-phosphonovaleric acid (D-APV), naloxone, met-enkephalin were purchased from Sigma Chemical Co. (USA). 6-cyano-7-nitroquinoxaline-2,3-dione (CNQX), 1-aminocyclopentane-1SR,3RS-carboxylic acid (t-ACPD), and L(+)-2-amino-4-phosphonobutyric acid (L-AP4) were purchased from Research Biochemicals International (RBI). CNQX was dissolved in dimethyl sulphoxide (DMSO) and the final concentration of DMSO in ACSF was 0.1-0.05%. The specific $GABA_B$ receptor blocker CGP 36742 was kindly donated by Dr, Jeffery A. Zidichouski, Ciba-Geigy (Canada).

2.8 Statistics

Data were analyzed using paired-student's *t*-tests, unpaired -student's *t*-tests and ANOVA unless otherwise stated. A probability less than 0.05 ($P<0.05$) was considered significant.

3.1 Introduction

The perforant pathway transmits information from entorhinal cortex to the dentate gyrus. The synapses of perforant path-dentate granule cells are the crucial site where this transmission occurs. The presynaptic transmitters, release properties of the presynaptic terminals, postsynaptic receptors, and spatial/temporal integration at the postsynaptic neurons are important factors which control the synaptic transmission. In order to understand synaptic transmission in the medial and lateral perforant pathways, the basic synaptic properties mentioned above should be explored. This knowledge will aid our understanding of LTP in these synapses. Furthermore, because of the convergence of the medial and the lateral perforant pathways on the dentate granule cells, discerning the basic synaptic properties of these pathways is the first step for studying the interactions of the pathways and how granule cells integrate the different inputs. Finally, recognizing the differences in synaptic properties of the two pathways can help future identification of the pathways. This chapter presents some basic physiological and pharmacological properties of the synapses in the medial and the lateral perforant pathways.

The glutamate receptors will be the main focus of this study because the perforant pathways use glutamate as their major neurotransmitter. Glutamate receptors can be divided into two major groups, the ionotropic glutamate receptors and the metabotropic glutamate receptors. The ionotropic glutamate receptors are responsible for the synaptic transmission in the perforant pathway synapses. Based on the sensitivity of various

ligands, the ionotropic glutamate receptors can be further divided into N-methyl-D-aspartate (NMDA) receptors and α-amino-3-hydroxyl-5-methyl-4-isoxazolepropionic acid (AMPA) receptors. AMPA receptors are responsible for fast cation currents during synaptic transmission while the NMDA current has a slower onset but lasts several tens of milliseconds. Furthermore, at resting membrane potential the NMDA receptor/channel pore is blocked by Mg^{2+} ion. Only when the Mg^{2+} ion is expelled by membrane depolarization, can current be conducted through the channel pore. Thus, this unique property makes the ligand-gated NMDA receptor also sensitive to voltage change. It is known that the NMDA receptor is important for certain types of LTP induction (for brief review, see Nicoll and Malenka, 1994). In the dentate gyrus, it has been shown that the medial pathway requires the activation of NMDA receptors for induction of LTP (Bramham et al., 1991b). The dependence of the lateral pathway LTP on NMDA receptor activation is uncertain. Dahl et al. (1990) reported that the NMDA receptor antagonist reduces only the EPSPs evoked by the medial pathway activation but not those evoked by the lateral pathway activation, implying that the lateral pathway has few NMDA receptors. It has also been reported from *in vivo* studies that lateral pathway does not need the activation of NMDA receptors for induction of LTP (Bramham et al., 1991b). However, Lambert and Jones (1990) demonstrated that both lateral and medial pathways have prominent NMDA components. Moreover, autoradiographic studies indicate considerable spread of NMDA receptors into the distal dendrites of dentate granule cells where the lateral pathway terminates (Monaghan et al., 1983). In a more recent paper, Colino and Malenka (1993) demonstrated that both the medial and the lateral pathways

express NMDA-dependent LTP. Thus, it is important to verify the earlier findings and further characterize the NMDA components in these two pathways.

In addition to the ionotropic glutamate receptors (AMPA and NMDA), glutamate also activates a group of G-protein linked metabotropic glutamate receptors. This group of receptors has eight subtypes known to date and the diversity of these receptors may be further expanded by alternative splicing (Schoepp and Conn, 1993). Activation of metabotropic receptors can lead to various second messenger cascades depending on subtype. For example, subtypes mGluR1 and mGluR5 are known to activate phosphoinositide-specific phospholipase C to cause phosphoinositide hydrolysis and subsequent intracellular Ca^{2+} mobilization (Watkins and Collingridge, 1994). The activation of mGluR2,3,4,6,7 is negatively coupled to adenylate cyclase activity (Watkins and Collingridge, 1994). The physiological functions of metabotropic glutamate receptors are currently unclear; however, there is evidence indicating that the metabotropic receptors are important for LTP induction (Bashir et al., 1993; Riedel et al., 1994; Riedel et al., 1995). I will examine the effects of exogenously applied metabotropic glutamate receptor agonists on synaptic transmission of the medial and the lateral pathways. This approach will provide some insight into how metabotropic glutamate receptors respond to synaptically released glutamate and how this might affect LTP induction.

Immunocytochemical and autoradiographical studies also showed that there were some differences in the transmitters (or modulators) and receptors of the two perforant pathways. The most distinct difference is that the lateral pathway contains opioid peptide, while the medial pathway contains cholecystokinin (CCK) (Fredens et al., 1984). In vivo

studies showed that opiate receptor activation is required to induce LTP in the lateral pathway but not in the medial pathway (Bramham et al., 1991a). Although only the lateral pathway contains opioid peptide (Fredens et al., 1984), autoradiographic studies showed that all three major opioid receptor subtypes (κ,δ,μ) are distributed throughout the dentate molecular layer, located in both the lateral and the medial pathway terminal fields (Crain et al., 1986; McLean et al, 1987; Plager and Vogt, 1988). The functional significance of the mismatch of opioid peptide release site and opioid receptor location is not clear at this point. Since it is thought that the opioid peptides are released only under high frequency pulsatile stimulation (Wagner et al., 1990; Caudle et al., 1991), it is quite possible that during the high frequency stimulation required for LTP induction, opioid peptide is released from the lateral perforant pathway. Furthermore, since the opioid peptides are only contained in the lateral pathway and there are receptors located in the medial pathway, a possible diffusion of the opioid peptides released from the lateral pathway to the medial pathway will be considered in this thesis. The function of the opioid receptors in the medial and lateral pathway terminal fields will be examined by exogenously applied opioid peptide and by application of an antagonist. The possible modulatory role of the opioid peptides in the lateral and the medial pathway will be discussed.

3.2 Results

The synaptic transmission in the medial and the lateral perforant pathways was

examined by whole-cell voltage-clamp and current-clamp recordings and the major differences will be presented in section 3.2.1. Some pharmacological properties of these synapses will be presented in section 3.2.2 - 3.2.4. These latter results were obtained by using both extracellular field potential recordings and single neuron whole-cell recordings.

3.2.1 Synaptic transmission

The evoked excitatory postsynaptic potentials (EPSPs) produced by medial pathway stimulation were similar to the EPSPs evoked by lateral pathway stimulation (Fig. 3-1A). However, a close examination of the response shape revealed differences in the rise time of the EPSPs (Fig.3-1B). The rise time was the time span measured from 10% to 90% of the peak response (Fig 3-2A).

On average, the medial pathway-evoked potentials had statistically significant shorter rise times (3.6 ± 0.4 ms, n = 12) while the lateral pathway-evoked potentials had longer rise times (4.2 ± 0.7 ms, n = 12) (Fig.3-2B,C). The half-width and time constant of the decay phase of the EPSPs were not different in the two pathways (Fig.3-2C). According to cable theory, the different rise times are expected since the lateral pathway's responses are conducted over a longer distance, and the RC filter effects of the neuron would slow the time course of the responses. This demonstrated that the lateral pathway-evoked responses indeed originated from the more distal dendrites.

The second noticeable difference between the medial and the lateral pathway evoked response was their depression to high frequency stimulation. This was best

Figure 3-1 Synaptic responses evoked by stimulating the medial and the lateral perforant pathways under current-clamp mode of whole-cell recording. **A**. Sample trace showing lateral and medial pathway responses. The boxed areas were enlarged and shown in panel **B** to illustrate the rise time differences seen in these two responses.

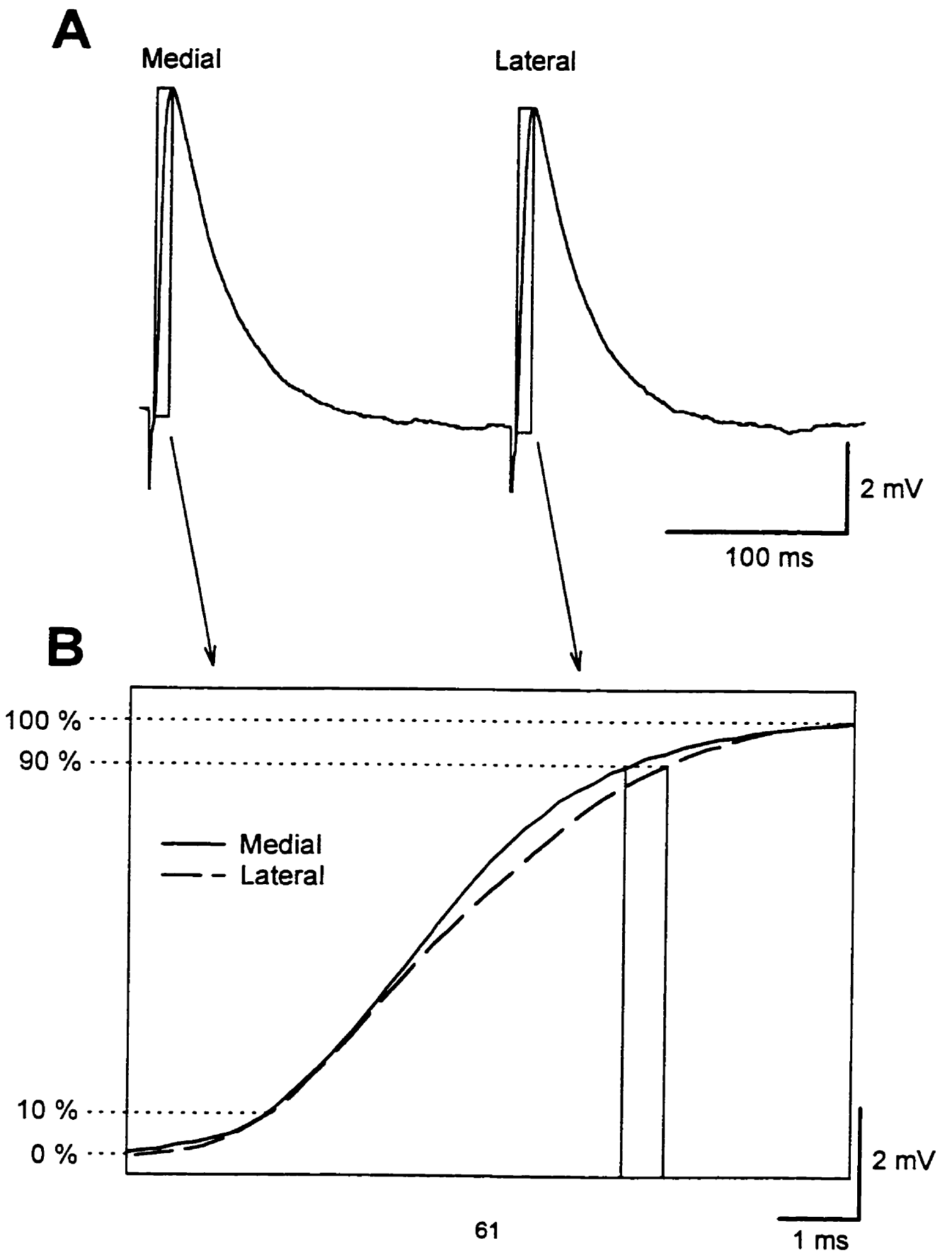
A
Medial
Lateral
2 mV
100 ms
B
100 %
90 %
Medial
Lateral
10 %
0 %
2 mV
1 ms

Figure 3-2 Shape parameters of medial and lateral perforant pathway stimulation-evoked responses. **A.** A sample trace illustrating the measurements of various parameters. The rise time of the response was measured from 10% to 90% of the response amplitude. Response half-width was measured from the time window where the response reaches 50% of the total amplitude in the rising phase and the falling phase. The falling phase time constant was measured from the peak of the response to when the response has fallen to 37% of the peak response. **B.** Comparison of rise time and half width of the lateral (empty circles) and medial (filled circles) pathway-evoked responses. Data were pooled from 12 experiments (12 cells, 1 cell/slice). The medial pathway and the lateral pathway-evoked responses from the same cell are linked by solid lines. The averaged results from all the experiments are shown by large circles with standard error bars. Note that in most of the cells the lateral pathway response has a longer rise time than the responses from the medial pathway, while the half width measurement from the two pathways did not show a significant difference. **C.** Summary table of the averaged results from 12 experiment shown in **B** (mean ± SD). Only the 10-90% rise time of the medial and the lateral pathways showed statistically significant difference (paired t-test, $P < 0.001$). The half width measurement was approaching significance (paired t-test, $P = 0.08$), whereas the falling phase time constant showed no difference in the two pathways.

A

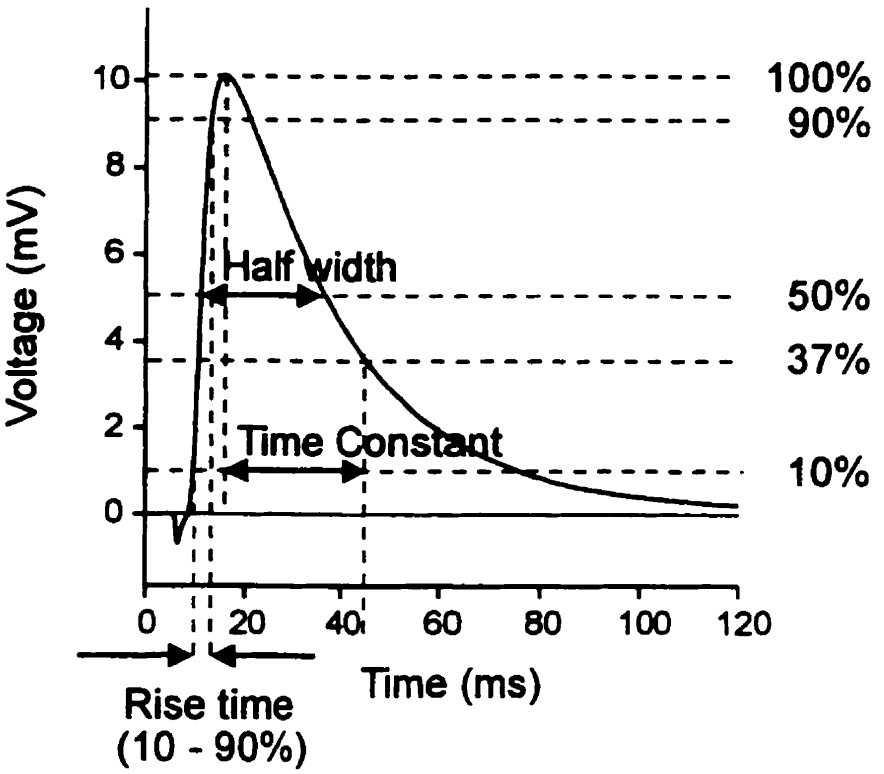

B

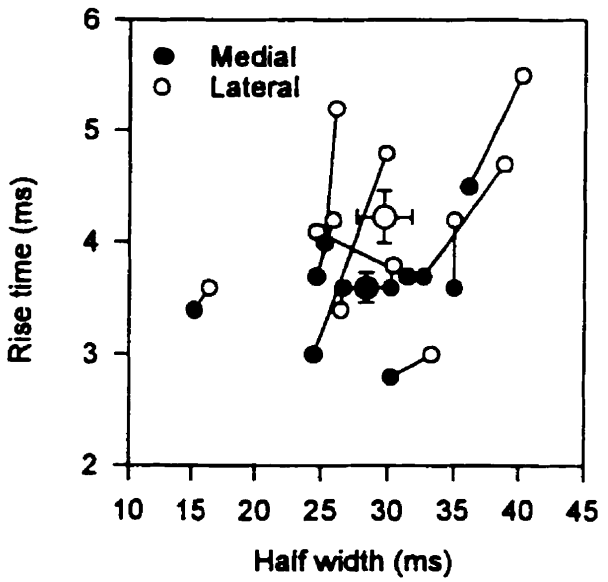

C

	Lateral	Medial
n	12	12
Amplitude (mV)	6.79 ± 3.33	6.88 ± 3.33
10-90% Rise Time (ms)	4.22 ± 0.76	3.60 ± 0.45*
Half-Width (ms)	29.70 ± 6.91	28.33± 5.96
Falling Phase Time Constant	33.10 ± 7.81	31.60 ± 7.56

demonstrated by whole-cell voltage-clamp recordings as in the examples shown in Figure 3-3. When a train of high frequency stimuli was applied to these pathways, the response of the medial pathway showed a clear depression towards the end of the train (Fig.3-3A). Those of lateral pathway, stimulated by the same stimulation paradigm, showed less depression (Fig.3-3B). This was shown by normalizing all the responses in the stimulation pulse trains to the first response of each train (100%). The medial pathway response depressed to 65.3 ± 4.5% (n = 5) after 6 pulses (interpulse interval 30 ms) while the lateral pathway response depressed to 77.9 ± 7.9% (n = 5). After 8 pulses, the medial pathway response further decreased to 55.5 ± 8.3% (n = 5) of the first response while the lateral pathway response only decreased to 75.4 ± 7.9% (n = 5) of the first response. Thus, the medial pathway response depresses more than the lateral pathway response when stimulated with high frequency pulse trains. Furthermore, this high frequency-induced depression was Ca^{2+} dependent. After reduction of Ca^{2+} ion concentration in the perfusion ACSF by partial substitution of the Ca^{2+} ions with Mn^{2+} ions (0.5 mM Ca^{2+}, 1.5 mM Mn^{2+}), the response size became smaller as expected, and the high frequency-induced depression evoked by the medial pathway stimulation was abolished (Fig.3-3C). This removal of high frequency depression was not due to a general reduction of response size in low Ca^{2+} solution, because in the standard solution, even after reducing the stimulation strength to create a small response matching the response size in low Ca^{2+} solution, the responses were still depressed by high frequency stimulation (Fig. 3-3C). This indicates that the synapses in the medial pathway behave like high-output synapses seen in the neuromuscular junction of the crayfish (see

Figure 3-3 High frequency depression of the medial and the lateral perforant pathway responses. **A**. The sample whole-cell voltage clamp responses of the lateral pathway to a train of high frequency stimuli. The interpulse interval was 30 ms (33.3 Hz). **B**. The medial pathway responses recorded from the same cell as **A** to high frequency stimuli. Note that the medial pathway responses depressed more than the lateral pathway responses after 6 pulses. **C**. The high frequency depression in the medial pathway was Ca^{2+} dependent. Lowering the Ca^{2+} concentration in the perfusion solution to 0.5 mM (substituting the removed Ca^{2+} with 1.5 mM Mn^{2+}) abolished the high frequency depression (thick line). This elimination of high frequency depression was not due to the general reduction in response size seen in low Ca^{2+} solution because when the stimulation strength was reduced to match the first response size in low Ca^{2+} solution, the small responses in normal solution (2 mM Ca^{2+}) still showed high frequency depression (thin line).

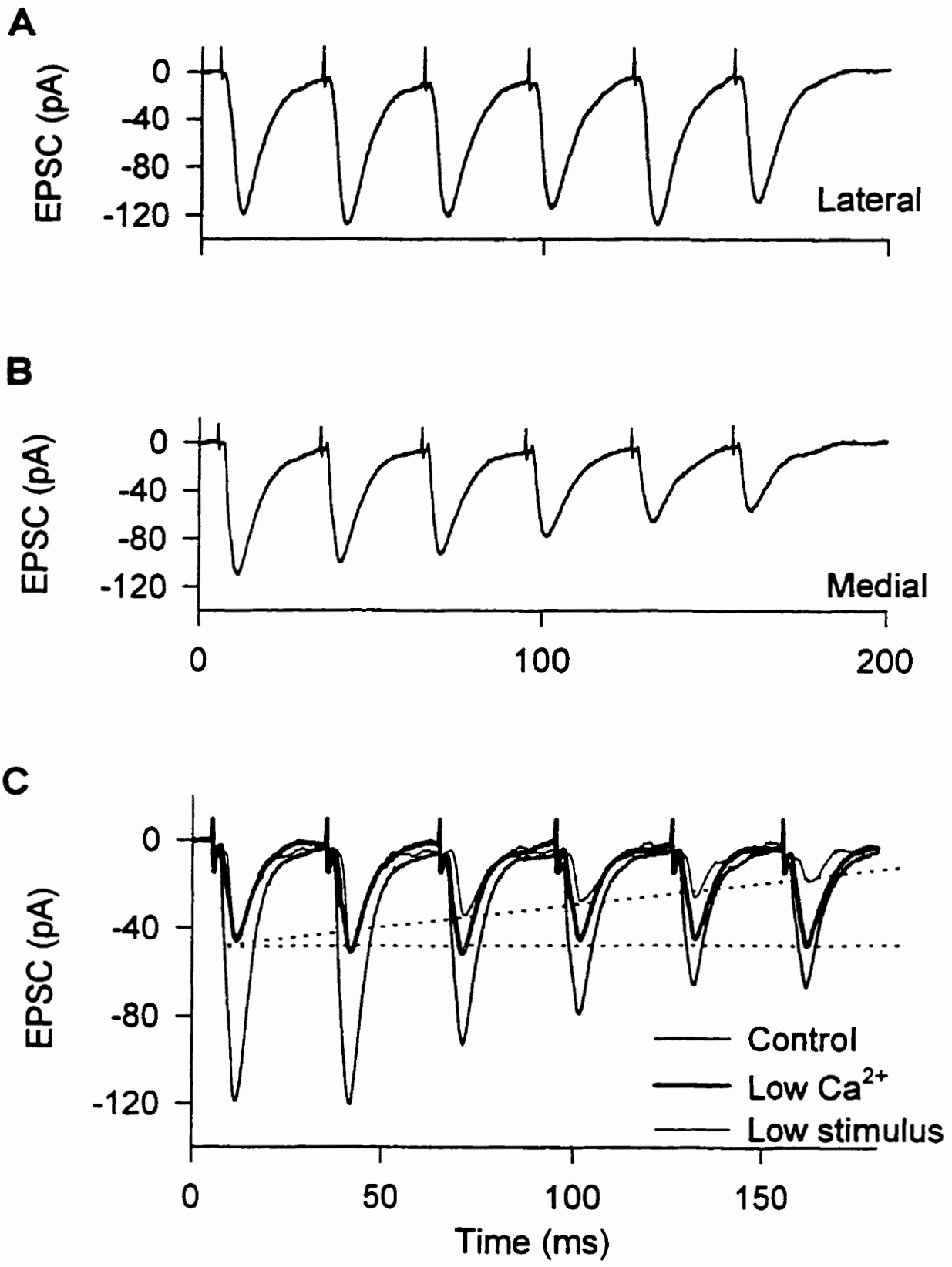
A
EPSC (pA)
0
-40
-80
-120
Lateral
B
EPSC (pA)
0
-40
-80
-120
Medial
0
100
200
C
EPSC (pA)
0
-40
-80
-120
Control
Low Ca2+
Low stimulus
0
50
100
150
Time (ms)

discussion). Thus, at high frequency transmission, there was a clear difference between the medial and lateral perforant pathways.

3.2.2 NMDA and AMPA receptors

The synaptic responses evoked by medial and lateral perforant pathway stimulation are mediated by ionotropic glutamate receptors. Measurements of excitatory postsynaptic currents (EPSCs) either at the resting membrane potential or during maintained depolarization revealed a strong voltage-dependence and the presence of two components: an early peak, and a late phase with slow decay (Fig 3-4A). Both the late and early phases of the EPSPs were voltage-dependent (Fig. 3-4B,C). I measured the early phase at the peak of response at each holding voltage and the late phase at 25 ms after the stimulus (Fig.3-4A). In both perforant pathways the peak current was bigger than the later current at -60 mV. However, the late phase grew gradually with progressive depolarization until it reached a maximum at about +10 mV. Generally, a plot of the membrane potential versus the ratio of late phase to early phase showed very similar curves in the medial and lateral pathways (Fig.3-5). These results showed that the effects of membrane potential changes on responses to medial and lateral pathway stimulation were very similar, suggesting the same ratio of AMPA and NMDA receptors at the synapses.

The peak and the late phase of the EPSCs were reduced by the specific NMDA receptor blocker D-APV (25 μM) (Fig.3-6B,C) in both pathways. Subtraction of the traces obtained before and after application of D-APV yielded a difference curve which had a

Figure 3-4 Voltage-clamp responses in lateral and medial perforant pathway under different membrane potentials. **A**. Sample traces of lateral and medial pathway responses held at different membrane potentials. Asterisk indicates the response peak measurement. Dashed line indicates 15 ms after stimulation when the late response was measured. **B**. The response peak measurement plotted against different holding potentials. The lateral and medial pathway responses had similar curve shapes. Note that the I-V curve is not linear. **C**. The late response plotted against different membrane potentials. Near the resting membrane potential of about 70 mV, the late response size was very small; however, the response size increased when the membrane potential was held at more depolarized levels. This late current peaked at -10 mV and reversed at +20 mV; these values were similar to the characteristics of NMDA current.

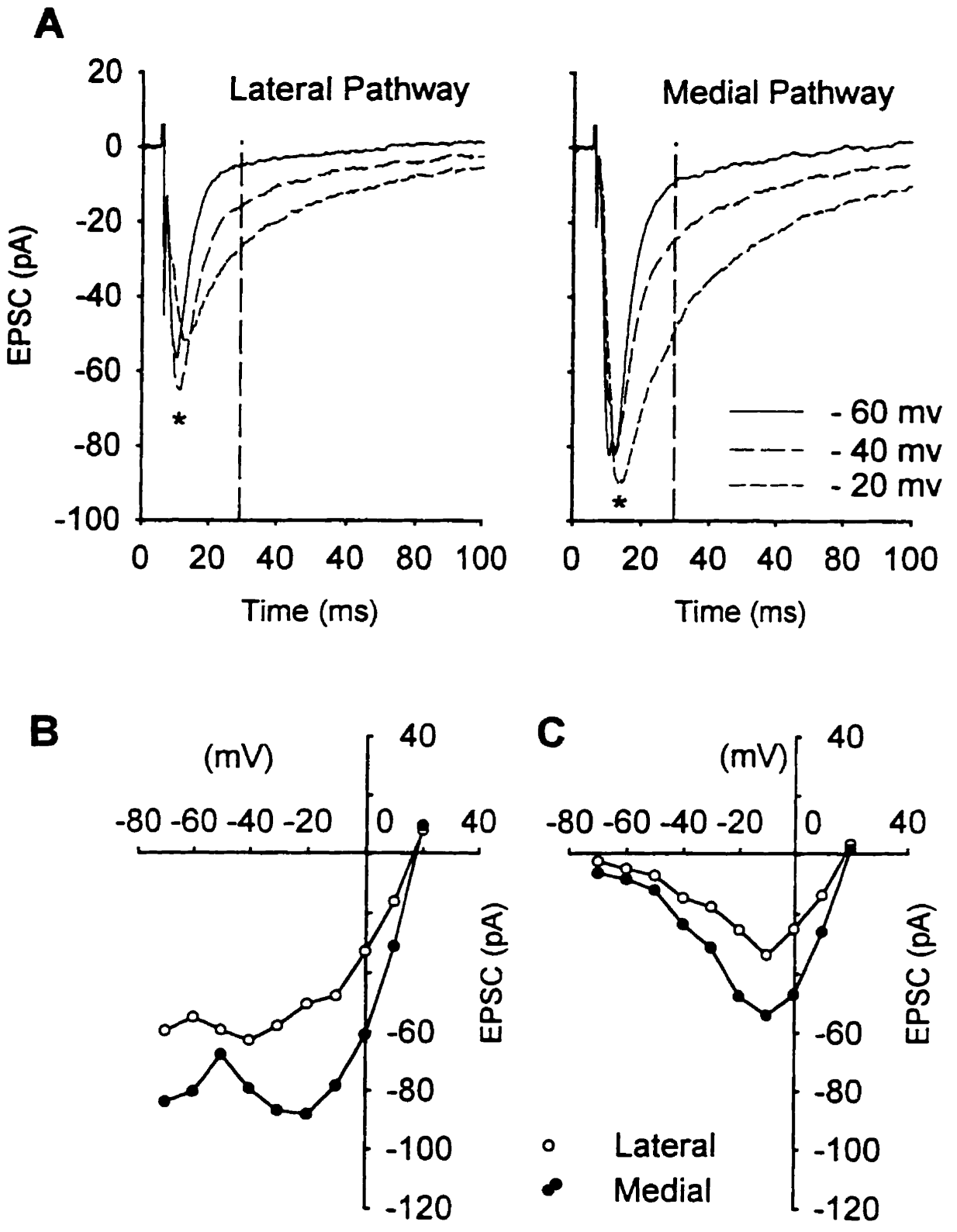
A
Lateral Pathway
Medial Pathway
EPSC (pA)
20
0
-20
-40
-60
-80
-100
0 20 40 40 80 100
Time (ms)
- 60 mv
- 40 mv
- 20 mv
B
C
(mV)
40
-80 -60 -40 -20
0
40
-60
-80
-100
-120
Lateral
Medial

Figure 3-5 The ratio of late response to peak response (late/peak) at various membrane potential measured in a single, representative experiment. This ratio is an estimation of the relative proportion of NMDA to AMPA currents (0% means pure AMPA current; 50% means 1:1 NMDA and AMPA; 100% means pure NMDA current). Clearly, the ratio is voltage dependent i.e. when membrane is depolarized, the contribution of NMDA component becomes larger. The medial and lateral pathway showed no significant difference in these ratios.

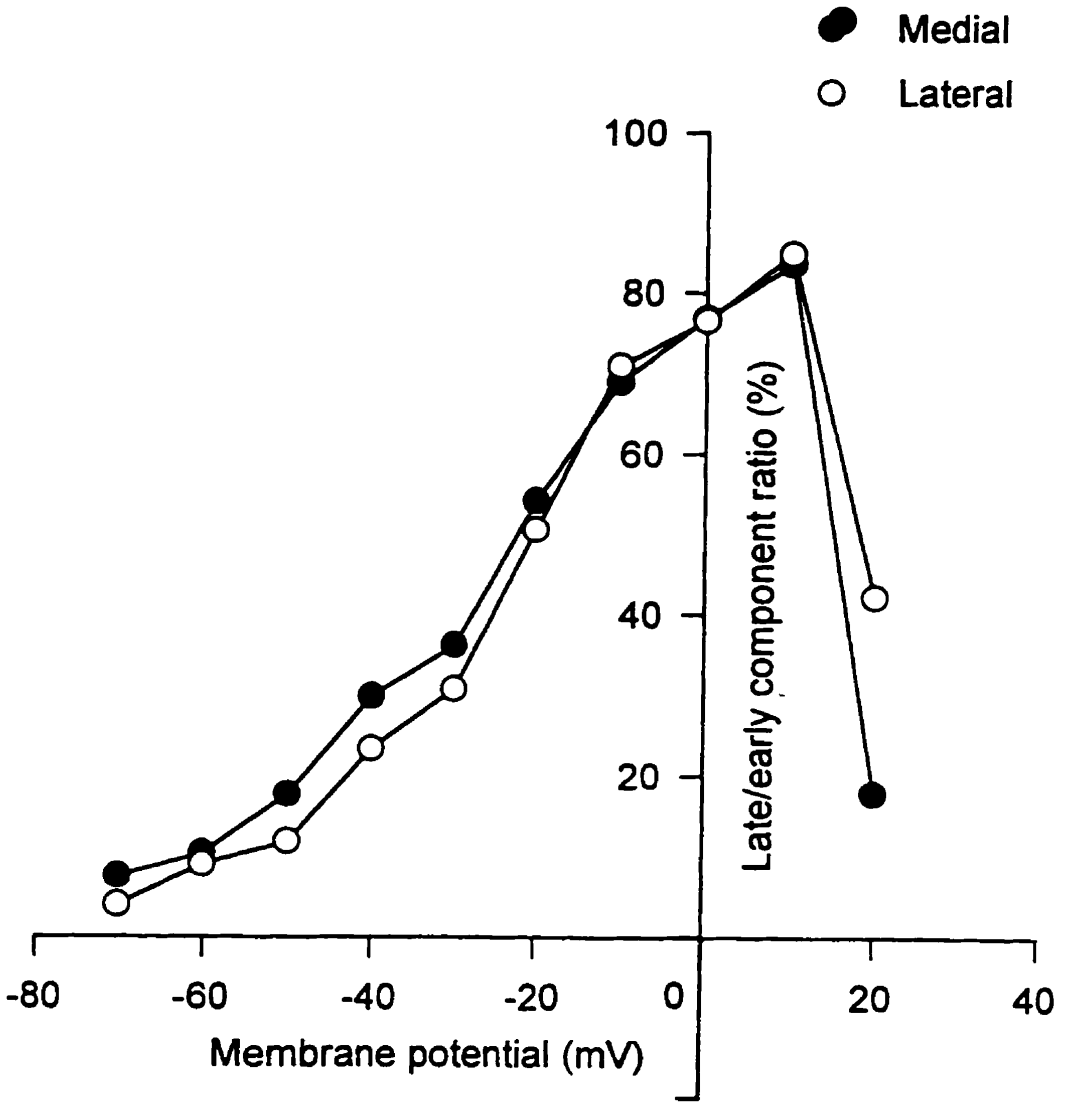
Medial
Lateral
100
80
60
40
20
Late/early component ratio (%)
-80
-60
-40
-20
0
20
40
Membrane potential (mV)

Figure 3-6 The NMDA component of the medial and lateral pathway responses. **A.** Sample traces from a voltage clamped cell held at -70 mV. NMDA receptor blocker D-APV reduced both the peak currents (indicated by asterisks) and the late currents (indicated by arrows). The blocked current (thick black lines) was demonstrated by subtracting the remaining current in D-APV from the control current. **B.** Plot of the percentage change of peak current in response to 25 μM D-APV. **C.** The late current change during D-APV application. Late current was measured 25 ms after stimulation started and was almost totally abolished by D-APV.

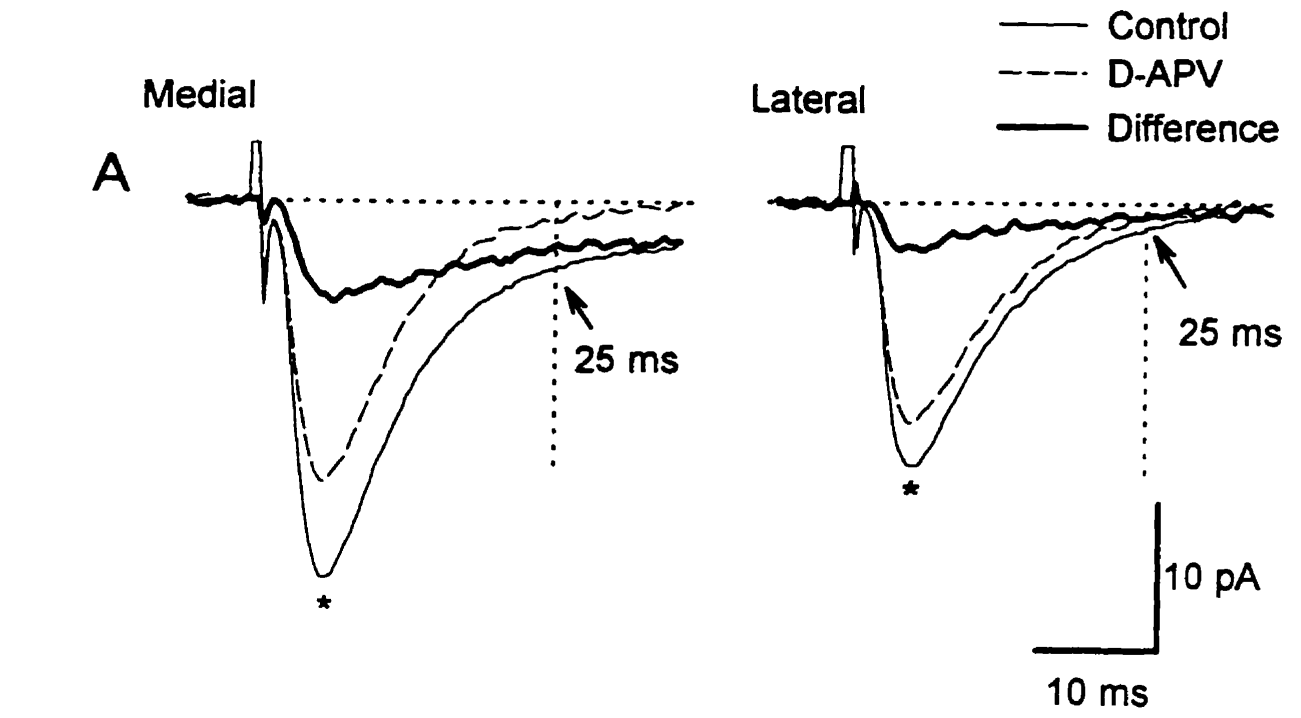
Control
D-APV
Difference
A
Medial
Lateral
25 ms
25 ms
10 pA
10 ms

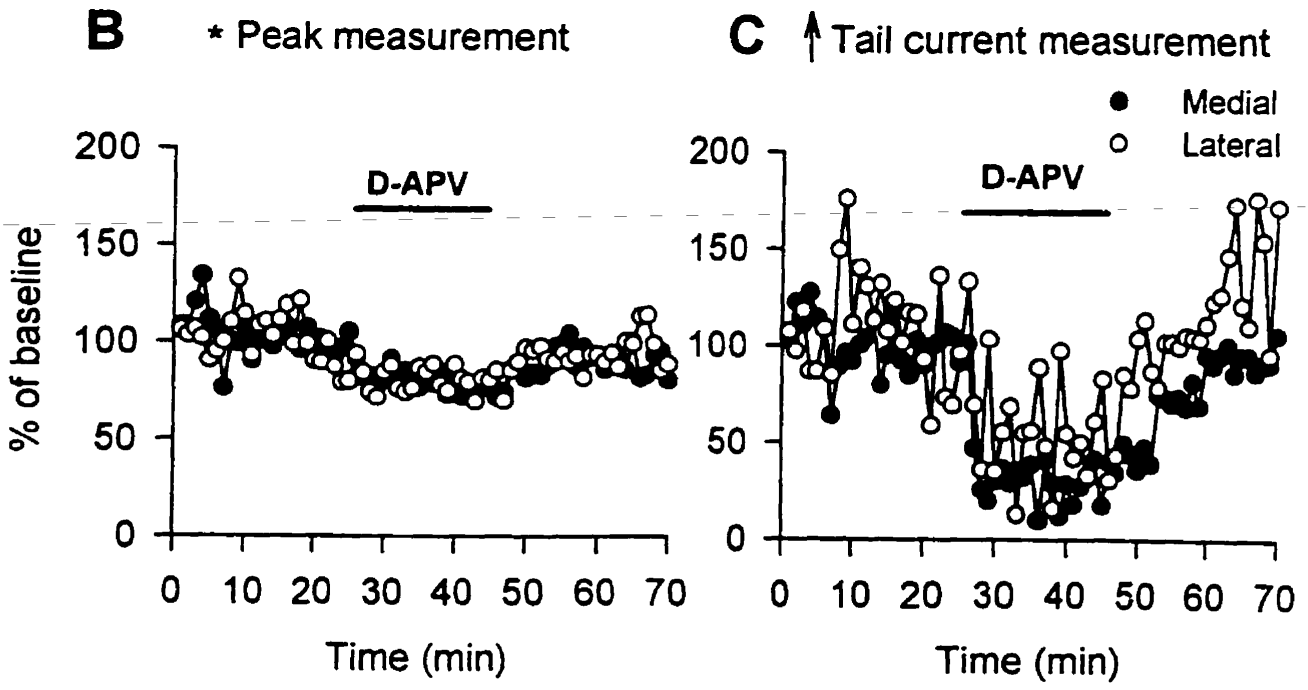
B
* Peak measurement
C
Tail current measurement
Medial
Lateral
D-APV
D-APV
% of baseline
200
150
100
50
0
0 10 20 30 40 50 60 70
Time (min)

long-lasting tail (Fig.3-6A). The slow decay time of this current is consistent with the involvement of NMDA type of glutamate receptors in the EPSCs. A similar type of current could be obtained with application of CNQX (5-10 μM), an AMPA receptor blocker which blocked only the peak current (Fig.3-7). In the presence of CNQX, the contribution of the NMDA component to the EPSC by peak measurement in the medial pathway was 15.1 ± 6.5% (s.d., n=8) and in the lateral pathway, 13.8 ± 6.3% (s.d., n=8). The residual current during CNQX application could be blocked by D-APV, indicating that this current was mediated by NMDA receptors (Fig. 3-7C).

The rise time of the NMDA EPSC was voltage-dependent. The average 10%-90% rise times in the presence of CNQX, at -60 mV were 2.50 ± 1.05 ms (s.d., n=5) in the medial pathway and 3.10 ± 0.8 ms (s.d., n=5) in the lateral pathway (Fig 3-7B). These values were significantly different from the rise time seen at -20 mV (5.88 ± 1.10 ms in the medial and 6.50 ± 2.10 ms in the lateral pathway)(Fig.3-7B).

3.2.3 Metabotropic glutamate receptors

The other major glutamate receptor subgroup, the metabotropic receptors are coupled to G proteins and various second messenger systems. I used the cyclic glutamate analogues 1-aminocyclopentane-1SR,3RS-carboxylic acid (t-ACPD) and L(+)-2-amino-4-phosphonobutyric acid (L-AP4) to specifically activate metabotropic receptors and examine their effects on synaptic transmission in the two pathways. t-ACPD is an agonist for mGluR1, mGluR2, mGluR3, and mGluR5 receptor subtypes while L-AP4 is agonist for mGluR4, mGluR6 and mGluR7 subtypes (Watkins and Collingridge, 1994).

Figure 3-7 Isolated NMDA currents in lateral and medial pathways. **A**. Sample whole-cell voltage clamp traces showing control responses and the remaining responses after 10 μM CNQX application. **B**. The remaining responses in CNQX showed voltage dependence. The responses increased with membrane depolarization. **C**. The remaining currents could be blocked by 25 μM D-APV, thus indicating they were NMDA receptor-mediated currents. Both the lateral pathway and the medial pathway evoked responses had NMDA currents.

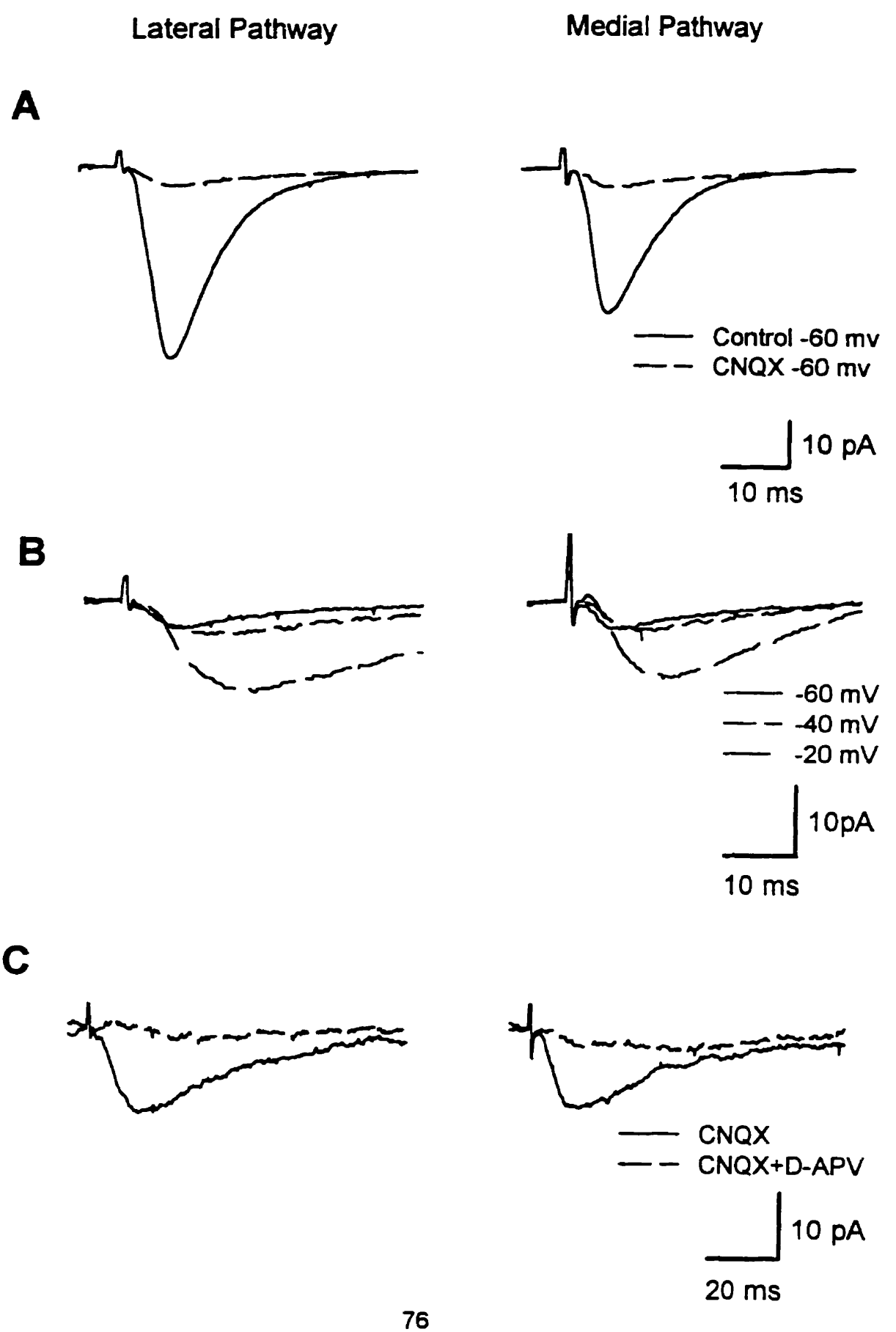
Lateral Pathway
Medial Pathway
A
Control -60 mv
CNQX -60 mv
10 pA
10 ms
B
-60 mV
-40 mV
-20 mV
10pA
10 ms
C
CNQX
CNQX+D-APV
10 pA
20 ms

Both t-ACPD and L-AP4 reduced the synaptic transmission. 50 μm trans-ACPD reduced the synaptic response to 54.5 ± 12.3% (n=8) of the baseline response in the medial pathway and to 52.3 ± 26.5% (n=8) in the lateral pathway (Fig.3-8). Thus, the effects of t-ACPD in the two pathways were similar. On the contrary, L-AP4 significantly reduced the response in the lateral pathway to 40.2 ± 12.3% of baseline response (Fig.3-9, n=11) but in the medial pathway, the response was only reduced to 80.2 ± 25.1% of the baseline value (Fig.3-9, n=11). Thus, there is a statistically significant ($p < 0.05$) preferential blockade of the lateral pathway response by L-AP4. A closer examination of the lateral pathway synaptic currents during L-AP4 perfusion revealed that the reduction of synaptic transmission is due to the increase of the number of cases where stimulation failed to induce a postsynaptic current. This "failed" response is usually considered as an indication of presynaptic terminal failure to release transmitter. Thus, the L-AP4 effect on the lateral pathway was likely due to a presynaptic mechanism. The difference in the response to L-AP4 application in the medial and the lateral pathway is one of the major differences between these pathways.

3.2.4 Opioid receptors

The terminal zone of the lateral pathway is characterized by a strong enkephalin-positive fiber plexus. Although it is believed that only the lateral pathway contains enkephalin or enkephalin-like peptide, the presence of opioid receptors in the medial pathway terminal area suggests that the opioid peptide released by the lateral pathway may diffuse to the medial pathway terminal region and exert its effect. When I applied

Figure 3-8 The effect of t-ACPD on synaptic transmission of medial and lateral perforant pathways. **A**. Sample traces obtained by field potential recordings before and after 50 μM t-ACPD application. **B**. Whole-cell voltage clamp recording traces showed a reduction of synaptic transmission by t-ACPD application (dashed line). The first response of each trace was evoked by lateral pathway stimulation whereas the second response was evoked by medial pathway stimulation. **C**. The effects of t-ACPD on the medial and lateral pathway responses were similar. The averaged results from eight experiments showed that the medial pathway synaptic responses were reduced to 54.5 ± 12.3% (S.D., n=8) of the baseline, and the lateral pathway responses were reduced to 52.3 ± 26.5% (S.D., n=8) of the baseline. The error bars on the graph indicates standard error (** , paired student t-test $P < 0.01$).

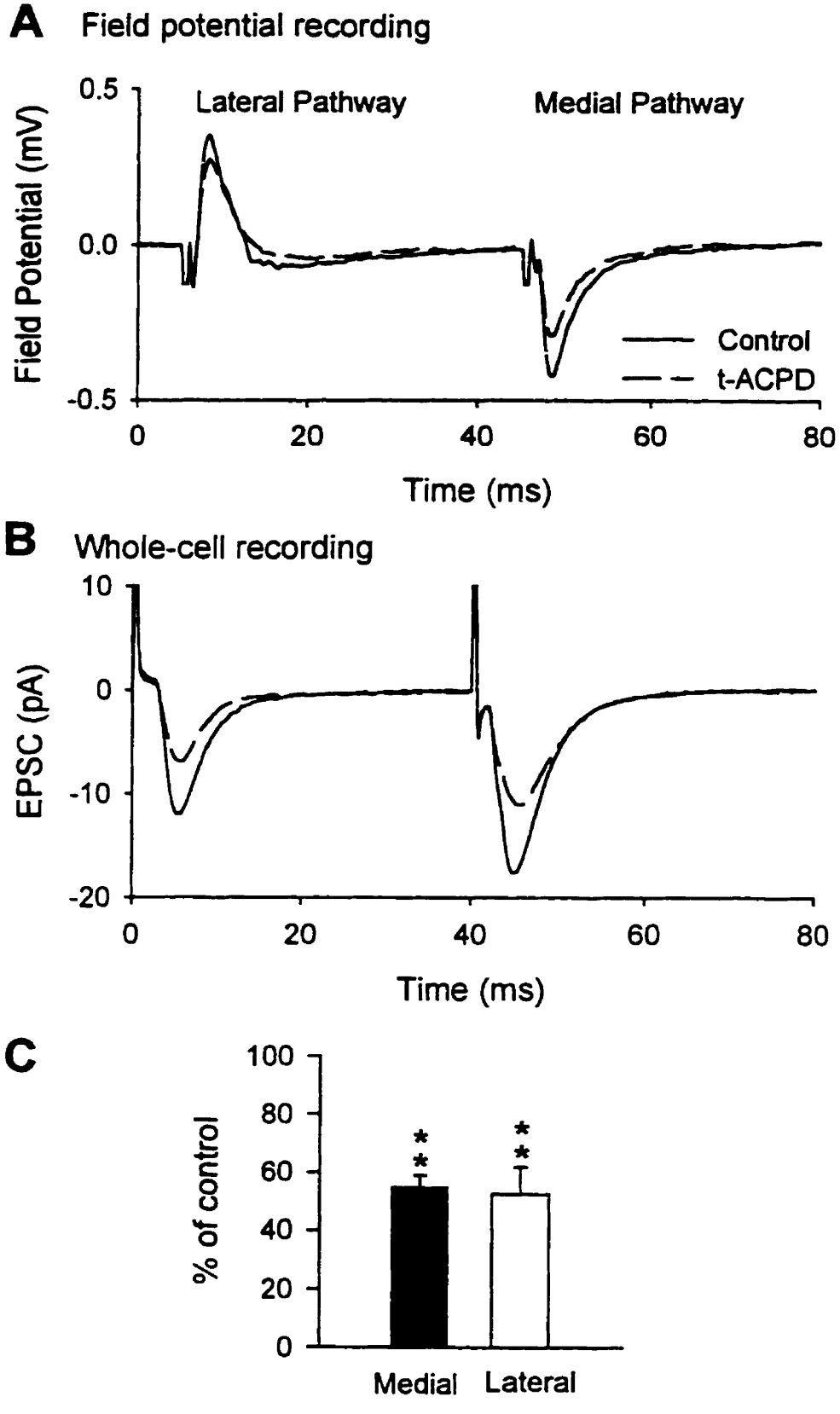
A
Field potential recording
Lateral Pathway
Medial Pathway
Field Potential (mV)
0.5
0.0
-0.5
Control
t-ACPD
0
20
40
60
80
Time (ms)
B
Whole-cell recording
EPSC (pA)
10
0
-10
-20
0
20
40
60
80
Time (ms)
C
% of control
100
80
60
40
20
0
Medial
Lateral

Figure 3-9 Effect of L-AP4 on synaptic transmission in the medial and lateral perforant pathways. **A**. An example of field potential recording experiment showing that the lateral pathway response was drastically reduced by 20 μM L-AP4 while the medial pathway response was minimally affected. **B**. In the whole-cell recordings the lateral pathway response was also preferentially reduced by L-AP4. The traces were obtained from a single granule cell and the first response was evoked by medial pathway stimulation; the second response was evoked by lateral pathway stimulation. **C**. The averaged results from eleven experiments showed that the lateral pathway responses were reduced to 40.2 ± 12.3 % (S.D., n=11) of the baseline whereas the medial responses were reduced to 80.2 ± 25.1 % (S.D., n=11) of the baseline. Standard errors are indicated (*, paired student t-test $P < 0.05$; **, paired student t-test $P < 0.01$).

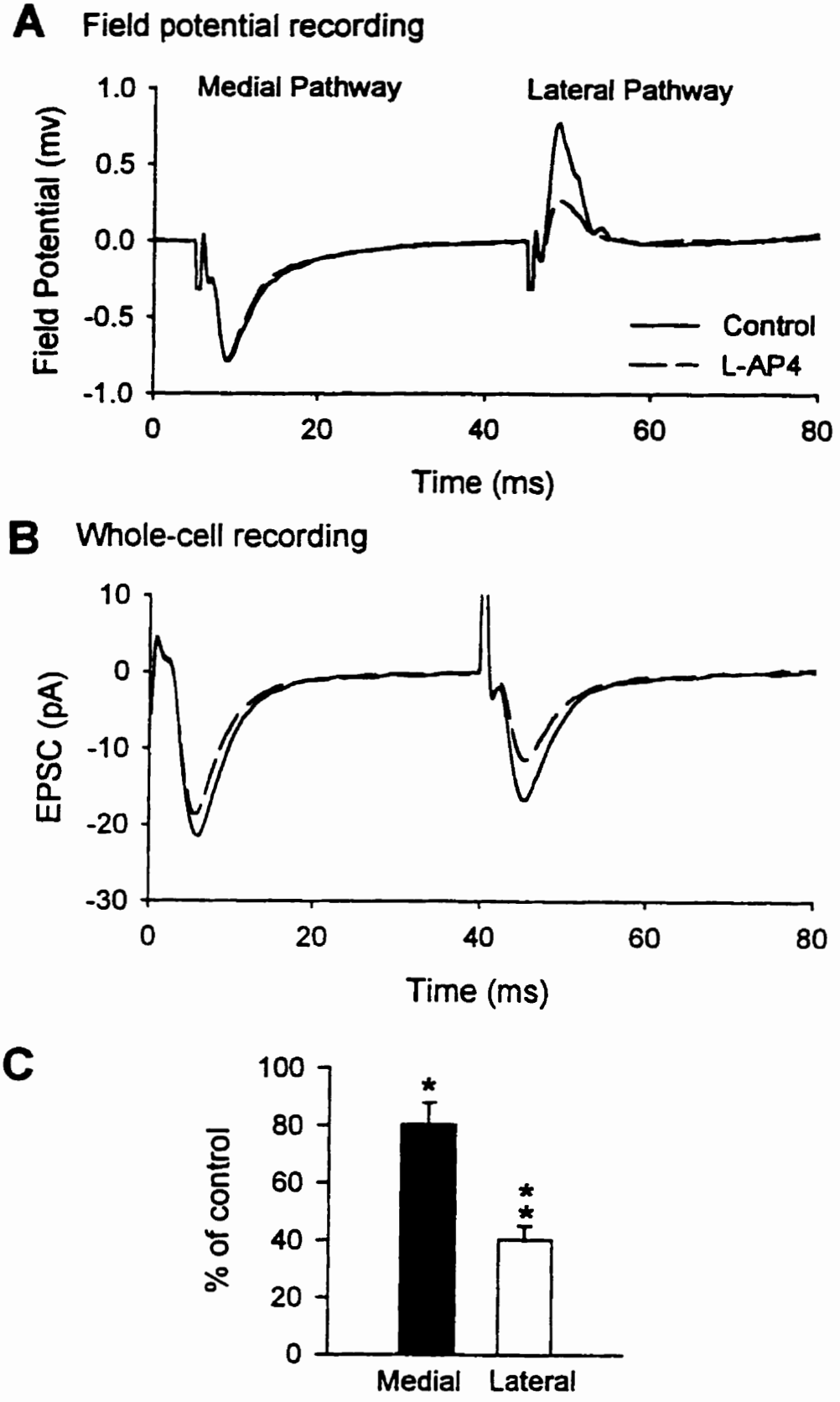
A
Field potential recording
Medial Pathway
Lateral Pathway
Field Potential (mv)
1.0
0.5
0.0
-0.5
-1.0
Control
L-AP4
0
20
40
60
80
Time (ms)
B
Whole-cell recording
EPSC (pA)
10
0
-10
-20
-30
0
20
40
60
80
Time (ms)
C
% of control
100
80
60
40
20
0
*
**
Medial
Lateral

the general opioid receptor blocker naloxone (2 μM) and monitored the changes in the synaptic transmission in the two pathways, naloxone had little effect on either lateral or medial pathway responses (medial 102.2 ± 10.2%, n=7; lateral 104.9 ± 9.9%, n=7, data obtained by field recordings and not illustrated). This indicated that during low frequency stimulation, there was no detectable opioid peptide mediated responses. In order to test whether opioid peptide was released during high frequency stimulation and whether it has any effect on lateral pathway LTP, I perfused the slice with 2 μM naloxone for 10 mins then applied high frequency tetanic stimulation to the lateral pathway. The lateral pathway LTP induced during naloxone perfusion was compared with LTP induced in normal medium (Fig. 3-10). The results showed that there was no difference in the magnitude of LTP induced in these two conditions (Fig. 3-10). Thus, either opioid peptide was not released during tetanic stimulation, or it was released but had no effect on lateral pathway LTP.

The effect of opioid peptide on medial pathway responses was tested by applying met-enkephalin exogenously. In the medial pathway, five minutes after enkephalin perfusion, the response size was 103.7 ± 8.4% of the baseline response taken immediately before enkephalin perfusion started. In the lateral pathway, the response to enkephalin was 103.6 ± 3.8% of the baseline. Thus, enkephalin had no significant effect on low frequency synaptic transmission (0.1 Hz). However, enkephalin clearly enhanced the medial pathway LTP size when it was applied during the tetanization period (Fig.3-11). The medial LTP size increased from 108.8 ± 52.7% (S.D., n=18) in control experiments to 162.3 ± 77.2% (S.D., n=9) (unpaired *t*-test, $p < 0.05$) in experiments with

Figure 3-10 Naloxone has no effect on lateral pathway LTP. **A**. Lateral pathway LTP induced in normal medium. The results were obtained from 7 granule cells recorded under voltage-clamp configuration. EPSC amplitudes were measured and normalized as % of control baseline (measured 10 mins before tetanic stimulation). Arrow indicates the tetanic stimulation. Standard deviations are indicated by vertical bars. **B**. Lateral pathway LTP induced during naloxone perfusion (2 μM). Naloxone was perfused for 10 mins before tetanic stimulation and left on for another 3 mins after tetanic stimulation. Data obtained by voltage-clamp recordings from 5 granule cells. Horizontal bar indicates naloxone perfusion. Standard deviations are plotted. **C**. Summary bar graph of results from **A** and **B**. Results from naloxone experiments are indicated by "Nal". LTP was measured and averaged from responses 16-10 mins after tetanic stimulation. In control experiments (**A**), lateral pathway LTP was 200.1± 201.0% (S.D.) whereas in naloxone experiments, lateral pathway LTP was 173.5 ± 105.2% (S.D.). There was no difference in LTP magnitude induced in these two conditions (unpaired *t*-test $P > 0.07$). Vertical bars are standard errors.

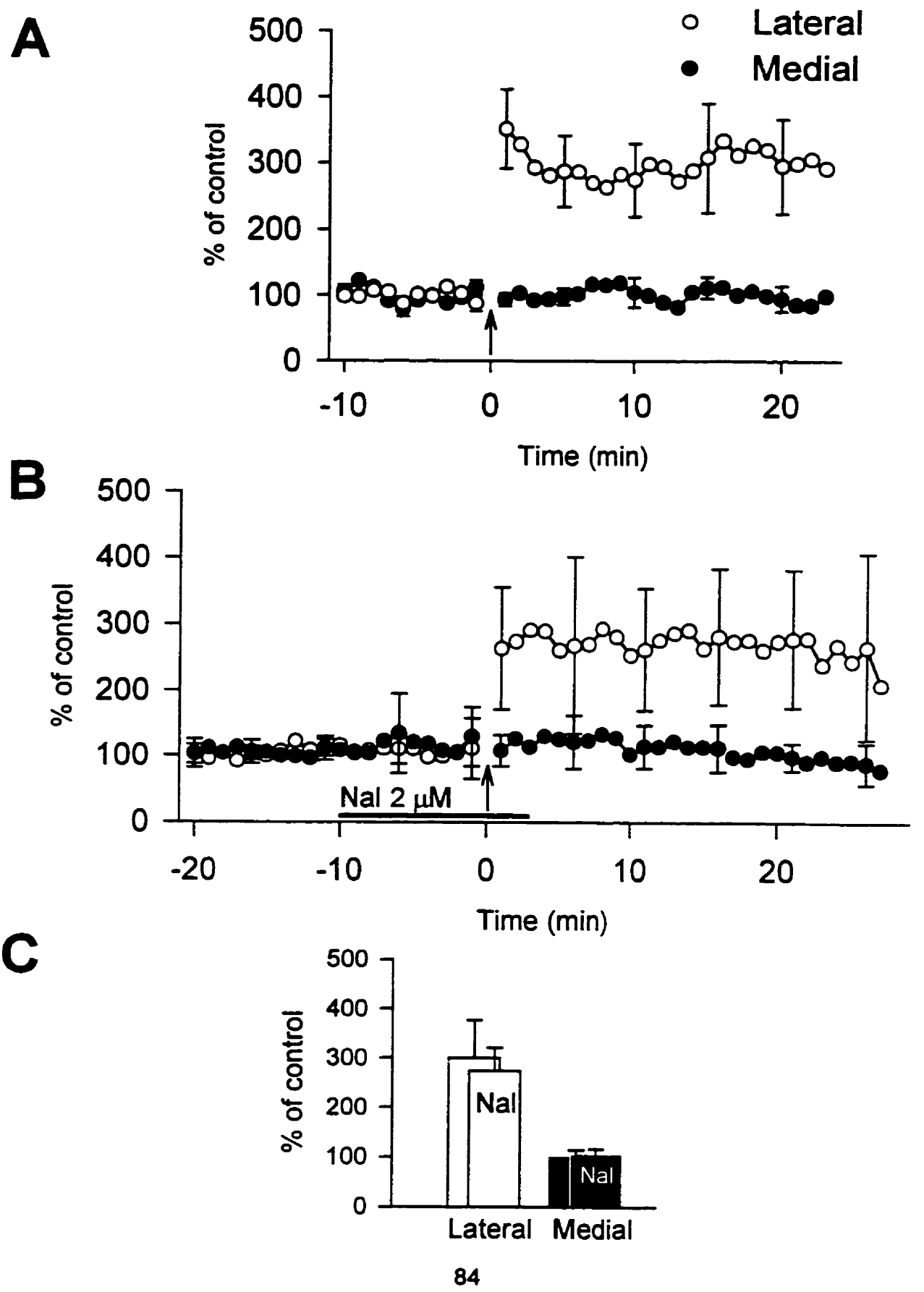
A
Lateral
Medial
500
400
300
200
100
0
% of control
-10
0
10
20
Time (min)
B
500
400
300
200
100
0
% of control
Nal 2 μM
-20
-10
0
10
20
Time (min)
C
500
400
300
200
100
0
% of control
Nal
Nal
Lateral
Medial

Figure 3-11 Effect of enkephalin on medial pathway LTP. **A**. Time course of medial pathway LTP in the presence of (filled circles) and without (filled squares) 2 μM enkephalin (Enk). Field potentials were used as a measure of synaptic responses. Vertical bars indicate standard errors. **B**. Bar graph plot of the response magnitude measured 16-20 minutes after LTP induction in the control experiments (208.8 ± 12.4% of baseline, S.E., n=18) and enkephalin experiments (262.3 ± 25.73% of baseline, S.E., n=9). LTP magnitude in enkephalin experiments was significantly larger than LTP magnitude in control experiments (unpaired t-test, $P < 0.05$).

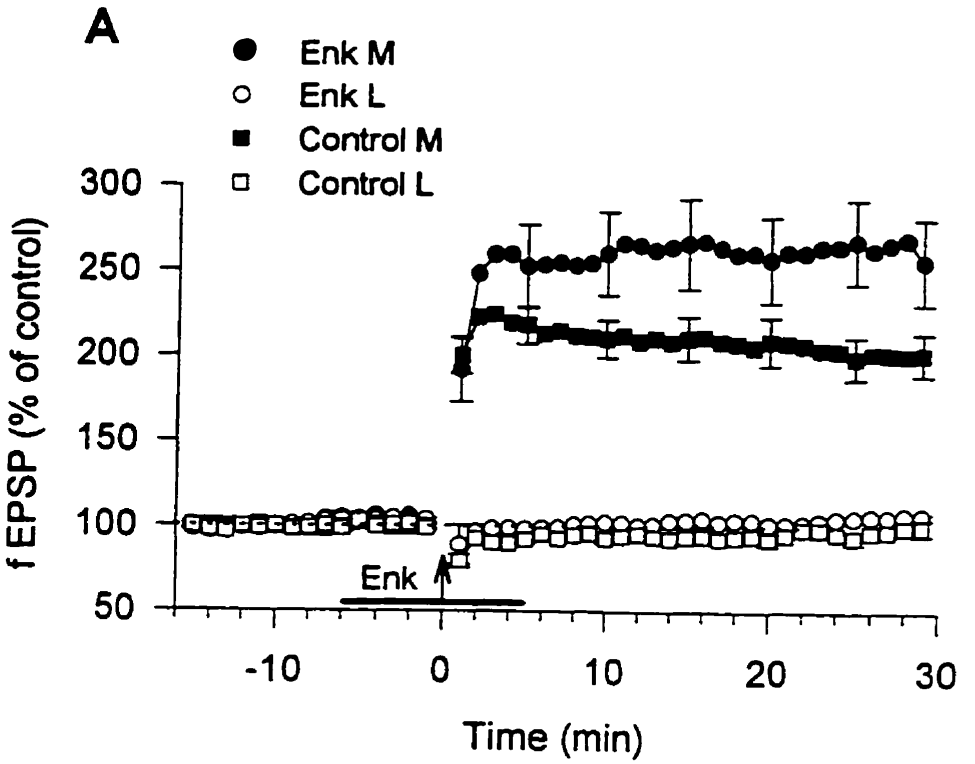
A
Enk M
Enk L
Control M
Control L
300
250
200
150
100
50
f EPSP (% of control)
Enk
-10
0
10
20
30
Time (min)

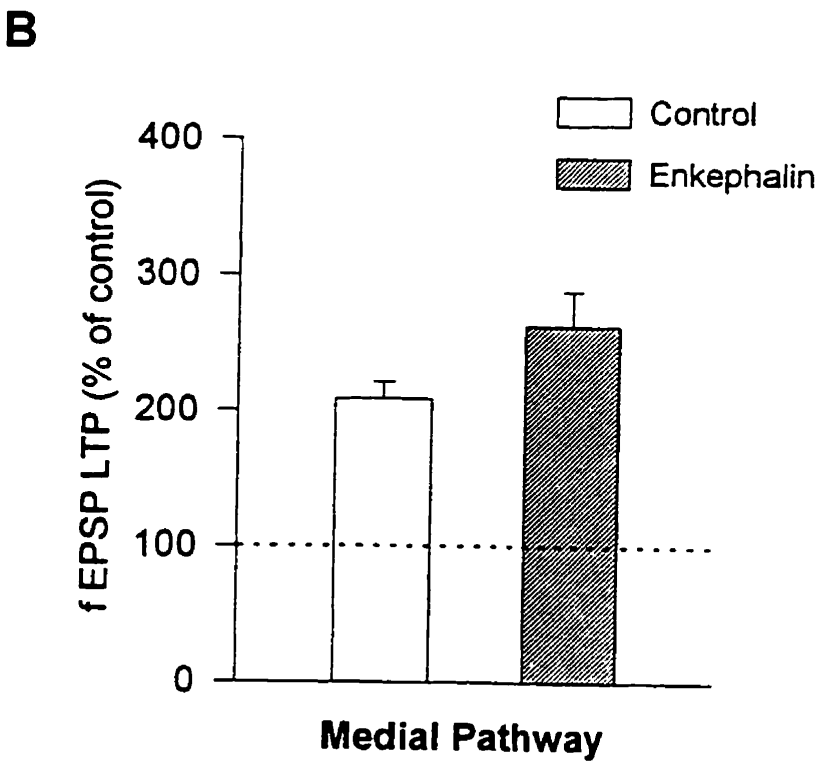
B
Control
Enkephalin
400
300
200
100
0
f EPSP LTP (% of control)
Medial Pathway

enkephalin perfusion. Nevertheless, a positive result from exogenously applied opioid peptide does not necessarily mean that the endogenous opioid peptide will have the same effect.

Although the results from naloxone experiments mentioned above (Fig. 3-10) showed no clear evidence that an opioid peptide was released by the lateral pathway during high frequency stimulation, there is still a possibililty that the released peptide exerts its effect on the nearby medial pathway terminal region. Thus, co-activation of both lateral and medial pathways with high-frequency stimulation could potentially release opioid peptides from the lateral pathway and affect the medial pathway LTP. On the other hand, perfusion of naloxone during co-activation should abolish any effect caused by the endogenous opioid peptide released by lateral pathway. The results from co-activation experiments are shown in Figure 3-12. Co-activation of both pathways produced larger LTP in the medial pathway while lateral pathway LTP remain unchanged (see Chapter 6, Table 6-I). However, this enhancement of medial LTP was not caused by opioid peptide released from lateral pathway because naloxone could not abolish this effect.

3.3 Discussion

The medial and the lateral perforant pathways originate from distinct parts of the entorhinal cortex. The medial entorhinal cortex gives rise to the medial pathway and the lateral entorhinal cortex give rise to the lateral perforant pathway. The medial and the

Figure 3-12 Co-activation of both medial and lateral pathway with high-frequency stimulation produced larger LTP in medial pathway. Perfusion of naloxone (2 μM) during co-activation had no effect on either medial or lateral pathway LTP. Data were obtained from 5 control experiments and 7 naloxone experiments using field potential recordings. Control: Medial LTP 167.2 ± 43.9% (S.D), Lateral LTP 86.8 ± 45.9% (S.D.); Naloxone: Medial LTP 197.0 ± 100.1% (S.D.), Lateral LTP 90.6 ± 56.3% (S.D.). On the graph, standard errors are shown by vertical bars.

Co-activation

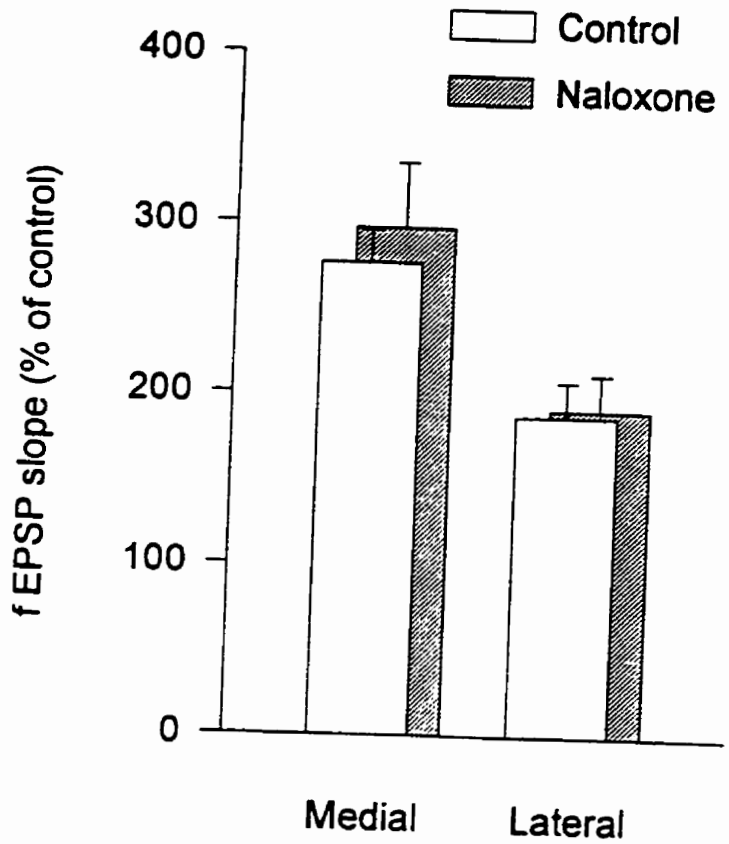

lateral entorhinal cortices are connected to different cortical areas. For example the medial entorhinal cortex has incoming fibers from the presubiculum and parasubiculum which contains highly processed visual inputs. The lateral entorhinal cortex receive predominately olfactory inputs from the lateral olfactory tract. Thus, the two divisions of the perforant pathway not only have different origins but also are different functionally.

The lateral perforant pathway terminates at the distal dendrites of the granule cell whereas the medial perforant pathway terminates at the middle region of the dendritic arborization. According to cable theory, the responses from the more distal synapses (lateral pathway) will have a slower rise time and decay time than the responses from the more proximal synapses (medial pathway). However, in the present study, only a difference in the rise time was observed in the responses from the lateral and medial pathways. Although the lateral pathway responses tend to have a longer decay time than the medial pathway responses, this comparison cannot reach a statistically significant level due to the large variation among the responses. One possible reason for the lack of difference in the decay phase is the compensatory mechanism consisting of faster kinetics of synaptic current in lateral perforant pathway.

3.3.1 High Frequency Depression

The medial pathway response depresses during repeated high frequency stimulation. This phenomenon had been observed in other synapses. For example, at the neuromuscular junction of a phasic motor neuron, a rapid depression of transmitter output was observed by repetitive stimulation (review Atwood and Wojtowicz, 1986). It

was suggested that the depletion of the readily available transmitter pool and relatively slow replenishment (lower supplies of energy from mitochondria and lower glutamate levels, Shupliakov et al., 1995) were responsible for the depression. At the tonic motor neuron of crayfish opener muscle, proximal synapses appear to release more neurotransmitter per impulse at low frequency stimulation and exhibit less short-term facilitation and more rapid depression under repetitive stimulation than distal synapses. These synapses are called "high-output" synapses in contrast to the distal "low-output" synapses (see review by Atwood and Wojtowicz, 1986). Ultrastructural study revealed that high-output synapses have a larger active zone per synapse than the low-output synapses (Atwood and Wojtowicz, 1986; Walrond et al., 1994). Quantal analysis revealed that these high-output synapses also have a high probability of transmitter release compared with distal low-output synapses (Cooper et al., 1996). The medial perforant pathway synapses certainly share some of the physiological properties of high-output synapses. On the other hand, lateral pathway synapses are more "depression-resistant". Although during repeated high-frequency stimulation the lateral pathway shows some depression eventually, it depresses less than the medial pathway for the same amount of stimulation. Whether the difference in high-frequency depression in perforant path synapses is correlated with their ultrastructure as observed in crayfish neuromuscular junctions is currently unknown. The physiological significance of the high-frequency depression is not clear; however, it could serve as a protective mechanism to prevent excitotoxicity caused by excessive Ca^{2+} entry to the postsynaptic neuron.

3.3.2 Ionotropic Glutamate Receptors

The NMDA current recorded in medial and lateral perforant pathway synapses showed an I-V curve which has a reversal potential around +10 mV. This is higher than the curve shown by others (Lambert and Jonse, 1990; Konnerth et al., 1990; Keller et al., 1991). However, the experimental conditions were not entirely comparable in the present and previous studies. In the Konnerth et al. (1990) and Keller et al. (1991) studies, the experiments were conducted at room temperature (21-24 °C) and the stimulated pathway was immediately adjacent to the granule cell layer. It had been shown by Petralia et al. (1994) that the NMDA GluR1 subunit is more densely distributed in the inner third of the molecular layer of dentate gyrus. Different subunit combinations will affect the channel properties. The NMDA receptor/channels in the inner third of the molecular layer could very well have different subunit combinations or subunit proportion differences than the NMDA receptor/channels in the outer two-thirds of the molecular layer where the perforant pathway terminates. Furthermore, Keller et al. (1991) reported that the NMDA current evoked by stimulating the inner third of the molecular layer contributed 23% of the peak current at resting membrane potential (eg. -60 to -70 mV). This value is slightly higher than that of the present study (medial pathway 15.1 ± 6.5%; lateral pathway 13.8 ± 6.3%). An NMDA sensitive L-[^{3}H]glutamate-binding method had shown that the inner molecular layer of the dentate gyrus has higher labelling than the outer molecular layer (Monaghan and Cotman, 1985). Unfortunately, in that study the molecular layer was divided into only the "inner" and "outer" halves; thus, the exact density of NMDA receptors in the inner third of the molecular layer is not known.

Although the different NMDA receptor density in different regions of molecular layer could account for the difference seen in the contribution of NMDA currents to peak EPSCs, it should be noted that this number is a ratio; thus, it also could be that the inner layer has less AMPA receptor mediated current instead of more NMDA receptor mediated current. Nevertheless, the medial and lateral pathways showed similar NMDA currents, which differs from a previous report stating that only the medial pathway has NMDA current (Dahl et al., 1990). My results are in agreement with those of Colino and Malenka (1994) who showed NMDA-dependent LTP in the lateral pathway but contradict the previous finding of Bramham et al. (1991b) indicating that NMDA receptor was not necessary for lateral pathway LTP.

3.3.3 Metabotropic Glutamate Receptors

The metabotropic glutamate receptor agonists t-ACPD and L-AP4 activate different subtypes of metabotropic glutamate receptors (Watkins and Collingridge, 1994). The active component of t-ACPD, 1S.3R-ACPD, is an agonist for mGluR1, mGluR2, mGluR3, and mGluR5 receptor subtypes while L-AP4 is agonist for mGluR4, mGluR6 and mGluR7 subtypes (Watkins and Collingridge, 1994). It is known that 1S.3R-ACPD has both presynaptic (Davies et al., 1993) and postsynaptic effects (Bashir et al., 1993) in hippocampal CA1 cells. The presynaptic effect was consistent with the present findings in the dentate gyrus granule cells i.e. through depression of transmitter release. In other regions of the hippocampal formation, 1S.3R-ACPD also has postsynaptic effects, i.e.

reduction of action potential accommodation and the ensuing afterhyperpolarization (Bashir et al., 1993).

The mechanism underlying the postsynaptic effect of 1S,3R-ACPD might be mediated by the activation of mGluR1 and/or mGluR5 receptors and blockade of a Ca^{2+} dependent K^+ current (Bashir et al., 1993; Watkins and Collingridge, 1994). In addition, mGluR1 and mGluR5 receptors are linked to the stimulation of phosphoinositide turnover (Houamed et al., 1991; Masu et al., 1991; Abe et al., 1992). It has been suggested by Futohi et al. (1994) that in the CA1 area it is mGluR5, linked to the IP3 receptor (through a pertussis-toxin insensitive G-protein), which mediates the PI-mediated Ca^{2+} release from internal store, required for the induction of LTP. On the other hand, the mechanism underlying the presynaptic effect of 1S,3R-ACPD might involve activation of mGluR2 (and/or mGluR3). It has been shown in motoneurons that agonists of mGluR2 (and/or mGluR3) receptors cause the presynaptically mediated depression of excitation (Ishida et al., 1993; Pook et al., 1992; Kemp et al., 1994), while MCPG ((RS)-α-methyl-4-carboxyphenylglycine), an antagonist at mGluR2 (Hayashi et al., 1994), blocks such synaptic depression (Kemp et al., 1994; Pook et al, 1992). This presynaptic depressive effect by metabotropic receptor activation suggests that glutamate can feed back and depress its own release.

In the medial and lateral perforant pathways, the effects of t-ACPD were very similar; thus, the negative feedback effect possibly mediated by mGluR2 (and/or mGluR3) receptors were similar in both pathways. However, the depression caused by L-AP4 application showed very different results in medial and lateral pathways. L-AP4

had a very strong depressive effect in the lateral pathway and a mild depressive effect in the medial pathway. Which metabotropic receptor subtype is mediating this depressive effect is less clear. Surprisingly, in neonatal rat motoneurons, MCPG, an mGluR2 antagonist (Hayashi et al., 1994), can antagonize the L-AP4-induced synaptic depression (Kemp et al., 1994; Pook et al., 1992). However, L-AP4 is not an agonist of mGluR2 (3). It was suggested by Watkins and Collingridge (1994) that among the three metabotropic glutamate receptor subtypes activated by L-AP4, mGluR4 can be excluded as the presynaptic receptor subtype mediating L-AP4-induced depression of neonatal rat motoneurons since MCPG is not an antagonist of L-glutamate-stimulated mGluR4 expressed in CHO cells (Hayashi et al., 1994). Whether this conclusion can hold for perforant pathways still awaits more experiments. It has been demonstrated by Trombley and Westbrook (1992) that in cultured olfactory bulb neurons, presynaptic L-AP4 receptors inhibit Ca^{2+} influx by a membrane-delimited action of a pertussis toxin-sensitive G-protein, and this effect may account for L-AP4-induced presynaptic inhibition. Whether this is the same mechanism underlying L-AP4-induced presynaptic depression in the lateral perforant pathway is less clear. However, it had been suggested that activation of presynaptic L-AP4 receptors can reduce Ca^{2+} influx into lateral perforant path presynaptic terminals (Harris and Cotman, 1983; Kahle and Cotman, 1993). From the above observations, it is clear that t-ACPD and L-AP4 act on different receptor subtypes. It seems that the lateral pathway, in addition to being regulated by the t-ACPD-activated negative feedback system, is also regulated by L-AP4-activated negative feedback system. Thus, synaptic transmission in the lateral pathway is more tightly regulated than

in the medial pathway.

The metabotropic receptors have been shown to be involved in LTP of the dentate gyrus in freely moving rats (Riedel et al., 1994; Riedel et al., 1995); in spatial learning (Riedel et al., 1994; Richter-Levin et al., 1994); in long-term memory consolidation (Rickard and Ng, 1995); and in depotentiation of LTP in CA1 (Bashir and Collingridge, 1994). However, there is also evidence indicating that activation of metabotropic receptors is not necessary for LTP induction (Manzoni et al., 1994; Brown et al., 1994; Hsia et al., 1995). A more recent report demonstrated that MCPG, a proposed mGluR2 receptor antagonist (Hayashi et al., 1994), failed to block LTP induced with either tetanic stimulation or theta-burst stimulation in CA1 pyramidal cells of rat hippocampus (Selig et al., 1995). Thus, mGluR2 receptors are not necessary for the induction of LTP. However, the roles of other MCPG-insensitive mGluRs in the induction of LTP still await further testing.

Although in this study I did not investigate the involvement of metabotropic receptors in perforant pathway LTP, certain suggestions can be made. The data showing that both pathways had similar responses to t-ACPD but different responses to L-AP4 argue against a significant involvement of the L-AP4 receptors in LTP because LTP was equal in the two pathways (see chapter 4). From the evidence provided above, this would rule out the involvement of mGluR4,6,and 7. Moreover, if there is no other regulation of L-AP4 activated metabotropic receptor during LTP, the prediction will be that during lateral pathway LTP expression, if LTP is mediated by more transmitter released from presynaptic terminals, we would expect that the L-AP4 receptor-mediated

negative feedback would be stronger than before LTP induction. This would limit the LTP magnitude of the lateral pathway. Theoretically, if LTP is mediated by increase in transmitter release, blocking of this negative feedback system in the lateral pathway should enhance LTP magnitude in this pathway. It would be interesting to test this hypothesis by applying newly developed potent and selective antagonists for presynaptic metabotropic glutamate receptors (RS)-α-methyl-4-phosphonophenylglycine (MPPG) or (RS)-α-methyl-4-sulphonophenylglycine (MSPG) (Jane et al., 1995) in potentiated lateral pathway.

3.3.4 Opioid Receptors

Although immuno-reactivity staining indicates that only the lateral pathway contains opioid peptide (enkephalin) (McLean et al., 1987; Fredens et al., 1984; Gall, et al., 1981), autoradiographic analysis shows that the three major opioid receptor subtypes, μ, δ, and κ are distributed throughout the molecular layer of the dentate gyrus. In the dentate gyrus molecular layer, μ receptors are the most abundant opioid receptors, followed by δ receptors, and finally κ receptors. While μ and κ receptors are particularly dense in the granule cell layer and adjacent zones on either side of it, δ receptors are preferentially distributed in the molecular layer (Crain et al., 1986; McLean et al., 1987; Plager and Vogt, 1988). The mismatch of transmitter releasing site and receptor locations seems perplexing. Herkenham and Mclean (1986) propose that the receptors, especially the receptors to which the endogenous ligand binds with high affinity, are not located at the synapses and may be sites of action of transmitters released from a distance. It is

possible that enkephalin released by lateral pathway diffuses to the medial pathway termination region and binds to the opioid receptors in that area.

From previous *in vivo* and *in vitro* studies, it was suggested that the major function of opioid peptides in the dentate gyrus is to "disinhibit" the granule cell (Wiesner et al., 1986; Wiesner and Henriksen, 1987; Neumaier et al., 1988; Xie and Lewis, 1991; Bramham, 1992; Piguet and North, 1993). Thus, the major site of action is on the inhibitory interneurons. However, this does not explain the function of the opioid receptors on granule cell dendrites. It has been shown that exogenously applied enkephalin or enkephalin analogue had no direct effect on membrane potential and resistance of granule cells (Haas and Ryall, 1980), although the excitability of granule cells is enhanced by activation of μ, δ, or κ opioid receptors with selective receptor agonists (Neumaier et al., 1988). Unfortunately, the inhibitory circuitry was intact in those experiments; thus, it is not clear whether this is a direct effect of the opioid peptide on granule cells or via disinhibition, or both.

I found that naloxone, a nonselective opioid receptor antagonist, has no effect on low frequency synaptic transmission between perforant pathway and granule cells in disinhibited preparation (Fig. 3-10; all experiments were done in 10 μM bicuculline to remove $GABA_A$ inhibition). This is consistent with previous findings (Tielen et al., 1981; Dunwiddie et al., 1982; Chavkin and Bloom, 1985). It is likely that opioid peptides are not released during low frequency stimulation (Caudle et al, 1991; Xie and Lewis, 1995). However, during high frequency stimulation, opioid peptides are presumably released. Naloxone had no visible effect on LTP induced in lateral pathway (Fig. 3-10). Thus, if

opioid peptide is released during high frequency stimulation, its site of action is probably not in the lateral pathway.

Exogenously applied met-enkephalin has no effect on low frequency synaptic transmission (Fig. 3-11). However, enkephalin clearly enhances the magnitude of LTP induced in the medial perforant pathway (Fig. 3-11). This enhancement might relate to increased cell excitability. The granule cells can produce more action potentials by the same stimulation during superfusion with enkephalin or enkephalin analogs (Neumaier et al., 1988; Xie and Lewis, 1991). The μ receptor agonist PL017 has been shown to facilitate the LTP of the population spike but did not show long-lasting effects on tetanus-induced potentiation of EPSP slope in the lateral pathway (Xie and Lewis, 1991). This enhancement in population spike is likely mediated by a disinhibition mechanism similar to the action of presynaptic $GABA_B$ receptors (Xie and Lewis, 1991). In addition, PL017 (1 μM) has been shown to enhance an NMDA receptor-mediated component in the single pulse-evoked field potential in the lateral pathway (Xie and Lewis, 1991). The enhancement in NMDA current could explain the larger LTP magnitude induced in the medial pathway during enkephalin perfusion. However, the same authors reported that PL017 at a higher concentration (3 μM) caused a 35% reduction in the amplitude of NMDA current in the granule cells (Xie et al., 1992). The authors suggest that at low concentrations the facilitatory effect of PL017 on NMDA current is the result of disinhibition; whereas at high concentration, PL017 has a genuine direct inhibitory effect on the NMDA current. Since the relative potency of PL017 compared with endogenous opioid peptides to μ receptors is not known, it is hard to grasp what, if any, is the opioid

peptide's effect on NMDA receptors at physiological concentrations.

Co-activation of both pathways produces larger LTP in the medial pathway while the lateral pathway LTP was not affected (Fig. 3-11, see also Chapter 6, Table 6-I). If this facilitation in the medial pathway were caused by opioid peptide diffusion from lateral pathway, pre-incubation of the slices with naloxone should abolish this effect. However, clearly this is not the case (Fig. 3-11). Thus, this facilitatory effect is not mediated by opioid peptide (this issue is further discussed in Chapter 6). The evidence presented thus far cannot prove that opioid peptide is released from the lateral pathway during tetanization. However, I cannot rule out the possibility that opioid peptide was released but had no effect on LTP of both lateral and medial pathway at physiological concentrations. Thus, the role of endogenous opioid peptides in excitatory synaptic transmission in the perforant pathway is still ambiguous.

4.1 Introduction

Long-term potentiation was discovered by Bliss and Lømo (1973) in the synapses between the perforant pathway and dentate gyrus granule cells in the rabbit brain. Subsequently this phenomenon has been shown to exist in the other two excitatory junctions of the trisynaptic circuitry of the hippocampal formation (CA1: Schwartzkroin and Wester, 1975; CA3: Alger and Teyler, 1976). However, the mechanisms of LTP induction and expression in these synapses are not uniform. A broad division can be made according to whether LTP induction requires the activation of the NMDA subtype of glutamate receptors. LTP of synapses between Schaffer collateral/commissural pathway and CA1 pyramidal cells and the synapses between perforant pathway and dentate granule cells depends on NMDA receptor activation and a subsequent rise in postsynaptic Ca^{2+} (Collingridge and Bliss, 1987; Bliss and Collingridge, 1993), whereas LTP of synapses between mossy fibers and CA3 pyramidal cells is independent of NMDA receptor activation but does require a rise in presynaptic Ca^{2+} (Harris and Cotman, 1986; Zalutsky and Nicoll, 1990).

Although the induction of LTP in the dentate gyrus and the CA1 region requires Ca^{2+} influx through postsynaptic NMDA receptors and a subsequent biochemical cascade to initiate LTP expression (for review see Nicoll and Malenka, 1995), the locus for LTP expression is still controversial. The persistent enhancement of synaptic transmission could result from an increase in neurotransmitter release, from an increased postsynaptic responsiveness to the released neurotransmitter, from addition of new synapses, or from

a combination of the three mechanisms.

4.1.1 Presynaptic vs. postsynaptic mechanisms for LTP expression

To resolve the problem of the locus of LTP expression, a number of different approaches have been employed. These approaches have included measurement of the amount of neurotransmitter released (Dolphin et al., 1982; Errington et al., 1983; Galley et al., 1993), and measurement of receptor sensitivity to the exogenously applied transmitter agonist before and after LTP induction (Lynch et al., 1977; Turner et al., 1982). However, neither of these methods provide conclusive evidence for either pre- or postsynaptic changes. The first method measures the transmitter released in the stimulated area, but has some sensitivity problems because the perfusion cannula which extracts the sample from the stimulated area is very large in comparison with the activated pathway. The collected transmitter could be released at the synapses between the stimulated pathway and target neurons, at synapses between the stimulated pathway and interneurons, or even released by the collateral axons of the stimulated neuron. Thus, an increase of collected neurotransmitter does not necessarily mean an increased release of transmitter at the synapses between the stimulated pathway and the target neurons. Furthermore, an increase in transmitter concentration does not necessarily mean that it will reach the postsynaptic receptors. The second method has a similar sensitivity problem, and in addition, desensitization of receptors is likely to occur.

Another popular, although controversial, approach has been to apply quantal analysis to the evoked synaptic responses (Voronin, 1993). In theory, if the synapses in

the central nervous system were exhibiting "quantal release", like the synapses at the neuromuscular junction, one could elucidate how quantal parameters change before and after LTP induction by using the quantal hypothesis which del Castilo and Katz (1954) first used in the frog neuromuscular junction to describe synaptic transmission. The change in quantal parameters can provide some insight into the locus of LTP expression. However, the application of quantal analysis to central nervous synapses has encountered many obstacles. The major problem is the validity of using the averaged, spontaneously released, miniature responses to estimate the mean quantal content (*m*). In the neuromuscular junction, the source of miniature responses is the same as the source of evoked responses, so *m* can be calculated from dividing averaged evoked response by averaged miniature response. However, in the central nervous system, these spontaneously released miniature responses could be generated anywhere along the dendritic tree of the neuron and not necessarily at the active synapses. Thus, the calculation of mean quantal content from averaged miniature events is an ambiguous method. Nevertheless, an attempt to use quantal analysis to investigate changes in quantal parameters during LTP was carried out in the present study and satisfactory results in the medial perforant pathway were obtained.

In this chapter, the main objective is to compare LTP in the medial and the lateral perforant pathways. A second objective is to investigate the possible mechanisms of LTP expression in the medial pathway by a quantal analysis method.

4.2 Results

4.2.1 LTP of the perforant pathway - extracellular field recordings

Local synaptic responses of the medial and the lateral perforant pathways were recorded by an extracellular field potential recording electrode placed in the medial pathway's terminal field. This recording configuration showed a current sink when the medial pathway was stimulated, and a current source when the lateral pathway was stimulated (see Chapter 2). Only the initial slope of the response was measured and used to quantify the synaptic response. Stimuli were applied every 10 seconds to both pathways. There was a 100 to 200 ms delay between the stimulation of the two pathways. In some experiments, stimulation of the lateral pathway preceded stimulation of the medial pathway, whereas in other experiments the reversed sequence was used. The different stimulation sequences were used to verify whether stimulation of the leading pathway had any influence on the response of the succeeding pathway. After a stable baseline had been acquired (> 10 mins), LTP was induced by high frequency tetanic stimulation in one of the two pathways at the test pulse strength. After application of this tetanic stimulus to one of the pathways, the stimulation pattern and frequency were returned to the ones used during the control period. The stimulation then continued for at least 20 more minutes to verify the establishment of LTP.

In the series of experiments where the medial pathway was tetanized, the medial pathway's responses potentiated to 208.8 ● 52.7 % (mean ± SD) of the control response (Fig.4-1A, n=18). In 6 of these 18 experiments, the medial pathway was the leading pathway and the averaged magnitude of the medial pathway LTP was 104.9 ± 44.6%

Figure 4-1 Comparison of field potential LTP in the medial and the lateral perforant pathways. **A**. Averaged LTP time course of the medial perforant pathway from 18 experiments. LTP was induced by tetanic stimulation as indicated by arrow at time 0. Note that immediately after medial pathway tetanization, the lateral pathway response showed heterosynaptic depression which lasted for only a few minutes. **B**. The time course of the lateral pathway LTP averaged from 13 experiments. After lateral pathway tetanization the medial pathway also showed heterosynaptic depression. **C**. The magnitude of potentiation, measured from responses 15-20 minutes after LTP induction was 208.8 ± 12.4% (mean ± SE, n=18) in the medial pathway and 190.0 ± 7.0% in the lateral pathway (**D**). Inset one shows a sample response during the control period (1) and inset two shows the potentiated response (2) in medial pathway (upper panel, recorded as current sink) and lateral pathway (lower panel, recorded as current source). • paired student t-test $P < 0.05$.

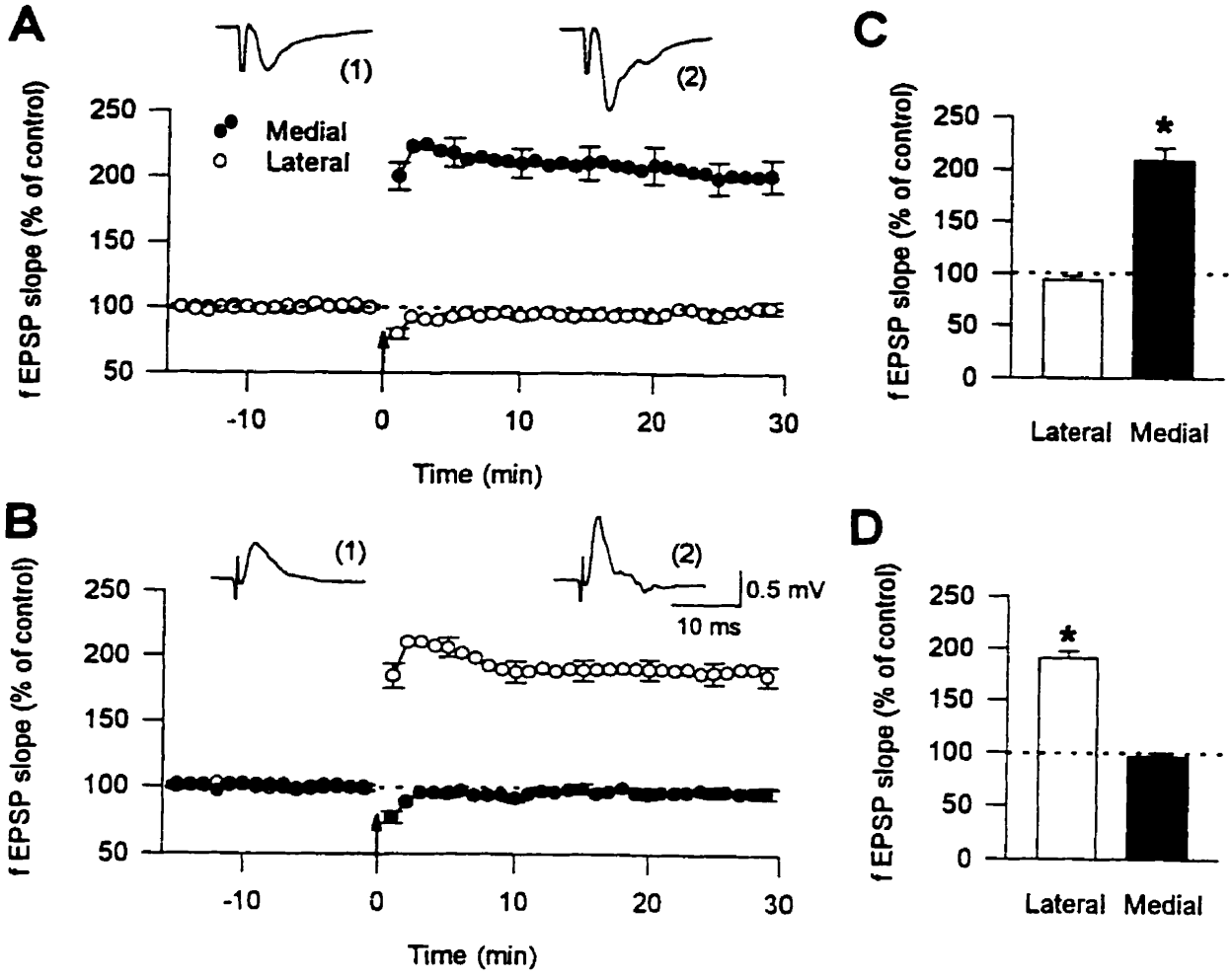
A
(1)
(2)
Medial
Lateral
f EPSP slope (% of control)
250
200
150
100
50
-10
0
10
20
30
Time (min)
C
f EPSP slope (% of control)
250
200
150
100
50
0
*
Lateral
Medial
B
(1)
(2)
0.5 mV
10 ms
f EPSP slope (% of control)
250
200
150
100
50
-10
0
10
20
30
Time (min)
D
f EPSP slope (% of control)
250
200
150
100
50
0
*
Lateral
Medial

above the control response. In the other 12 experiments the lateral pathway was leading and LTP was 110.7 ± 58.2% above control response. The sequence of stimulation does not appear to affect the size of the LTP (Figure 4-2). Immediately after medial pathway tetanization, the lateral pathway showed a heterosynaptic depression, and this depression lasted for only a few minutes (Fig.4-1).

LTP induced in the lateral pathway had an average magnitude of 189.8 ± 25.2 % (mean ± SD) of the control reponse (Fig.4-1B, n=17). Although the magnitude of LTP of the lateral pathway was smaller than the magnitude of the medial pathway LTP, the difference was not statistically significant. The sequence of stimulation, again, has no effect on the magnitude of LTP induced in the lateral pathway (Figure 4.-2). In the experiments where the lateral pathway was the leading pathway, the LTP magnitude was 186.0 ± 24.2% of control (n=10). When the medial pathway stimulation was leading the lateral pathway stimulation, the lateral pathway LTP was 188.1 ± 27.1%. After the lateral pathway tetanization, the medial pathway also showed a brief heterosynaptic depression.

The magnitude of LTP in the medial and the lateral pathway did not show any clear correlation with the age of the rat (Fig. 4-3). In the medial pathway the age of the rat and LTP magnitude was slightly negatively correlated, however, the correlation coefficient is a weak one (r = 0.19).

4.2.2 LTP of the perforant pathway - whole-cell recordings

Whole-cell recordings were used to further examine the properties of LTP in the medial and the lateral perforant pathways. Both current-clamp recordings and voltage-

clamp recordings were used. Before the establishment of whole-cell recordings, a field recording electrode was placed in the medial pathway terminal field to verify the separation of the pathways via the current source and sink method. After establishing the whole-cell voltage clamp recordings, the stimulation strength was further lowered to activate a minimum number of fibers and allow occasional synaptic transmission failure to occur. This minimum stimulation further ensured the independence of the stimulation to the two pathways, and the small number of activated axons simplified and facilitated quantal analysis.

Although in field potential recordings the success rate of inducing LTP in either pathway was close to 100%, in the whole-cell recording configuration the success rate of LTP induction was much lower. Different induction methods were used to induce LTP in the whole-cell current clamp and voltage clamp recordings. The most effective method in the voltage-clamp mode was to apply high frequency tetanic stimulation to the perforant pathway while artificially clamping the cell to -20 mV during the tetanic stimulation. The success rates of LTP induction by different methods under current clamp configuration are presented in Table 4-1. Afferent stimulation alone was not very effective in inducing LTP in either the medial or the lateral pathways. Pairing the afferent stimulation with postsynaptic depolarization is a more efficient way to induce LTP. Under the voltage clamp condition, three different methods were used to induce LTP. The success rates for different induction methods are presented in Table 4-2.

In the whole cell voltage clamp condition, when presynaptic tetanic stimulation was paired with postsynaptic depolarization, the medial pathway LTP ranged from 135.0% to

Figure 4-2 Comparison of LTP of field potential induced by different stimulation sequences. The LTP magnitude in the lateral pathway stimulation followed 100-200 ms later by the medial pathway stimulation sequence (LM series) and the reversed stimulation sequence (ML series) are compared. **A**. In medial pathway, the LTP induced in the LM stimulation sequence is 210.7 ± 58.2% and in the ML sequence is 205.0 ± 44.6% (mean ± SD). **B**. In the lateral pathway, the LTP induced in the LM series is 186.0 ± 24.2% while in the ML series LTP is 188.1 ± 27.1% (mean ± SD). The magnitudes of LTP induced in the different stimulation sequences (LM series and ML series) are not statistically significant in either medial pathway or lateral pathway ($P > 0.05$).

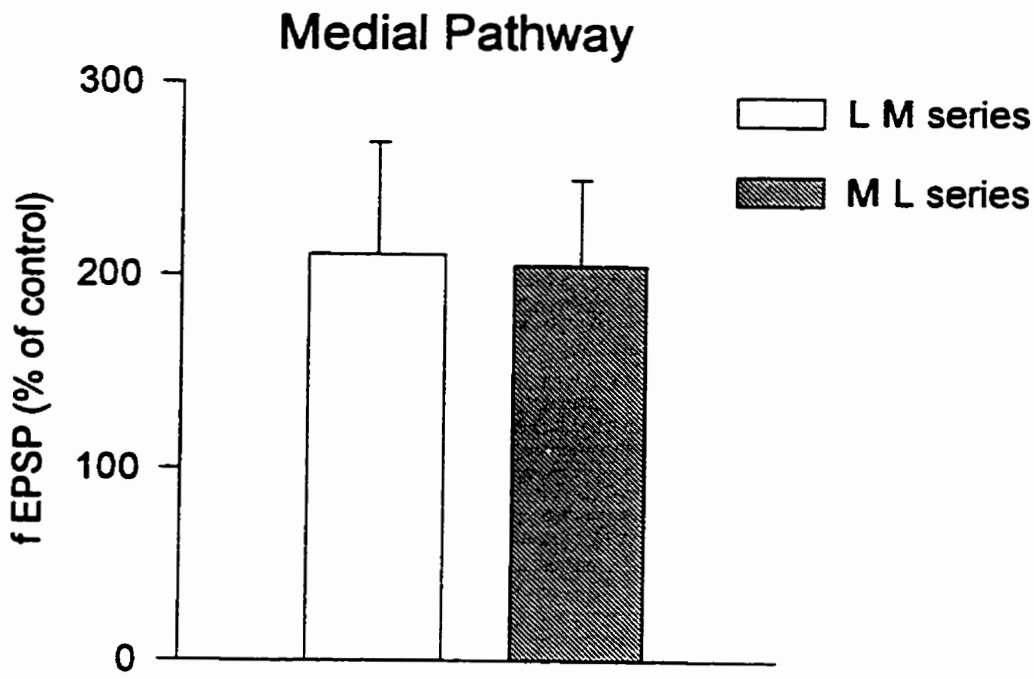
Medial Pathway
300
200
100
0
f EPSP (% of control)
L M series
M L series

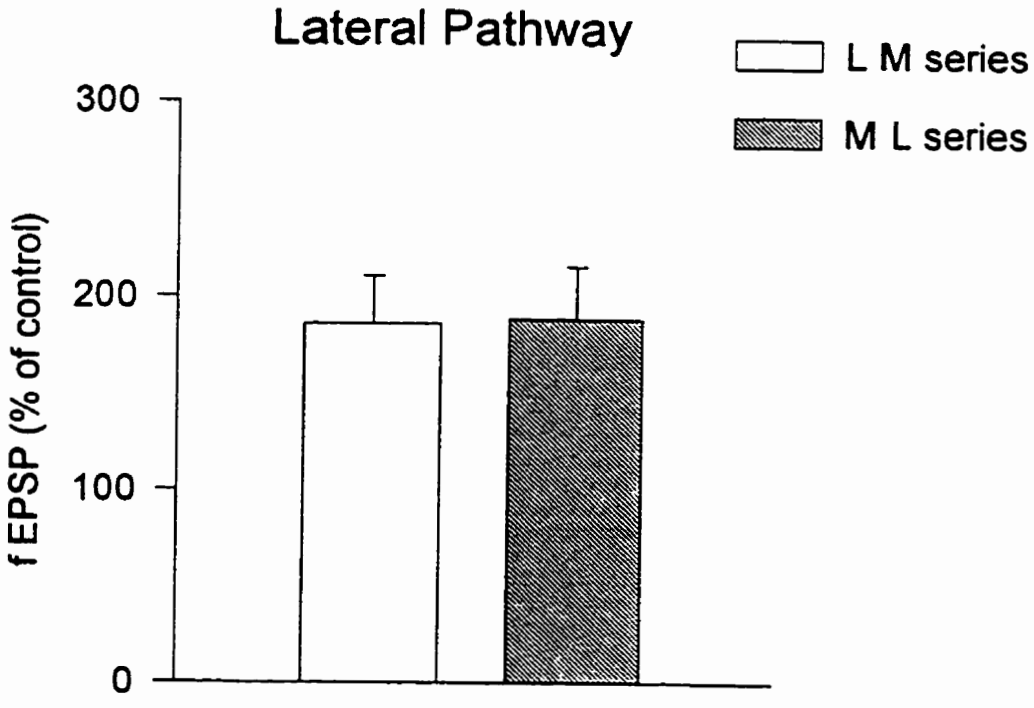
Lateral Pathway
300
200
100
0
f EPSP (% of control)
L M series
M L series

Figure 4-3 Correlation of LTP magnitude and rat age. The age of the rat is plotted against the LTP magnitude induced in the medial and the lateral pathways. In the medial pathway (filled circle), the LTP magnitude has a slight tendency to be negatively correlated with age (solid regression line). However, the correlation coefficient was $r = 0.19$, which is not considered to be a strong correlation. In the lateral pathway (open circle), the age has no effect on the LTP magnitude as can be seen in the horizontal regression line (dash line, correlation coefficient $r = 0.05$).

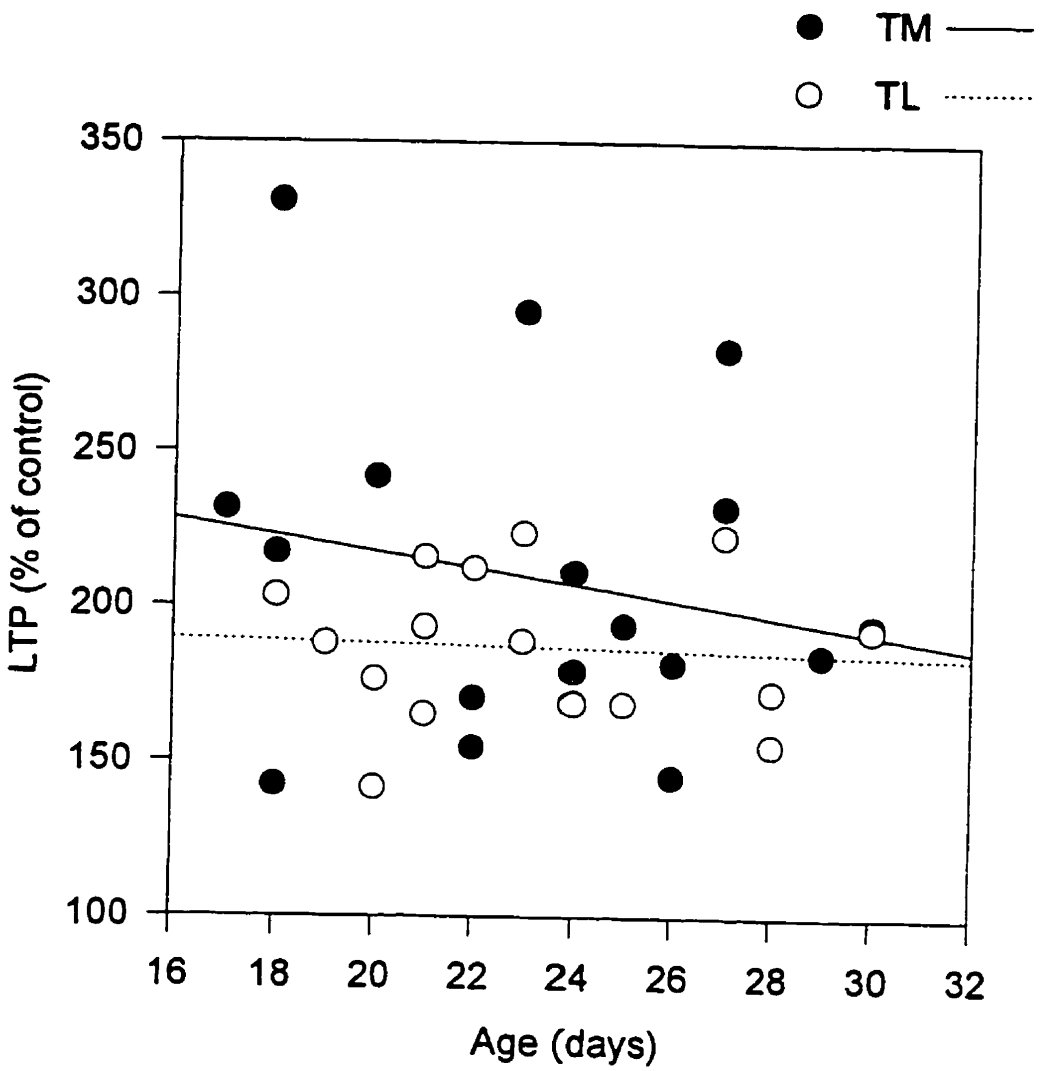
TM
TL
350
300
250
200
150
100
LTP (% of control)
16
18
20
22
24
26
28
30
32
Age (days)

Table 4-1 Induction of LTP in the medial and the lateral perforant pathways under current-clamp

Method of Induction	Success Rate	
	Medial pathway	Lateral pathway
Afferent stimulation (100 Hz, 1s, 4X)	6/17 cells (35%)	2/4 cells (50%)
Afferent stimulation paired with postsynaptic depolarization (100 Hz, 0.5s, 4X, -20 mV)	3/4 cells (75%)	1/1 cells (100%)

Table 4-2 Induction of LTP in the medial and the lateral perforant pathways under voltage-clamp

Method of Induction	Success Rate	
	Medial pathway	Lateral pathway
Afferent stimulation (100 Hz, 1s, 2X)	1/10 cells (10%)	1/7 cells (14%)
Afferent stimulation paired with postsynaptic depolarization (100 Hz, 1s, 2X, -20 mV)	2/8 cells (25%)	1/7 cells (14%)
Afferent stimulation paired with postsynaptic depolarization (100 Hz, 0.5s, 4X, -20 mV)	9/18 cells (50%)	7/20 cells (35%)

Figure 4-4 LTP induced in the medial and lateral perforant pathway under whole-cell voltage clamp configuration. **A**. The time course of medial pathway LTP (filled circle) averaged from 11 cells. Arrow at time 0 indicates the application of tetanic stimulation paired with the postsynaptic cell artificially clamped to -20 mV. Standard error bars are shown for every fifth data point for clarity. The lateral pathway (open circle) showed little potentiation after medial pathway tetanization. **B**. The lateral pathway LTP time course averaged from 7 cells. The averaged magnitude of LTP measured from responses 16-20 minutes after induction are shown in bar graph **C** and **D**. **C**. The averaged magnitude of medial pathway LTP is 350.2 ± 248.5 % (mean ± SD, n=11) of control response. **D**. The averaged LTP of lateral pathway is 300.1± 201.0 % (mean ± SD, n=7). * paired student t-test $P < 0.05$.

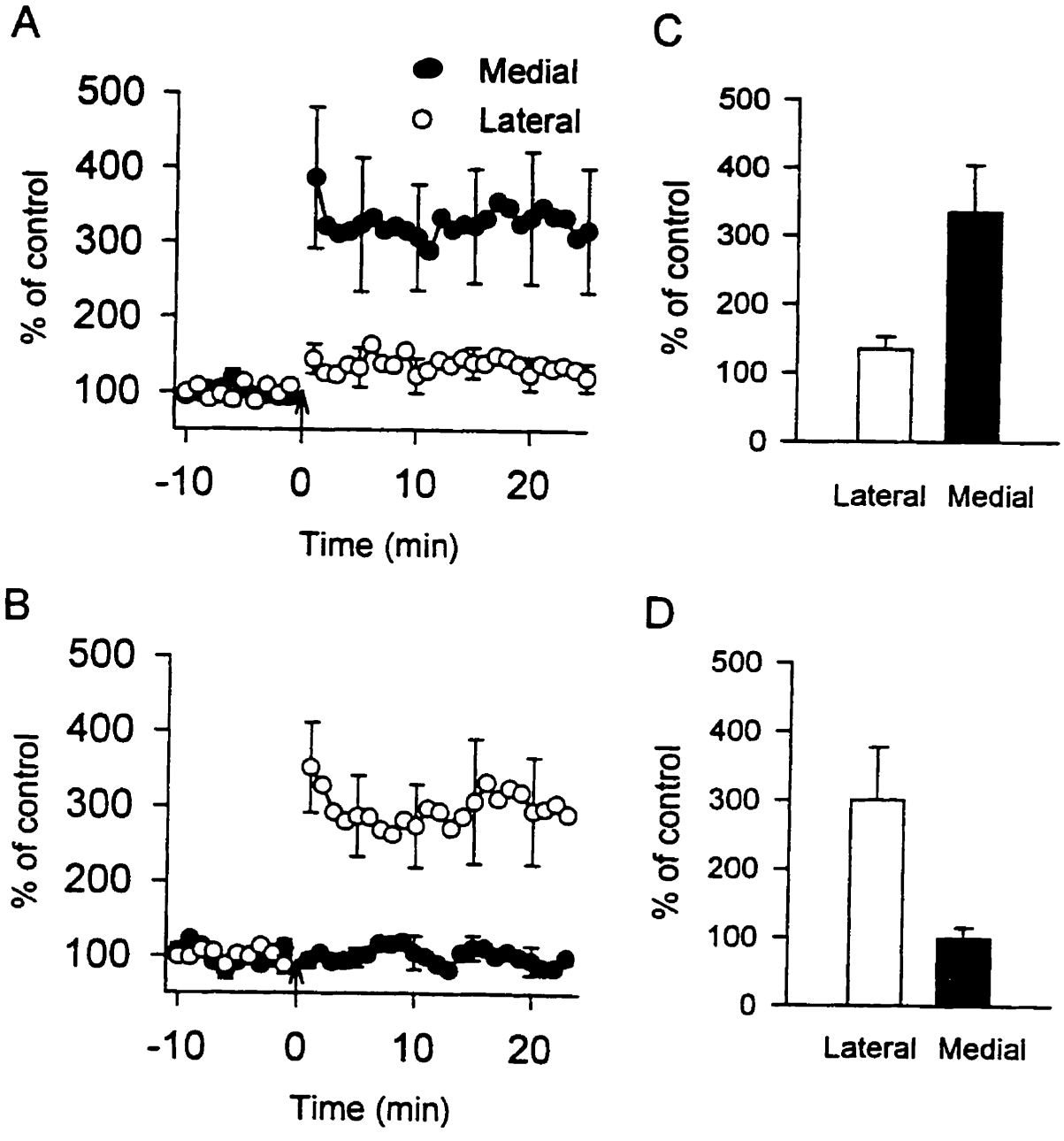
A
Medial
Lateral
500
400
300
200
100
% of control
-10
0
10
20
Time (min)
C
500
400
300
200
100
0
% of control
Lateral
Medial
B
500
400
300
200
100
% of control
-10
0
10
20
Time (min)
D
500
400
300
200
100
0
% of control
Lateral
Medial

943.3% and on average was 350.2 ± 248.5% (mean ± SD, n=11) of control (Fig.4-4A). The lateral pathway LTP was 300.1 ± 201.0% (mean ± SD, n=7) (range from 141.3% to 680.2%, Fig.4-4B). Clearly the LTP magnitudes recorded from single granule cells were larger than the ones acquired by extracellular field recordings. However, when the success rate of LTP induction in a single cell is considered, the corrected average LTP magnitude in the population of neurons was 177% which was not very different from the results obtained by extracellular field recordings. Curiously, the heterosynaptic depression seen in the field potential recordings was not observed in the whole-cell voltage recordings. However, in many cells the membrane potential hyperpolarized after tetanization, as judged by the positive current passed by the clamping circuitry to hold the membrane potential constant (data not shown). The hyperpolarization of the cell could contribute to the heterosynaptic depression seen in the field potential recordings. To further verify this issue, whole-cell current clamp recordings, which did not manipulate membrane potential of the cell as did the voltage-clamp recordings, were used in order to imitate the field recording conditions.

In whole-cell current clamp recording, the stimulation strengths were usually larger than the ones used in the voltage clamp recordings, and similar to the ones used in the field recordings. The stronger stimulation strength usually triggered the granule cells to fire action potentials. Thus, the initial slope of the response, instead of the amplitude of the response, was used to quantify the results. Furthermore, during tetanic stimulation, the cell membrane potential was not manipulated, in order to mimic the field potential recording conditions. Interestingly, under the current clamp recording condition, the

membrane potential after tetanization was stable (Fig. 4-5A). This observation ruled out the possibility that heterosynaptic depression was caused by cell hyperpolarization. However, in a few cells the membrane potential was artificially depolarized to about -20 mV during tetanization, and the membrane potential did show a brief hyperpolarization after tetanization and returning the cells from the clamped membrane potential (Fig.4-5B). Thus, the hyperpolarization of cell membrane potential could be an artifact caused by clamping the cell at a depolarized state for a short period and cannot account for the heterosynaptic depression.

The success rate of inducing LTP in the current clamp condition (Table 4-1) was higher than the success rate under the voltage clamp condition (Table 4-2). However, this could be related to the relatively high stimulation strength used in the current clamp experiments. Nevertheless, depolarization of the cell to a more positive membrane potential did facilitate the induction of LTP as shown in the voltage clamp experiments. In the cases where membrane potential was not manipulated, the stimulating pulse trains could depolarize the cell by 40-50 mV, the degree of depolarization being similar to that obtained by clamping the cell artificially to 20mV. However, the duration of depolarization was variable and never exceeded the duration of the pulse train, ie 500 ms (Fig. 4-6).

During tetanic stimulation, four 500 ms pulse trains were used. The granule cell responded to the first stimulation train with an initial depolarization which was followed by a train of action potentials that soon ceased firing. Meanwhile, the membrane potential gradually repolarized and by the time the stimulation train ended the membrane potential was only a few millivolts higher than resting membrane potential. In subsequent

Figure 4-5 The effects of different tetanization methods under whole-cell current clamp configuration. **A**. The membrane potential was not manipulated during tetanic stimulation. The tetanic stimulation consists of four 100 Hz high frequency trains (0.5 s train duration) indicated by four asterisks. Note that shortly after tetanization the membrane potential hyperpolarized 2-3 mV. **B**. The membrane potential was artificially depolarized to -20 mV during tetanic stimulation. After removial of the depolarizing current, the membrane potential showed hyperpolarization for several tenths of seconds and the degree of hyperpolarization was higher than the one produced by the method shown in A. Each vertical response during control period and potentiated phase is composed of both the medial and the lateral pathway responses due to the poor time resolution of the chart recorder. LTP was induced in both A and B.

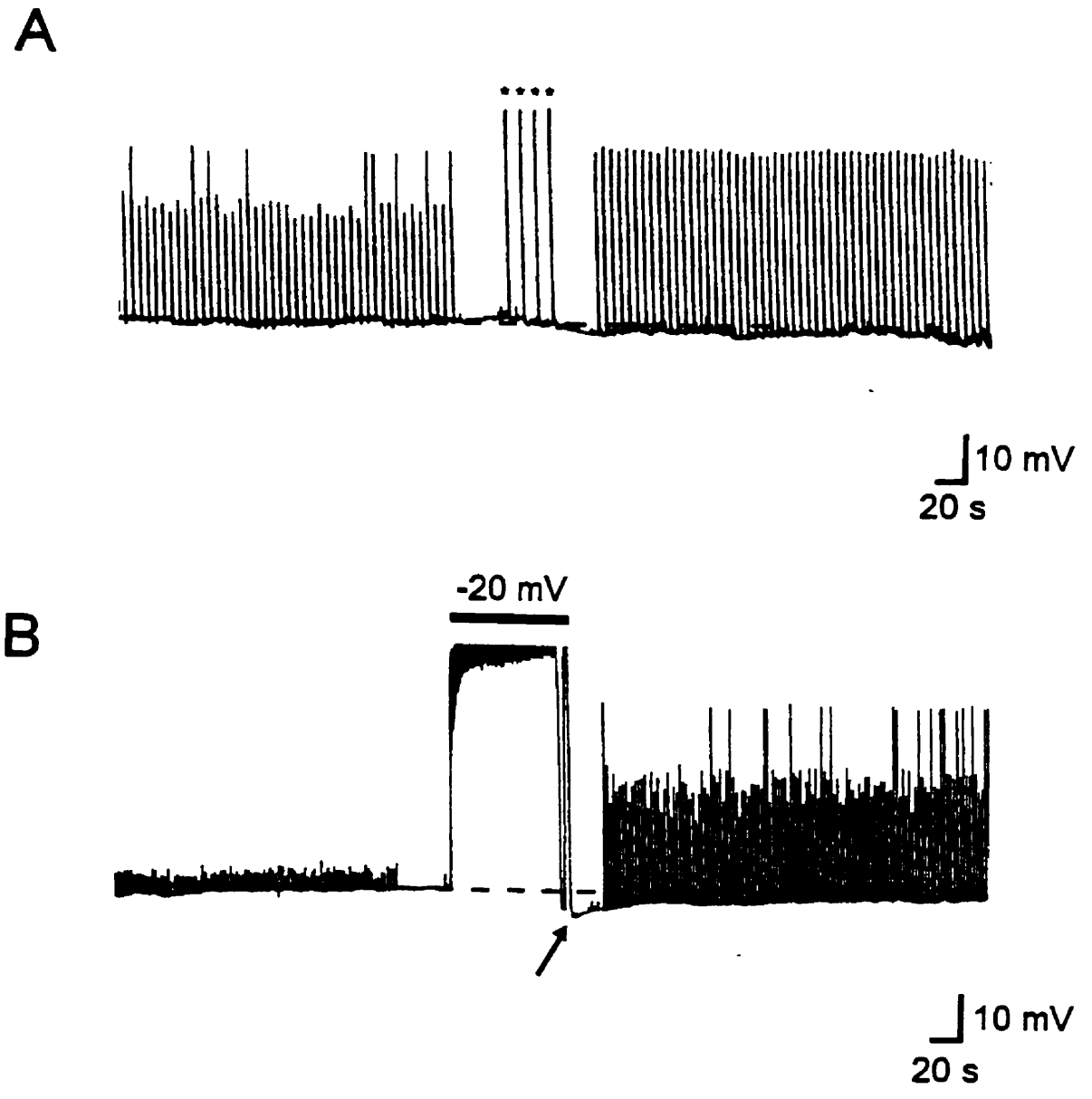
A
10 mV
20 s
-20 mV
B
10 mV
20 s

Figure 4-6 Single cell response during four tetanization trains resulting in successful LTP. In the whole-cell current clamp configuration, the cell responded to the first tetanization train with a membrane depolarization and on top of the depolarization, a train of action potentials. In each of the following trains, the duration of membrane depolarization was increased and the number of action potentials was also increased. Note that the strong membrane depolarization never lasted the full duration of the train (indicated by the horizontal bar, 0.5 s). By the time the tetanization train stopped, the membrane potential had already repolarized to less than 10 mV above the resting membrane potential. There is 10 seconds delay between each tetanization train.

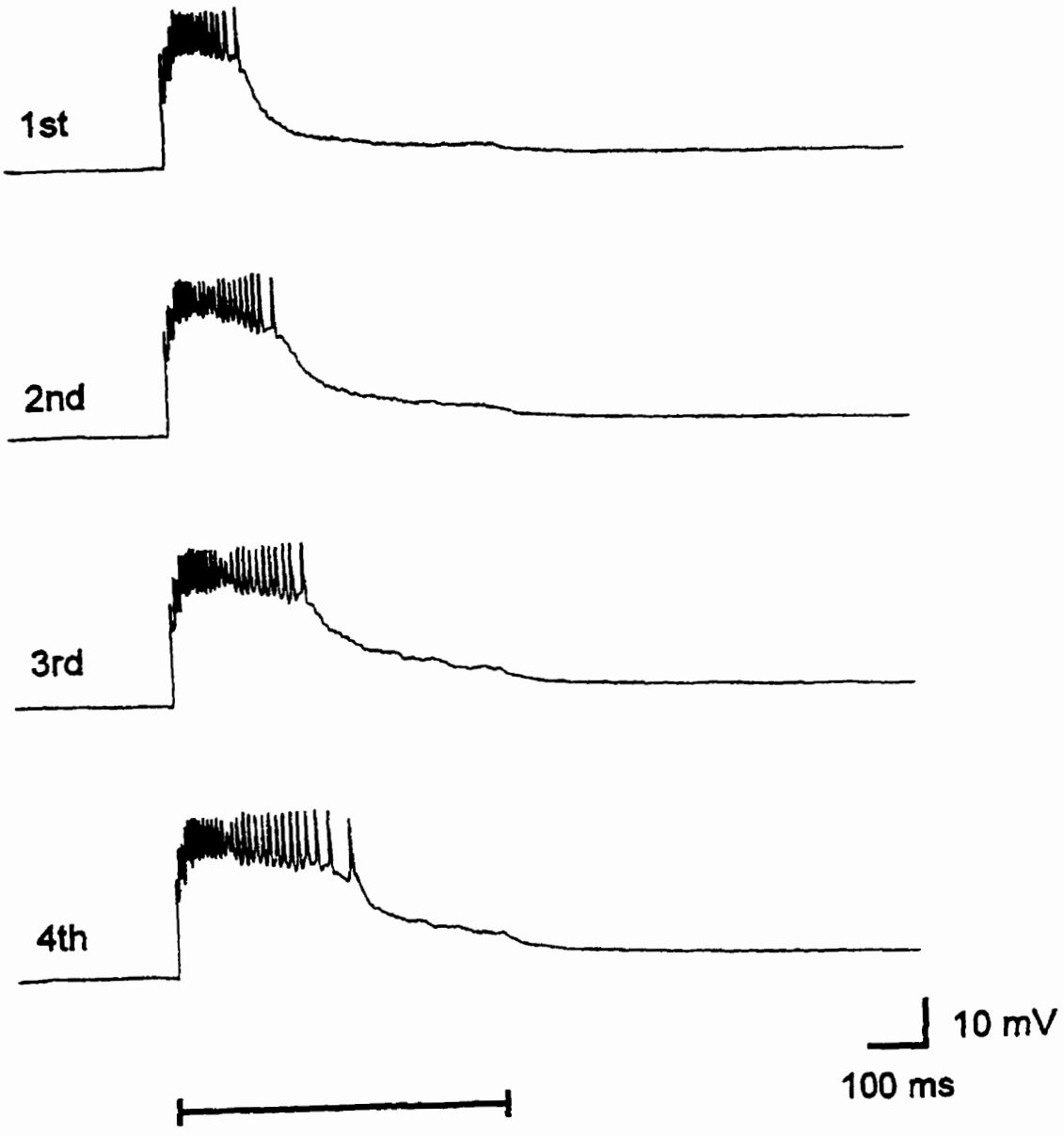
1st
2nd
3rd
4th
10 mV
100 ms

Figure 4-7 Single cell response during four tetanization trains. Under whole-cell current clamp configuration, the first tetanization train produced membrane depolarization and a train of action potentials. In the subsequent tetanic stimulation, there was little change in the duration of membrane depolarization or the number of action potentials. The cells which showed this kind of response did not exhibit LTP after tetanic stimulation.

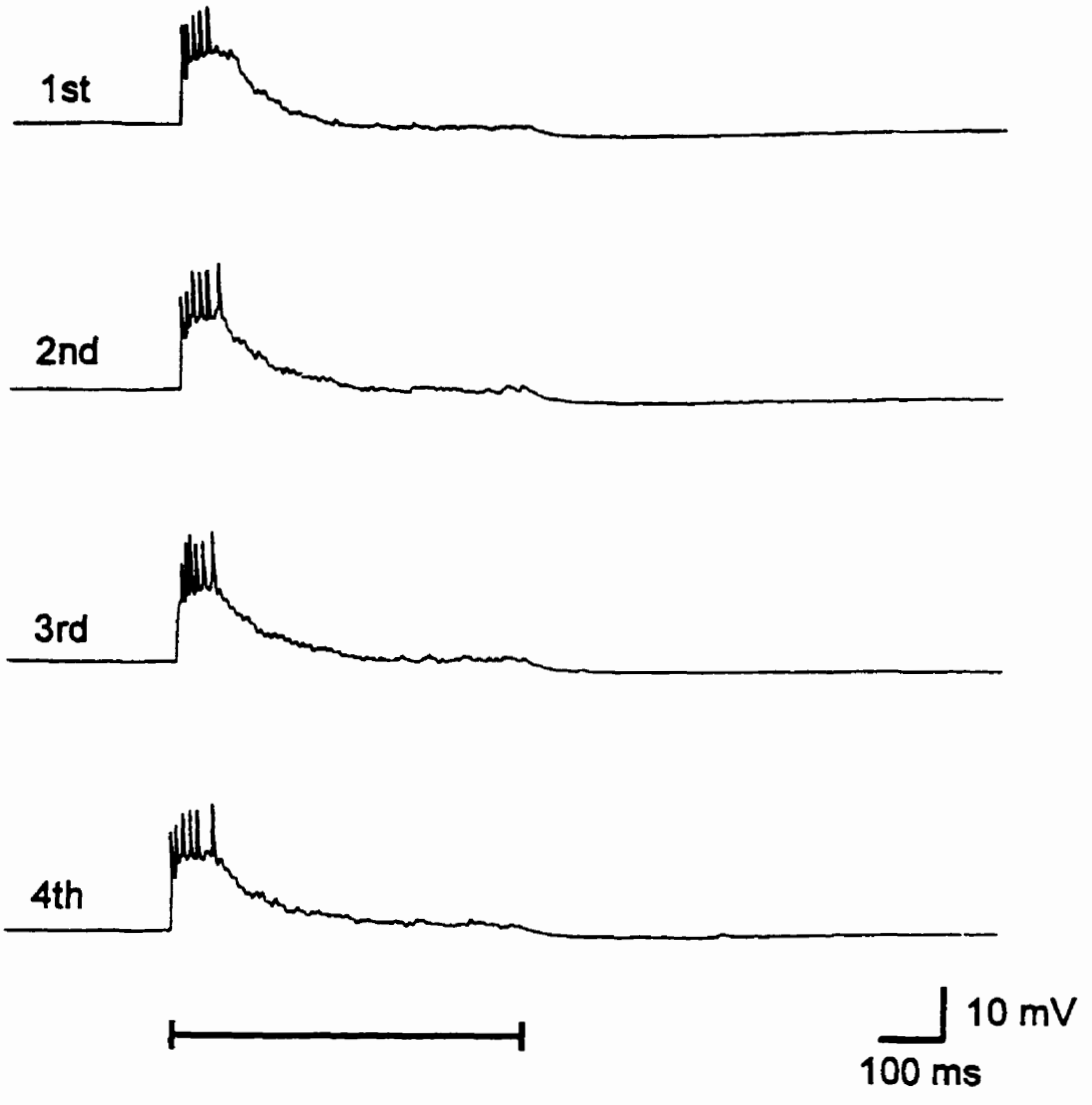
1st
2nd
3rd
4th
10 mV
100 ms

stimulation trains, the membrane depolarization was prolonged and the number of action potential increased; however, the cell always began to repolarize before the stimulation train ended (Fig. 4-6). Curiously, in the cells which did not display LTP the granule cell spike train did not increase during the subsequent stimulation trains (Fig. 4-6). In one cell the initial attempt to induce LTP in the medial pathway failed and the cell's responses to stimulation trains were typical of the kind of responses exhibited by cells which did not potentiate (Fig.4-7). However, in the same cell, a lateral pathway LTP was later induced, and this time the cell's response to stimulation trains was typical of the ones which displayed LTP, i.e. prolonged membrane depolarization and increase in the number of action potentials.

4.2.3 Quantal analysis

The analysis of statistical fluctuations of the evoked synaptic responses was performed on four representative data sets (four cells) of the medial perforant pathway. The observed LTP magnitude ranged from 16% (not statistically significant, used as a control) to 450% of the control baseline value. In three other data sets the analysis was attempted but results did not satisfy the criteria for stationarity of the responses and reliability of the procedure. Thus these latter data are not included in this chapter.

The estimated statistical parameters of synaptic transmission before and after LTP in the four data sets mentioned above are listed in Table 3. In all cases the control data suggest a rather small number of quantal units (n) but a high average probability of release (p). This is consistent with the findings on high frequency synaptic depression

Table 4-3 Quantal parameters before and after LTP induction

Exp.	% LTP	Control parameter estimates					LTP parameter estimates			
		n	p̄	varp	q ± s.d.	**Obs. q ± s.d.	n	p̄	varp	q ± s.d.
I	16	2	0.64	0.13	12.3±5.8pA	10.7±9.2pA	3	0.66	0.11	9.4±5.1pA
II	63	5	0.31	0.15	7.2±3.0pA	4.7±4.1pA	4	0.56	0.09	7.9±3.7pA
III	400	3	0.47	0.21	6.7±2.5pA	6.5±2.6pA	12	0.39	0.00	6.8±2.5pA*
IV	450	3	0.5	0.19	9.3±3.3pA	7.9±4.3pA	11	0.60	0.00	7.9±3.3pA*

Four representative experiments were examined with quantal analysis to determine parameters *n* (# of quantal units), p̄ (average probability of transmission), q (mean quantal size) and var *p* (variance of *p*) according to the procedure described in Chapter 2 (2.6.2).

* Parameters p and *n* in experiments III and IV were calculated assuming same quantal size as in control period and a uniform binomial distribution (using equations 3-5 from Wojtowicz & Atwood, 1986).

** Observed values of q were caculated by measuring the spontaneous "minis" before induction of LTP.

in the medial pathway (see Chapter 3). Moreover, in all cases, the deconvolved binomial distributions were non-uniform, indicating variance among probabilities at single synapses. For all data sets, the mean estimated quantal sizes (q) were slightly larger but the variances smaller than the values obtained from measurements of spontaneous EPSCs. Such estimates suggest that the quantal units participating in the evoked EPSCs belong to a population of synapses giving rise to spontaneous EPSCs, and originating at synapses located relatively close to the somatic recording site. The standard deviations of estimated q were nevertheless quite large (Table 3). The calculated coefficients of variation ranged between 0.36 and 0.47.

In experiments I and II the estimated quantal parameters before and after the attempted induction of LTP were obtained. In the first case there was no significant LTP; correspondingly, no significant changes in the estimated parameters were seen. In the second case there was an increase in p, corresponding to the larger mean EPSC (63% larger than control) during LTP. Small changes (± 1) in parameter n are not considered to be significant (see Chapter 2 methods).

In experiments III and IV the estimates of n demanded by the LTP data were apparently large but beyond the capabilities of the quantal analysis procedure used (see Chapter 2 methods). In these cases n and p were calculated by using equations for the binomial distributions available in the literature (Robinson, 1976; Wojtowicz and Atwood, 1986). These calculations require prior knowledge of q and the variance of q. These values are assumed to be the same as the values estimated from the control data. The analysis in Table 3 suggests that large LTP (> 100%) is primarily due to increased

Figure 4-8 Analysis of evoked and spontaneous EPSCs during the control period before induction of LTP in a single cell. **A**. Each point represents the charge measured for each response in the medial pathway. The mean of the evoked responses and its standard deviation are shown. **B**. Histogram of charge distribution of 144 spontaneous EPSCs observed during the control period. **C**. Charge distribution of evoked EPSCs and two Poisson distributions. Both Poisson distributions are calculated on the basis of measured quantal size q = 63 ± 25 pA∘ ms, and recording noise = 25 ± 15 pA∘ ms. In curve #1 the quantal content is determined by the direct method and the result is m = 1.8. In curve #2, the method of failures was used to calculate quantal content, and the result was m = 3.2. Note that both curves failed to predict the shape of the histogram. The theoretical distribution assumed Gaussian distributions of noise and quantal sizes. Due to relatively large standard deviations of the spontaneous miniature events and the noise, the peaks of the individual quantal components do not show in the overall distributions. **D**. Cumulative distribution plot obtained for the data and for the predicted Poisson distributions. In both cases, the theoretical distributions were different from the observed values on the basis of the Kolmogorov-Smirnov test (P.0.3). **E**. Non-uniform binomial distribution derived from the data by a curve fitting procedure. The derived parameters were n = 3, $\bar{p}$ = 0.5, q = 74 pA∘ms. **F**. Cumulative distribution plots of data and the predicted binomial distributions show a good fit.

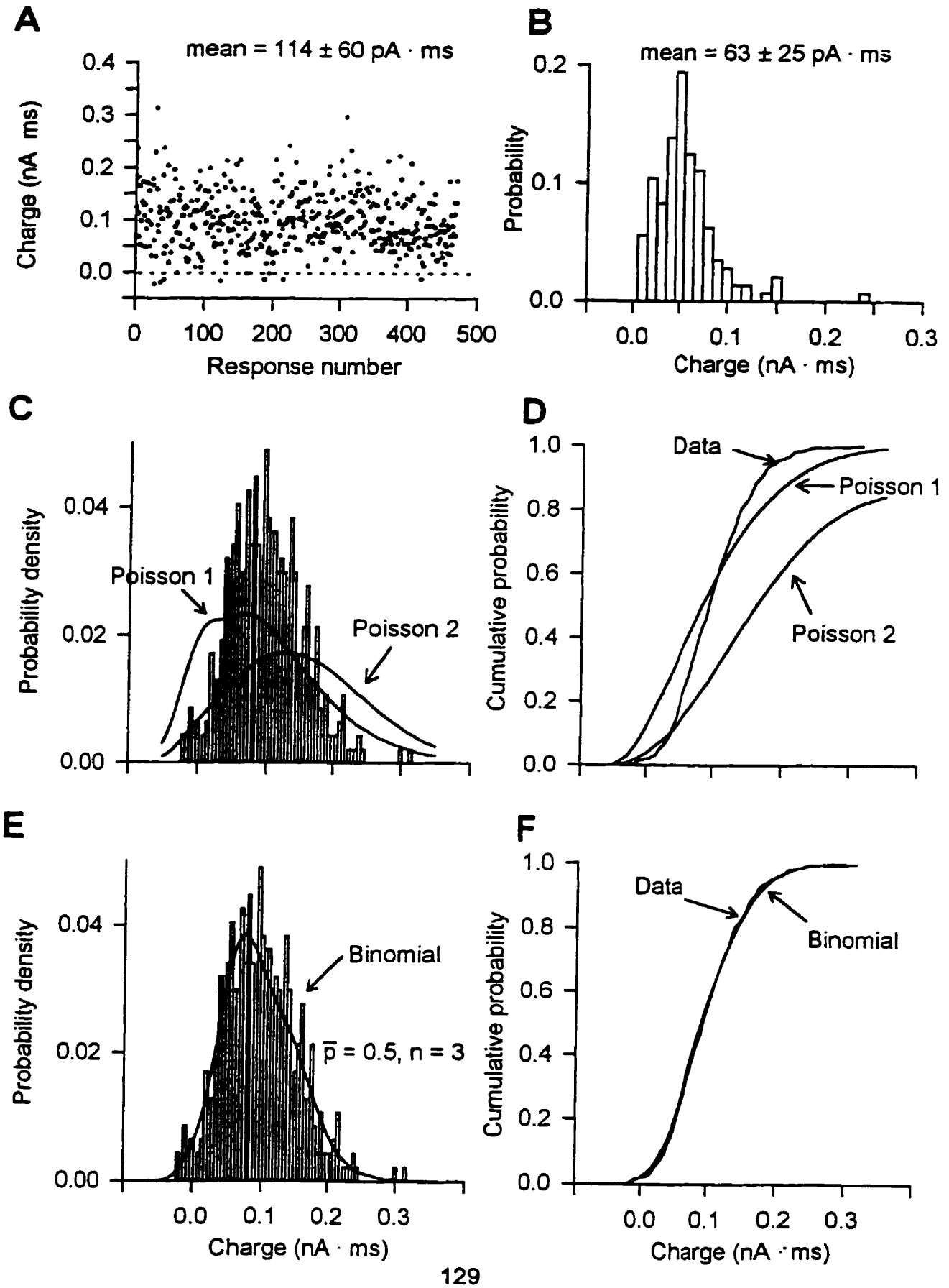
A
mean = 114 ± 60 pA · ms
Charge (nA ms)
0.4
0.3
0.2
0.1
0.0
0
100
200
300
400
500
Response number
B
mean = 63 ± 25 pA · ms
Probability
0.2
0.1
0.0
0.0
0.1
0.2
0.3
Charge (nA · ms)
C
Probability density
0.04
0.02
0.00
Poisson 1
Poisson 2
D
Cumulative probability
1.0
0.8
0.6
0.4
0.2
0.0
Data
Poisson 1
Poisson 2
E
Probability density
0.04
0.02
0.00
Binomial
p̄ = 0.5, n = 3
0.0
0.1
0.2
0.3
Charge (nA · ms)
F
Cumulative probability
1.0
0.8
0.6
0.4
0.2
0.0
Data
Binomial
0.0
0.1
0.2
0.3
Charge (nA · ms)

Figure 4-9 Analysis of evoked and spontaneous EPSCs after induction of LTP (same experiment as in Figure 4-8). **A**. Each point represents evoked EPSCs at the same stimulus intensity as in control (Figure 4-8). The mean response was potentiated approximately 4.5 times. **B**. The charge distribution of 150 spontaneous events observed during LTP period. The distribution was not significantly different from the control set shown in Figure 4-8B (Kolmogorov-Smirnov test, $p > 0.3$). **C**. The histogram of charge distribution of evoked EPSCs is superimposed on two predicted binomial distribution. "High q" shows a distribution obtained by increasing the quantal size and its variance 4.5 times, in correspondence with 4.5 fold increase of evoked responses. "High p&q" is a distribution predicted on the assumption that parameter p increases 2 times and parameter q increases 2.25 times, again corresponding to the 4.5 fold increase in evoked responses. **D**. Plots of cumulative distributions show that predicted and observed distributions are different (Kolmogorov-Smirnov test, $p > 0.5$). **E**. A predicted binomial distribution with $n = 14$, $p = 0.5$, and $q = 74$ pA∘ms superimposed on the histogram of the data. **F**. The predicted binomial distribution with high *n* fits the data well (Kolmogorov-Smirnov test $p < 0.05$).

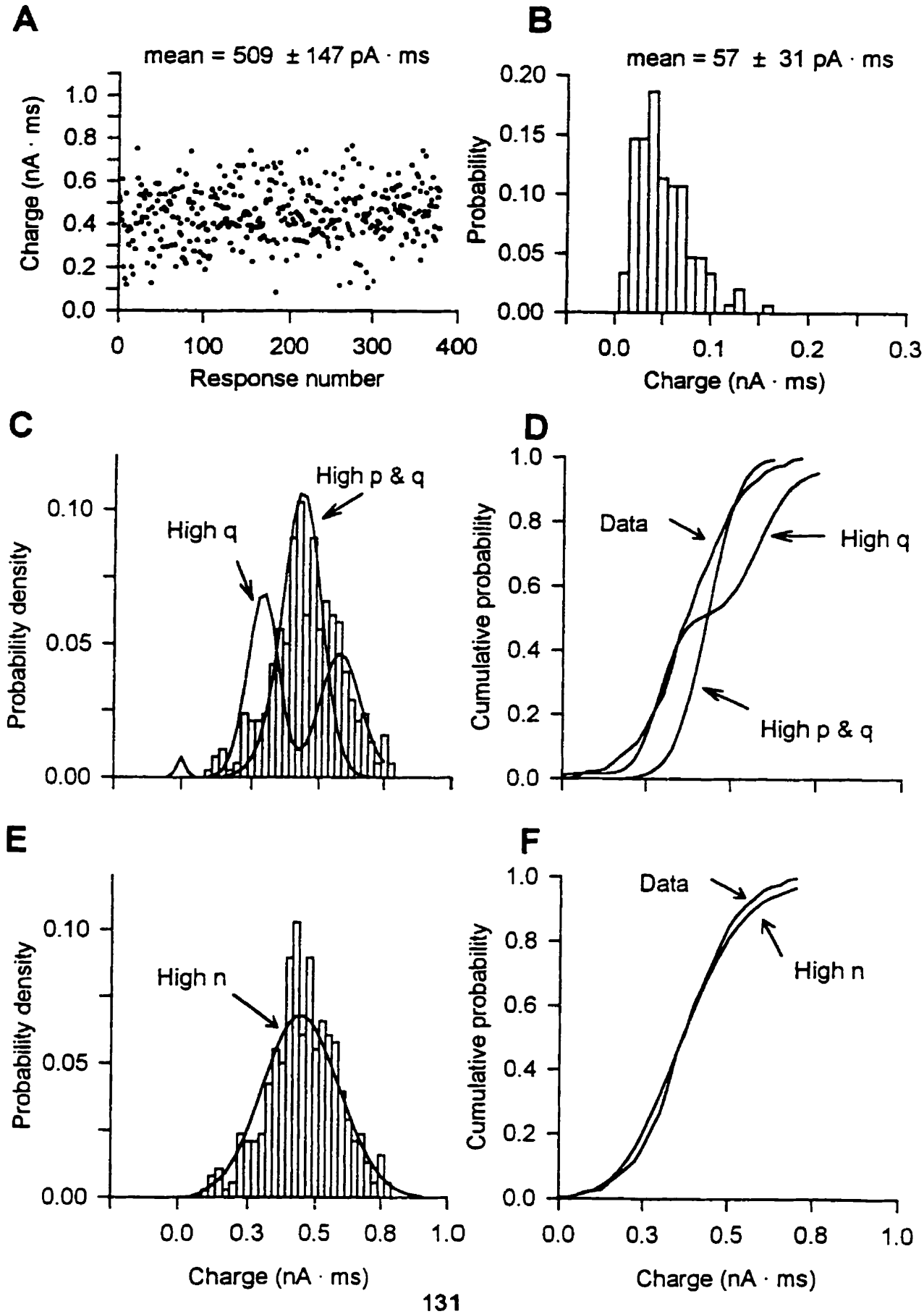
A
mean = 509 ± 147 pA · ms
Charge (nA · ms)
1.0
0.8
0.6
0.4
0.2
0.0
0
100
200
300
400
Response number
B
mean = 57 ± 31 pA · ms
Probability
0.20
0.15
0.10
0.05
0.00
0.0
0.1
0.2
0.3
Charge (nA · ms)
C
Probability density
0.10
0.05
0.00
High q
High p & q
D
Cumulative probability
1.0
0.8
0.6
0.4
0.2
0.0
Data
High q
High p & q
E
Probability density
0.10
0.05
0.00
High n
0.0
0.3
0.5
0.8
1.0
Charge (nA · ms)
F
Cumulative probability
1.0
0.8
0.6
0.4
0.2
0.0
Data
High n
0.0
0.3
0.5
0.8
1.0
Charge (nA · ms)

number of active synapses and not due to increased probability of transmitter release. The assumption of constant *q* in experiments III and IV is supported by the consistent lack of any detectable changes in the mean quantal size of spontaneous EPSCs during LTP (Figure 4-8B, Figure 4-9B). However, these EPSCs probably originated from many synapses which were not potentiated. In order to increase the number of potentiated synapses I increased the stimulation strength.

In two such additional experiments in which LTP was induced by relatively large (approximately three-fold higher than usual) stimulus intensities to produce an increase of the strength in many synapses, I did not observe a change in either frequency or amplitude of the spontaneous EPSCs. Thus, even when many input fibers were activated during induction of LTP, there was no indication of any change in amplitude of mean quantal size as judged by the spontaneous events.

An independent method to examine the consequences of possible changes in *q* and in the other quantal parameters is to model mathematically the expected statistical distributions by changing one parameter (*q*, *p*. or *n*) at a time. This procedure is particularly revealing when cases of large LTP, such as shown in experiments III and IV in Table 3, are examined.

The analysis of experiment IV is illustrated in figure 4-8 and 4-9. In this case the quantal analysis was performed on the charge measures of EPSPs (see Chapter 2 methods); however, an analysis of peak amplitudes gave very similar results. In Figure 4-8A, the magnitudes of individual evoked EPSCs measured before LTP were plotted to illustrate their range and stationarity. In Figure 4-8B, the magnitude-distribution of

spontaneous EPSCs (presumed miniature, quantal EPSCs) were illustrated. A histogram of the evoked responses is shown in Figure 4-8C, superimposed on two Poisson distributions (1 and 2). The first curve assumed quantal content (m) of 1.8, calculated by dividing the mean of evoked responses by the mean of spontaneous responses. The second curve assumed m of 3.2 for EPSCs calculated from the method of failures (Poisson distribution) (Voronin 1993). In both cases I assumed that the quantal size to be equal to the mean size of spontaneous EPSCs as would be expected if the evoked EPSCs originated at a large number of synapses. These methods serve as first pass approximations of quantal content. Neither curve fitted the data. This can be seen clearly from a comparison of shapes of the cumulative distribution in Figure 4-8D. These two examples show that the data were incompatible with a Poisson distribution requiring a large number of quantal components with a low probability of occurrence.

Next, a binomial distribution was considered. In Figure 4-8E the histogram of evoked EPSCs is superimposed on the fitted non-uniform binomial distribution with n = 3, p = 0.5. The match between the fitted and the observed curves was very good (Fig. 4-8F).

To further explore the predicted changes in the distributions resulting from changes of parameters q, p and n during LTP, the following calculations were performed to fit the LTP portion of data set IV. In this data set, the observed evoked responses were enhanced about 4.5 times (Fig. 4-9A) while the spontaneous EPSCs remained unchanged (Fig. 4-9B, compare with Fig. 4-8B) during LTP. In Figure 4-9C the histogram of the evoked EPSCs is superimposed on a predicted binomial distribution with the same

n and *p* as in control but with parameter *q* increased 4.5 times ("high q" curve). This curve clearly does not coincide with the data. The second curve ("high p and q" curve) simulates the expected changes in the distribution of *p* is changed from 0.5 to its maximum possible value of 1, and *q* is also increased 2.25 times to produce an overall increase of the mean response of 4.5 times, as observed experimentally. This curve did not fit the data either, as shown on the cumulative probability plots in Figure 4-9D. This simulation demonstrates that an increase of p alone cannot account for LTP, even when large changes in q are allowed.

A much better fit was obtained when parameter *n* was increased approximately 4.5 times (from 3 to 14) simulating an increase in the number of responding synapses. This result is shown in Figure 4-9E and Figure 4-9F. Very similar results were obtained during simulation of Expt. III in Table 3. From these comparisons of observed and theoretical distributions, it is clear that increased *n*, which probably corresponds to an increased number of active synapses, can alone account for most of the observed large LTP, although relatively small contributions from *p* and *q* cannot be rigorously excluded on present data.

To further examine whether the increase in parameter *n* is not due to recruitment of additional axons by tetanic stimulation, I used a graphical coefficient of variation analysis. In two additional experiments (see Chapter 2 Methods), the stimulation intensity was increased after collecting the control responses, to mimic the condition where additional axons were recruited. Figure 4-10A and 10B shows that the response histogram is shifted to the left after the stimulation intensity was increased. Calculating

Figure 4-10 Effect of increasing stimulation intensity on the response size and coefficient of variation analysis. **A**. The histogram of control responses where weak stimulation was used. The mean response amplitude is 20.0 ● 7.3 pA (n = 500). **B**. The histogram of responses after the stimulation intensity was increased to recruit more axons. The mean response amplitude is 50.3 ± 9.4 pA (n = 500). **C**. Coefficient of variation analysis of experiments of LTP (filled circles) and experiments where stimulation intensity were increased (open squares). The experiment shown in A and B is the square on the left hand side. Note that all the LTP experiments were under the diagonal line whereas the stimulation intensity change experiments were above the diagonal line. The solid line is the regression line of the LTP experiments and the curves indicate the 95% confidence area.

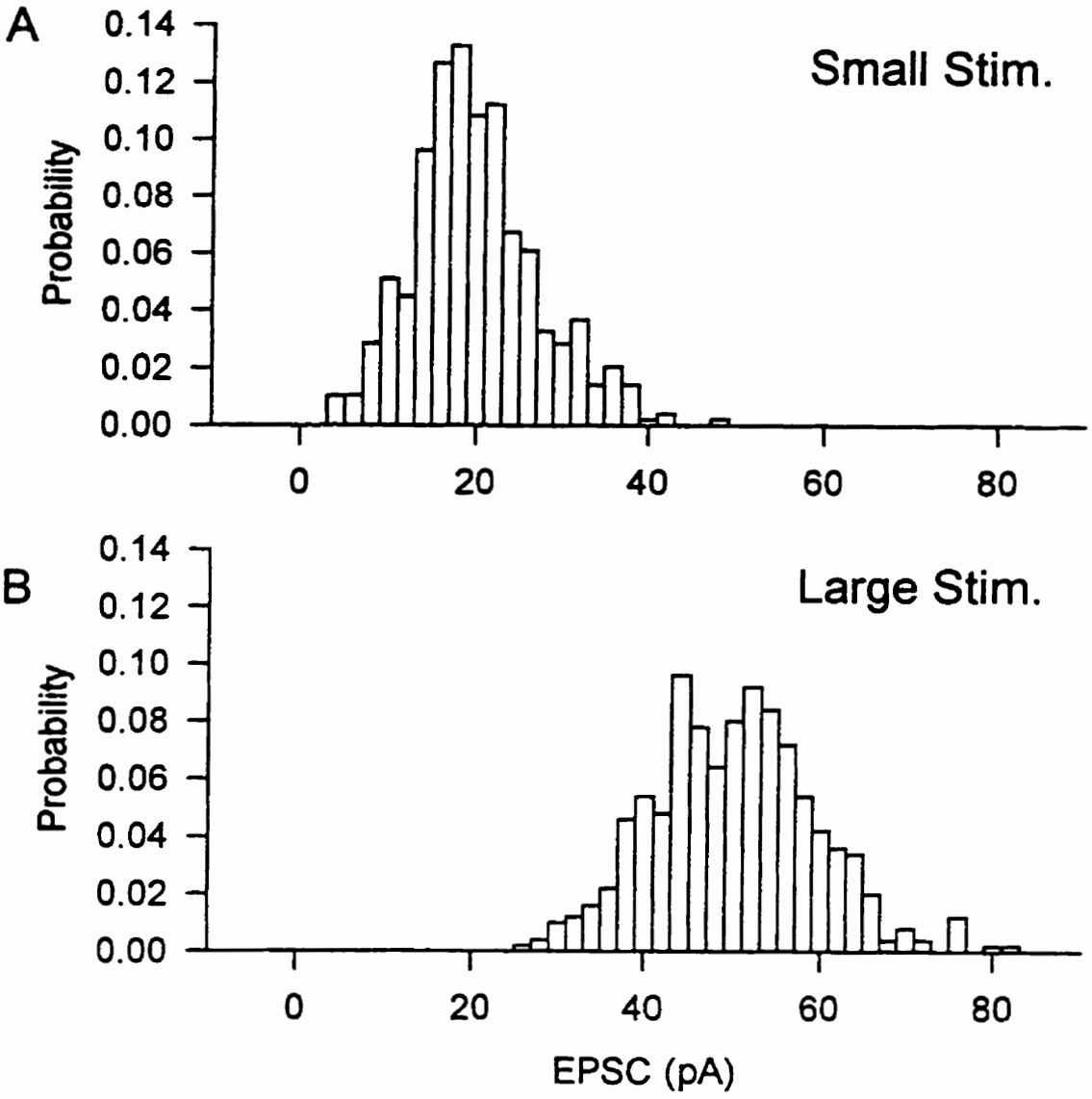
A
Small Stim.
Probability
0.14
0.12
0.10
0.08
0.06
0.04
0.02
0.00
0
20
40
60
80
B
Large Stim.
Probability
0.14
0.12
0.10
0.08
0.06
0.04
0.02
0.00
0
20
40
60
80
EPSC (pA)

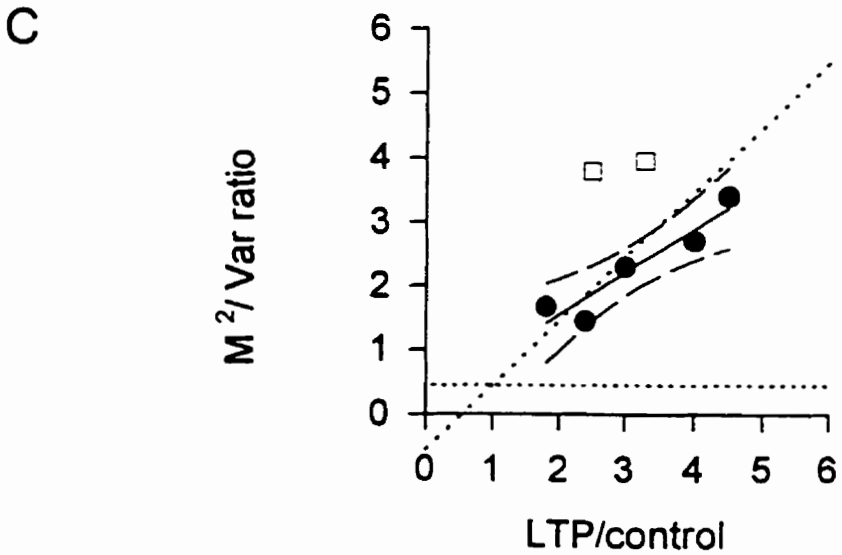
C
M 2/ Var ratio
6
5
4
3
2
1
0
0
1
2
3
4
5
6
LTP/control

the M^2/CV ratio in these two experiments and comparing them with the coefficient of variation of the LTP experiments, revealed that the distribution of the data points is clearly different (Figure 4-10C). All of the LTP experiment data points fall below the diagonal line, while the two data points from increased intensity experiments are above the diagonal line. Thus, the pattern of quantal variability resulting from recruiting more axons is different from the pattern of recruiting synapses. Detailed description of the coefficient of variation method and results is included in the following chapter.

4.3 Discussion

The medial and the lateral perforant pathways are different in a number of their basic properties (see chapter 3). However, when considering the LTP size in the perforant pathway, the lateral division and the medial division do not show any difference.

4.3.1 Success rate of LTP induction

The success rate of inducing LTP under whole-cell configuration, compared with the success rate in field potential recording experiments, was relatively low. There are several possible reasons for this low success rate of LTP induction in whole-cell configuration. The first one is that the whole-cell configuration might produce so called "wash-out" effect. Some important factors for LTP induction may have been washed out due to the perfusion of the inside of the cell by the intracellular recording solution in the

pipette. In CA1 pyramidal cells, it was believed that by 20 minutes after establishment of the whole-cell configuration, it is impossible to induce LTP in the well-washed cell (Malinow and Tsien, 1990). However, in the present studies LTP had been induced well after the 20-minute limit in some cells. Furthermore, in several cases the first attempt to induce LTP in one pathway failed. However, 30 minutes later, LTP was successfully induced in the other pathway. Moreover, there was no correlation between occurrence of LTP and the duration of recording prior to the induction. These observations suggest that "wash-out" effect might not be a serious problem in the dentate granule cells, although we cannot rule it out.

The second possible cause of the low success rate under the whole-cell recording configuration is that the relatively weak stimulation might not activate enough synapses or produce large enough depolarization for LTP induction. It has been shown by Wigström and Gustafsson (1986) that LTP requires a certain number of fibers to be activated for its successful induction in the perforant pathway. It is very likely that with the minimum stimulation used in the voltage clamp experiments, there were not enough fibers activated to induce LTP, even though the postsynaptic cell was artificially depolarized to facilitate LTP induction. This hypothesis was supported by the observation that in current clamp experiments, when stronger stimulation was used to mimic the extracellular field recording conditions, the LTP success rate was much higher than in the voltage clamp experiments where minimal stimulation was used.

The magnitude of the LTP induced in single cells was on average larger than the LTP induced in the extracellular field potential recording experiments (field potential

recording: lateral LTP, 190 ± 7%; medial LTP, 209 ± 12%; whole cell recording: lateral LTP, 300.1 ± 201.0%; medial LTP, 350.2 ± 248.5%). However, if the success rate of LTP induction in single cell recordings is taken into consideration, the re-calculated LTP magnitude is not too far off from the field potential LTP magnitude (medial: 125%; lateral: 70%). This further suggests that it is possible that some granule cells do not exhibit LTP. Otherwise, if every granule cell exhibited LTP (success rate 100%), the averaged LTP magnitude from a single cell would be too large when compared with the field potential LTP (assumed to be from the same population of cells).

4.3.2 Changes during tetanization

The prolonged depolarization and the increase in the number of spikes observed during tetanization in the current-clamp mode is of interest for several reasons. First, it is a reliable way to predict whether LTP will be successfully induced in the cell. The cells which displayed this phenomenon during the four successive tetanic stimulation trains expressed LTP while the ones that failed to show changes did not express LTP. Secondly, the cause of this phenomenon is still not known. Thirdly, whether this phenomenon is necessary for LTP induction or is merely the "byproduct" of successful LTP induction is unclear. If there is a link between this phenomenon and LTP induction, what is the mechanism underlying this linkage? Although no further experiments were conducted to elucidate these unanswered questions, possible causes for the prolonged depolarization and the increase in number of spikes and their connection with LTP induction will be discussed in the following paragraphs.

The most probable cause of prolonged depolarization and increased action potential numbers is a blockade of repolarization current or after-hyperpolarization potential (AHP). In dentate granule cells, a Ca^{2+}-activated K^+ conductance is thought to cause after-hyperpolarization current (I_{AHP}) and spike accommodation following repetitive firing (Stanton et al., 1989). Although the phenomenon I observed during the tetanic stimulation was not entirely the same as spike accommodation, it does share some similar features. First of all, the action potentials produced by each tetanic stimulation are few in number. The membrane depolarization and action potential firing never persist for the full duration of the tetanic stimulation (0.5 s). Thus, the excitatory responses are turned off by some mechanism before the stimulation ended. In spike accommodation, the membrane depolarization is provided by a depolarizing pulse, and the action potentials produced by the cell never persist throughout the full length of the pulse, which is similar to the limited number of action potentials observed during tetanic stimulation. If I_{AHP} is responsible for turning off membrane depolarization and limiting the action potential number during tetanic stimulation, then the prolonged membrane depolarization and increased action potential number should be the result of reducing I_{AHP}.

There are a number of neurotransmitters and receptors known to modulate I_{AHP} in the dentate granule cells. Thus, they are the possible candidates for producing prolonged membrane depolarization and increased action potential numbers during tetanic stimulation. This might in turn affect the LTP induction.

4.3.2.1 Norepinephrine

Stanton et al. (1989) demonstrated that norepinephrine blocks spike accommodation and I_{AHP} of granule cells. These effects are antagonized by the β-adrenergic receptor blocker propranolol and the β1-adrenergic antagonist metoprolol; while forskolin, which bypasses the β-adrenergic receptor activation and directly activates adenylate cyclase, can mimic the norepinephrine effects. Although the elevated cyclic AMP (cAMP) concentration induced by adenylate cyclase activation is related to the blockade of Ca^{2+}-activated K^+ conductance, the exact mechanism by which cAMP exerts its effect is still unknown. Interestingly, norepinephrine itself can produce a LTP -like potentiation in the granule cells (Neuman and Harley, 1983; Stanton and Sarvey, 1985).

The noradrenergic innervation of the dentate gyrus originates in the locus coeruleus, with norepinephrine-containing terminals found throughout the dentate gyrus and concentrated in the hilar region (Jones and Yang, 1985). Binding studies have indicated distribution of β-adrenergic receptors throughout the dentate gyrus (Rainbow et al., 1984). Thus, it is possible that during tetanic stimulation, some noradrenergic fibers were also stimulated. As a result, norepinephrine released by these terminals could have produced the progressive prolongation of membrane depolarization and increasing action potential number during tetanic stimulation. However, Dahl and Sarvey (1989) reported that norepinephrine only potentiates the responses evoked by medial perforant pathway stimulation while depressing the responses evoked by the lateral perforant pathway activation. This pathway-specific effect of norepinephrine is difficult to explain by blockade of I_{AHP} because the changes observed during tetanic stimulation are

observed in both the medial and the lateral pathways. Alternatively, norepinephrine might not be the modulator for the phenomenon observed during tetanic stimulation.

4.3.2.2 Acetylcholine

Spike accommodation in the dentate gyrus can also be reduced by carbachol, a cholinergic receptor agonist. Carbachol is known to inhibit a potassium conductance called M current; however, the contribution of M-current in spike accommodation of granule cells is not clear. Thus, it is questionable whether the carbachol effect on spike accommodation is mediated by the blockade of the M current. It had been shown by Müller and Misgeld (1986) that muscarinic M1 receptor activation produces a slow depolarization in dentate gyrus granule cells. This effect could lead to an increased excitability of granule cells and facilitate LTP induction by increasing granule cell depolarization during high frequency stimulation. Indeed, Burgard and Sarvey have shown that muscarinic receptor activation can facilitate LTP induction in the dentate gyrus, probably through the activation of muscarinic M1 receptors. This slow depolarizing potential could explain the prolonged membrane depolarization and increase in number of action potentials.

Muscarinic M1 receptor activation in CA1 pyramidal cells also reduces the slow I_{AHP}. Whether the same holds for dentate gyrus is not known. In addition, M1 receptor activation has been linked to phospholipase C and phosphoinositol turnover (Gil and Wolfe, 1985; Peralta et al., 1988). The second messengers produced by phosphoinositol turnover might exert their effects by phosphorylating certain cellular proteins (Van Hoof

et al., 1989). These second messengers may also play a role in the induction of LTP. For example, the product of phosphoinositol breakdown, diaceylglycerol, could activate PKC which is known to be activated during LTP induction (Linden and Routtenberg, 1989). Thus, these cellular processes could underlie the facilitation of LTP induction by M1 receptor activation. However, the source of acetylcholine is ambiguous. The known cholinergic fibers in the dentate gyrus are from the septum and terminate mainly around granule cell soma and the proximal dendrites in the inner one-third of the molecular layer (Frotscher and Leranth, 1985). It is not clear whether tetanic stimulation in the medial or the lateral perforant pathway in the outer two-thirds of molecular layer also causes acetylcholine release. In fact, it is quite possible that PKC is part of the second messenger pathway activated by receptors other than M1, for example the metabotropic glutamate receptors (see below). Activated PKC could subsequently phosphorylate the Ca^{2+}-activated K^+ channel and modulate spike accommodation by reducing the channel conductance.

4.3.2.3 Glutamate

Finally, the most likely candidate for modulating spike accommodation is glutamate itself. I am in favour of this candidate because clearly, the source of glutamate is not hard to explain, unlike the source of acetylcholine and norepinephrine. In the CA1 area, the metabotropic glutamate receptor agonist 1S-3R-ACPD can reduce spike accommodation and this effect is antagonized by MCPG. Although 1S-3R-ACPD is an agonist for metabotropic glutamate receptor subtype mGluR1,2,3, and 5, its effect on

Figure 4-11 Possible second messenger mechanisms underlying the changes observed during tetanic stimulation. Activation of the muscarinic M1 receptors could lead to phosphoinositol (PIP2) turnover by the action of phospholipase C (PLC) and produce diacylglycerol (DG) and phosphoinositoltriphosphate (IP3) (pathway I). Activation of metabotropic glutamate receptor subtypes 1 and 5 could also result in the production of DG and IP3 via phosphoinositol turnover. The DG produced by either pathway can activate protein kinase C (PKC) which could phosphorylate the calcium activated potassium channel (K_{Ca}) and reduce the conductance of the channel (pathway II). Protein kinase C is also known to be one of the key enzymes for LTP induction. Meanwhile, IP3 could trigger Ca^{2+} release from internal stores and this Ca^{2+} could act in synergy with the Ca^{2+} that enters via the NMDA receptor-channels, thereby activating calcium calmodulin kinase II and induce LTP. An alternative pathway is via the activation of the β adrenergic receptor. The G protein coupled with the β adrenergic receptor could turn on adenylyl cyclase upon activation. Adenylyl cyclase activation would produce cyclic AMP (cAMP) which is known to have a direct action on the K_{Ca} channel (pathway III). Thus, multiple second messenger pathways could lead to a similar effect. The effector which turns off the K_{Ca} channel conductance could also act in the LTP induction process.

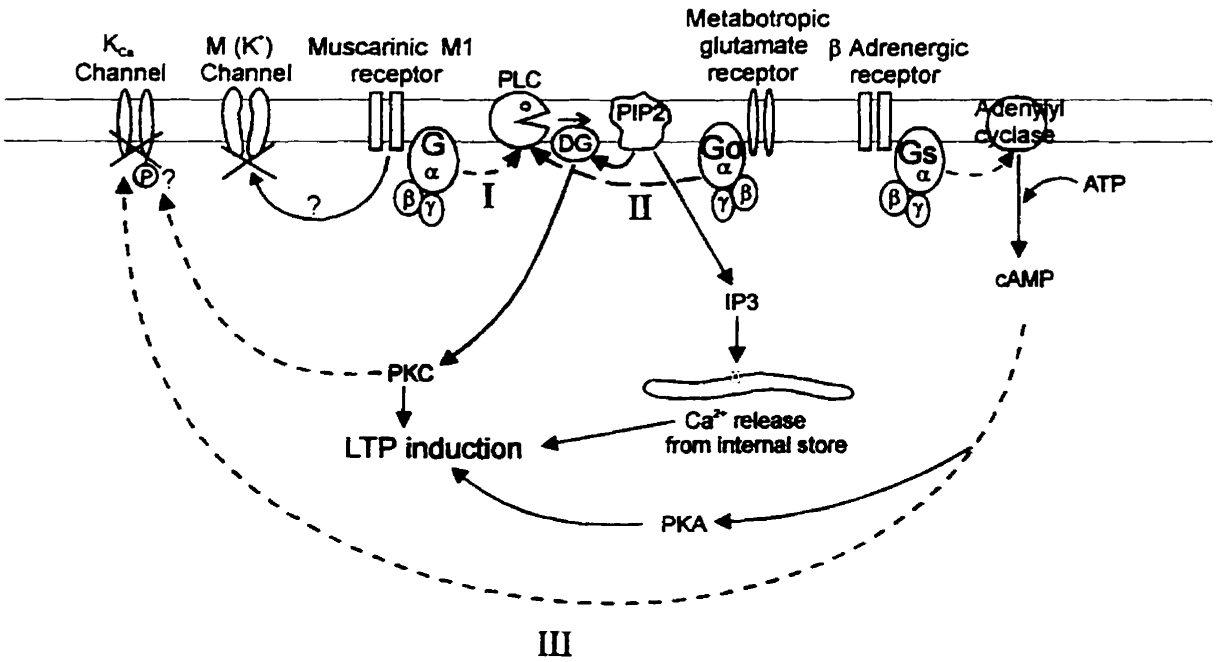
K_{Ca} Channel
M (K^+) Channel
Muscarinic M1 receptor
PLC
PIP2
DG
Metabotropic glutamate receptor
β Adrenergic receptor
Adenylyl cyclase
ATP
cAMP
G α β γ
Go α β γ
Gs α β γ
P
?
?
I
II
IP3
PKC
Ca^{2+} release from internal store
LTP induction
PKA
III

spike accommodation is probably mediated by mGluR1 and/or mGluR5 (Watkins and Collingridge, 1994). It has been shown that 1S-3R-ACPD could inhibit Ca^{2+}-activated K^+ conductance which produces spike accommodation and this effect is antagonized by MCPG (Bashir et al., 1993; Hurke and Hablitz, 1996). Activation of metabotropic glutamate receptor subtypes mGluR1 and mGluR5 cause phosphoinositide hydrolysis (Hayashi et al., 1994). This process will create diacylglycerol which could activate PKC (Figure 4-11). Again, this activated PKC could phosphorylate Ca^{2+}-activated K^+ channel to reduce spike accommodation and/or proteins which induce LTP. Alternatively, Abdul-Ghani et al (1996a,b) have shown that in the granule cells metabotropic receptor activation blocks the long-lasting AHP via tyrosin kinase and IP3 mediated mechanisms. It has been shown that MCPG inhibits the induction of LTP in the dentate gyrus in vivo (Riedel and Reymann, 1993; Richter-Levin et al., 1994). However, which metabotropic receptor subtype is involved in this effect is not clear.

Thus, the second messenger systems involved in LTP induction could also reduce spike accommodation. Alternatively, LTP induction and the reduction of spike accommodation could be two independent events; but the prolonged depolarization caused by the reduction of spike accommodation could contribute to LTP induction. The relationship of spike accommodation reduction and LTP induction is not clear at present. However, the possible linkages above can be tested experimentally.

4.3.3 Quantal analysis and recruitment of "silent" synapses

Traditionally, discussion of the mechanism of LTP expression has revolved around

three factors: increased transmitter release, increased sensitivity of postsynaptic receptors and the recruitment of additional synapses. In terms of the quantal analysis of synaptic transmission, these factors generally correspond to changes in parameters *p*, *q* and *n* respectively. From the results of examining these parameters in various ways and taking advantage of the large magnitude of LTP induced in this study, it would appear that quantal size (*q*) alone cannot account for LTP in this system. Judged by direct measurements of spontaneous EPSCs, the quantal size did not increase in proportion to the potentiation observed after LTP induction. Thus, while it remains possible that an increase in quantal size may contribute to LTP, it is not the major factor.

The results of experiments III and IV support an increase in the number of available quantal units (n), with little change in mean probability of release. Probability of release at initially active synapses is fairly high, and it is not possible to get the magnitude of the LTP observed simply by increasing p at these synapses. More synapses must be added to the responding population. The addition of effective synapses is supported by the results obtained by quantal analysis (Table 4-3) and by quantal simulation (Figure 4-9). There are two possible mechanisms to increase the number of effective synapses. The first one is recruitment of additional axons by tetanic stimulation. However, the coefficient of variation analysis of evoked response does not support this mechanism (Figure 4-10). The variance of the evoked responses will change by recruiting additional axons and this change is not consistent with the change observed during LTP (Figure 4-10).

The other possible mechanism of increasing effective synapses is to recruit previously "silent" synapses during LTP. These silent synapses might have a low level transmission, but not necessarily a low probability of release. The low level of transmission could be caused by low concentration of transmitter released by each vesicle, obstacles in the synaptic cleft affecting transmitter diffusion, low number of responding receptors in the postsynaptic membrane, or improper alignment of the release site and the receptor location. The real number of transmitter molecules in a vesicle is currently unknown; however, it is believed that the number is usually constant and estimates of the concentration of glutamate range from 60-210 mM have been proposed (Burger et al., 1989; Riveros et al., 1986; Nicolls and Attwell, 1990; Shupliakov et al., 1992). Thus, the low concentration of transmitter in vesicles seems an unlikely explanation for the low level of transmission. The obstacles in the synaptic cleft could be physical properties of the cleft or re-uptake of the transmitter; the concentration of transmitter reaching the postsynaptic side could thus be reduced. Since the synaptic cleft is only 20-30 nm (Faber et al., 1992), the transmitter molecule can reach the postsynaptic site in ns, as revealed by computational modelling (Clements, 1996). Because we know very little about the physical properties of the synaptic cleft, what might happen in such a short time span is currently unknown. Although changes in the synaptic cleft could provide a possible mechanism for manipulating the transmitter concentration, this is an unlikely mechanism. Isaac et al. (1995) discovered that at CA1 pyramidal cells, depolarizing the cell from resting membrane potential to a positive membrane potential could turn the previously silent synapses into active ones. In their

experiments, the only change made to alter synapse behaviour is postsynaptically depolarizing the cell and this indicates that the alteration happened in the postsynaptic receptors and not in the presynaptic release or diffusion of the transmitters.

There are several possible mechanisms to modulate the postsynaptic receptors. It has been shown for example that the AMPA receptors can be modulated by phosphorylation (Blackstone et al., 1994). There might be a mechanism like phosphorylation to turn the receptor "on" or "off". It is also possible that the release sites and the receptors are not aligned (extra-synaptic receptors), and thus, the transmitter concentration becomes too low by the time it reaches the receptor. Thus, to achieve a larger postsynaptic response, like the ones after LTP induction, the receptor has to shift towards the release site, which will be called receptor translocation here (Xie et al., 1995, personal communication). Another type of receptor translocation is that the receptors are already assembled in the cytoplasm near the synapse, and upon LTP induction, they will be inserted into the postsynaptic membrane to express their function.

The mechanism of recruiting "silent" synapses might have a postsynaptic origin or a presynaptic origin. In the postsynaptic theory, the silent synapse is due to inactive AMPA receptors (Figure 4-12). The transmitter is released by the presynaptic terminals however, the postsynaptic AMPA receptors do not respond. This, in turn, would cause insufficient membrane depolarization and inability to expel the Mg^{2+} ion blocking NMDA channel pores. Alternatively, the NMDA channels might be open due to the depolarization provided by neighbouring synapses. However, the NMDA current may be too small and masked by the background noise. After LTP induction, the AMPA receptors

Figure 4-12 Two models of silent synapse hypothesis. The postsynaptic model suggests that at the silent synapse the presynaptic terminal releases transmitter, but the AMPA receptors in the postsynaptic site are inactive. Thus, there is no depolarization to expel the Mg^{2+}- block in the NMDA channel pore, and no postsynaptic response is detected. After LTP induction, various protein kinases are activated by Ca^{2+} and some might phosphorylate the AMPA receptors and make them active. In the presynaptic hypothesis, the transmitter concentration is too low to activate the low-affinity AMPA receptor. Thus, although the high-affinity NMDA receptor might be opened by the low concentration of transmitter, there is not enough membrane depolarization to remove the Mg^{2+}-block. After LTP induction, the Ca^{2+} entering via the NMDA receptor channels triggers a retrograde messenger systems, and a retrograde messenger diffuses back to the presynaptic terminal to facilitate transmitter release.

Recruitment of "silent" synapse models

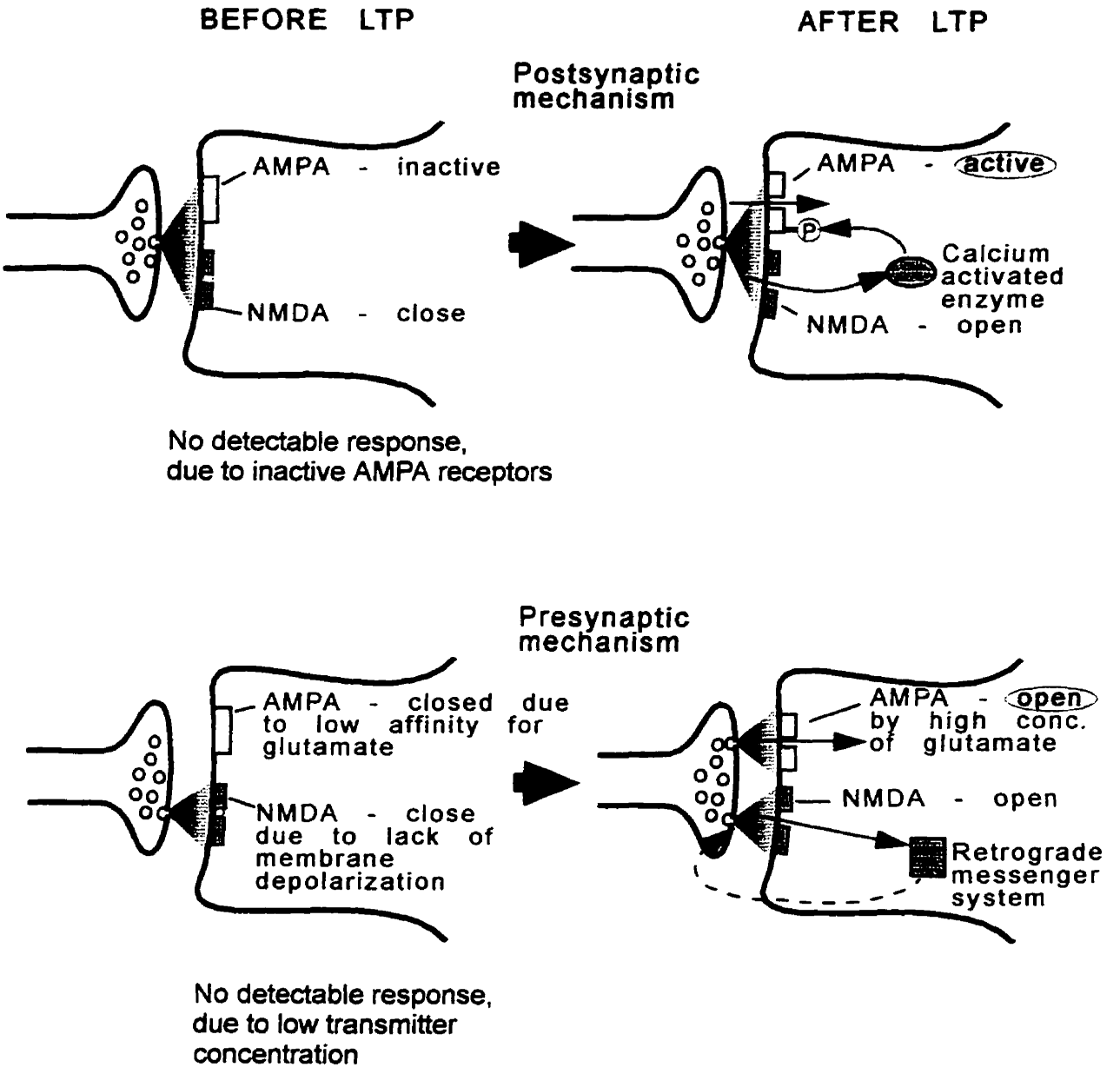

can become active by phosphorylation or by other as yet to be discovered mechanisms. The postsynaptic hypothesis is supported by the evidence for silent synapses in CA1 obtained by Isaac et al. (1995) and Liao et al. (1995).

The presynaptic theory hinges on the fact that the NMDA receptor has a much higher affinity for glutamate than for the AMPA receptor (Figure 4-12). If the transmitter concentration is low, then only the high affinity NMDA receptor will bind with the transmitter while the low affinity AMPA receptor remains inactive. After LTP induction, a retrograde messenger released from the postsynaptic site would stimulate more transmitter release from the presynaptic terminals; thus, leading to a higher transmitter concentration which could now activate the previously inactive AMPA receptors. The idea of more glutamate release after LTP induction is supported by the findings of Dolphin et al. (1982), which showed an elevation of glutamate concentration after LTP induction in the dentate gyrus. One of the proposed retrograde messenger, arachidonic acid has a time course which is too slow to account for the early phase of LTP (Bliss and Collingridge, 1993). The other proposed retrograde messenger, nitric oxide, has been shown to stimulate transmitter release in the CA1 region (Segovia et al., 1994). Several groups have reported that blockade of nitric oxide synthase (enzyme for nitric oxide production) does not prevent the induction of LTP (Bannerman et al., 1994; Boulton et al., 1994; Cummings et al., 1994). However, it was since found that it may be the so-called "endothelial", as opposed to the "neuronal", form of nitric oxide sythase that is the principle source of nitric oxide in CA1 pyramidal cells (Dinerman et al., 1994; O'Dell et al., 1994). O'Dell et al. (1991) have shown evidence for nitric oxide as a possible early

retrograde messenger.

The evidence presented here is more in favour of the postsynaptic model for recruiting silent synapses. The following chapter will provide further evidence for a postsynaptic mechanism for LTP expression.

Chapter 5 Synaptic recruitment during long-term potentiaion at synapses of the medial perforant pathway in the dentate gyrus of the rat brain

Results of this section have been published in Wang, S.; Wojtowicz, J.M.; and Atwood, H.L. (1996) Synaptic recruitment during long-term potentiation at synapses of the medial perforant pathway in the dentate gyrus of the rat brain. Synapse 22:78-86.

5.1 Abstract

Long-term potentiation (LTP) in synapses of the medial perforant pathway of the rat dentate gyrus has been studied using the whole-cell voltage clamp technique and a standard hippocampal slice preparation. The rate of LTP induction by 2-4 brief trains of stimuli at 100 Hz, paired with postsynaptic depolarization to -20 mV, in individual granule neurons was only 42% but the average magnitude was large. In a representative series of nine experiments the average potentiation was 339% (s.d. 255%). The variable magnitude of LTP appeared to be related to the relative size of the NMDA receptor dependent current in individual neurons. LTP was further characterized by the selective enhancement of the AMPA (but not the NMDA) component in the excitatory synaptic responses. This selective enhancement of the AMPA component and a graphical variance analysis suggest that the large magnitude of LTP in dentate gyrus can be best explained by recruitment of previously silent synapses by a combination of pre and postsynaptic mechanisms.

5.2 Introduction

Long term potentiation (LTP) is known to occur in all three regions of the hippocampal trisynaptic circuit: dentate gyrus, CA3, and CA1 areas (Berger and Yeckel,

1991). Of the three areas, the perforant path-dentate gyrus projection has been least well characterized by intracellular recordings, undoubtedly due to difficulties with stable recordings from relatively small granule neurons. With the advent of the whole-cell patch recording technique, stable recordings from the dentate granule neurons are now possible and the mechanisms of LTP in these cells are open for investigation. The afferent axons of the perforant path converge on dendrites of the granule neurons but retain their segregation into the functionally different lateral (LPP) and medial (MPP) perforant pathways (Witter, 1989). Anatomical studies show termination of the LPP on the distal one third, and of the MPP, on the middle one third of the dendritic tree (Witter, 1993). In a recent paper by Colino and Malenka (1993) it was found that both MPP and LPP require participation of N-methyl-D-aspartate (NMDA) glutamate receptors for induction of LTP *in vitro*. This finding confirms earlier observations based upon field potential recordings (Hanse and Gustafsson, 1992). Thus, with regard to the types of glutamate receptors required, the mechanism of LTP induction in dentate granule neurons is similar to that found in CA1. However, in addition, LTP in the medial pathway is modulated by muscarinic cholinergic receptors (Burgard and Sarvey, 1990), noradrenergic receptors (Dahl and Sarvey, 1990), and $GABA_B$ receptors (Mott and Lewis, 1991). The lateral pathway has been reported to be strongly influenced by opioid peptides *in vivo* (Bramham et al., 1991).

The mechanism of expression and maintenance of LTP is less well understood. Quantal analysis can, in principle, determine whether the expression of LTP is pre- or postsynaptic but its use in the dentate gyrus has been limited to a single, preliminary

study which did not distinguish between the two divisions of the perforant pathway (Baskys et al., 1991). A recent report by Christie and Abraham (1994) compared LTPs in medial and lateral perforant pathways *in vivo* using the paired-pulse paradigm as an assay for possible presynaptic effects. They concluded that an increase in probability of transmitter release plays a role in the lateral but not in the medial perforant path.

In the present investigation, we have extended our analysis of the mechanism of LTP expression in the medial perforant pathway. We observed that induction of LTP in this pathway resulted in large increases in the excitatory currents in some (but not all) of the cells receiving input synapses. Analysis of evoked responses suggests recruitment of previously inactive AMPA component at synapses by induction of LTP. A preliminary account of these results has been presented (Wojtowicz et al., 1994, Soc. Neurosci. Abstr., vol 20, p.847).

5.3 Materials and methods

5.3.1 Brain Slice Preparation

Hippocampal slices were prepared from 16-30 day old Wistar rats of either sex. The rats were anaesthetized with halothane and decapitated by a guillotine. Hippocampi were quickly removed from the brain and sliced by tissue chopper into 400 μm transverse slices. Slices were kept in a moist and oxygenated holding chamber for over 1 hour at room temperature, before being transferred to a recording chamber for experimentation. In the recording chamber, the slice was continuously superfused with

artificial cerebrospinal fluid (ACSF) (2ml/min) that had been saturated with 95% O_2-5% CO_2. The composition of the ACSF was (in mM): 124 NaCl, 3 KCl, 1.25 $NaHPO_4$, 1 $MgCl_2$, 2 $CaCl_2$, 26 $NaHCO_3$, 10 dextrose, and 0.01 bicuculline methiodide. The temperature of the medium was kept at 30-32°C.

5.3.2 Stimulation and Recording Techniques

Two bipolar tungsten electrodes were placed at the outer and middle thirds of the dentate gyrus molecular layer to stimulate the lateral and medial perforant paths, respectively. "Blind" whole-cell patch-clamp recordings were made from dentate granule cells with patch electrodes (1-2 µm outside tip diameter, 5-8 MΩ) filled with (in mM) : 142.5 potassium gluconate, 17.5 $KMeSO_4$, 8 NaCl, 10 HEPES, 0.1 EGTA, 2 MgATP, 0.2 GTP, pH=7.3, osmolality=290-300 mOsm. Recordings were performed with an Axopatch-1D patch clamp amplifier (Axon Instruments) and monitored by a computer. The signals were also recorded via Neuro-Corder (Neuro Data Instruments Corp.) to VCR tapes for additional off-line analysis. During synaptic stimulation, cells were held under voltage clamp at a constant membrane potential ranging from -55 to -75 mV. All membrane potentials presented in the RESULTS refer to the potential recorded at the soma. Records illustrated in the RESULTS were digitized at 100-200 µs/bin: averaged traces included 400-500 individual sweeps.

Excitatory synaptic currents (EPSCs) were elicited by test pulses applied once every 2 seconds to the medial perforant pathway (MPP) and to the lateral perforant pathway (LPP) with 50 -200 ms delay between the two pathways. It was determined that

this procedure produced no mutual facilitation or depression between synapses of the two pathways. Thus, the stimulation of the lateral pathway provided a useful measure of the stability of synaptic transmission unaffected by tetanic stimulation.

Before starting whole-cell patch recordings, an extracellular field potential electrode (5 μm tip diameter, filled with ACSF) was placed at the MPP to verify separation of MPP and LPP pathways by activating them while recording current sinks and sources. The slices which failed to show distinct current sinks and sources for the different pathways were rejected. In the accepted slices, the stimulating electrodes were kept at the same place throughout the experiment while the intensity of the stimulation was further reduced during whole-cell recordings to obtain "minimal" stimulation, with occasional failures of synaptic transmission. It is not certain how many axons were stimulated by this technique and if stimulation always reached threshold at the participating axons but we made sure that stimulation gave stationary EPSCs and that it was not changed during LTP (see Results). The distance between the two stimulating electrodes was 80-100 μm. Stimulus intensity ranged from 0.1-1.2 mA, and stimulus duration was 10 μs. These minimal stimulus intensities further reduced the possible overlap of the stimulation fields of the two pathways.

Three methods were employed to induce LTP in MPP synapses. The first was to release the cell from voltage-clamp during tetanic stimulation consisting of two 100 Hz trains (1 s duration) at test pulse intensity, applied 10 s apart. This method proved not to be very effective in inducing LTP. The second and more effective method was to voltage-clamp the cell to -20 mV while applying tetanic stimulation consisting of two 100

Hz trains (1 s duration) at test pulse intensity applied at 10 second intervals. The third and most effective method was to voltage-clamp the cell to -20 mV while applying four 100 Hz trains (0.5 s duration) at test pulse intensity (10 sec intervals). The success rates for these two procedures among the cells analyzed is shown in Table I. It is likely that the intracellular depolarization had a strong effect on synapses of the MPP which are about 100 μm distant from the cell body layer. Estimates of cable properties of the granule cell dendrites suggest only a minimal decrement of steady state signal over such a short distance (Staley et al., 1992).

5.3.3 Curve fitting

To evaluate the rates of decay of the evoked synaptic currents we fitted double exponentials to the decay phases of averaged traces of EPSCs using the curve fitter in Sigma Plot Scientific Graphing Software, Jandel Scientific (1993). Only traces giving two clear exponentials fitted with standard errors of less than 5% of the estimated values of parameters were accepted for analysis. The linear regression in Figure 4 was obtained using the least squares method (Sigma Plot, Jandel Scientific, 1993).

5.3.4 The coefficient of variation analysis of LTP

Four to five hundred stationary, evoked responses were used to calculate the ratio of the mean of the evoked responses squared, to their variance (M^2/var) (Bekkers and Stevens, 1990; Malinow and Tsien, 1990; Xiang et al., 1994). This ratio is equal to the inverted and squared coefficient of variation. As shown originally by del Castillo and Katz

(1954), the coefficient of variation varies in a predictable way with quantal content of synaptic transmission but is independent of the quantal size. However, the relationship between the variance and quantal content depends on the characteristics of the release process. Thus it will be different for Poisson and binomial distributions. The calculated change in the M^2/var ratio associated with a five-fold increase in quantal content for a Poisson distribution should be equal to five. For a simple binomial distribution the ratio is also five if the change is due to increased parameter n but larger if the change is due to increased probability of release. Lower slopes indicate a larger change in variance than expected from the simple binomial or Poisson distributions. It can be shown that for a non-uniform binomial distribution, characterized by variable probability (p) of release among synapses, the variance of EPSCs is strongly (inversely) dependent on the variance of p (del Castillo and Katz, 1954). This dependence can produce low (<45°) slopes on the graphical variance plots under certain conditions when, for example, the variance of p is reduced as the responses are increased in size. However, changes of the mean responses caused by increases in quantal size would not be expected to alter M^2/var ratios (Malinow and Tsien, 1990).

Faber and Korn (1991) pointed out certain caveats in the coefficient of variation method when probabilities among the quantal units are non-uniform. Given many hypothetical factors which can alter the coefficient of variation of evoked EPSCs, one should use it carefully. For example, we have addressed a hypothetical situation given by Faber and Korn with an experiment where additional axons are recruited during an experimental manipulation and found a predicted change in the M^2/var ratio (see Results).

5.3.5 Drugs

The chemicals used to make ACSF and the intracellular solution were purchased from BDH, Baker and Sigma. Bicuculline methiodide and D-2-amino-5-phosphonovaleric acid (D-APV) were purchased from Sigma. 6-cyano-7-nitroquinoxaline-2,3-dione (CNQX) was purchased from Research Biochemicals International (RBI). CNQX was dissolved in dimethyl sulphoxide (DMSO) and the final concentration of DMSO in ACSF was 0.1-0.05%.

5.4 Results

5.4.1 Long-term potentiation in medial perforant pathway

In this study we have concentrated on the mechanism of LTP in the medial perforant pathway. Synapses of this pathway terminate relatively near (100-200 μm) the cell body of the granule neurons and should be easily accessible to the whole-cell recordings. The responses of the lateral pathway were monitored in all experiments and served as useful controls for stability of the recordings and selectivity of the LTP effects.

In our initial series of experiments in which voltage clamp control of the resting membrane potential was released for the duration of tetanic stimulation, it was noted that the rate of LTP induction with "minimal" (low intensity) stimulation was low (see Table 5-I). This resuit may have been due to insufficient depolarization of the cells by this type of synaptic stimulation. Consequently in the remaining experiments we paired the tetanic stimulation of afferents with postsynaptic depolarization to -20 mV, imposed by the

voltage clamp circuit (Wigström and Gustafsson, 1986). This latter procedure produced significant LTP in 42% of cases (11/26 cells; Table 5-I). LTP was considered significant if the evoked excitatory postsynaptic currents (EPSCs) 15-20 minutes after tetanization were significantly greater than the controls (paired t-test $P<0.05$).

Figure 1 illustrates the time course and magnitude of synaptic enhancement following successful induction. In this series of experiments there was more than a 3-fold enhancement in amplitude of the EPSCs 20 minutes after tetanization (mean 339%, s.d. 255%, n=9). LTP in individual experiments ranged between 135% and 943% of control values. The large LTP in the medial pathway was accompanied by a smaller and statistically insignificant enhancement (paired t-test $P>0.1$) of responses elicited by stimulation of the control, lateral pathway (Figure 5-1).

It should also be noted that the magnitude of medial pathway LTP calculated on the basis of all 36 cells listed in Table 5-I was 177% of the baseline. This average is similar to the values frequently reported for these synapses using the field recording measurements (Hanse and Gustafsson, 1992, Colino and Malenka, 1993). We have determined that during tetanic stimulation with strong stimuli, such as used for evoking the field responses, the membrane potential of unclamped granule neurons reaches at least -20mV, a level comparable to that used during the paired paradigm described above.

Table 5-I. Induction of LTP in medial perforant pathway

Method of Induction	Success rate of Induction	Magnitude of LTP (% of control)	Overall LTP (% of control)
Afferent stimulation (100 Hz, 1s, 2 trains)	1/10 cells (10%)	610%	151% (n=10)
Afferent stimulation paired with post-synaptic depolarization (100 Hz, 1s, 2 trains, -20 mV)	2/8 cells (25%)	175% ± 22 (S.D.)	119% (n=8)
Afferent stimulation paired with post-synaptic depolarization (100Hz, 0.5s, 4 trains, -20 mV)	9/18 cells (50%)	339% ± 256 (S.D)	218% (n=18)

Induction of LTP was considered successful when the mean of evoked EPSCs 15-20 min after tetanization reached a level statistically different (paired t-test, $P<0.05$) from control. Only such significant LTP cases are listed in columns 2 and 3. Column 4 gives the overall, average enhancement in all cells.

Figure 5-1 Top: experimental arrangement for the whole-cell recordings and for stimulation of medial (MPP) and lateral (LPP) perforant pathways. Bottom: time course and magnitude of LTP in the MPP. Whole-cell synaptic currents were measured. Results from nine experiments show large but variable effect for MPP synapses. Tetanic stimulation consisting of 4 trains of pulses at 100 Hz, lasting 500ms and repeated every 10 seconds was applied at time zero. Data from the same series of experiments is presented in the last row of Table I. A smaller, statistically insignificant (paired t-test, $P>0.1$) effect was seen in the untetanized lateral perforant pathway (LPP). Both pathways were stimulated continuously at 0.5 Hz. Each point in the graph represents an average of 30 stimulations. Standard error bars are indicated at 5 minute intervals.

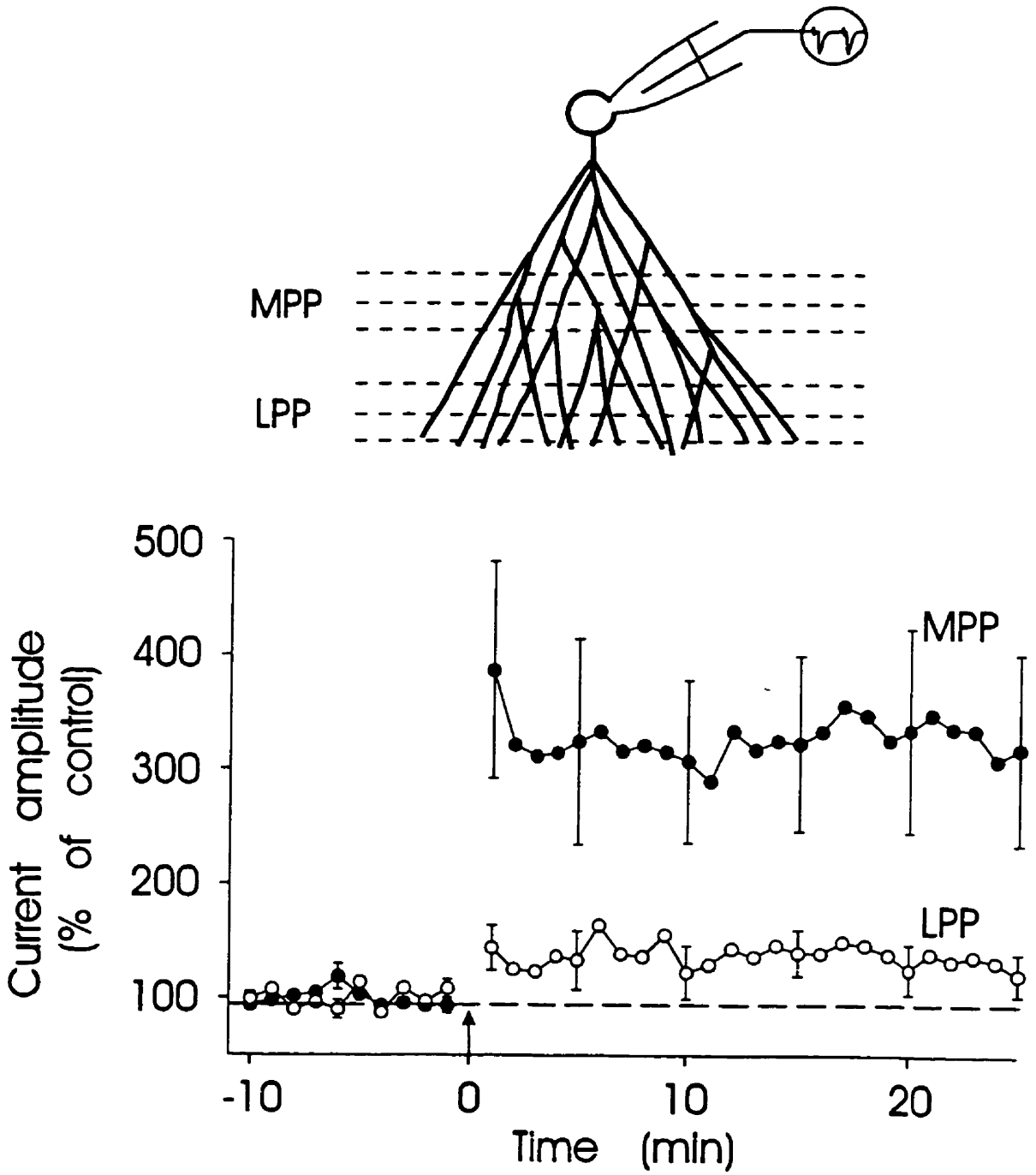
MPP
LPP
500
400
300
200
100
Current amplitude
(% of control)
MPP
LPP
-10
0
10
20
Time (min)

5.4.2 Selective LTP of "early" EPSCs

Synaptic responses at the perforant path synapses are composed of early and late components corresponding to activation of AMPA (α-amino-3-hydroxy-5-methyl-4-isoxazoleproprionic acid) and NMDA receptors, respectively (Lambert and Jones, 1990). In contrast with pyramidal neurons in CA1, granule neurons exhibit a significant NMDA component at resting membrane potentials and in the presence of 1 mM Mg^{2+}(Keller et al., 1991).

In several cells showing robust LTP, we fitted the decay phases of the EPSCs with double exponentials to confirm the presence of early and late components (Table 5-II). Consistently, only the fast component increased significantly during LTP. This was particularly well seen in experiments where LTP was large. In Figure 5-2, for example, the amplitude of the fast component, given by the intercept of the first exponential, increased about seven-fold while that of the slow component remained virtually unchanged. The magnitudes of the two components obtained from curve fitting corresponded closely to the relative contributions of the early and late components defined pharmacologically . In a series of experiments, the peak amplitudes of the evoked EPSCs were reduced by 85.5% (s.d.=6.14, n=8) in presence of 5 μM 6-cyano-7-nitroquinoxaline-2,3-dione (CNQX) indicating the dominant but not exclusive involvement of AMPA receptors in the peak responses of EPSCs. The smaller but more prolonged component was blocked selectively by 25 μM D-2-amino-5-phosphonovaleric acid (D-APV) (n=10).

Direct comparison of the slow component derived from the exponential fitting

Table 5-II. Analysis of the decay rates of evoked EPSCs in four experiments

Exp.	Control				LTP			
	a_1 (pA)	τ_1 (ms)	a_2 (pA)	τ_2 (ms)	a_1 (pA)	τ_1 (ms)	a_2 (pA)	τ_2 (ms)
1	15.8	6.3	2.8	29.0	104.7	7.8	2.8	30.7
2	21.2	8.4	1.0	48.7	59.5	9.3	0.9	70.1
3	14.8	3.7	1.0	31.3	29.5	4.3	1.0	59.8
4	9.5	5.8	2.4	23.2	51.3	7.0	1.3	44.5
	15.3±4.8	6.1±1.9	1.8±0.94	33.1± 11.0	61.3±31.6*	7.1±2.1	1.5±0.9	51.3±17.3

The fast components are the postulated responses of AMPA receptors and slow components are postulated to be due to activation of NMDA receptors. In all cases the decay phases of EPSCs were well fitted by double exponentials. Parameters a_1 and a_2 indicate the x-axis intercepts of the fast and slow components respectively. Parameters τ_1 and τ_2 indicate the corresponding time constants. In Mg^{2+}-free medium or at depolarized membrane potentials the decay of the NMDA component should follow two exponentials. We did not detect the second exponential presumably due to partial blockade by ambient Mg^{2+} (see Keller et al.,1991).

* Note that only a_1 shows a significant change after LTP induction (Paired t-test, $P<0.05$).

Figure 5-2 **A**. Time course of a single experiment showing a large LTP in medial pathway. **B**. Superimposed averaged traces of the evoked EPSCs during the control period (a), 15-20 minutes after tetanus (b), and 40-45 minutes after tetanus (c). TM indicates the time of tetanic stimulation applied to the medial pathway. Note that the lateral pathway remained essentially unchanged. **C**. Superimposed control (1) and potentiated (3) responses with double exponential curves fitted to the descending phases. The time constant of the rapid component in the control curve was 6.3 ms and the slow one was 29 ms. In the potentiated response the corresponding values were 7.8 ms and 30.7 ms. The intercept of the fast component increased approximately 7 times during LTP. The intercept of the slow component did not change (curves 2&4). Note: the data from the same cell are presented in experiment 1 in Table 5-II.

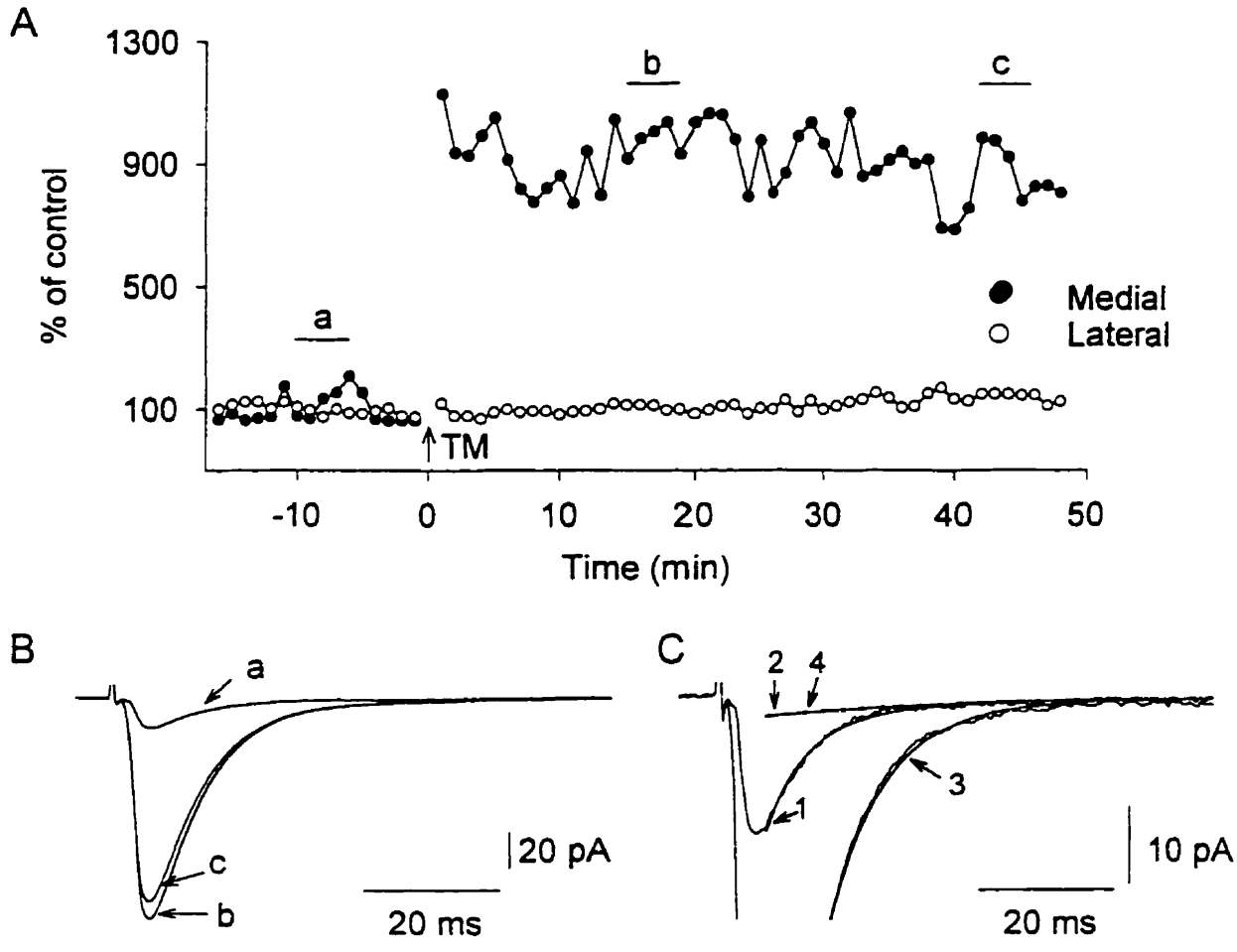
A
1300
900
500
100
% of control
a
b
c
TM
Medial
Lateral
-10
0
10
20
30
40
50
Time (min)
B
a
c
b
20 pA
20 ms
C
2
4
1
3
10 pA
20 ms

with the NMDA-dependent component obtained in the presence of CNQX confirmed the former procedure as a reliable and non-invasive method to measure the NMDA currents in granule neurons (Figure 5-3A) . These results argue that the early and late components are mediated by AMPA and NMDA receptors, respectively, and that there is a selective increase in the AMPA-receptor mediated component of the EPSCs during LTP.

We confirmed this observation in a series of experiments where the typical, large LTP was induced and CNQX was applied to the potentiated responses (Figure 5-3B). In these experiments the average percentage of NMDA current before LTP induction was 17% (s.d.=2.5%). In three experiments, in which induced LTP averaged 389% (s.d.=71%), the proportion of the NMDA current in the potentiated response was reduced to 4%. The results clearly indicate that the magnitude of NMDA component did not change during LTP, and that the non-NMDA component was selectively enhanced.

Among neurons where the NMDA component was isolated and measured, the magnitude of LTP was positively correlated with the initial relative size of the NMDA current. In seven cells which did not show LTP, the NMDA component was on average 9% of the total synaptic current. In five cells which showed large LTP (>3 fold), the NMDA component was 19% (s.d.=4%).

5.4.3 The coefficient of variation analysis of LTP

It has been shown theoretically and experimentally that changes in the Mean^2/variance (M^2/var) ratio of EPSCs are independent of quantal size but vary in a

predictable manner with quantal content (Malinow and Tsien, 1990; Xiang et al., 1994). Data from five representative experiments plotted in the graph in Figure 4 indicate clearly that increase of quantal content contributes to LTP, because the linear regression vector on the graphical variance display has a slope significantly greater than zero but smaller than the 45° line. However, the slope indicates a departure from predictions based on either Poisson or simple binomial distributions which require the M^2/var ratio to fall on or above the diagonal (45°) line. To explain the low slope, we propose that the statistical distribution of evoked EPSCs in dentate gyrus is a non-uniform binomial. In such distributions, the variance of EPSCs is less than that of a simple binomial distribution with equal probabilities among the release sites (McLachlan, 1978; Brown et al., 1976). Consequently, the relationship in Figure 4 can be explained if the initially large variance of probability was reduced during LTP. This would occur, for example, if a small number of non-uniform, active synapses was replaced by a larger number of strong, more uniform synapses. Alternatively, the low slope can be obtained by simply increasing the number of synapses without changes in the variance among synapses.

To test the effects of a simple recruitment of axons, we conducted two experiments in which EPSCs were increased by increasing the stimulus intensity. In these experiments much larger changes of M^2/var were observed (Figure 5-4, open squares). In three other experiments, the concentration of extracellular Ca^{2+} was lowered from 2 to 0.5 mM in order to change the probability of release at synapses. The resulting changes in the M^2/var ratios fell well above the diagonal, 45° line (Figure 5-4, open circles), in accordance with expectations.

Figure 5-3 **A**. Representative traces from CNQX experiments. The control currents were superimposed with double exponential curves (τ_1 + τ_2) fitted to the descending phases of the currents (dashed lines). The residual currents in CNQX (NMDA component) correspond well with the τ_2 trace, derived from the second component of the double exponential curve fitted to the control current. **B**. Effects of CNQX on potentiated EPSCs. The NMDA current measured after induction of LTP, contributed only a very small portion (3%) of the potentiated response (LTP trace). Inset: expanded view of NMDA component after induction of LTP and the control EPSC. Note that the ratio of the NMDA to control current is about 15%, which is in the normal range.

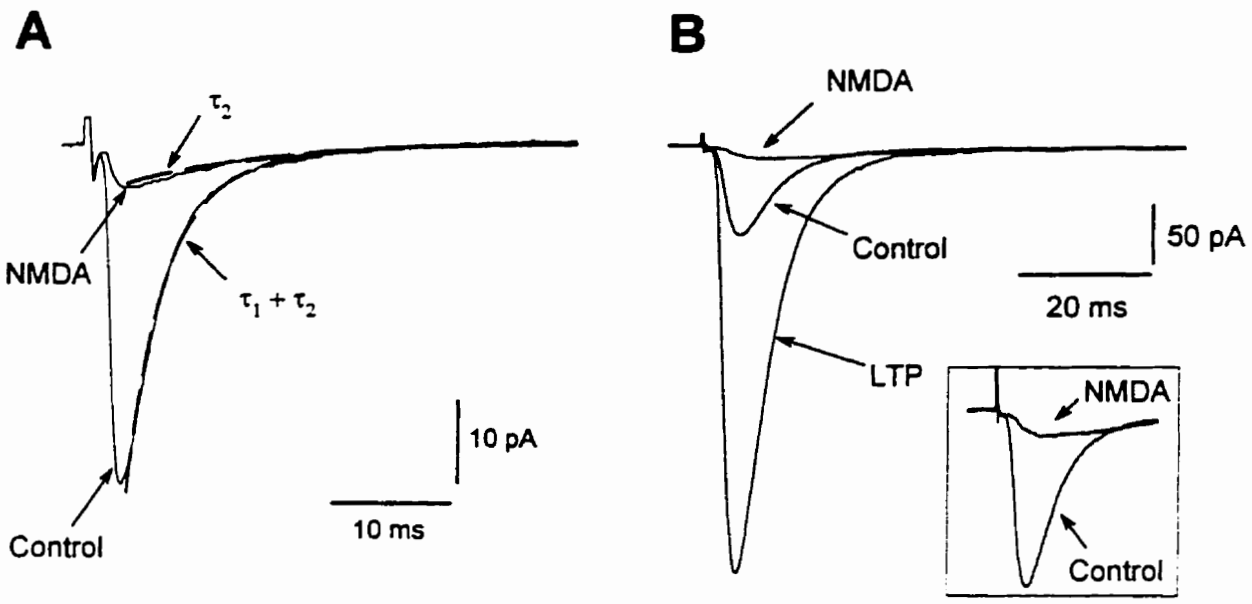
A
τ_2
NMDA
$\tau_1 + \tau_2$
10 pA
10 ms
Control
B
NMDA
Control
50 pA
20 ms
LTP
NMDA
Control

Figure 5-4 Results of five LTP experiments (filled circles) showing large increases of synaptic currents associated with consistent increases of the M^2/variance ratios. The linear regression line is drawn through the data points and the broken lines indicate the 95% confidence limits. Note that the values of M^2/var ratios fall significantly below the diagonal, 45° line (dotted) and are consistent with our own calculated values in a representative non-uniform binomial distribution with increased parameter *n* and reduced variance of parameter *p* (see Methods). For comparison, we have plotted results from two experiments where the stimulus intensity was increased to recruit additional axons (open squares). In this case the points fall above the diagonal as would be expected from increased *n* with larger variance of *p*. Calculated values of the M^2/var ratio for changes in the probability of release would also be expected to fall above the diagonal. This was confirmed in three experiments where the probability was changed by lowering the extracellular Ca^{2+} concentration (open circles). Hypothetical changes in quantal size during LTP would not be expected to alter M^2/var ratios and data points would fall on the dotted horizontal line.

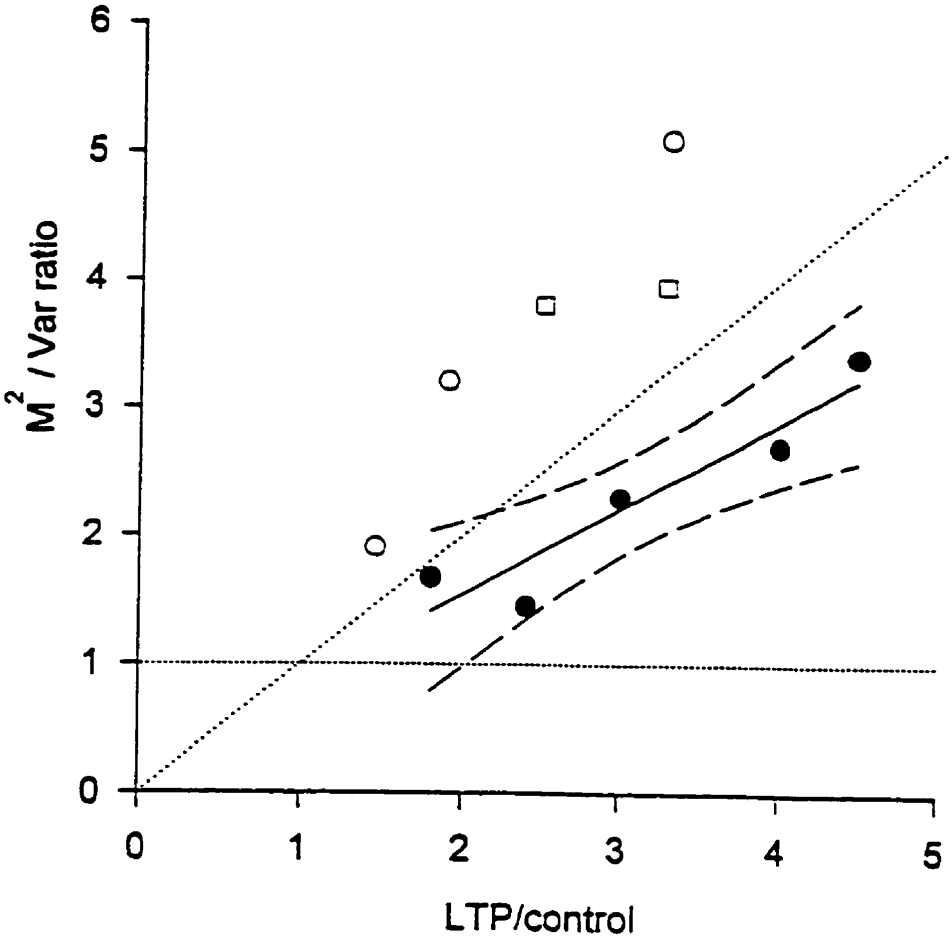
6
5
4
3
2
1
0
M^2 / Var ratio
0
1
2
3
4
5
LTP/control

We employed a further test to confirm that the lowering of calcium concentration suppressed transmission by reducing the probability of transmitter release. In each experiment, a brief train of stimuli at 30 Hz was applied to evoke high-frequency synaptic depression. Such depression is a characteristic feature of synapses in MPP. After lowering the calcium concentration from a normal 2 mM to 0.5 mM and substituting manganese for the removal of calcium, the high-frequency depression was abolished. Control experiments showed that simply lowering the stimulus intensity did not reduce the depression (Fig.5-5). The tendency of the MPP synapses to depress during repeated stimulation in normal calcium places them in a "high output" category. Such synapses have been well characterised in other, extensively studied preparations such as the frog neuromuscular junction and are known to have a relatively high probability of transmitter release (see Discussion).

5.5 Discussion

5.5.1 Properties of LTP in MPP synapses

The termination of MPP on the central portions of the granule cell dendrites offers favourable conditions for electrophysiological recording of small synaptic currents due to the relatively short distance between terminating synapses and the site of recording, and the laminar arrangement of afferent synapses on dendrites (Witter, 1989). Moreover, the properties of the medial synapses are distinct from those of the lateral synapses and perhaps from other synapses in the hippocampus. When stimulated at intervals of 40-

Figure 5-5 High-frequency synaptic depression in MPP. Low calcium concentration in the perfusion solution reduces the responses and abolishes the high-frequency depression. A third trace shows that after wash-out of the low Ca^{2+} solution, reducing the stimulation strength to the level matching the smaller responses seen in low Ca^{2+} does not diminish the depression.

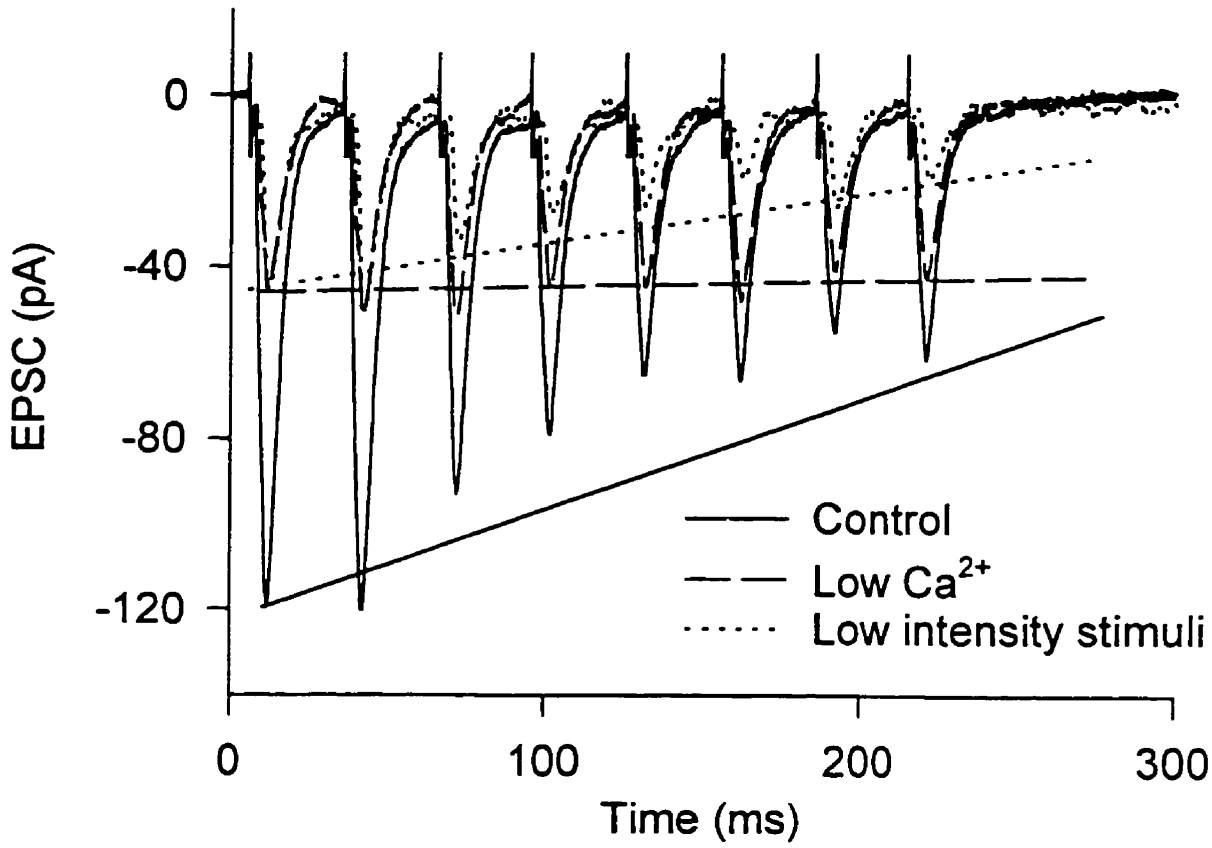
0
-40
-80
-120
EPSC (pA)
Control
Low Ca2+
Low intensity stimuli
0
100
200
300
Time (ms)

1000 ms, the synapses of the medial pathway show paired-pulse depression rather than facilitation (McNaughton, 1980; Hanse and Gustafsson, 1992; Colino and Malenka, 1993). Such short-term depression is a characteristic feature of the high-output synapses seen in the vertebrate neuromuscular junctions, the squid giant synapse, and certain crustacean synapses (reviewed in Atwood and Wojtowicz, 1986). Similar differentiation between facilitating (initially "weak") and depressing (initially "strong") synapses in the mammalian cortex have been described recently by Thompson et al. (1993).

It would appear that quantal size alone cannot account for LTP in this system. We see no evidence of increased quantal size from the coefficient of variation analysis of evoked EPSCs. However, a combination of increased quantal size and increased probability could account for the observed changes in M^2/var ratios.

It is very unlikely that the increase of responses during LTP could have resulted from recruitment of additional axons by tetanic stimulation because this latter mechanism, when activated, has an entirely different effect on the coefficient of variation (see Figure 5-4) and would be expected to recruit AMPA and NMDA components equally, which is not the case (Figures 5-2 and 5-3). On balance, the results argue against simple mechanisms of LTP such as increased quantal size, increased overall probability of release, or recruitment of additional axons. Instead, the analysis suggests a modification of transmission consisting of a recruitment of previously silent synapses. This mechanism is in agreement with the *in vivo* observations of Christie and Abraham (1994) who found a reduction in the paired-pulse facilitation in the lateral but not the medial perforant pathway. A change in the paired-pulse facilitation would indicate a change in probability

of transmitter release.

The very large magnitude of LTP seen in some granule cells could be explained by the relatively large ratios of NMDA to AMPA current (see Results and Table 5-II). At this time it is difficult to ascertain if the differences in the magnitude of the NMDA current were due to "wash out" or to normal variability among neurons.

5.5.2 Recruitment of AMPA receptors

The selective enhancement of the early, AMPA component of EPSCs seems to point to a postsynaptic mechanism, unless it is assumed that recruited synapses have only AMPA and not NMDA receptors, which is contrary to other evidence in the literature (Bekkers and Stevens, 1989). Mechanisms have been suggested previously for AMPA receptor enhancement. According to one proposal (Lynch and Baudry, 1984; Gustafsson and Wigström, 1988), calcium ions, admitted via NMDA channels, could trigger an enhancement of AMPA receptors which are believed to be co-localized at the same synapses with the NMDA channels. Supporting evidence for this mechanism has been provided by Kauer et al. (1988) and Muller et al. (1989) who found selective enhancement of the AMPA component and not of the NMDA component during LTP in CA1 pyramidal neurons, in agreement with our present results from granule neurons. Postsynaptic modification of AMPA receptors, for example by phosphorylation (Blackstone et al., 1994; Wang et al., 1991) could lead to selective increase in the AMPA component with minimal change in quantal size, if the enhanced AMPA component occurs at synapses which were effectively silent or possessed only the NMDA

component prior to LTP. Another possible mechanism leading to recruitment of AMPA receptors would entail presynaptic modification of transmitter release sites resulting in greater concentration of glutamate in the synaptic cleft after LTP. This type of mechanism is supported by reports of increased release of glutamate during LTP in dentate gyrus (Errington et al., 1987; Feasey et al., 1986). The increased glutamate release could selectively enhance the AMPA component of EPSCs through a mechanism whereby the NMDA receptors are fully saturated prior to LTP by the released glutamate, and additional release of glutamate after LTP induction could recruit more AMPA receptors. This type of recruitment, dependent on altered transmitter release due to presynaptic modification, is based on the recognized large differences in the binding affinity of glutamate to NMDA and AMPA receptors. The half-maximal concentration of glutamate required to saturate NMDA receptors is 2-3 μM and that for AMPA receptors is about 350 μM (Patneau and Mayer, 1990). However, it remains to be determined if the conditions in the synaptic cleft, where receptor binding can be strongly altered by the time course of transmitter diffusion, permit full differences in the affinities of the two receptor classes to be expressed (Perkel and Nicoll, 1993). The two mechanisms acting in concert would provide particularly effective quantal recruitment.

Significant increases of both AMPA and NMDA components of the synaptic responses were seen during LTP of the commissural/associational pathway in the dentate granule neurons (O'Connor et al., 1994). It should be noted that the magnitudes of these effects were relatively small (about 50% enhancement) in comparison to LTP seen in MPP in our study. Moreover, the changes in the NMDA component were

noticeable only at depolarized membrane potentials (-30mV) and not at the resting membrane potential (-70 mV). An interesting concept arising from these studies is that the enhancement of the NMDA-receptor dependent current reflects a change in voltage dependence of the NMDA channels. Such changes may entail different mechanisms than the selective recruitment of previously inactive AMPA channels proposed in the present paper.

5.5.3 Comparison with LTP in CA1

The mechanism of LTP expression in the medial perforant pathway may be different than in the more commonly studied synapses on CA1 pyramidal neurons. In CA1 the magnitude of LTP is usually smaller and the mechanism of its expression could involve a combination of increased probability of release and/or increased quantal size, depending on experimental conditions (Manabe et al., 1992; Stevens and Wang, 1994; Manabe and Nicoll, 1994, Manabe et al., 1993). An exhaustive review by Voronin (1993) concluded that changes in quantal size can contribute a modest (30-50%) part of LTP. A large but transient increase in size of miniature EPSCs can occur after application of repeated voltage pulses to CA1 pyramidal neurons (Wyllie et al., 1994). In still other experiments, an increase of the NMDA component did occur, indicating a possible additional mechanism which may serve to enhance LTPs during repeated inductions (Tsien and Malinow, 1990; Bashir et al., 1991; Asztely et al., 1992). These observations suggest that LTP in the CA1 synapses could involve mechanisms different from those likely to operate in the MPP. The difference may be related to the low average probability

of transmitter release estimated for these synapses (Rosenmund et al., 1993; Hessler et al., 1993).

5.6 Acknowledgements

This work was supported by an MRC Group grant to H.L.A. and J.M.W. We thank Steve Jones of the Medical Computing Division at the University of Toronto for writing data acquisition and analysis programs.

Chapter 6 Effect of $GABA_B$ receptors on synaptic interactions in dentate gyrus granule neurons of the rat.

Results of this chapter have been accepted for publication in Wang, S. and Wojtowicz, J.M. (1997) Effect of $GABA_B$ receptors on synaptic interactions in dentate gyrus granule neurons of the rat. Neurosci. (in press).

6.1 Abstract

Dendritic arborization permits convergence of synaptic inputs and their integration in single neurons. The granule neuron in the dentate gyrus represents a relatively simple example where anatomically and functionally distinct medial and lateral perforant pathways terminate on different regions of the dendritic tree. High frequency stimulation of either pathway alone results in the induction of long-term potentiation. However, whether the potentiated synapses in different parts of the dendrites interact is not known. In this study we have compared long-term potentiation and synaptic interactions in the lateral and medial perforant pathways in the "disinhibited" hippocampal slice preparation in the presence of the $GABA_A$ receptor blocker bicuculline.

The data show that the magnitude of long-term potentiation induced by tetanic stimulation was similar in both pathways, but differences between the two pathways were revealed after two or more tetanizations. A significantly smaller capacity for further long-term potentiation in the lateral, as compared to the medial, perforant pathway was found and can be attributed to stronger postsynaptic $GABA_B$ inhibition in distal dendrites of granule neurons. Blockade of $GABA_B$ inhibition with CGP36742 (100 μM) unmasked additional long-term potentiation in the lateral pathway. Presynaptically, $GABA_B$ receptors

produced a short lasting heterosynaptic depression in the medial pathway, which was reduced by CGP36742. Coincident activation of the two pathways boosted long-term potentiation only in the medial pathway. We propose that the interactions between the two pathways are orchestrated to maximize associative long-term potentiation in the medial pathway; this may be important for types of learning attributed to the hippocampus.

Key words: Dentate gyrus, Perforant pathway, LTP, $GABA_B$, Hippocampus.

6.2 Introduction

Spatial and temporal summation as well as inhibitory shunting mechanisms are the basic integrative mechanisms in dendrites of central neurons. Additional mechanisms relying on voltage-dependent glutamate N-methyl-D-aspartate (NMDA) channels (Thomson et al., 1993) and voltage-dependent sodium and calcium channels (Regehr et al., 1993; Kim and Connors, 1993), could provide amplifying mechanisms to boost the conduction of synaptic depolarization from distal dendrites towards the soma. In the hippocampal neurons a strong synaptic input can potentiate a weak synaptic input (Levy and Steward, 1983; Barrionuevo and Brown, 1983), presumably by providing membrane depolarization which relieves NMDA receptors from the magnesium blockade in other parts of the dendrites receiving the weak input (Gustafsson and Wigström, 1988; Lynch and Baudry, 1984). Another special case of such a facilitatory mechanism has been proposed by Thomson and Deuchars (1994) who considered a case of coincident synaptic inputs converging on the same cortical pyramidal neurons but terminating on

separate regions of the dendritic tree. In this case NMDA receptors would ensure summation and mutual boosting of the two inputs. Thus, when considering more than one synaptic pathway, the location of NMDA receptors, in addition to the temporal pattern of the stimulation, could affect the integration of synaptic inputs.

The NMDA receptors are known to play a crucial role in long-term potentiation (LTP) induction in the hippocampal CA1 pyramidal neurons and the dentate gyrus granule neurons (Colino and Malenka, 1993). Induction of LTP involves repeated dendritic stimulation at high frequencies. The resulting summation of postsynaptic responses could enhance dendritic interactions of multiple inputs. The inhibitory inputs must also be taken into account when considering synaptic integration. It had been shown that the efficacy of excitatory synaptic responses on the dendrites of granule neurons is regulated by powerful $GABA_A$ inhibition (White et al., 1990; Tomasulo et al., 1993; Sloviter and Brisman, 1995). Furthermore, presynaptic $GABA_B$ receptors on inhibitory interneurons in dentate gyrus are thought to be involved in the induction of LTP in the perforant pathway during theta-frequency stimulation (Mott and Lewis, 1994). In support of this concept, bath applications of a $GABA_B$ agonist baclofen have an overall potentiating effect on synaptic transmission in the dentate gyrus, presumably by activation of autoreceptors on the inhibitory interneurons (Burgard and Sarvry, 1991). Thus, the location and temporal pattern of inhibitory inputs are also very important in shaping the excitatory responses in the postsynaptic cell.

In this study, we took advantage of the presence of two anatomically and functionally distinct medial and lateral pathways terminating on separate regions of the

granule cell dendrites (Witter, 1993) to study synaptic interactions between pathways. Synapses of both medial and lateral perforant pathways possess NMDA receptors and express NMDA receptor-dependent LTP (Colino and Malenka, 1993; Hanse and Gustafsson, 1992); thus, a mechanism for potential dendritic interactions during LTP is present in this system. This has never been demonstrated experimentally. Published data indicate high concentration of $GABA_B$ receptors on dendrites of the granule neurons in dentate gyrus (Bowery et al., 1987; Solís and Nicoll, 1992). Because of postsynaptic $GABA_B$ receptors' dendritic location and their prolonged effects (>200 ms) on the membrane potential (Newberry and Nicoll, 1984) they may affect LTP induction by opposing the action of NMDA receptors during tetanic stimulation (Swearengen and Chavkin, 1989). In the present study we eliminated $GABA_A$ inhibition with bicuculline and examined the role of $GABA_B$ receptors on LTP induction and interactions of two perforant pathways.

6.3 Experimental Procedures

6.3.1 Brain Slice Preparation

Experiments were performed on 16-30 day old Wistar rats of either sex supplied by Charles River. Although neurogenesis proceeds at high rate at this age, the immature neurons are primarily restricted to the inner granule layer bordering the hilus (Cowan et al., 1980). The majority of the neurons appear to have fully extended dendrites although synaptic spines are not fully developed (Cowan et al., 1980). The smaller and fewer

spines present on immature dendrites make the young granule neurons more electrically "compact" than the fully mature adult neurons (Jou, 1995). This could enhance the synaptic interactions that we study. In view of the reported developmental changes in LTP during the first two postnatal weeks in the CA1 area of rat hippocampus (Jackson et al., 1993), we examined the possible age-related differences in the magnitude of LTP in dentate gyrus. In the two to four weeks old animals the magnitude of LTP induced in the lateral and medial pathways showed no correlation with age.

Preparation of hippocampal slices and the recording set-up were standard and have recently been described (Wang et al., 1996). Briefly, transverse hippocampal slices, 400 μm in thickness, were prepared using a manual tissue chopper and kept in a holding chamber at room temperature for at least one hour before being transferred to a recording chamber. In the recording chamber, the slice was submerged in the continuously superfused (2ml/min) standard artificial cerebrospinal fluid (ACSF) saturated with 95% O_2-5% CO_2. The temperature was maintained at 30-32° C. The composition of the ACSF was (in mM): 124 NaCl, 3 KCl, 1.25 NaH_2PO_4, 1 $MgCl_2$, 2 $CaCl_2$, 26 $NaHCO_3$, 10 dextrose, and 0.01 bicuculline methiodide. All efforts were made to minimize animal suffering, and to reduce the number of animals used. University of Toronto animal experiments protocol number 4460.

6.3.2 Stimulation and Recording Techniques

In this study, both extracellular field potential recordings and whole-cell current clamp recordings were used. Bipolar tungsten electrodes were placed in the outer and

middle molecular layers of the dentate gyrus in order to stimulate axons in the lateral and medial perforant pathways and to evoke synaptic responses in the distal and middle regions of the granule cell dendrites, respectively. For extracellular recordings we used a single glass micropipette filled with ACSF, placed in the middle molecular layer. The positions of the stimulating electrodes were further adjusted so that the recording electrode detected a current sink when the medial pathway was stimulated and current source when the lateral pathway was stimulated. This procedure ensured separation of the two bands of stimulated afferents. In the presence of a $GABA_A$ blocker bicuculline (10 μM), there was no detectable facilitation or inhibition between the pathways when they were stimulated separately at 200 ms intervals every 10 seconds. Prolonged $GABA_B$-mediated inhibition produced predominantly in the lateral pathway, could in principle, interfere with the subsequent responses in the medial pathway. However, under the condition of low frequency and low intensity stimulation, we did not observe any detectable effect on the initial slope of the field EPSPs. Furthermore, there was no difference in the initial slopes of field EPSPs when the sequence of the pathway's stimulation was altered. Moreover, the magnitude of LTP in the lateral and the medial pathways was not affected by the stimulation sequence or by recording mode (current sink or current source).

To induce LTP in the perforant pathways, four 100 Hz trains (0.5 s duration), at test pulse intensity were applied to the selected pathway at 10 sec intervals. When the two perforant pathways were co-activated, each pathway received the same stimulation paradigm as stated above, however, there was a 4 ms phase shift between the pulses

applied to each pathway. The 4 ms interval was arbitrarily selected for convenient splicing of 100 Hz stimulus trains from both pathways.

In a separate series of experiments we used "blind" whole-cell patch recordings in current-clamp mode from dentate granule cells. The patch electrodes had tips measuring 1-2 µm and resistances of 5-8 MΩ. They were filled with (in mM) : 142.5 potassium gluconate, 17.5 $KMeSO_4$, 8 NaCl, 10 HEPES, 0.1 EGTA, 2 MgATP, 0.2 GTP, pH = 7.3, osmolality = 290-300 mOsm.

6.3.3 Materials

The chemical reagents used to make ACSF and the intracellular solution were purchased from BDH Inc. (Canada), J.T. Baker Inc. (Canada), and Sigma Chemical Co. (USA). CGP36742 was a gift from CIBA-GEIGY (Canada).

6.3.4 Statistical analyses

Data were analyzed using paired student's *t*-tests and ANOVA unless otherwise stated. A probability less than 0.05 ($P < 0.05$) was considered significant.

6.4 Results

6.4.1 $GABA_B$-mediated IPSPs in medial and lateral perforant pathways

When recorded intracellularly with whole-cell recordings under current-clamp

mode, the evoked excitatory postsynaptic potentials (EPSPs) in medial and lateral perforant pathways were followed by long lasting inhibitory postsynaptic potentials (IPSPs) which persisted for over 200 ms. These IPSPs were only noticeable when the intensity of stimulation was sufficiently high, to produce EPSPs of 5 mV or larger, or when stimuli were applied at high frequency. Having blocked $GABA_A$ receptors with bicuculline we could proceed to identify the IPSPs as $GABA_B$ receptor-mediated responses. In five experiments, CGP36742 (100 μM) a specific $GABA_B$ receptor blocker (Olpe et al., 1993), reversibly reduced the slow IPSP (Fig. 6-1A). At comparable amplitudes of evoked EPSPs in medial and lateral perforant pathways, the lateral perforant pathway showed more pronounced $GABA_B$ IPSPs. The larger slow IPSP in the lateral pathway was particularly well demonstrated during stimulation with a train of pulses at the frequency of 100 Hz (Fig. 6-1B) but was also evident after stimulation with single pulses (Fig. 6-1C).

6.4.2 Capacity for LTP induction in medial and lateral perforant pathways

The stronger $GABA_B$ IPSP seen in the lateral perforant pathway, particularly during 100 Hz high frequency stimulation, could hinder LTP induction in this pathway. However, in the initial set of experiments a comparison of LTP sizes in the medial and lateral perforant pathways showed no significant difference (Fig. 6-2, Lateral LTP:89.8 ± 7.0% S.E., n=13 ; Medial LTP: 108.8 ± 12.4% S.E., n=18; t-test, $P>0.05$). In both pathways, we observed a highly robust and reproducible LTP of similar magnitude.

We subsequently examined the capacity for LTP in the two pathways. To test the

Figure 6-1 Intracellularly recorded EPSPs and IPSPs in dentate granule neurons. **A**. EPSPs and slow IPSP evoked by a train of stimuli (100 Hz) to the lateral perforant pathway. The slow IPSP could be reversibly blocked by CGP36742 (100 μM). A brief train of seven stimuli was chosen to produce a significant IPSP without induction of LTP. **B**. Comparison of slow IPSPs in lateral and medial pathways. Note that the initial EPSPs were of similar size in the medial and lateral pathways (marked by a large arrow) while the IPSPs were significantly larger in the lateral pathway. **C**. For a similar EPSP amplitude evoked with single stimuli, the IPSPs were larger in the lateral pathway than in the medial pathway. On average the amplitude of the lateral IPSP was 290 ± 100% (S.E.) of medial IPSP (n=5). Arrows underneath the records indicate the stimulation pulses. Baseline potential was held at -60 mV in **A**, **B** and at -70 mV in **C**. Holding potentials in this range enlarge the slow, potassium-dependent $GABA_B$ IPSPs, which are not apparent at more hyperpolarized levels.

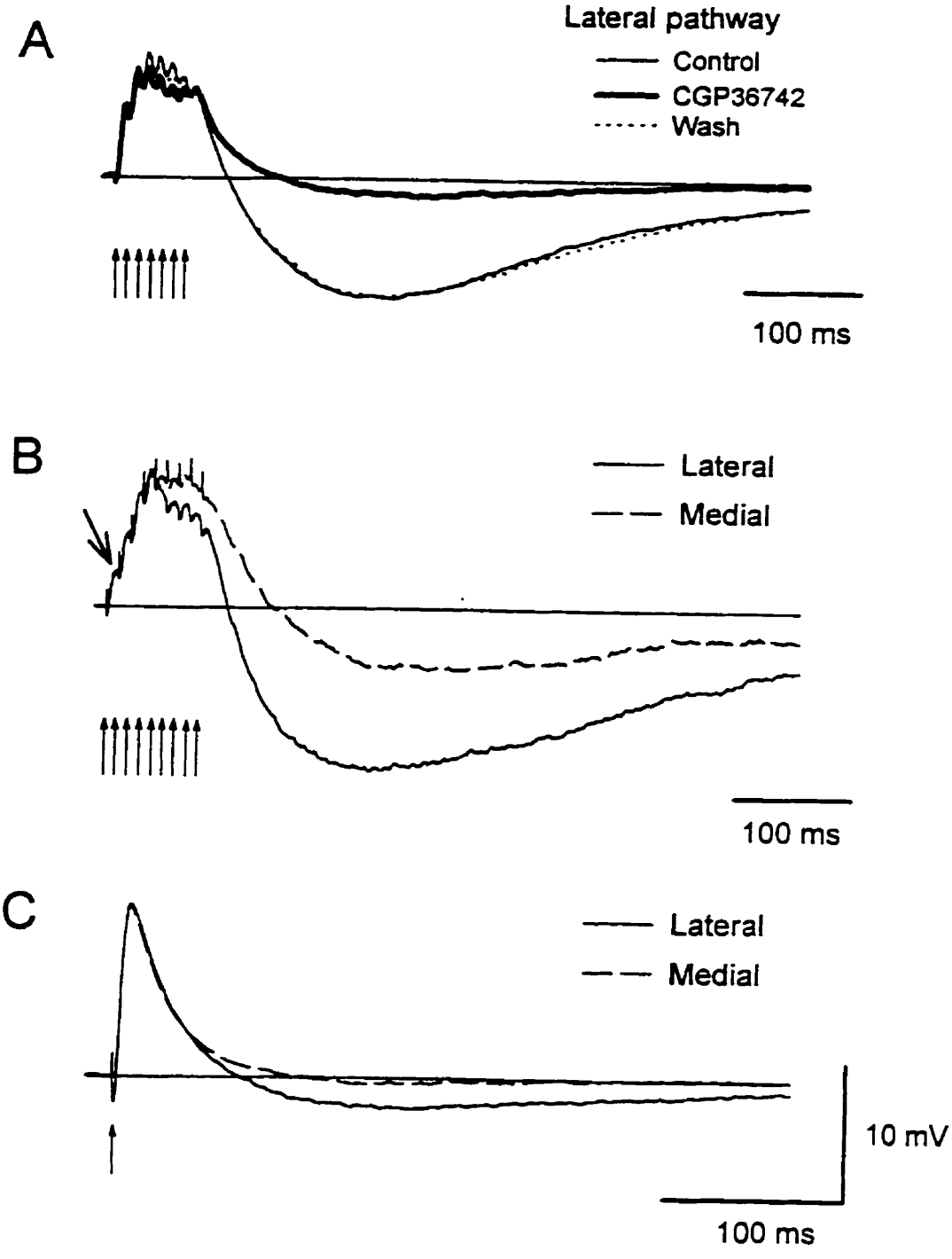
A
Lateral pathway
Control
CGP36742
Wash
100 ms
B
Lateral
Medial
100 ms
C
Lateral
Medial
10 mV
100 ms

Figure 6-2 LTP in medial and lateral perforant pathways. **A**. Extracellular, field EPSPs show the time course of LTP in the lateral perforant pathway (n=13). The initial slopes of EPSPs were measured and expressed as the percentage of control baseline level. The standard errors for every fifth point (minute) are indicated. **B**. Time course of the medial pathway LTP (n=18). LTPs were induced at time 0 indicated by the arrows in **A** and **B**. Representative samples of field EPSPs above the graphs illustrate the control responses (1) and the responses after LTP induction (2). **C**. Lateral pathway potentiation measured from responses 16-20 minutes after LTP induction (190 ± 7% S.E., n=13). **D**. The medial pathway responses, measured during the same time period, potentiated to 209 ± 12% (S.E., n=18). Asterisks indicate statistically significant differences between baseline and potentiated responses at $P < 0.05$.

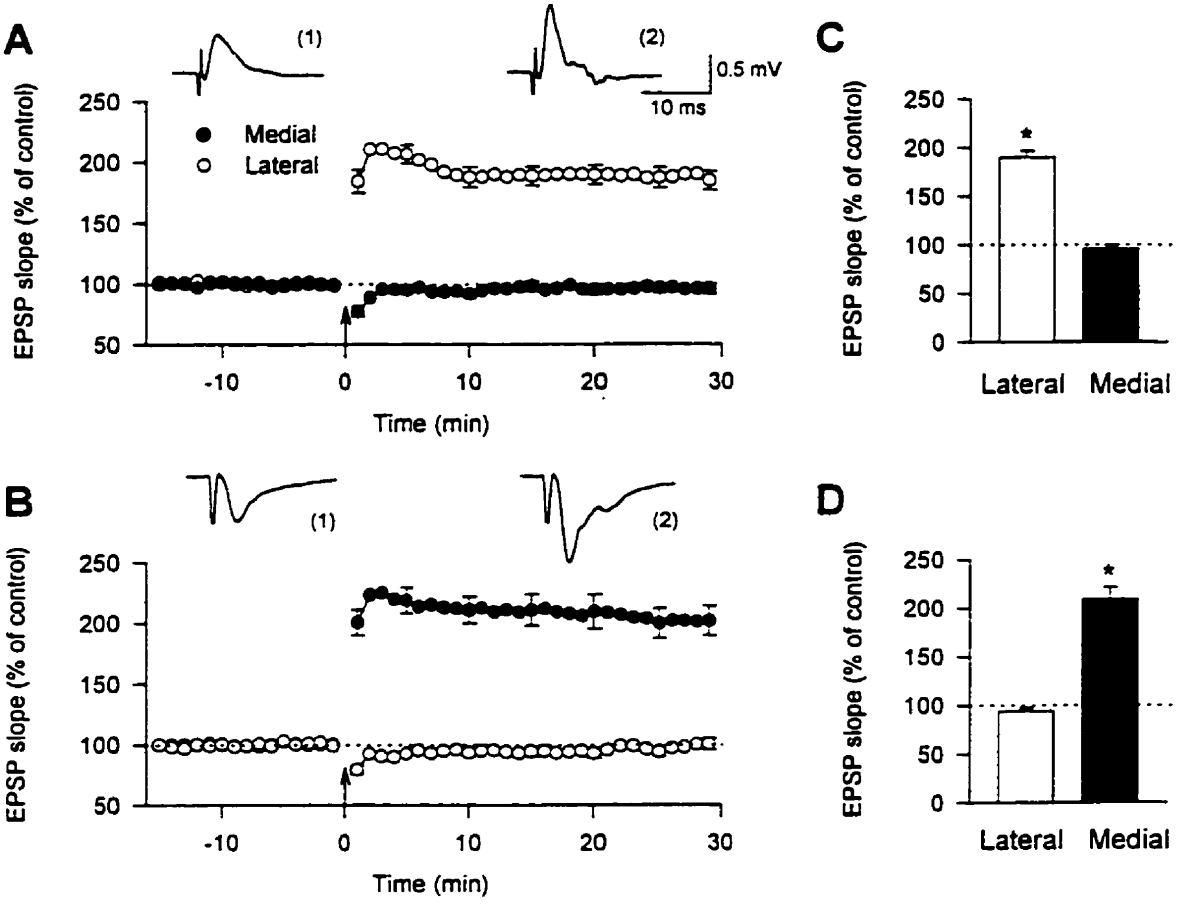
A
(1)
(2)
0.5 mV
10 ms
Medial
Lateral
EPSP slope (% of control)
250
200
150
100
50
-10
0
10
20
30
Time (min)
B
(1)
(2)
EPSP slope (% of control)
250
200
150
100
50
-10
0
10
20
30
Time (min)
C
EPSP slope (% of control)
250
200
150
100
50
0
*
Lateral
Medial
D
EPSP slope (% of control)
250
200
150
100
50
0
*
Lateral
Medial

hypothesis that $GABA_B$ IPSPs alter the capacity for LTP in synapses on dentate granule neurons, we induced LTP four times in each pathway. We found that the medial pathway reliably potentiated after second, third, and fourth induction episodes (Fig. 6-3) and produced a statistically significant effect after these repeated tetanization. The lateral pathway, on the other hand, did not show a significant potentiation even after the four tetani (Detailed statistics are presented in Fig. 6-3). Thus, the medial perforant pathway showed a larger capacity for LTP than the lateral pathway. This was particularly well illustrated by comparing differences between the first and fourth LTPs in the medial and lateral pathways (Fig. 6-3; inset).

To test whether the limited capacity in the lateral pathway was related to the larger $GABA_B$ IPSP response, we induced LTP in the lateral pathway twice in a paradigm similar to that used in Figure 6-3, while perfusing the slices with CGP36742 during each induction. If the $GABA_B$-mediated IPSP was the limiting factor in the ability of the lateral pathway to produce LTP, blocking the $GABA_B$ receptors should enlarge the potentiation. Indeed, in five out of five experiments, the lateral pathway showed significant LTP after the second induction in the presence of CGP36742 (Fig. 6-4B, $P<0.05$). This is in contrast to the results of experiments done without CGP36742 (Fig. 6-4A), where in only three out of seven cases the second induction showed a noticeable potentiation, however, the total averaged effect was not statistically significant. However, neither baseline nor potentiated synaptic responses in the lateral pathway were directly affected by CGP36742 suggesting that the induction rather than the expression of LTP is altered by $GABA_B$-mediated IPSPs. These experiments demonstrated that $GABA_B$

Figure 6-3 Different capacities for LTP in the medial and the lateral perforant pathways. In each pathway, LTP was induced four times at 20-30 min intervals. The medial perforant pathway potentiated after each induction, from 241 ± 23% (T1) to 390 ± 130% (T4) (mean ± S.E.; n=7). The lateral perforant pathway potentiated from 198 ± 8% after the first induction to 247 ± 10% after the fourth induction (mean ± S.E.; n=7). Two-way repeated measures ANOVA indicated significant difference in LTPs between the two pathways ($t = 2.62$, $P < 0.05$). A multiple comparison (Bonferroni's method) test demonstrated a significant LTP between first (T1) and fourth (T4) tetanizations in the medial pathway. No additional LTP was induced in the lateral pathways after the first tetanus ($P > 0.05$) indicating that the total capacity for LTP in this pathway has been used up by the first tetanus. Inset demonstrates the difference between LTP expressed after first and fourth induction in medial and lateral perforant pathways. The difference seen in the medial pathway was significantly larger than that seen in the lateral pathway (t-test, $P < 0.05$). Error bars are indicated for each group.

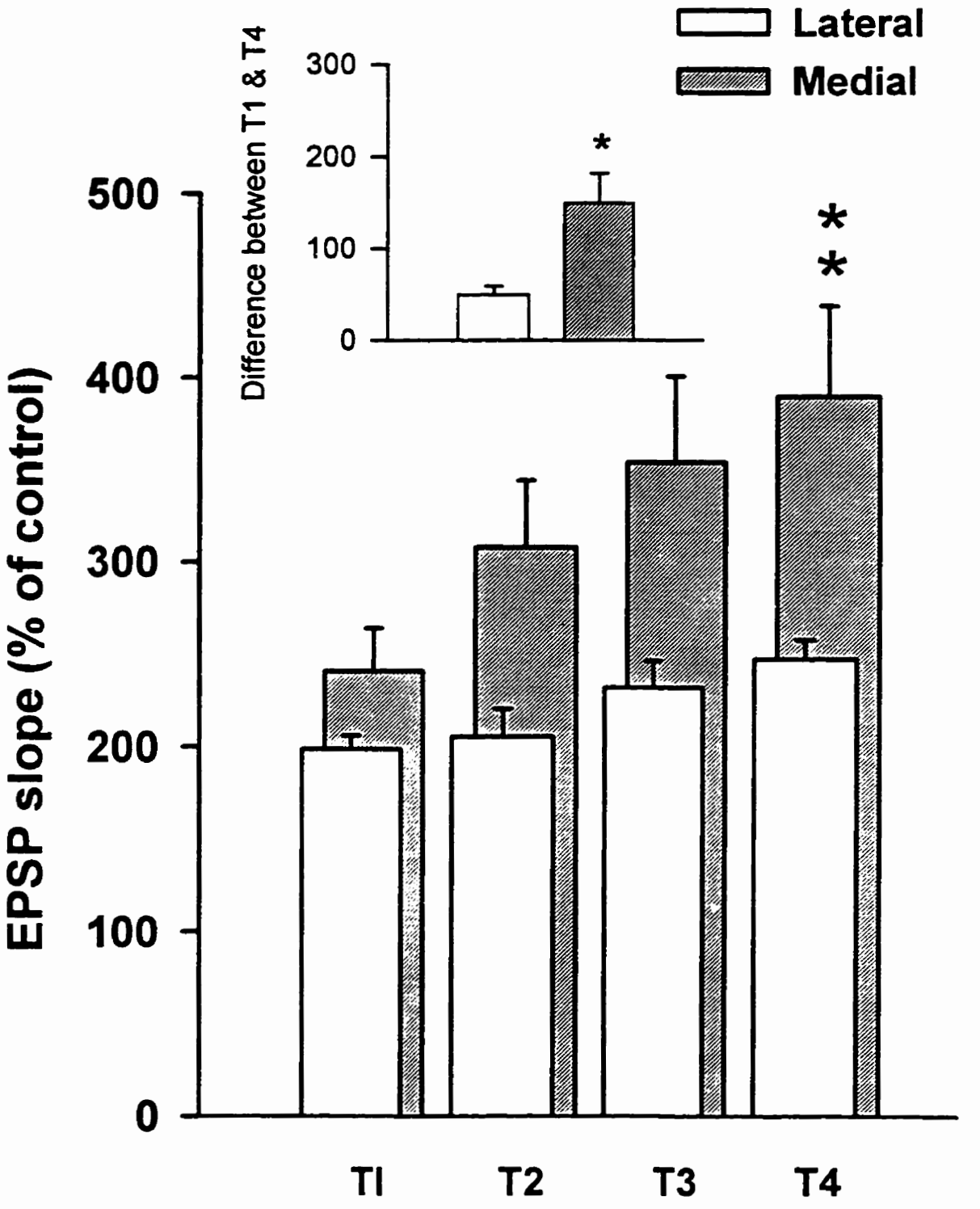
Lateral
Medial
Difference between T1 & T4
300
200
100
0
*
500
400
300
200
100
0
EPSP slope (% of control)
**
TI
T2
T3
T4

receptors reduce the capacity for LTP induction in the lateral pathway.

In addition to altering the capacity for LTP induction in the lateral pathway, CGP36742 reduced the heterosynaptic depression of the medial pathway (compare filled symbols in Fig.6-4 A and B) suggesting that this depression is also mediated by $GABA_B$ receptors. In order to distinguish between a possible pre- and postsynaptic loci of the heterosynaptic depression, we employed the paired-pulse stimulation paradigm in the medial pathway. In previous studies of this pathway a change from paired-pulse depression to paired-pulse facilitation was thought to be caused by a reduction of transmitter release (Harris and Cotman, 1985). Under normal circumstances, medial pathway usually showed paired-pulse depression when the interpulse interval was 40 to 50 ms as originally showed by Harris and Cotman (1985). This phenomenon is probably related to the relatively high probability of transmitter release in the medial pathway and can be reversed to facilitation by lowering of the extracellular calcium concentration (Zucker, 1989; Wang et al., 1996). Tetanization of the lateral pathway suppressed synaptic transmission in the medial pathway with concomitant reversal of the paired-pulse depression to the paired-pulse facilitation, indicating a presynaptic action (Fig. 6-4C). These results supported the hypothesis of the reduction of transmitter release during the heterosynaptic depression period in the medial pathway.

6.4.3 LTP of $GABA_B$-mediated IPSPs

Considering that the magnitudes of single LTPs in the lateral and the medial pathways were similar after the first induction episode but clearly different during

Figure 6-4 Removal of $GABA_B$ inhibition unmasks additional potentiation in the lateral perforant pathway and reduces heterosynaptic depression in the medial perforant pathway. **A**. Lateral pathway LTP was induced twice (indicated by arrows T1 and T2), but the second induction (T2) did not lead to additional potentiation in this pathway ($P > 0.05$, n=7). Dashed line indicates the averaged response size before the second potentiation. Note that in these experiments the heterosynaptic depression in the medial pathway significantly increased after the second tetanization ($P<0.01$, n=7). **B**. Lateral pathway LTP was induced twice in presence of CGP36742 (CGP, 100 μM) indicated by horizontal bars. The responses after the second induction (T2) were significantly larger than the baseline ($P < 0.05$, n=5). The magnitude of the heterosynaptic depression was reduced by CGP36742 and its potentiation was blocked. Standard error bars are shown on every fifth point for clarity. **C**. Sample field responses from a single experiment were taken from the medial pathway to illustrate the changes of paired-pulse responses during different experimental manipulations. During the heterosynaptic depression period after lateral pathway tetanization, medial pathway paired-pulse depression (-5.3 ± 3.3%, n =5) changed into paired-pulse facilitation (+19.0 ± 18.9%, n = 5). In contrast, after tetanization of the medial pathway, paired-pulse depression was enhanced by 68% during the period of post-tetanic potentiation (n = 4). These results show that the paired-pulse stimulation is a sensitive measure of presynaptic effects and suggest a presynaptic locus of heterosynaptic depression.

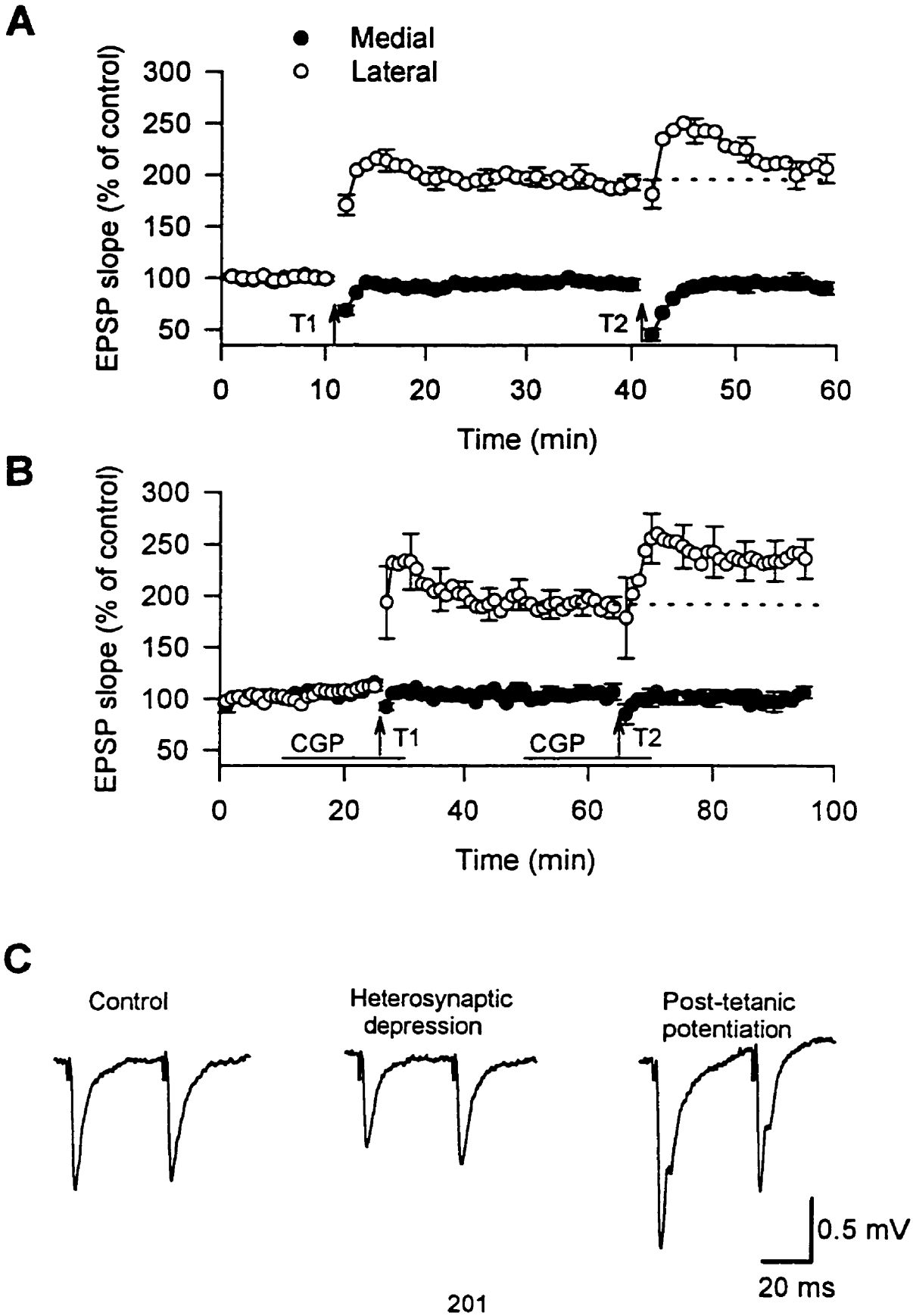
A
Medial
Lateral
EPSP slope (% of control)
300
250
200
150
100
50
T1
T2
0
10
20
30
40
50
60
Time (min)
B
EPSP slope (% of control)
300
250
200
150
100
50
CGP
T1
CGP
T2
0
20
40
60
80
100
Time (min)
C
Control
Heterosynaptic depression
Post-tetanic potentiation
0.5 mV
20 ms

subsequent inductions, we hypothesised that during the first induction, the $GABA_B$ IPSP in the lateral pathway was potentiated and consequently limited the induction of the subsequent LTP of EPSP. We examined this hypothesis with the use of the whole-cell current clamp recordings. The results showed that in three out of four cells, the slow $GABA_B$-mediated IPSP underwent long lasting (>20 min) potentiation by the same induction paradigm as was used to potentiate the field EPSP (Fig. 6-5). The fourth cell was also potentiated; however, in this case the potentiation lasted only 10 minutes. The average IPSP potentiation was 85.3 ● 38.7 % (S.E., range from 44% to 163%, n=3). A complete block of the slow IPSP by CGP36742 after the induction of LTP confirmed the involvement of $GABA_B$ receptors.

An independent measure of LTP in the inhibitory interneurons in the lateral pathway is given by the relative increase of the second heterosynaptic inhibition in the medial pathway, compared with the first heterosynaptic inhibition, illustrated in Figure 6-4A. The average magnitude of this increase was 92 ± 39% (S.E., n=7), similar to the magnitude of LTP of the IPSPs illustrated in Figure 6-5. In contrast, the reverse experiment showed no such effect. The heterosynaptic depression of the lateral pathway was reduced by 6.1 ± 3.4% (S.E., n=7) during repeated tetanizations of the medial pathway (data not illustrated).

6.4.4 Interactions of medial and lateral perforant pathways

One possible explanation for the heterosynaptic depression seen in the medial pathway after tetanization of the lateral pathway was that we directly stimulated axonal

Figure 6-5 LTP of $GABA_B$ IPSP in the lateral perforant pathway. **A**. Sample traces of intracellular recordings show potentiation of $GABA_B$ IPSPs in a cell held at -70 mV. LTP trace was taken at 15 mins after LTP induction. 100 μM CGP36742 was applied at the end of the experiment to verify the presence of $GABA_B$ component. **B**. Representative time course of $GABA_B$ IPSP LTP. Arrow indicates the time of LTP induction. The potentiated IPSPs were blocked by CGP36742 at the end of the experiment. The IPSP amplitudes were measured at the peak.

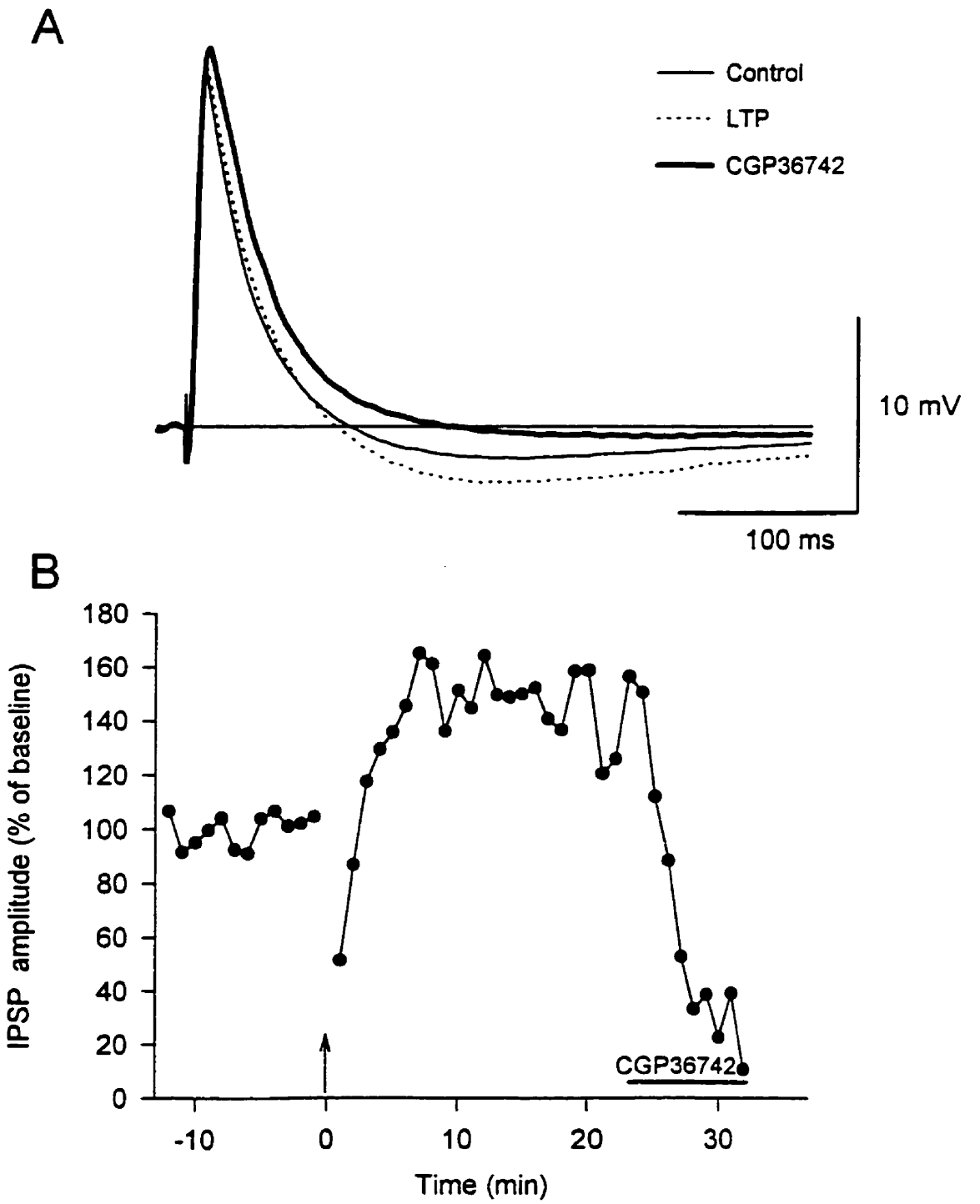
A
Control
LTP
CGP36742
10 mV
100 ms
B
IPSP amplitude (% of baseline)
180
160
140
120
100
80
60
40
20
0
-10
0
10
20
30
Time (min)
CGP36742

branches of inhibitory interneurons which may be spanning the molecular layer (see Discussion). In the case of such an indiscriminate stimulation the inhibitory $GABA_B$ synapses on both the distal and medial dendrites of granule neurons could be stimulated and would be expected to have indiscriminate effects on potentiation in both pathways. The results in Figure 6-6 show that such an effect did not occur. After the first tetanization of the medial pathway (Fig. 6-6A, C), the subsequent LTP in the lateral pathway was unchanged. This is in sharp contrast to the effect on the lateral pathway shown in Figures 6-3 and 6-4. The complementary experiment shown in Figure 6-6B, D further emphasizes the independence of LTPs in the two pathways whenever they were induced separately. However, the results were different after co-activation of both pathways which always produced additional long-term potentiation in the medial pathway, whereas the lateral pathway was unchanged. Overall, the results shown in Figure 6-6 demonstrated that the medial pathway became potentiated by 117.3 ± 16.0% (S.E., n=17) during co-activation, whereas the lateral pathway became potentiated by only 13.9 ± 5.3% (S.E., n=17). Furthermore, the data illustrated in Figure 6-6 highlight strong heterosynaptic depression in the potentiated medial pathway by the lateral pathway (Fig. 6-6A, see large asterisk).

6.4.5 Lateral pathway facilitates the responses of the medial pathway during co-activation

The larger LTP in the medial pathway during co-activation could be due to a larger capacity of this pathway for expression of LTP or to additional "boosting" of the medial

Figure 6-6 Interactions of medial and lateral pathways. **A**. Representative experiment showing effects of inducing LTP first in the medial pathway (TM) then in the lateral pathway (TL), followed by co-activation (TB). Asterisk in A indicates a large heterosynaptic depression resulting in a complete, transient de-potentiation of the medial pathway by the lateral pathway. This occurred in 6 out of 9 experiments. In the other 3 experiments a partial de-potentiation was observed. **B**. Representative experiment of alternate induction sequence. Arrows indicate the time of LTP induction. **C**. The averaged results from the first series of experiments (example in A) are shown in the form of bar graph (n=9, one asterisk, $P < 0.05$; two asterisks, $P < 0.01$). **D**. The averaged results from the second series of experiments (example in B, n=8, one asterisk, $P < 0.05$; two asterisks, $P < 0.01$). Note that after co-activation the medial pathway further potentiated while the lateral pathway did not change, regardless of the induction sequence. Standard error bars are indicated.

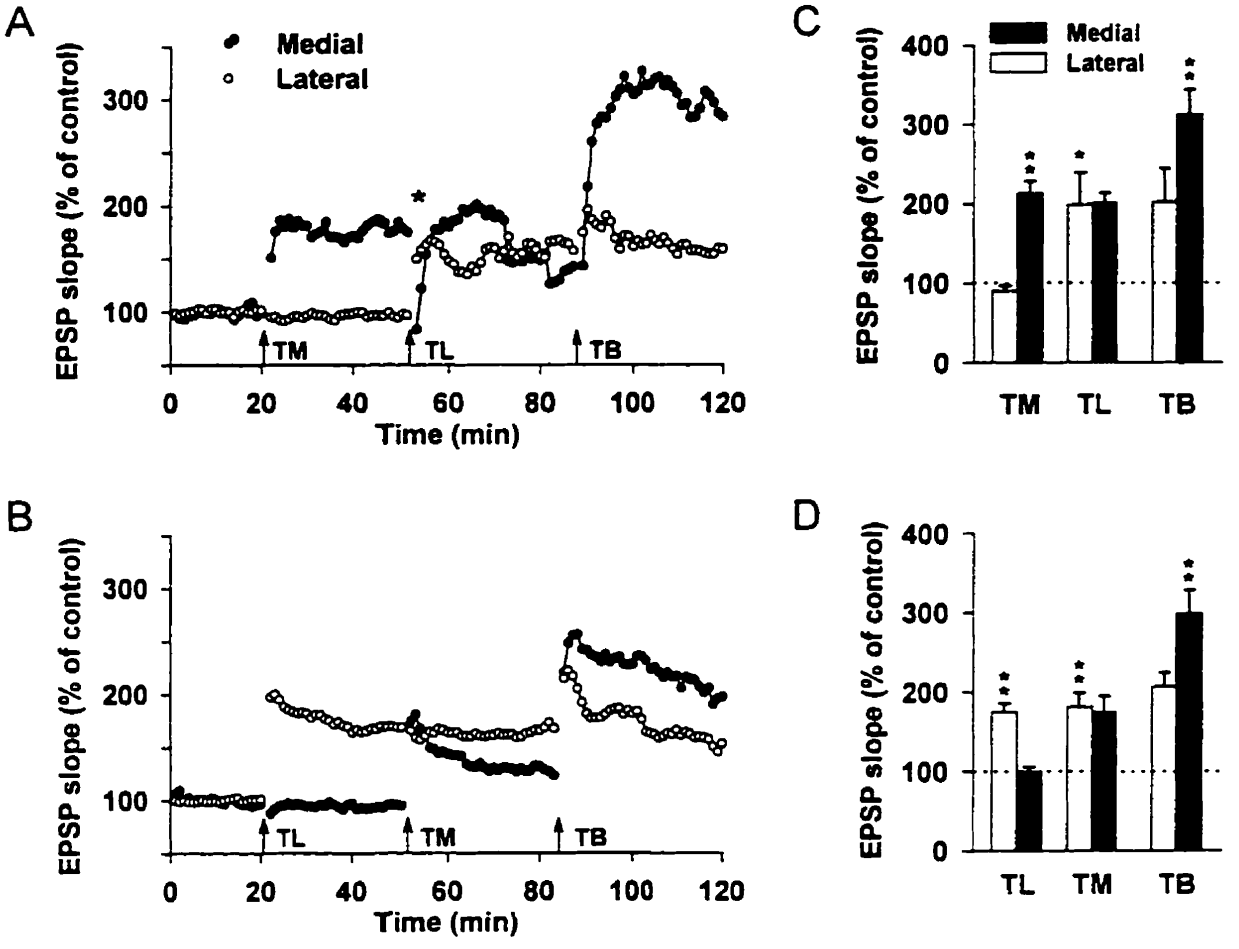
A
Medial
Lateral
EPSP slope (% of control)
300
200
100
TM
TL
TB
0
20
40
60
80
100
120
Time (min)
B
EPSP slope (% of control)
300
200
100
TL
TM
TB
0
20
40
60
80
100
120
Time (min)
C
Medial
Lateral
EPSP slope (% of control)
400
300
200
100
0
TM
TL
TB
D
EPSP slope (% of control)
400
300
200
100
0
TL
TM
TB

pathway by the lateral input during induction of LTP. To distinguish between these possibilities we co-activated the two pathways together once. We argued that if the medial pathway and lateral pathway acted independently of each other during co-activation, the LTP induced by a single co-activation should have similar magnitude to the LTP induced separately in each pathway. On the other hand, if the lateral pathway facilitated the medial pathway LTP when they were co-activated, the medial LTP induced by co-activation should be larger than when induced alone. The experimental results clearly favoured the latter hypothesis (Table 6-1). The medial pathway showed 67.4% larger LTP during co-activation (unpaired t-test, $P<0.05$), but LTP in the lateral pathway was unchanged. These results showed that the lateral pathway had a facilitatory (boosting) effect on the medial pathway during co-activation but not *vice versa*. CGP36742 had no effect on this facilitation (unpaired t-test, $p>0.05$, $n=3$; data not illustrated).

6.5 Discussion

6.5.1 Capacity of medial and lateral synapses for LTP

The study demonstrated a relatively high capacity for LTP induction in the medial pathway (Fig. 6-3). This finding implied that either the capacity of the lateral pathway was limited by some inhibitory mechanism or that the medial pathway was inherently more plastic. We propose that the difference in the relative capacity for LTP in the two pathways results primarily from the selective inhibition of distal dendrites of granule

Table 6-1 The effect of co-activation of lateral and medial pathways.

Tetanization	Lateral LTP	Medial LTP
Each pathway independently	89.8 ± 25.2% (n=13)	108.8 ± 52.7% (n=18)
Co-activation	86.8 ± 45.8% (n=5)	176.2 ± 43.9%* (n=5)

The facilitatory, associative effect of lateral pathway on medial pathway. In medial perforant pathway the LTP induced by co-activation paradigm was larger than LTP induced by tetanizing the medial pathway alone (unpaired t-test, $P < 0.05$). However, lateral perforant pathway LTP induced by the co-activation paradigm was not different from the LTP induced in the lateral pathway alone (unpaired t-test, $P > 0.05$).

neurons by slow $GABA_B$-mediated IPSPs. These IPSPs appeared larger in the lateral pathway (Fig. 6-1) but, more importantly, were further potentiated by tetanic stimulation (Fig. 6-5). Under low frequency and low intensity stimulation, the slow IPSPs do not inhibit the monosynaptically evoked excitatory responses at the lateral or medial perforant path synapses. Thus applications of a $GABA_B$ receptor blocker had no effect on the magnitude of EPSPs (Fig. 6-4, Fig. 6-5). Only during repeated stimulation at high frequencies, such as those used during the induction of LTP, did the $GABA_B$-mediated inhibition of EPSPs become apparent (Fig. 6-1A, B).

Although stronger $GABA_B$ inhibition in the lateral pathway can partly explain the difference between the relatively low capacity for LTP in this pathway, other factors may also play a role. For example, the medial pathway was shown to express a particularly powerful form of LTP by recruitment of synapses with AMPA receptors (Wang et al., 1996). It is not yet known if the lateral pathway utilizes a similar mechanism.

6.5.2 Inhibitory interneurons in dentate gyrus

In dentate gyrus the distal dendrites of granule neurons receive selective input from the lateral perforant pathway which is functionally distinct from the medial pathway terminating on the middle portions of the dendrites (Bowery et al., 1993; Witter, 1993). We have now demonstrated that the two pathways differ in their capacities for LTP and that slow IPSPs in distal dendrites contribute to this difference. Anatomical studies show the presence of a class of interneurons which terminate on distal dendrites of granule cells (Halasy and Somogyi, 1993; Buckmaster and Schwartzkroin, 1995). The synapses

of these interneurons may be responsible for the inhibitory effects we observed. The evidence for feedforward inhibition in dentate gyrus is well established (Busáki 1984), but it is not known whether this inhibition involves $GABA_B$ receptors. Furthermore, a quantitative immunocytochemical study by Woodson et al. (1989) demonstrated that the outer one third of the molecular layer of dentate gyrus contained more GABA-like-immunoreactive grain density than the inner two-thirds of the molecular layer. These anatomical findings correlate well with our physiological data, which indicate stronger postsynaptic $GABA_B$ inhibition in the lateral perforant pathway.

6.5.3 Mechanisms of interactions between lateral and medial perforant pathways

The most evident interaction between medial and lateral perforant pathway is the short-lasting heterosynaptic depression seen immediately after LTP induction. This heterosynaptic depression can be potentiated by repeated tetanizations (Fig. 6-4A) and is sensitive to CGP36742 (Fig. 6-4B). It appears to be caused by presynaptic action of $GABA_B$ receptors as shown by the reversal of paired-pulse depression to paired-pulse facilitation (Fig. 6-4C). These results are in agreement with Mott and Lewis (1994), who showed that the $GABA_B$ agonist baclofen reduces extracellular field EPSPs in the medial perforant pathway while the lateral pathway showed little effect. This effect is to be expected since the initial phase of the field EPSP is much more sensitive to presynaptic inhibition than to a postsynaptic conductance change. They concluded that the reduction in the medial pathway synaptic transmission is mediated by a presynaptic mechanism because the paired-pulse depression in the medial pathway changed into paired-pulse

facilitation. Furthermore, the large depression in the potentiated medial pathway seen in this study (Fig. 6-6A) was difficult to explain by postsynaptic $GABA_B$ receptor activation however, it can be readily explained by reduced transmitter release caused by presynaptic $GABA_B$ receptors.The presynaptic $GABA_B$ receptor mediated reduction of transmitter release in the excitatory synapses has also been shown in CA1 area of the hippocampus (Isaacson et al., 1993). We propose that the CGP-sensitive heterosynaptic depression in the medial pathway seen in the present study is caused by the diffusion of GABA from inhibitory terminals in the region of lateral pathway to the nearby medial pathway (Fig. 6-7). It is unlikely that this transient inhibition is a direct effect of inhibitory synapses terminating on the granule cell dendrites, because its short-lasting time course does not correlate with the time course of the potentiation of the $GABA_B$ IPSP. Furthermore, the LTP induction in the medial pathway is not inhibited by co-activation of the two pathways (Table 6-1). Thus diffusion of GABA from one pathway to another emerges as the most likely mechanism.

Why doesn't the presynaptic, heterosynaptic depression of the medial pathway prevent associative LTP? We propose that diffusion of GABA across a short distance from the lateral towards the medial pathway may take in excess of several hundred milliseconds and produce maximal depression after the co-incident afferent impulses to the medial region have already passed. We anticipate that the delay to maximal presynaptic depression in our experiments may be considerably longer than the 300 ms observed by Isaacson et al. (1993), due to the longer distance separating the two pathways. However, the exact time course was not measured in our experiments. One

Figure 6-7 Schematic illustration of proposed presynaptic and postsynaptic $GABA_B$ receptor mediated inhibitory systems in dentate gyrus. High frequency activation of the lateral pathway is postulated to cause massive GABA release from inhibitory interneurons in that region. In addition to having a direct postsynaptic effect, GABA diffuses to the medial pathway and activates presynaptic $GABA_B$ receptors and decreases transmitter release from the excitatory terminals.

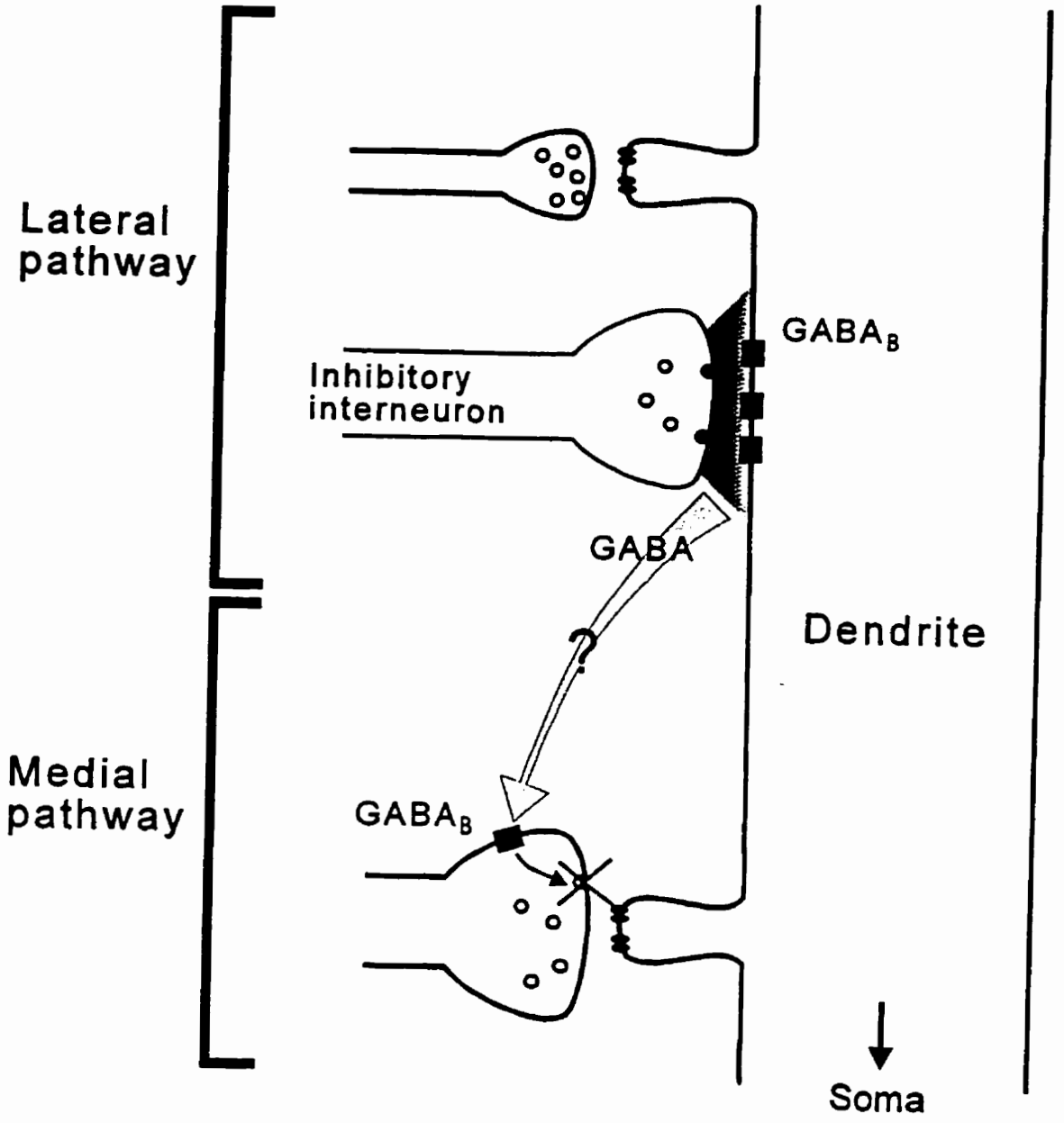
Lateral pathway
Medial pathway
Inhibitory interneuron
GABA$_B$
GABA
?
Dendrite
GABA$_B$
Soma

possible function of such a delayed gating mechanism is to emphasize the associative interactions between the two pathways but prevent extraneous, possibly irrelevant, inputs from entering the hippocampus.

It has been previously established that GABAergic inhibition via $GABA_A$ receptors plays an important role in synaptic interactions within hippocampus. For example, in the presence of the $GABA_A$ blocker bicuculline, the magnitude of LTP in dentate gyrus is enhanced (Wigström and Gustafsson, 1983) and the heterosynaptic interactions are revealed (Tomasulo et al., 1993). A new aspect of such interactions during co-activation of the two perforant pathways shown by our study is a selective enhancement of the medial pathway. This effect does not appear to be directly related to the preferential $GABA_B$ inhibition of the lateral pathway but may be a result of the topographic arrangement of the two pathways. The distal dendrites of the granule neurons are thinner and may have a higher input resistance than the middle dendrites. Computational analyses in a geometrically realistic model of the granule neuron have shown that for equal synaptic currents at two locations there would be an expected larger depolarization in the distal dendrite. Consequently, a net axial current would be expected to flow proximally thus contributing to the depolarization of the medial dendritic region (Jou, 1995; Jou et al., 1995).

Interactions between lateral and medial pathways have been examined previously *in situ*. McNaughton et al. (1978) were first to propose cooperative interactions between perforant afferents. In their experiments, performed on anesthetized animals, LTP induced by concurrent activation of medial and lateral pathways was larger than during

activation of either pathway alone. This result is apparently different from ours where selective enhancement of medial pathway was observed. However, it should be noted that in their experiments the magnitude of LTP was much lower, presumably due to effect of anaesthesia on $GABA_A$ inhibition. Thus, experimental conditions could account for the different results. Tomasulo et al. (1993) had found that the blockade of $GABA_A$ inhibition in the lateral pathway enhances LTP to the extent that the subsequent co-activation of both pathways has no additional effect. This finding is in agreement with our data.

Abraham et al. (1985) observed mutual long-lasting, heterosynaptic depression between the two pathways. This was recently confirmed by Christie et al. (1995) who studied heterosynaptic long-term depression (LTD) of the lateral pathway by repeated tetanizations of the medial pathway. White et al. (1990) demonstrated cooperative LTP and LTD between the overlapping ipsilateral and contralateral projection of the perforant pathway. All of the studies were performed on anaesthetized animals where synaptic inhibition is greatly enhanced, possibly diminishing the cooperative effects and enhancing synaptic depression. In our experiments, we have reduced the inhibitory effects by using an *in vitro* slice preparation continuously perfused with a $GABA_A$ blocker bicuculline. In reality, the degree of inhibition is probably in between these two extremes.

6.5.4 Physiological significance

The $GABA_B$ inhibitory system provides the lateral pathway with a mechanism to control the medial pathway. Further evidence of this control mechanism is the strong

depression of the medial pathway after it had been potentiated (Fig. 6-6A). This provides a mechanism for effective transient de-potentiation of the medial pathway during increased activity in the lateral pathway alone. At the same time the lateral pathway possesses a mechanism to prevent its own LTP by powerful postsynaptic $GABA_B$ inhibition. We suggest that this inhibition, together with a dendritic boosting mechanism function in tandem to maximize associative LTP in the medial pathway. Such a mechanism may be related to the recognized role of the hippocampus in associative (e.g. spatial) memory (Cohen and Eichenbaum, 1993). The medial pathway originates in the medial entorhinal cortex which connects to various regions of the brain and could integrate spatial information. In contrast, the lateral perforant pathway is anatomically connected to the olfactory system (Witter et al., 1989). Our results suggest a possible cellular mechanism for a link between the two pathways in the hippocampus resulting in a unilateral association of signals from different sources. This mechanism is in agreement with the behavioral evidence supporting the hippocampal involvement in association of olfactory and spatial cues (Lynch and Baudry, 1988; Cohen and Eichenbaum, 1993; Lynch and Baudry, 1984; Bunsey and Eichenbaum, 1996). In addition, other neurotransmitter systems including opioid peptides (Bramham et al., 1991a) and acetylcholine (Burgard and Sarvey, 1990) are likely to be involved in the associative interactions between the lateral and medial perforant pathways.

6.6 Conclusions

In summary, we have shown a difference between the capacity for LTP in the two subdivisions of the perforant pathway and a number of novel interactions during LTP. Most effects can be, attributed at least in part to the larger demonstrated strength of the $GABA_B$ inhibition in the lateral pathway.

7.1 Synaptic properties of lateral and medial pathways

The differences in synaptic properties between lateral and medial pathways are summarized in Table 7-1 and discussed in detail below. A few other features such as the ratio of AMPA/NMDA receptors at synapses and the involvement of opiate receptors in LTP were initially postulated to be different in the two pathways, but the data didn't support those hypotheses.

7.1.1 High frequency depression

The medial pathway has more Ca^{2+}-dependent high frequency depression than the lateral pathway (Chapter 3). From this observation and quantal analysis results (Chapter 4), the synapses in the medial pathway can be characterized as high output synapses with high probability of release.

The difference in high frequency depression can be seen in Figure 3 of the *in vivo* study of perforant pathways by McNaughton and Barnes (1977) in which they used 100 Hz stimulation to examine the monosynaptic connections. Although no quantitative comparison was made from these traces, the authors did notice that the medial pathway responses "follow less well [to the 100 Hz stimulation], i.e., show greater attenuation than later peaking ones [lateral pathway]". Thus, the difference in high frequency depression in medial and lateral pathways observed in the slice preparation are consistent with the observations made *in vivo* and are not an artifact created by *in vitro* conditions. In a subsequent report, McNaughton (1980) further examined the properties of the medial and

Table 7-1 Difference between lateral and medial perforant pathways

Synaptic Properties	Lateral	Medial
High Frequency Depression	Weak	Strong
Presynaptic L-AP4 receptors	Numerous	Few
Inhibitory Input	Strong	Weak
LTP Capacity	Low	High

lateral divisions of the perforant pathway. He found that the ratio of EPSP size to presynaptic fiber response was greater in the medial pathway, implying that the same presynaptic discharge causes a larger postsynaptic response in the medial pathway than in the lateral pathway. Furthermore, in response to a paired-pulse paradigm with interpulse pulse interval less than 2 s, the medial pathway showed depression whereas the lateral pathway showed facilitation. The depression in the medial pathway can be converted to facilitation upon reduction of extracellular Ca^{2+} concentration. Thus the author concluded that the medial perforant pathway releases a larger fraction of its available transmitter per impulse than the lateral pathway. This conclusion is consistent with the current study, i.e. Ca^{2+}-dependent high frequency depression and quantal analysis showed that the medial pathway synapse is a high-output synapse with higher probability of release.

The lateral pathway showed less high-frequency depression than the medial pathway. A lower probability of transmitter release could account for the reduced high-frequency depression. However, I do not have satisfactory results from quantal analysis for this pathway. Thus, it is not known whether this pathway has low probability of transmitter release. The presynaptic L-AP4 receptor in this pathway could limit the transmitter release by an autoinhibitory mechanism and contribute to high frequency depression resistance (see below).

7.1. 2 L-AP4 metabotropic receptor in the lateral pathway

The lateral pathway has more presynaptic L-AP4 sensitive metabotropic receptors

than the medial pathway (Chapter 3). Thus, if this receptor is involved in the negative feedback control of transmitter release as observed in the rat olfactory cortex (Anson and Collins, 1987), then the lateral pathway response is under stronger presynaptic control than the medial pathway response. Furthermore, the relative resistance to depression during high-frequency stimulation in the lateral pathway could be the result of such a feedback system. L-AP4 has been shown to enhance paired-pulse facilitation in the lateral pathway (Harris and Cotman, 1983), possibly by inhibiting Ca^{2+} influx into the presynaptic terminal (Cotman et al., 1986; Trombley and Westbrook, 1992). Thus, the reduced Ca^{2+} influx may reduce the probability of transmitter release and lead to reduced depression. Unfortunately a specific antagonist for this receptor is currently not available and a direct link between the reduction of high-frequency depression and the presynaptic L-AP4-sensitive receptor is not established.

The negative feedback control of transmitter release by L-AP4-sensitive receptors could potentially affect LTP induction in the lateral pathway. The high frequency tetanic stimulation used for LTP induction could create a higher glutamate concentration in the synaptic cleft, and the negative feedback system could reduce transmitter release by the subsequent impulses, thus creating a limiting factor for transmitter release and the availability of transmitter to the postsynaptic receptors. It would be interesting to see if blocking presynaptic L-AP4-sensitive receptors could enhance LTP induction and expression in the lateral pathway.

Recently, Pekhletski et al. (1996) generated and studied knockout mice lacking the mGluR4 subtype of mGluR that displays a high affinity for L-AP4. They found that

the mGluR4 knockout mice have an impaired ability to learn complex motor tasks. Patch-clamp and extracellular field recording from Purkinje cells in cerebellar slices demonstrated that L-AP4 had no effect on synaptic responses in the mutant mice, whereas in the wild-type mice 100 μM L-AP4 produced a 23% depression of synaptic responses. In mutant mice, paired-pulse facilitation normally seen in the parallel fiber-Purkinje cell synapses was significantly reduced and the post-tetanic potentiation seen in wild-type mice was reversed to post-tetanic depression. However, LTD of Purkinje cells produced by activation of parallel fibers in conjuction with a depolarizating postsynaptic voltage step was not affected in mutant mice. These results suggest that presynaptic mGluR4 receptors play a role in short-term plasticity by regulating presynaptic transmitter release in the cerebellum. Whether the mutant mice have a similar change in short-term plasticity of the lateral perforant pathway still awaits further exploration. If the result is negative, it would help to rule out the involvement of presynaptic mGluR4 receptors in the lateral pathway and direct future research towards presynaptic mGluR6 and 7 receptors.

Although the identity of the L-AP4-sensitive receptor is currently unknown, recent immunocytochemical studies using subtype-specific antibodies against mGulR4a (one of the splice variants of mGluR4; the other one is mGluR4b) and mGluR7 receptors revealed a very interesting and somewhat surprising pattern in the dentate gyrus (Bradley et al., 1996). First of all, mGluR4a immunoreactivity is most intense in the cell body layer and less dense in the molecular layer of the dentate gyrus. The labelling in the molecular layer is rather uniform and no specific bands corresponding to lateral and

medial pathways can be seen. Some of the basket cells in the hilus are also densely labelled. Although no detailed electron microscopic examination has been carried out in the dentate area, the results from examining CA1 and CA3 areas revealed heavy postsynaptic localization of mGluR4a at asymmetrical synapses (presumably glutamatergic) onto pyramidal cells, and the presynaptic localization of mGluR4a at both asymmetrical and symmetrical synapses. This suggests that the mGluR4 receptor could be an autoreceptor for both excitatory and inhibitory terminals. Secondly, the immunoreactivity of mGluR7 is very light or absent from the cell bodies and proximal dendrites of granule cells but there is intense staining in the middle third of the molecular layer, whereas the outer third of the molecular layer is virtually free of immunoreactivity for mGluR7. Analysis at the EM level shows that the presynaptic mGluR7 receptors are mostly localized in asymmetrical synapses. The distribution pattern of the mGluR7 receptor in the dentate gyrus is somewhat unexpected because it is the lateral pathway that showed a strong L-AP4 effect and yet it lacks mGluR7 receptors. In contrast, the medial pathway terminal field has a high density of mGluR7 receptors but produces little L-AP4 related activity. This suggests that the L-AP4 activity in the lateral pathway is probably not mediated by mGluR7. However, the function of the mGluR7 receptor in the medial pathway remains unknown.

7.1. 3 More inhibition in the lateral pathway than the medial pathway

Lateral pathway activation produces stronger $GABA_B$ inhibitory responses than medial pathway activation (Chapter 6). Interneurons possessing elaborate axon

ramifications in the lateral pathway terminal zone could provide both feed-forward and feedback inhibition to reduce the lateral perforant pathway responses (Chapter 1, 1.3.1.1). However, whether $GABA_A$ inhibition is also stronger in the lateral pathway has not been determined.

The lateral pathway is known to contain the opioid peptide enkephalin (McLean et al., 1987; Fredens et al., 1984; Gall et al., 1981). This opioid peptide is co-released with glutamate during high frequency stimulation (Caudle et al., 1991; Wagner et al., 1989) and has been shown to have a "disinhibitory" effect on granule cells (Xie et al., 1992; Bramham, 1992; Xie and Lewis, 1991). Furthermore, it has been shown that naloxone, a nonselective opioid receptor antagonist, blocks the induction of LTP in the dentate gyrus of anesthetized rats after high frequency stimulation of the lateral pathway but not the medial pathway (Bramham et al., 1988). The fact that naloxone can block the lateral pathway's LTP (Bramham et al., 1988) suggests that the disinhibitory mechanism mediated by opioid peptide has a very powerful control of LTP induction in the lateral pathway. This also suggests that the inhibition in this area is very strong and needs to be reduced in order to induce LTP.

In the current study, $GABA_A$ inhibition was artificially removed by bicuculline and therefore the experimental condition is different from the *in vivo* situation where $GABA_A$ inhibition is intact. Nevertheless, the interactions of the two pathways observed in current study could still occur when *in vivo* conditions are right. For example, as mentioned above, the opioid peptids released by the lateral pathway could serve as a "natural bicuculline" to remove $GABA_A$ inhibition.

Xie et al., (1992) have shown that in the lateral pathway, both the $GABA_A$ and $GABA_B$ IPSCs can be reduced by bath application of PL107, a μ opioid agonist. These authors suggested that at low concentrations, the μ receptor agonist PL017 has a facilitatory effect on the NMDA current due to disinhibition of IPSC and could contribute to the LTP induction in this pathway (Xie et al., 1992). Furthermore, Xie and Lewis (1995) reported that high frequency stimulation delivered to the lateral perforant pathway in the presence of naloxone could induce a long-lasting potentiation of the amplitude of $GABA_A$ receptor- mediated inhibitory postsynaptic current of granule cells and that this potentiation was not observed in control medium without naloxone. They further demonstrated that blocking δ, but not μ and κ, receptors is critical for inducing LTP of $GABA_A$ IPSCs in granule cells. These authors suggest that the opioid peptide may act at δ receptors on interneurons to hyperpolarize their dendrites, which reduces Ca^{2+} influx through NMDA channels and hence inhibits induction of LTP, whereas activation of the μ receptor may primarily act at the interneuronal terminals to directly inhibit GABA release (Xie et al., 1992; Capogna et al., 1993; Xie and Lewis, 1995). Thus, during high frequency stimulation, opioid peptide released by the lateral pathway could reduce inhibitory response in this area and facilitate LTP induction. However, the results presented in Chapter 6 clearly showed that the $GABA_B$ IPSCs in the lateral pathway can be enhanced after tetanic stimulation. Thus, the opioid peptide release by the lateral pathway during tetanic stimulation, if present, does not appear to act on $GABA_B$ interneurons.

A major difference between the current results and the results from Xie and Lewis

(1995) is that the potentiation of inhibitory responses can be observed without naloxone. One explanation is that there was no opioid peptide released by the tetanic stimulation paradigm used in the current study. Indeed, naloxone did not alter lateral pathway LTP nor did it change LTP induced by co-activation of both pathways (Chapter 3). However, this negative result cannot be seen as conclusive evidence that the opioid peptide is not released. Another explanation is that there are two groups of inhibitory interneurons, of which one group forms $GABA_A$ receptor synapses and is strongly inhibited by opioid peptide, while the other group forms $GABA_B$ receptor synapses and is not affected by opioid peptide. Discrete localization of $GABA_A$ and $GABA_B$ receptors has been proposed in a number of brain areas (Segal, 1990; Otis and Mody, 1992; Sugita et al., 1992). In the dentate gyrus Otis and Mody (1992) observed that spontaneous IPSCs do not show a slow $GABA_B$-receptor mediated component. Yet, at the same time, stimulus-elicited responses or those elicited by a burst discharge of GABA neurons induced by a convulsant consistently display a prominent $GABA_B$-receptor-mediated component (Otis and Mody, 1992). Furthermore, $GABA_A$-receptor-mediated miniature IPSCs appear to originate at proximal dendrites of dentate granule cells (Mody et al.,1994). There are at least five different types of inhibitory neurons in the dentate gyrus (Mody et al., 1994). Mody et al., (1994) suggest that $GABA_A$ receptors might be activated mostly by interneurons innervating the proximal membrane regions of granule cells, whereas other interneurons innervating distal dendrites might exert their actions through $GABA_B$ receptors. If this assumption is correct, the interneurons which produce LTP of $GABA_B$ current might be different from the interneurons which produce LTP of the $GABA_A$

current, as observed by Xie et al. (1994) in agreement with my results. This scheme suggests a very complex fine tuning machanism of local inhibition circuitry by opioid peptides and is worth further exploration.

7.1.4 High LTP capacity in medial pathway in comparison to the lateral pathway

After repeated tetanization, medial pathway stimulation produces more LTP than the lateral pathway (Chapter 6). The results presented in chapter 6 showed that the difference between lateral and medial pathway activation on LTP capacity is related to the larger postsynaptic $GABA_B$ inhibition in the lateral pathway. By removing this inhibition, the lateral pathway responses can be further potentiated by subsequent tetanization. Most importantly, this inhibition itself can be potentiated by tetanic stimulation; thus, the strength of inhibition is greater after the first tetanization. The degree of potentiation in the inhibitory response can then set the threshold of LTP induction in lateral pathway.

7.1. 5 Unidirectional facilitatory effect of the lateral pathway on the medial pathway

When co-activating the lateral and medial pathways, the lateral pathway facilitates the medial pathway LTP but not vice versa. Tomasulo et al. (1993) have found that removing $GABA_A$ inhibition in the lateral pathway enhances LTP to the extent that the subsequent co-activation of both pathways has no additional effect. This finding is in agreement with my observations (Chapter 6). However, the mechanism underlying the facilitatory effect of the lateral pathway on the medial pathway LTP is still not explored.

In the first attempt to answer this question, I tested the effect of enkephalin in the medial pathway. The rationale was that during co-activation, the opioid peptide released from the lateral pathway might diffuse to the medial pathway and facilitate the medial LTP. Exogenously applied met-enkephalin did facilitate the medial pathway LTP. However, the complementary experiment in which naloxone was used to block the endogenous peptide effects did not reveal reduction of the facilitatory effect of the lateral pathway on the medial pathway.

From the computer simulation work done by Jou et al. (1995) using a geometrically realistic granule cell model, it has been shown that for the same amount of conductance change, the local depolarization produced by lateral pathway activation is two-fold larger than that produced by medial pathway activation. Thus, this larger depolarization could generate axial current passing through the dendrites in the medial region of the molecular layer (medial pathway) en route to the soma, and could provide additional depolarization of the dendrites in the medial pathway. This additional depolarization could help to remove Mg^{2+} block of the NMDA receptor and facilitate the medial pathway LTP. During co-activation the depolarization current produced by dendrites in the medial pathway could propagate in both directions (towards the soma or the lateral pathway terminal field). However, due to the higher resistance of the distal dendrites as they taper towards the lateral pathway, the propagation towards the lateral pathway direction will be limited. Furthermore, even if the extra depolarization reaches the lateral pathway terminal field, the postsynaptic $GABA_B$ conductance in the lateral pathway could easily shunt this depolarization current. Consequently, the end product

of co-activating lateral and medial pathways will favour more LTP in the medial pathway.

7.2 Differential potentiation of AMPA and NMDA components

In the medial perforant pathway the AMPA and NMDA components of the EPSCs showed different amounts of potentiation after LTP induction (Chapter 5). This is particularly clear for cases in which a large magnitude LTP was induced. For the experiments in which CNQX was applied after LTP induction to isolate the NMDA component, the isolated NMDA component did not change in parallel with the AMPA component. However, the percentage of the isolated NMDA current to total current was towards the high end of the average obtained from control experiments (Chapter 3). Since the ratio of NMDA component before LTP induction was unknown, this result can not rule out the possibility that a small amount of potentiation (10-20%) was expressed in the NMDA current and thus might account for the slightly larger ratio of the NMDA component in the potentiated preparation.

Xie et al. (1996) recently reported that in the rabbit medial perforant pathway, the pharmacologically isolated NMDA component showed 50% potentiation by 100 Hz tetanization. In their study, the tetanic stimulation was applied to the isolated NMDA responses (AMPA component was blocked by 10 μM CNQX) and the extracellular Mg^{2+} concentration was arbitrarily reduced to 0.1 mM. Lowering the extracellular Mg^{2+} concentration was, presumably, to compensate for the lacking of the AMPA component

which, in the natural condition, can produce the membrane depolarization required to remove the Mg^{2+} blockade in the NMDA receptor. Potentiation of the NMDA receptor-mediated response was also observed in a special form of LTP termed "anoxic LTP" (Gozlan et al., 1995a,b; Gozlan et al., 1994; Crépel et al., 1993). This form of LTP was induced by a brief anoxic episode; upon re-oxygenation, a long-lasting potentiation (around 50%) of the NMDA receptor-mediated EPSP was observed (Crépel et al., 1993). Gozlan et al. (1994, 1995a,b) demonstrated that the redox site on the NMDA receptor is responsible for the induction and expression of anoxic LTP; that is, anoxia triggers anoxic LTP only when at least part of the redox site of the NMDA receptor is in a reduced form. Furthermore, Hammond et al. (1994) demonstrated that the potentiation of NMDA receptor normally would not occur in conventional tetanic LTP, except in special experimental conditions where AMPA receptors are partly or fully blocked and NMDA receptors boosted by reducing extracellular Mg^{2+}. Under those special conditions, the tetanic stimulation could produce LTP of the NMDA receptor-mediated responses and this form of LTP was sensitive to redox reagents (Hammond et al., 1994). Indeed, in most of the reports where LTP of the NMDA receptor-mediated responses were observed, the experiments were done in the special condition mentioned above (Asztely et al., 1992; Xie et al., 1992; Clark and Collingridge, 1995; Xie et al., 1996). However, how blockade of AMPA receptors and reduced Mg^{2+} concentration lead to changes of the redox site in the NMDA receptor and produce the potentiation of the NMDA responses remains obscure.

7.3 Silent synapse

The data presented in Chapter 5 demonstrate selective recruitment of AMPA receptors during LTP expression. Two models for recruitment of silent synapses are proposed in Chapter 4. In a recent report, Desmond and Weinberg (1996) demonstrated a differential synaptic localization of AMPA and NMDA receptor subunits in the dentate gyrus of adult rats. They used postembedding immunogold labelling for three glutamate receptor subunits (GluR1, GluR2/3, and NMDAR1) to characterize AMPA and NMDA receptors in axospinous synapses in the medial pathway area. They found that the axospinous synapses were substantially more likely to be NMDAR immunopositive than GluR1 or GluR2/3 immunopositive. This suggests that there are some synapses which have only NMDA receptors (silent synapses). When they subsequently grouped the synapses into synapses with a perforated postsynaptic density and synapses with a nonperforated postsynaptic density, they found these two groups are equally likely to be NMDAR immunopositive. On the other hand, the probability of axospinous synapses with perforated postsynaptic density being AMPAR (GluR1 or GluR2/3) immunopositive is about twice that of synapses with nonperforated postsynaptic density. Given that synapses with perforated postsynaptic density are hypothesized to be potentiated synapses (Geinisman et al., 1993), the authors concluded that these data suggest that LTP leads to the insertion of AMPA receptors at the postsynaptic density. These results are in agreement with my observation of selective recruitment of AMPA receptors during LTP expression.

7.4 Interaction of lateral and medial perforant pathways

The data presented thus far indicate that medial pathway is designed to pass the inputs from medial entorhinal cortex to dentate granule cells with ease. Compared with the lateral pathway, the medial pathway has high output synapses which more readily release transmitter when an action potential arrives. The medial pathway has less negative feedback control for the transmitter release than the lateral pathway (fewer L-AP4 receptors). Furthermore, this pathway readily potentiates after each tetanic stimulation, thus displaying more capacity for LTP induction and expression. When co-activated with the lateral pathway, the medial pathway response is enhanced by the lateral pathway activation. On the other hand the lateral pathway's synaptic transmission seems to be under more strict control. It has more autoreceptors for negative feedback of transmitter release (L-AP4 receptors). This pathway also receives more feed-forward inhibition than the medial pathway. Furthermore, repeated tetanic stimulation applied to this pathway produces little additional potentiation. When co-activated with the medial pathway, this pathway is not facilitated by medial pathway activation. In general, when compared with the medial pathway, the lateral pathway showed less plasticity and more rigid controls on transmitting inputs from lateral entorhinal cortex to dentate granule cells. In addition, acetylcholine and norepinephrine, the two neuromodulators known to facilitate LTP induction, act in a pathway-specific manner; that is, they facilitate medial pathway LTP but not lateral pathway LTP (Kahle and Cotman, 1989; Burgard and Sarvey, 1990; Dahl and Sarvey; 1989; Harley, 1991). The conclusion from the above observations is that the whole system design of the dentate gyrus seems to be in favour of passing on

the inputs from medial entorhinal cortex rather than from the lateral entorhinal cortex.

The scheme of input processing and interactions in dentate gyrus might be related to the function of this structure. The hippocampal formation is involved in generating spatial maps of the surrounding environment (O'Keefe and Nadel, 1978; O'Keefe and Burgess, 1996) and spatial memory (Morris et al., 1982,1986). More recently Bunsey and Eichenbaum (1996) demonstrated that the hippocampal formation is also critical for non-spatial declarative memory in rats (humans too). Part of this memory processing involves forming integrated representations of overlapping stimulus associations (Bunsey and Eichenbaum, 1996). Considering the different sensory inputs to the lateral and medial entorhinal cortices, dentate granule cells may play an important role in this kind of information processing. As mentioned above, the dentate gyrus more readily passes the inputs from the medial pathway (medial entorhinal cortex) than those of the lateral perforant pathway (lateral entorhinal cortex) and co-activation of both pathways enhances the medial pathway LTP. Thus, the information carried by the medial pathway, and not the lateral pathway, is emphasized by processing in dentate gyrus. Based on the anatomical connections, the medial pathway may relay visual information into the dentate gyrus. The emphasis of visual input in the dentate gyrus certainly fits the role of hippocampal formation as a spatial memory center. On the other hand, the olfactory input from the lateral pathway is less emphasized in the dentate gyrus. In fact, the olfactory memory could be processed in other cortical areas. Lesion of the hippocampus does not affect odour discrimination memory (Eichenbaum et al., 1988). Thus, the olfactory information may not be very important in the dentate gyrus in terms of olfactory memory

consolidation or storage. However, this olfactory input when coinciding with a visual input, is important to create an association between the two inputs and helps to consolidate the visual input.

7.5 Summary

In this project I characterized the properties of synaptic transmission in the medial and the lateral pathways in detail. The major findings include: (1) that the medial pathway is prone to high frequency depression while the lateral pathway is more resistant to high frequency depression; (2) that both medial and lateral pathways contain a prominent NMDA component in synaptic transmission at resting membrane potential. Thus, I have clarified some of the previous confusion in the literature. I also found that the endogenous opioid peptide released from the lateral pathway has no effect on lateral pathway LTP and on co-activation of both pathways. The main function of the opioid peptide released by the lateral pathway is probably restricted to inhibitory interneurons.

LTP studies in the lateral and medial pathways revealed that during tetanic stimulation there are changes in evoked responses (prolonged depolarization and increased number of action potentials) which can be used to predict a successful LTP induction. This phenomenon can be used to study various modulators and second messenger systems in LTP induction. In addition, I found that medial pathway LTP expression is mediated by a non-parallel potentiation of AMPA and NMDA components of the potentiated responses. This selective recruitment of AMPA receptors, with the addition of quantal analysis and variance analysis, leads me to propose the silent

synapse hypothesis. Anatomical support for this hypothesis from other research groups is starting to emerge.

The stronger postsynaptic $GABA_B$ inhibition in the lateral pathway is another important finding of this project. More importantly, I demonstrated that the $GABA_B$ IPSP can be potentiated by tetanic stimulation and that this potentiation is a long-lasting one. This LTP of the $GABA_B$ IPSP is a novel finding in the dentate gyrus. I also demonstrated that the LTP of the $GABA_B$ IPSP has an impact on LTP capacity of the lateral pathway. In the medial pathway I found that the presynaptic $GABA_B$ receptors played a major role in heterosynaptic depression. This short-term depression can serve as a gating mechanism to eliminate unrelated "noise". The differential LTP capacity of the medial and lateral pathways is another novel finding in the perforant pathway. In addition, I found that co-activation of the lateral and medial pathways leads to enhanced potentiation in the medial pathway whereas potentiation in the lateral pathway is not affected. Thus, the lateral pathway can facilitate the medial pathway and this is probably related to their physiological functions.

To summarize from above findings: the medial and the lateral perforant pathways have different physiological properties, are under different inhibitory modulations, show different LTP capacities, and exhibit facilitation of medial pathway by lateral pathway activation but not vice versa. Clearly, even in this much reduced preparation, with limited neuronal circuitry, relatively free from many modulatory inputs from other brain circuitries, the activity and interactions of two closely related but very different pathways can be controlled/modulated at many different levels. Presynaptically, the transmitter release

mechanism of the "high-output" medial pathway synapses is probably different from that of the lateral pathway. In the lateral pathway, there are opioid peptides which can be co-released with glutamate when stimulation pattern or frequency is appropriate. There are also presynaptic autoreceptors which regulate transmitter release in both pathways. Postsynaptically, the receptors can be modulated by phosphorylation and new receptors can be inserted into the membrane. Feed-forward Inhibition certainly plays a role in modulating postsynaptic responses. The distribution of $GABA_A$ and $GABA_B$ receptors and their different properties further complicates the situation. Factors modulating various inhibitory interneurons in this area have to be considered i.e. serotonin, CCK, opioid peptides. The conductance properties of granule cell dendrites are yet another factor which could affect temporal and spatial summation of the responses. Thus, the "simple" system is not simple at all. There are many "unknowns" in this system. My research helped to answer some of the questions and elucidated some possible mechanisms. This knowledge provides the necessary background for understanding more complex cognitive functions carried out by the hippocampal formation.

7.6 Future directions

There are many unanswered questions left by the current study. In order to fully understand the function and interactions of the lateral and medial pathways, the following issues have to be clarified.

7.6.1 Ultrastructure of the perforant pathway

The correlation of presynaptic ultrastructure and release properties in the medial and the lateral pathways certainly merits more detailed quantitative studies. Previous studies using the crayfish neuromuscular junction have revealed that the high-output synapses have a larger active zone per synapse than the low-output synapses (review Atwood and Wojtowicz, 1986). Current studies revealed that the output synapses of medial pathway can be characterized as high-output synapses on the basis of their release properties and that they are very different from the lateral pathway synapses. It would be important to verify whether the release properties are correlated with the ultrastructure of the synapses. This study will contribute to our knowledge of perforant pathways and to general transmitter release mechanisms. If no ultrastructural differences can be seen in the two perforant pathways, it is possible that the difference is in the calcium channels and/or proteins involved in the transmitter release machinery. However, to quantify Ca^{2+} channels in the presynaptic active zone is not trivial. Furthermore, our understanding of how Ca^{2+} triggers transmitter release and the release mechanism is currently far from complete. Thus, the question of which presynaptic proteins are the possible candidates underlying the differences in release properties in the medial and lateral pathway awaits further research.

7.6.2 Inhibitory interneurons and GABA receptors

The modulation of inhibitory interneurons is an important issue needing further exploration. There are at least 5 types of inhibitory interneurons in the dentate gyrus

(review, Mody et al., 1994). The morphology and distribution of these interneurons suggest that they have specific functions. Some of these interneurons inhibit granule somas and proximal dendrites (HICAP cells and basket cells), some inhibit the distal dendrites of the granule cell in the outer two-third of the molecular layer (HIPP cells and MOPP cells), and some inhibit axon initial segments of the granule cells (axon-axonic cells). These interneurons could be modulated by serotonin, CCK and opioid peptide (Chapter 1), depending on their localization and receptor types. More detailed systematic studies of each type of inhibitory interneuron are required in order to understand their functions in the dentate gyrus. Furthermore, with the aid of advanced optical equipment, it is now possible to visually identify interneurons in the slice preparation and record from them. Paired whole-cell patch recordings from inhibitory interneurons and granule cells can be obtained. This is a crucial experiment for the study of spatial and temporal effects of inhibition on excitatory responses of granule cells. We can also verify whether there is a group of interneurons which produces solely $GABA_A$ responses and which are modulated by opioid peptide. And whether there is another group of interneurons that produces $GABA_B$ responses and is not sensitive to opioid peptides. The morphology of the interneuron recorded from can later be identified by including fluorescent dye in the recording electrode, thus filling the cell while physiological recordings are obtained. Furthermore, special emphasis should be directed to understanding the LTP of the IPSP. With paired recordings from inhibitory interneurons and granule cells, we could then demonstrate that it is the synapses between perforant pathway and the inhibitory interneuron (feedforward inhibition) that underwent potentiation as proposed in Chapter

6.

The localization of $GABA_A$ and $GABA_B$ receptors in the dentate gyrus has to be studied at the EM level in order to settle the argument of whether they are co-localized in the same synapses. One feasible method is double-labeling immunocytochemistry, using the combination of the two primary antibodies, monoclonal anti-rat $GABA_A$ receptor and monnclonal anti-rat $GABA_B$ receptor. The secondary antibodies will be conjugated with colloidal gold of different sizes (for example, 10 and 30 nm diameters) to distinguish the labeled $GABA_A$ and $GABA_B$ receptors. Using EM methods to examine the distribution of different sized gold particles in the synapses of the dentate granule cell would provide the details of the location of different GABA receptors.

7.6.3 More realistic stimulation

The current study used stimulations with very regular intervals. In reality, however, the neuronal firing pattern is very irregular. This is particularly important when considering two or more inputs with some special temporal pattern because the temporal pattern alone could be important for information processing. The co-activation stimulation paradigm used in this study is far from ideal. In reality, neurons don't all fire at exactly 100 Hz and with exactly 4 ms phase shift to other firing neurons (as in the arbitrary stimulation pattern used in this study). It would be interesting to use single unit recordings to acquire realistic firing patterns from neurons in the entorhinal cortex and to use this firing pattern to drive a stimulator to stimulate the perforant pathway. Using simultaneous recordings from lateral and medial entorhinal neurons (ideally from awake

animals performing distinct behaviours) and replaying the pattern to stimulate lateral and medial perforant pathways while recording from dentate granule cells, we could acquire more knowledge about temporal integration of two inputs under more realistic operating conditions.

References

Abdul-Ghani, M.A.; Valiante, T.A. ; Carlen, P.L.; and Pennefather, P.S. (1996a) Tyrosine kinase inhibitors enhance a Ca^{2+}-activated K^+ current (I_{AHP}) and reduce I_{AHP} supression by a metabotropic glutamate receptor agonist in rat dentate granule neurons. J. Physiol. 496:139-144.

Abdul-Ghani, M.A.; Valiante, T.A.; Carlen, P.L.; and Pennefather, P.S. (1996b) Metabotropic glutamate receptors coupled to IP3 production mediate inhibition of I_{AHP} in rat dentate granule neurons. J. Neurophysiol. 76:2691-2700.

Abe, T.; Sugihara, H.; Nawa, H.; Shigemoto, R.; Mizuno, N.; and Nakanishi, S. (1992) Molecular characterization of a novel metabotropic glutamate receptor mGluR5 coupled to inositol/phosphate/Ca2+ signal transduction. J. Biol. Chem. 267:13361-13368.

Abraham, W.C.; Bliss, T.V.P.; and Goddard, G.V. (1985) Heterosynaptic changes accompany long-term but not short-term potentiation of the perforant path in the anaesthetized rat. J. Physiol. 363:335-349.

Abraham, W.C. and Goddard, G.V. (1983) Asymmetric relationships between homosynaptic long-term potentiation and heterosynaptic depression. Nature 305:717-719.

Akers, R.; Lovinger, D.; Colley, P.; Linden, D.; and Routtenberg, A. (1986) Translocation of protein kinase C activity may mediate hippocampal long-term potentiation. Science 231:587-589.

Alger, B.E. and Teyler, T.J. (1976) Long-term and short-term plasticity in the CA1, CA3 and dentate region of the rat hippocampal slice. Brain Res. 110:463-480.

Alonso, A. and Köhler, C. (1984) A study of the reciprocal connections between the septum and the entorhinal area using anterograde and retrograde axonal transport methods in the rat brain. J. Comp. Neurol. 225:327-343.

Alonso, A.; DeCurtis, M.; and Llinas, R. (1990) Postsynaptic Hebbian and non-Hebbian long-term potentiation of synaptic efficacy in the entorhinal cortex in slices and in isolated adult guinea pig brain. Proc. Natl. Acad. Sci. USA 87:9280-9284.

Amaral, D.G. (1978) A Golgi study of cell type in the hilar region of the hippocampus in the rat. J. Comp. Neurol. 132:851-914.

Amaral, D.G. and Kurz, J. (1985) An analysis of the origins of cholinergic and noncholinergic septal projections to the hippocampal formation of the rat. J. Comp.

Neurol. 240:37-59.

Amaral, D.G.; Ishizuka, N.; and Claiborne, B. (1990) Neurons, numbers and the hippocampal network. In "Progress in Brain Research: Understanding the Brain through the Hippocampus: The Hippocampal Region as a Model for Studying Structure and Function." (Storm-Mathisen, J.; Zimmer, J.; and Ottersen, O.P., Eds.), pp 1-11.

Amaral, D.G. and Witter, M.P. (1995a) The three-dimensional organization of the hippocampal formation: A review of anatomical data. Neuroscience 31:571-591.

Amaral, D.G. and Witter, M.P (1995b) Hippocampal formation. In Paxinos, G. (Ed), The rat nervous system (pp.443-493), San Diego:Academic Press.

Aniksztejn, L.; Ben-Ari, Y. (1991) Novel form of long-term potentiation produced by a K^+ channel blocker in the hippocampus. Nature 349:67-69.

Anson, J. and Collins, G.G.S. (1987) Possible presynaptic actions of 2-amino-4-phosphonobutyrate in rat olfactory cortex. Br. J. Pharmacol. 91:753-761.

Aroniadou, V.A. and Teyler, T.J. (1992) Induction of NMDA receptor-independent long-term potentiation (LTP) in visual cortex of adult rats. Brain Res. 584:169-173.

Artola, A. and Singer, W. (1987) Long-term potentiation and NMDA receptors in rat visual cortex. Nature 330:649-652.

Asztely, F.; Wigström, H.; and Gustaffson, B. (1992) The relative contribution of NMDA receptor channels in the expression of long-term potentiation in the hippocampal CA1 region. Eur. J. Neurosci. 4:681-690.

Atwood, H.L. and Wojtowicz, J.M. (1986) Short-term and long-term plasticity and physiological differentiation of crustacean motor synapses. Int. Rev. Neurobiol. 28:275-362.

Bannerman, D.M.; Chapman, P.F.; Kelly, P.A.T.; Butcher, S.P.; and Morris, R.G.M. (1994) Inhibition of nitric oxide synthase does not prevent the induction of long-term potentiation *in vivo*. J. Neurosci. 14:7415-7425.

Bannerman, D.M.; Good, M.A.; Butcher, S.P.; Ramsay, M.; and Morris, R.G.M. (1995) Prior experience and N-methyl-D-aspartate receptor blockade dissociate components of spatial learning in the watermaze. Nature 378:182-186.

Baranyi, A. and Szente, M.B. (1987) Long lasting potentiation of synaptic transmission requires postsynaptic modification in the neocortex. Brain Res. 423:378-384.

Barrionuevo, G. and Brown, T.H. (1983) Associative long-term potentiation in hippocampal slices. Proc. Natl. Acad. Sci. USA 80:7347-7351.

Bashir, Z.I.; Alford, S.; Davies, S.N.; Randall, A.D.; and Collingridge, G.L. (1991) Long-term potentiation of NMDA receptor-mediated synaptic transmission in the hippocampus. Nature 349:156-158.

Bashir, Z.I. and Collingridge, G.L. (1994) An investigation of depotentiation of long-term potentiation in the CA1 region of the hippocampus. Exp. Brain Res. 100:437-443.

Bashir, Z.I.; Bortolotto, Z.A.; Davies, C.H.; Berretta, N.; Irving, A.J.; Seal, A.J.; Henley, J.M.; Jane, D.E.; Watkins, J.C.; and Collingridge, G.L. (1993) Induction of LTP in the hippocampus needs synaptic activation of glutamate metabotropic receptors. Nature 363:347-350.

Baskys, A.; Carlen, P.L.; and Wojtowicz, J.M. (1991) Long-term potentiation of synaptic responses in the rat dentate gyrus is due to increased quantal content. Neurosci. Lett. 127:169-172.

Bayer, S.A. (1982) Changes in the total number of dentate granule cells in juvenile and adult rats: A correlated volumetric and ^{3}H-thymidine autoradiographic study. Exp. Brain Res. 46:315-323.

Bayer, S.A.; Yackel, J.W.; and Puri, P.S. (1982) Neurons in the rat dentate gyrus granular layer substantially increase during juvenile and adult life. Science 216:890-892.

Beckstead, R.M. (1978) Afferent connections of the entorhinal area in the rat as demonstrated by retrograde cell-labelling with horseradish peroxidase. Brain Res. 152:249-264.

Bekkers, J.M. and Stevens, C.F. (1989) NMDA and non-NMDA receptors are co-localized at individual excitatory synapses in cultured rat hippocampus. Nature 341:230-233.

Bekkers, J.M. and Stevens, C.F. (1990) Presynaptic mechanism for long-term potentiation in the hippocampus. Nature 346:724-729.

Bekkers, J.M. and Stevens, C.F. (1991) Application of quantal analysis to the study of long-term potentiation: errors, assumptions, and precautions. In Long-term Potentiation. A Debate of Current Issues, M. Baudry and J. L. Davis, eds. (Cambridge, Massachusetts: MIT Press), pp. 63-76.

Ben-Ari, Y.; Aniksztejn, L.; and Bregestovski, P. (1992) Protein kinase C modulation of

NMDA currents: an important link for LTP induction. TINS 15:333-22--339.

Berger, T.W. and Yeckel, M.F. (1991) Long-term potentiation of entorhinal afferents to the hippocampus: enhanced propagation of activity through the trisynaptic pathway. In Long-Term Potentiation. A Debate of Current Issues, M. Baudry and J. L. Davis, eds. (Cambridge, Massachusetts: MIT Press), pp. 327-356.

Bindman, L.J.; Meyer, T.; and Pockett, S. (1987) Long term potentiaion in rat neocortical neurons in slices produced by repetitive pairing of an afferent volley with intracellular depolarizing current. J. Physiol. 386:90.

Blackstad, T.W. (1956) Commissural connections of the hippocampal region in the rat, with special reference to their mode of termination. J. Comp. Neurol. 105:417-537.

Blackstad, T.W. (1958) On the termination of some afferents to the hippocampus and fascia dentata. Acta. Anat. 35:202-214.

Blackstone, C.; Murhpy, T.H.; Moss, S.J.; Baraban, J.M.; and Huganir, R.L. (1994) Cyclic AMP and synaptic activating-dependent phosphorylation of AMPA-preferring glutamate receptors. J. Neurophysiol. 69:1150-1159.

Bliss, T.V.P. and Collingridge, G.L. (1993) A synaptic model of memory: long-term potentiation in the hippocampus. Nature 361:31-39.

Bliss, T.V.P.; Lancaster, B.; and Wheal, H.V. (1983) Long-term potentiation in commissural and Schaffer projection to hippocampal CA1 cells: an *in vivo* study in the rat. J. Physiol (Lond.) 341:617-626.

Bliss, T.V.P. and Lømo, T. (1973) Long-lasting potentiation of synaptic transmission in the dentate area of the anaesthetized rabbit following stimulation of the perforant path. J. Physiol. (Lond.) 232:331-356.

Bliss, T.V.P. and Richter-Levin, G. (1993) Spatial learning and the saturation of long-term potentiation. Hippocampus 3:123-126.

Bohme, G.A.; Bon, C.; Stutzmann, J.M.; Doble, A.; and Blanchard, J.C. (1991) Possible involvement of nitric oxide in long-term potentiation. Eur. J. Pharmacol. 199:379-381.

Bortolotto, Z.A. and Collingridge, G.L. (1993) Characterization of LTP induced by the activation of glutamate metabotropic receptors in area CA1 of the hippocampus. Neuropharmacology 32:1-9.

Boss, B.D.; Peterson, G.M.; and Cowan, W.M. (1985) On the number of neurons in the dentate gyrus of the rat. Brain Res. 338:144-150.

Boulton, C.H.; Irving, A.J.; Southam, E.; Potier, B.; Garthwaite, J.; and Collingridge, G.L. (1994) The nitric oxide-cyclic GMP pathway and synaptic depression in rat hippocampal slices. Eur. J. Neurosci. 6:1528-1535.

Bourtchuladze, R.; Frenguelli, B.; Blendy, J.; Cioffi, D.; Schutz, G.; and Silva, A.J. (1994) Dificient long-term memory in mice with a targeted mutation of the cAMP-responsive element-binding protein. Cell 79:59-68.

Bowery, N.G., Hudson, A.L., and Price, G.W. (1987) $GABA_A$ and $GABA_B$ receptor site distribution in the rat central nervous system. Neurosci. 20:365-383.

Bradley, S.R.; Levey, A.I.; Hersch, S.M.; and Conn, P.J. (1996) Immunocytochemical localization of group III metabotropic glutamate receptors in the hippocampus with subtype-specific antibodies. J. Neurosci. 16:2044-2056.

Bramham, C.R.; Milgram, N.W.; and Srebro, B. (1991a) Opioid receptor activation is required to induce LTP of synaptic transmission in the lateral perforant path in vivo. Brain Res. 567:42-50.

Bramham, C.R.; Milgram, N.W.; and Srebro, B. (1991b) Activation of AP5-sensitive NMDA receptors is not required to induce LTP of synaptic transmission in the lateral perforant path. Eur. J. Neurosci. 3:1300-1308.

Bramham, C.R. (1992) Opioid receptor dependent long-term potentiation: peptidergic regulation of synaptic plasticity in the hippocampus. Neurochem. Int. 20:441-455.

Bredt, D.S.; Ferris, C.D.; and Snyder, S.H. (1992) Nitric oxide synthase regulatory sites. Phosphorylation by cyclic AMP-dependent protein kinase, protein kinase C, and calcium/calmodulin protein kinase; indentification of flavin and calmodulin binding sites. J. Biol. Chem. 267:10976-10981.

Brown, T.H.; Perkel, D.H.; and Feldman, M.W. (1976) Evoked neurotransmitter release: statistical effects of nonuniformity and nonstationarity. Proc. Natl. Acad. Sci. USA 73:2913-2917.

Brown, R.E.; Rabe, H.; and Reymann, K.G. (1994) (RS)-alpha-methyl-4-carboxyphenylglycine (MCPG) does not block theta burst-induced long-term potentiation in area CA1 of rat hippocampal slices. Neurosci. Lett. 170:17-21.

Buckmaster, P.S. and Schwartzkroin, P.A (1995) Interneurons and inhibition in the

dentate gyrus of the rat *in vivo*. J. Neurosci. 15:774-789.

Bunsey, M. and Eichenbaum, H. (1996) Conservation of hippocampal memory function in rats and humans. Nature 379:255-257.

Burgard, E.C. and Sarvey, J.M. (1990) Muscarinic receptor activation facilitates the induction of long-term potentiation (LTP) in the rat dentate gyrus. Neurosci. Lett. 116:34-39.

Burgard, E.C. and Sarvey, J.M. (1991) Long-lasting potentiation and epileptiform activity produced by $GABA_B$ receptor activation in the dentate gyrus of rat hippocampal slice. J. Neurosci. 11:1198-1209.

Burger, P.M.; Mehl, E.; Cameron, P.L.; Maycox, P.R.; Baumert, M.; Lottspeich, F.; De Camilli, P.; and Jahn, R. (1989) Synaptic vesicles immunoisolated from rat cerebral cortex contain high levels of glutamate. Neuron 3:715-720.

Burke, J.P. and Hablitz, J.J. (1996) G-protein activation by metabotropic glutamate receptors reduces spike frequency adaptation in neocortical neurons. Neuroscience 75:123-131.

Buzsáki, G. (1984) Feed-forward inhibition in the hippocampal formation. Prog. Neurobiol. 22:131-153.

Cahusac, P.M.; Miyashita, Y.; and Rolls, E.T. (1989) Responses of hippocampal formation neurons in the monkey related to delayed spatial response and object-place memory tasks. Behav. Brain Res. 33:229-240.

Cain, D.P.; Hargreaves, E.L.; Boon, F.; and Dennison, Z. (1993) An examination of the relations between hippocampal long-term potentiaiton, kindling, afterdischarge, and place learning in the water maze. Hippocampus 3:153-164.

Capochhi, G.; Zampolini, M.; and Larson, J. (1992) Theta burst stimulation is optimal for induction of LTP at both apical and basal dendritic synapses on hippocampal CA1 neurons. Brain Res. 591:332-336.

Capogna, M.; Gähwiler, B.H.; and Thompson, S.M. (1993) Mechanism of mu-opioid receptor mediated presynaptic inhibition in the rat hippocampus in vitro. J. Physiol. (Lond) 470:539-558.

Castillo, P.E.; Weisskopf, M.G.; and Nicoll, R.A. (1994) The role of Ca^{2+} channels in hippocampal mossy fiber synaptic transmission and long-term potentiation. Neuron 12:261-269.

Castro, C.A.; Silbert, B.L.; McNaughton, E.L.; Barnes, C.A. (1989) Recovery of spatial learning deficits after decay of electrically induced synaptic enhancement in the hippocampus. Nature 342:545-548.

Caudle, R.M.; Wagner, J.J.; and Chavkin, C. (1991) Endogenous opioids released from perforant path modulate norepinephrine actions and inhibitory potentials in guinea pig CA3 pyramidal cells. J. Pharmacol. Exp. Ther. 258:18-26.

Chavkin, C. and Bloom, F.E. (1985) Opiate antagonists do not alter neuronal responses to stimulation of opioid-containing pathways in rat hippocampus. Neuropeptides 7:19-22.

Chen, L. and Huang, L.-Y. M. (1992) Protein kinase C reduces Mg^{2+} block of NMDA-receptor channels as a mechanism of modulation. Nature 356:521-523.

Chetkovich, D.M.; Gray, R.; Johnston, D.; and Sweatt, J.D. (1991) N-methyl-D-asparate receptor activation increases cAMP levels and voltage-gated Ca2+ channel activity in area CA1 of hippocampus. Proc. Natl. Acad. Sci. USA 88:6467-6471.

Christie, B.R. and Abraham, W.C. (1994) Differential regulation of paired pulse plasticity following LTP in the dentate gyrus. NeuroReport 5:385-388.

Christie, B.R.; Stellwagen, D.; and Abraham, W.C. (1995) Evidence for common expression mechanisms underlying heterosynaptic and associative long-term depression in the dentate gyrus. J. Neurophysiol. 74:1244-1247.

Claiborne, B.J.; Amaral, D.G.; and Cowan, W.M. (1986) A light and electron microscopic analysis of the mossy fibers of the dentate gyrus. J. Comp. Neurol. 246:435-458.

Clark, K.A. and Collingridge, G.L. (1995) Synaptic potentiation of dual-component excitatory postsynaptic currents in the rat hippocampus. J. Physiol. 482:39-52.

Cohen, N.J. and Eichenbaum, H. (1993) Memory, Amnesia and the Hippocampal System. The MIT Press, Cambridge, Massachusetts.

Cohen, N.J. and Squire, L.R. (1980) Preserved learning and retention of pattern analyzing skill in amnesia: Dissociation of knowing how and knowing that. Science 210:207-209.

Conard, L.C.A.; Leonard, C.M.; and Pfaff, D.W. (1974) Connections of the median and dorsal raphe nuclei in the rat: An autoradiographic and degeneration study. J. Comp. Neurol. 156:179-206.

Colino, A and Malenka, R.C. (1993) Mechanisms underlying induction of long-term

potentiation in rat medial and lateral perforant paths in vitro. J. Neurophysiol. 69:1150-1159.

Collingridge, G.L. (1985) Long term potentiation in the hippocampus: mechanisms of initiation and modulation by neurotransmitters. Trends Pharmacol. Sci. 6:407-411.

Collingridge, G.L and Bliss, T.V.P. (1987) NMDA receptors - their role in long-term potentiation. Trends Neurosci, 10:288-293.

Cooper, R.L.; Harrington, C.C.; Marin, L. and Atwood, H.L. (1996) Quantal release at visualized terminals of a crayfish motor axon: Intraterminal and regional differences. J. Comp. Neurol. 375:583-600.

Cotman, C.W.; Flatman, J.A.; Ganong, A.H.; and Perkins, M.N. (1986) Effects of excitatory amino acid antagonists on evoked and spontaneous excitatory potentials in guinea-pig hippocampus. J. Physiol (Lond). 378:403-415.

Cowan, W.M.; Stanfield, B.B.; and Kishi K. (1980) The development of the dentate gyrus. Curr. Topics. Dev. Biol. 15:103-157.

Crépel, V.; Hammond, C.; Krnjevic, K.; Chinestra, P.; and Ben-Ari, Y. (1993) Anoxia-induced LTP of isolated NMDA receptor-mediated synaptic responses. J. Neurophysiol. 69:1774-1778.

Crain, B.J.; Chang, K.-J.; and McNamara, J.O. (1986) Quantitative autoradiographic analysis of mu and delta opioid binding sites in the rat hippocampal formation. J. Comp. Neurol. 246:170-180.

Cummings, J.A.; Nicola, S.M.; Malenka, R.C. (1994) Induction in the rat hippocampus of long-term potentiation (LTP) and long-term depression (LTD) in the presence of a nitric oxide synthase inhibitor. Neurosci. Lett. 176:110-114.

Dahl, D. (1987) Systemically administered cholecystokinin affects an evoked potential in the hippocampal dentate gyrus. Neuropeptide 10:165-173.

Dahl, D. and Sarvey, J.M. (1989) Norepinephrine induces pathway-specific long-lasting potentiation and depression in the hippocampal dentate gyrus. Proc. Natl. Acad. Sci. USA 86:4776-4780.

Dahl, D. and Sarvey, J.M. (1990) β-adrenergic agonist-induced long-lasting synaptic modifications in hippocampal dentate gyrus require activation of NMDA receptors, but not electrical activation of afferents. Brain Res. 526:347-350.

Dahl, D; Bugard, E.C. and Sarvey, J.M. (1990) NMDA receptor antagonists reduce medial, but not lateral, perforant path-evoked EPSPs in dentate gyrus of rat hippocampal slice. Exp. Brain Res. 83:172-177.

Davies, S.; Butcher, S.P.; Morris, R.G.M. (1992) The NMDA receptor antagonist D-2-amino-5-phosphonopentanoate (D-AP5) impairs spatial learning and LTP in vivo at intracerebral concentrations comparable to those that block LTP *in vitro*. J. Neurosci. 12:21-34.

Davies, C.H.; Jane, D.E.; Sunter, D.C.; Watkins, J.C.; and Collingridge, G.L. (1993) Antagonism of presynaptic mGluRs in the hippocampus. Soc. Neurosci. Abstr. 19:276.

Del Castillo, J. and Katz, B. (1954) Quantal components of the end-plate potential. J. Physiol. 124:560-573.

Desmond, N.L. and Weinberg, R.J. (1996) Differential synaptic localization of AMPA and NMDAR1 receptor subunits in the rat hippocampal dentate gyrus. Soc. Neurosci. Abstr. 22:441.

Di Lauro, A.; Schmid, R.W.; and Meek, J.L. (1981) Is aspartic acid the neurotransmitter of the perforant pathway? Brain Res. 207:476-480.

Dinerman, J.L.; Dawson, T.M.; Schell, M.J.; Snowman, A.; and Snyder, S.H. (1994) Endothelial nitric oxide synthase localized to hippocampal pyramidal cells: implications for synaptic plasticity. Proc. Natl. Acad. Sci. USA 91:4214-4218.

Dolphin, A.C., Errington, M.L., and Bliss, T.V.P. (1982) Long-term potentiation of the perforant path *in vivo* is associated with increased glutamate release. Nature 297:496-498.

Dunwiddie, T.V. and Lynch, G. (1979) The relationship between extracellular calcium concentrations and the induction of hippocampal long-term potentiation. Brain Res. 169:103-110.

Dunwiddie, T.V.; Perez-Reyes, E.; and Rice, K.C. (1982) Stereoselectivity of opiate antagonists in rat hippocampus and neocortex: Responses to (+)- and (-)-isomers of naloxone. Neurosci. 7:1691-1702.

Eichenbaum, H. (1996) Learning from LTP: A comment on recent attempts to identify cellular and molecular mechanisms of memory. Learning & Memory 3:61-73.

Eichenbaum, H. (1994) The hippocampal system and declarative memory in humans and animals: Experimental analysis and historical origins. In Schacter,D and

Tulving, E. (Eds.), Memory systems 1994 (pp.147-201). Cambridge, The MIT Press.

Eichenbaum, H.; Cohen, N.J., Otto, T.; and Wible, C.G. (1992) Memory representation in the hippocampus: Functional domain and functional organization. In Squire, L.R.; Lynch, G.; Weinberger, N.M.; and McGaugh, J.L. (Eds.), Memory: organization and locus of change (pp. 163-104). Oxford: Oxford University Press.

Eichenbaum, H.; Otto, T.; and Cohen, N.J. (1992) The hippocampus - What does it do? Behavioral and Neural Biology 57:2-36.

Eichenbeum, H; Fagan, A.; and Mathews, P. (1988) Hippocampal system dysfunction and odour discrimination learning in rats: impairment or facilitation depending on representational demands. Behav. Neurosci. 102:331-339.

Eichenbaum, H.; Fagan, A.; Cohen, N.J. (1986) Normal olfactory discrimination learning set and facilitation of reversal learning after combined and separate lesions of the fornix and amygdala in rats: Implications for preserved learning in amnesia. J. Neurosci. 6:1876-1884.

Eichenbaum, H.; Kuperstein, M.; Fagan, A.; and Nagode, J. (1986) Cue-sampling and goal-approach correlates of hippocampal unit activity in rats performing an odour discrimination task. J. Neurosci. 7:716-732.

Eichenbaum, H.; Mathews, P.; Cohen, N.J. (1989) Further studies of hippocampal representation during odour discrimination learning. Behavioral Neuroscience 103:1207-1216.

Errington, M.L., Dolphin, A.C., and Bliss, T.V.P. (1983) A method for combining field potential recording with local perfusion in the hippocampus of the anaesthetized rat. J. Neurosci. Methods 7:353-357.

Errington, M.L.; Lynch, M.A.; and Bliss, T. V. P. (1987) Long-term potentiation in the dentate gyrus: induction and increased glutamate release are blocked by D(-) aminophosphonvalerate. Neuroscience 20:279-284.

Evans, R.H.; Francis, A.A. and Watkins, J.C. (1977) Selective antagonism by Mg^{2+} of amino acid-induced depolarization of spinal neurones. Experientia 33:489-491.

Faber, D.S. and Korn, H. (1991) Applicability of the coefficient of variation method for analyzing synaptic plasticity. Biophys. J. 60:1288-1294.

Faber, D.S.; Young, W.S.; Legendre, P.; and Korn, H. (1992) Intrinsic quantal variability due to stochastic properties of receptor-transmitter interactions. Science 258:1494-

1498.

Feasey, K.J.; Lynch, M.A.; and Bliss, T.V. P. (1986) Long-term potentiation is associated with an increase in calcium-dependent potassium-stimulated release of [^{14}C] glutamate from hippocampal slices: an ex vivo study in the rat. Brain Res. 364:39-44.

Finch, D.M.; Derian, E.L.; and Babb, T.L. (1983) Demonstration of axonal projections of neurons in the rat hippocampus and subiculum by intracellular injection of HRP. Brain Res. 271:201-216.

Fotuhi, M.; Standaert, D.G.; Testa, C.M.;Penny Jr., J.B.; and Young, A.B. (1994) Differential expression of metabotropic glutamate receptors in the hippocampus and entorhinal cortex of the rat. Mol. Brain Res. 21:283-292.

Fredens, K.; Steengaard-Pedersen, K; and Larsson, L.I. (1984) Localization of enkephalin and cholecystokinin immunoreactivities in the perforant path terminal fields of the rat hippocampal formation. Brain Res. 304:255-263.

Frey, U.; Huang, Y.Y.; and Kandel, E.R. (1993) Effects of cAMP stimulate a late stage of LTP in hippocampal CA1 neurons. Science 260:1661-1664.

Frotscher, M. and Léránth, C. (1985) Cholinergic innervation of the rat hippocampus as revealed by choline acetyltransferase immunocytochemistry: A combined light and electron microscopic study. J. Comp. Neurol. 239:237-246.

Frotscher, M. and Léránth, C. (1986) The cholinergic innervation of the rat fascia dentata:identification of target structures on granule cells by combining choline acetyltransferase immunocytochemistry and Golgi impregnation. J. Comp. Neurol. 243:58-70.

Gaarskjaer, F.B. (1978) Organization of the mossy fiber system of the rat studied in extended hippocampi. I. Terminal area related to number of granule and pyramidal cells. J Comp. Neurol. 178:49-72.

Gall, C.; Brecha, N.; Karten, H.J.; and Chang, K.-J. (1981) Localization of enkephalin-like immunoractivity to identified axonal and neuronal populations of the rat hippocampus. J. Comp. Neurol. 198:335-350.

Galley, P., Errington, M.L., and Bliss, T.V.P. (1993) Sustained increase in basal and stimulus-dependent glutamate efflux during LTP in dentate gyrus: real-time *in vivo* measurement using a dialysis electrode. Soc. Neurosci. Abstr. 19.

Geinisman, Y.; deToledo-Morrell, L.; Morrell, F.; Heller, R.E.; Rossi, M.; and Parshall,

R.F. (1993) Structural synaptic correlate of long-term potentiation: formation of axospinous synapses with multiple, complete partitioned transmission zones. Hippocampus 3(4):435-446.

Gil, D.W. and Wolfe, B.B. (1985) Pirenzepine distinguishes between muscarinic receptor-mediated phosphoinositide breakdown and inhibition of adenylate cyclase. J. Pharmacol. Exp. Thr. 232:608-616.

Goldowitz, D.W.; White, F.; Steward, O.; Cotman, C.W.; and Lynch, G.S. (1975) Anatomical evidence for a projection from the entorhinal cortex to the contralateral dentate gyrus of the rat. Exp. Neurol. 47:433-441.

Gozlan, H.; Chinestra, P.; Diabira, D.; and Ben-Ari, Y. (1995a) In CA1 hippocampal neurons, the redox state of NMDA receptors determines LTP expressed by NMDA but not AMPA receptors. J. Neurophysiol. 73:2612-2617.

Gozlan, H.; Khazipov, R; and Ben-Ari, Y. (1995b) Multiple forms of long-term potentiation and multiple regulatory sites of N-methyl-D-asparate receptors: role of the redox site. J. Neurobiol. 26:360-369.

Gozlan, H.; Diabira, D.; Chinestra, P.; and Ben-Ari, Y. (1994) Anoxic LTP is modulated by the redox modulatory site of the NMDA receptor. J. Neurophysiol. 72:3017-3022.

Grant, S.G.N.; O'Dell, T.J.; Karl, K.A.; Stein, P.L.; Soriano, P.; and Kandel, E.R. (1992) Impaired long-term potentiation, spatial learning, and hippocampal development in *fyn* mutant mice. Science 258:1903-1910.

Greenwood, R.S.; Godar, S.E.; Reaves, T.A. Jr.; and Hayward, J.N. (1981) Cholecystokinin in hippocampal pathways. J. Comp. Neurol. 203:335-350.

Gustafsson, B. and Wigström, H. (1988) Physiological mechanisms underlying long-term potentiation. TINS 11:156-162.

Haas, H.L. and Ryall, R.W. (1980) Is excitation by enkephalins of hippocampal neurons in the rat due to presynaptic facilitation or to disinhibition? J. Physiol. 308:315-330.

Haas, H.L. and Konnerth, A. (1983) Histamine and noradrenaline decrease calcium-activated potassium conductance in hippocampal pyramidal cells. Nature 302:432-434.

Haberly, L.B. and Price, J.L. (1978) Association and commissural fiber systems of the olfactory cortex in the rat. I. Systems originating in the piriform cortex and

adjacent areas. J. Comp. Neurol. 178:711-740.

Halasy, K. and Somogyi, P. (1993) Subdivisions in the multiple GABAergic innervation of granule cells in the dentate gyrus of the rat hippocampus. Eur. J. Neurosci. 5:411-429.

Halasy, K. and Miettinen, R.; Szabat, E.; and Freund, T.F. (1992) GABAergic interneurons are the major postsynaptic targets of medial raphe afferents in the rat dentate gyrus. Eur. J. Neurosci. 4:144-153.

Halliwell, J.V. and Adams, P.R. (1982) Voltage-clamp analysis of muscarinic excitation in hippocampal neurons. Brain Res. 250:71-92.

Hammond, C.; Crépel, V.; Gozlan, H.; and Ben-Ari, Y. (1994) Anoxic LTP sheds light on the multiple facets of NMDA receptors. TINS 17:497-503.

Han, Z.-S.; Buhl, E.H.; Lörinczi, Z.; and Somogyi, P. (1993) A high degree of spatial selectivity in the axonal and dendritic domains of physiologically identified local-circuit neurons in the dentate gyrus of the rat hippocampus. Eur. J. Neurosci. 5:395-410.

Hanse, E. and Gustafsson, B. (1992) Long-term potentiation and field EPSPs in the lateral and medial perforant paths in the dentate gyrus *in vitro*: a comparison. Eur. J. Neurosci. 4:1191-1201.

Harley, C.W. (1991) Noradrenergic and locus coeruleus modulation of the perforant path-evoked potential in rat dentate gyrus supports a role for the locus coeruleus in attentional and memorial processes. Prog. Brain Res. 88:307-320.

Haring, J.H. and Davis, J.N. (1983) Topography of locus coeruleus neurons projecting to the area dentata. Exp. Neurol. 79:785-800.

Haring, J.H. and Davis, J.N. (1985a) Differential distribution of locus coeruleus projections to the hippocampal formation: Anatomical and biochemical evidence. Brain Res. 325:366-369.

Haring, J.H. and Davis, J.N. (1985b) Retrograde labelling of locus coeruleus neurons after lesion-induced sprouting of the coeruleohippocampal projection. Brain Res. 360:384-388.

Harris, E.W.; Lasher, S.S.; and Steward, O. (1979) Analysis of the habituation-like changes in transmission in the temporodentate pathway of the rat. Brain Res. 162:21-32.

Harris, E.W. and Cotman, C.W. (1983) Effects of acidic amino acid antagonists on paired-pulse potentiation at the lateral perforant pathway. Exp. Brain Res. 52:455-460.

Harris, E.W. and Cotman, C.W. (1985) Effects of synaptic antagonists on perforant path paired-pulse plasticity: differentiation of pre- and postsynaptic antagonism. Brain Res. 334:348-353.

Harris, E.W. and Cotman, C.W. (1986) Long-term potentiation of guinea pig mossy fiber responses is not blocked by N-methyl-D-aspartate antagonists. Neurosci. Lett. 70:132-137.

Hayashi, Y.; Sckiyana, N.; Nakanishi, S.; Jane, D.E.; Sunter, D.C.; Birse, E.F., Udvarhelyi, P.M.; and Watkins, J.C. (1994) Analysis of agonist and antagonist activities of phenylglycine derivatives for different cloned metabotropic glutamate receptor subtypes. J. Neurosci. 14:3370-3377.

Heimer, L. (1968) Synaptic distribution of centripetal and centrifugal nerve fibers in the olfactory system of the rat: an experimental anatomical study. J. Anat. 103:413-432.

Hendry, S.H.C. and Jones, E.G. (1985) Morphology of synapses formed by cholecystokinin-immunoreactive axon terminals in regio superior of rat hippocampus. Neuroscience 16:57-68.

Herkenham, M. and Mclean, S. (1986) Mismatches between receptor and transmitter localization in the brain. In Boast, C.A.; Snowhill, E.W.; and Altar, C.A.(eds): Quantitative receptor autoradiography. New York: Alan R. Liss, pp.137-171.

Herron, C.E.; Lester, R.A.; Coan, E.J.; and Collingridge, G.L. (1986) Frequency-dependent involvement of NMDA receptors in the hippocampus: a novel synaptic mechanism. Nature 322:265-268.

Hessler, N.A.; Shirke, A.M.; and Malinow, R. (1993) The probability of transmitter release at a mammalian central synapse. Nature 366:569-572.

Higashima, M. and Yamamoto, C. (1985) Two components of long-term potentiation in mossy fiber-induced excitation in hippocampus. Exp. Neurol. 90:529-239.

Hirsh, R. (1974) The hippocampus and contextual retrieval of information from memory: A theory. Behavioral Biology 12:421-444.

Hjorth-Simonsen, A. (1972) Projection of the lateral part of the entorhinal area to the hippocampus and fascia dentata. J. Comp. Neurol. 146:219-232.

Hjorth-Simonsen, A. and Jeune, B. (1972) Origin and termination of the hippocampal perforant path in the rat studied by silver impregnation. J. Comp. Neurol. 144:215-231.

Houamed, K.M.; Kuijper, J.L.; Gillbert, T.L.; Haldeman, B.A.; O'Hara, P.J.; Mulvihill, E.R.; Almers, W.; and Hagen, F.S. (1991) Cloning, expression and gene structure of a G protein-coupled glutamate receptor from rat brain. Science 252:1318-1321.

Hsia, A.Y.; Salin, P.A.; Castillo, P.E.; Aiba, A.; Abeliovich, A.; Tonegawa, S.; and Nicoll, R.A. (1995) Evidence against a role for metabotropic glutamate receptors in mossy fiber LTP: the use of mutant mice and pharmacological antagonists. Neuropharmacol. 34:1567-1572.

Hu, G.Y.; Havlby, O.; Walaas, S.I.; Albert, K.A.; Skjeflo, P.; Andersen, P.; and Greengard, P. (1987) Protein kinase C injection into hippocampal pyramidal cells elicits features of long-term potentiation. Nature 328:426-429.

Huang, Y.Y. and Malenka, R.C. (1993) Examination of TEA-induced synaptic enhancement in area CA1 of the hippocampus: the role of voltage-dependent Ca^{2+} channels in the induction of LTP. J. Neurosci. 13:568-576.

Hyman, B.T.; Van Hasten, G.W.; and Damasio, A.R. (1987) Alzheimer's disease: glutamate depletion in the hippocampal perforant pathway zone. Annals of Neurology 22:37-40.

Isaac, J.T., Nicoll, R.A., and Malenka, R.C. (1995) Evidence for silent synapses: implication for the expression of LTP. Neuron 15:427-434.

Isaacson, J.S.; Solís, J.M.; and Nicoll R.A. (1993) Local and diffuse synaptic actions of GABA in the hippocampus. Neuron 10:165-175.

Ishida, M; Saitoh, T.; Shimamoto, K.; Ohfune, Y.; and Shinozaki, H. (1993) A novel metabotropic receptor agonist: marked depression of monosynaptic excitation on the new born isolated spinal cord. Br. J. Pharmacol. 109:1169-1177.

Ito, I. and Sugiyama, H. (1991) Roles of glutamate receptors in long-term potentiation at hippocampal mossy fiber synapses. Neuroreport 2:333-336.

Jackson, P.S.; Suppes, T.; and Harris, K.M. (1993) Stereotypical changes in the pattern and duration of long-term potentiation expressed at postnatal days 11 and 15 in the rat hippocampus. J. Neurophysiol. 70:1412-1419.

Jane, D.E.; Pittaway, K.; Sunter, D.C.; Thomas, N.K.; and Watkins, J.C. (1995) New phenylglycine derivatives with potent and selective antagonist activity at

presynaptic glutamate receptors in neonatal rat spinal cord. Neuropharmacol. 34:851-856.

Jarrard, L.E. (1993) On the role of the hippocampus in learning and memory. Behav. Neural Biol. 60:9-26.

Jaffery, K.L. and Morris, R.G.M. (1993) Cumulative long-term potentiation in the rat dentate gyrus correlated with, but does not modify, performance in the water maze. Hippocampus 3:133-140.

Jarrard, L.E. (1986) Selective hippocampal lesions and behaviour: Implications for current research and theorizing. In Isaacson, R.L. and Pribram, K.H. (Eds.), The hippocampus. Vol.4 (pp. 93-126). New York: Plenum Press.

Jarrard, L.E.; Ringland, J.M.; and Johnson, L.S. (1987) Increased rate of forgetting of spatial information in rats with ibotenate lesions of hippocampus. Soc. Neurosci. Abstr. 13:802.

Jones, B.E. and Yang, T.-Z. (1985) The efferent projections from the reticular formation and the locus coeruleus studied by anterograde and retrograde axonal transport in the rat. J. Comp. Neurol. 242:56-82.

Jou, S.F. (1995) Simulation and analysis of synaptic transmission in hippocampal dentate gyrus granule cells. University of Toronto MSc Thesis.

Jou, S.F.; Winslow, J.L.; Wang S.; and Wojtowicz J.M. (1995) Families of generated hippocampal dentate granule shapes used to determine effects of location on synaptic response. Soc. Neurosci. Abs. 21:584.

Kahle, J. S. and Cotman, C.W. (1989) Carbachol depresses synaptic responses in the medial but not the lateral perforant pathway. Brain Res. 482:159-163.

Kahle, J.S. and Cotman, C.W. (1993) Adenosine, L-AP4, and baclofen modulation of paired-pulse potentiation in the dentate gyrus: interstimulus interval-dependent pharmacology. Exp. Brain Res. 94:97-104.

Kanter, E.D. and Haberly, L.B. (1990) NMDA-dependent induction of long-term potentiation in afferent and association fiber systems of piriform cortex *in vitro*. Brain Res. 525:175-179.

Kato, K.; Uruno, K.; Saito, K.; and Kato, H. (1991) Both arachidonic acid and 1-oleoyl-2-acetyl-glycerol in low magnesium solution induce long-term potentiation in hippocampal CA1 neurons *in vitro*. Brain Res. 563:95-100.

Kauer, J.A.; Malenka, R.C.; and Nicoll, R.A. (1988). A persistent postsynaptic modification mediates long-term potentiation in the hippocampus. Neuron 1:911-917.

Keller, B.U.; Konnerth, A.; and Yaari, Y. (1991) Patch clamp analysis of excitatory synaptic currents in granule cells of rat hippocampus. J. Physiol. 435:275-293.

Kelly, P.T.; McGuinness, T.L.; and Greengard, P. (1984) Evidence that the major postsynaptic density protein is a component of a Ca^{2+}/calmodulin-dependent protein kinase. Proc. Natl. Acad. Sci. USA 81:945-949.

Kelso, S.R.; Ganong, A.H.; and Brown, T.H. (1986) Hebbian synapses in hippocampus. Proc. Natl. Acad. Sci. USA 83:5326-5330.

Kelso, S.R.; Nelson, T.E.; and Leonard, J.P. (1992) Protein kinase C mediated enhancement of NMDA currents by metabotropic glutamate receptors in Xenopus oocytes. J. Physiol. 449:705-718.

Kemp, M.; Roberts, P.; Pook, P.C.; Jane, D.E.; Jones, A.W.; Jones, P.L.; Sunter, D.C.; Udvarhelyi, P.M.; and Watkins, J.C. (1994) Antagonism of presynaptically mediated depressant responses and cyclic-AMP coupled metabotropic glutamate receptors. Eur. J. Pharmacol.- Mol. Pharmacol. Sect. 266:187-192.

Kennedy, M.B.; Bennett, M.K.; and Erondu, N.E. (1983) Biochemical and immunochemical evidence that the "major postsynaptic density protein" is a subunit of a calmodulin-dependent protein kinase. Proc. Natl. Acad. Sci. USA 80:7357-7361.

Kim, H.G. and Connors, B.W. (1993) Apical dendrites of the neocortex: Correlation between sodium- and calcium-dependent spiking and pyramidal cell morphology. J. Neurosci. 13:5301-5311.

Kim, J.J.; DeCola, J.P.; Landeira-Fernandez, J.; and Fanselow, M.S. (1991) N-methyl-D-aspartate receptor antagonist APV blocks acquisition but not expression of fear conditioning. Behav. Neurosci. 105:126-133.

Klann, E.; Chen, S.J.; and Sweatt, J.D. (1991) Persistent protein kinase activation in the maintance phase of long-term potentiation. J. Biol. Chem. 266:24253-24256.

Koda, L.Y.; Schulman, J.A.; and Bloom, F.E. (1978a) Ultrastructural identification of noradrenergic terminals in rat hippocampus: Unilateral destruction of the locus coeruleus with 6-hydroxydopamine. Brain Res. 145:190-195.

Koda, L.Y.; Schulman, J.A.; and Bloom, F.E. (1978b) Light and electron microscopic

changes in the rat dentate gyrus after lesions or stimulation of ascending locus coeruleus pathway. Brain Res. 144:363-368.

Köhler, C.; Chan-Palay, V.; and Wu, J.Y. (1984) Septal neurons containing glutamic acid decarboxylase immunoreactivity project to the hippocampal region in the rat brain. Anat. Embryol. 169:41-44.

Köhler, C. (1985) Intrinsic projections of the retrohippocampal region in the rat brain. I. The subicular complex. J. Comp. Neurol. 236:504-522.

Köhler, C. (1986) Intrinsic connections of the retrohippocampal region in the rat brain. II. The medial entorhinal area. J. Comp. Neurol. 246:149-169.

Köhler, C. (1988) Intrinsic connections of the retrohippocampal region in the rat brain. III. The lateral entorhinal area. J. Comp. Neurol. 271:208-228.

Konnerth, A.; Keller, B.U.; Ballanyi, K.; and Yaari, Y. (1990) Voltage sensitivity of NMDA-receptor mediated postsynaptic currents. Exp. Brain Res. 81:209-212.

Korol, D.L.; Abel, T.W.; Church, L.T.; Barnes, C.A.; and McNaughton, B.L. (1993) Hippocampal synaptic enhancement and spatial learning in the Morris swim task. Hippocampus 3:127-132.

Kosaka, T.; Kosaka, K.; Tateishi, K.; Hamaoka, Y.; Yanaihara, N.; Wu, J.Y.; and Hama, K. (1985) GABAergic neurons containing CCK-8-like and/or VIP-like immunoreactivities in the rat hippocampus and dentate gyrus. J. Comp. Neurol. 239:420-430.

Kosel, K.C.; Van Hasten, G.W.; West, J.R. (1981) Olfactory bulb projections to the parahippocampal area of the rat. J. Comp. Neurol. 198:467-482.

Lacaille, J.-C. and Harley, C.W. (1985) The action of norepinephrine in the dentate gyrus: Beta-mediated facilitation of evoked potentials *in vitro*. Brain Res. 358:210-220.

Lambert, J.D.C. and Jones, R.S.G. (1989) Activation of N-methyl-D-aspartate receptors contributes to the EPSP at perforant path synapses in the rat dentate gyrus in vivo. Neurosci. Letters 97:323-328.

Lambert, J.D.C. and Jonse, R.S.G. (1990) A reevaluation of excitatory amino acid-mediated synaptic transmission in rat dentate gyrus. J. Neurophysiol. 64:119-132.

Lancaster, B. and Adams, P.R. (1987) Calcium-dependent current generating the afterhyperpolarization of hippocampal neurons. J. Neurophysiol. 55:1268-1282.

Lancaster, B., Nicoll, R.A., and Perkel, D.J. (1991) Calcium activates two types of potassium channels in rat hippocampal neurons in culture. J. Neurosci. 11:23-30.

Larson, J.; Wong, D.; and Lynch, G. (1986) Patterned stimulation at the theta frequency is optimal for the induction of long-term potentiation. Brain Res. 368:347-350.

Laurberg, S. and Sorensen, K.E. (1981) Associational and commissural collaterals of neurons in the hippocampal formation (hilus fasciae dentatae and subfield CA3). Brain Res. 212:287-300.

Lee, K.S. (1983) Cooperativity among afferents for the induction of long-term potentiation in the CA1 region of the hippocampus. J. Neurosci. 7:1369-1372.

Levy, W.B. and Steward, O. (1979) Synapses as associative memory elements in the hippocampal formation. Brain Res. 175:233-245.

Levy, W.B. and Steward, O. (1983) Temporal contiguity requirements for long-term associative potentiation/depression in the hippocampus. Neurosci. 8:791-797.

Lewis, P.R. and Shute, C.C.D. (1967) The cholinergic limbic system: Projections to hippocampal formation, medial cortex, nuclei of the ascending cholinergic reticular system, and the subfornical organ and supra-optic crest. Brain 90:521-590.

Liao, D., Hessler, N.A., and Malinow, R. (1995) Activation of postsynaptically silent synapses during pairing-induced LTP in CA1 region of hippocampal slice. Nature 375:400-404.

Linden, D.J. and Routtenberg, A. (1989) The role of protein kinase C in long-term potentiation: a testable model. Brain Res. Rev. 14:279-296.

Lingenhöhl, K. And Finch, D.M. (1991) Morphological characterization of rat entorhinal neurons in vivo: soma-dendritic structure and axonal domains. Exp. Brain Res. 84:57-74.

Lömo, T. (1966) Frequency potentiation of excitatory synaptic activity in the dentate area of the hippocampal formation. Acta Physiol. Scand. 68:277-281.

Lynch, G. and Baudry, M. (1984) The biochemistry of memory: a new and specific hypothesis. Science 224:1057-1063.

Lynch, G. and Baudry, M. (1988) Structure-function relationships in the organization of memory. In Perspectives in memory research (ed. Gazzaniga M.S.), pp 23-92. The MIT Press, Cambridge, Massachusetts.

Lynch, G.S.; Gribkoff, V.K.; and Deadwyler, S.A. (1977) Long term potentiation is accompanied by a reduction in dendritic responsiveness to glutamic acid. Nature 363:151-153.

Lynch, G.; Larsen, J.; Kelso, S.; Barrionuevo, G.; and Schottler, F. (1983) Intracellular injection of EGTA block induction of hippocampal long-term potentiation. Nature 305:719-721.

MacDonald, R.J. and White, N.M. (1993) A triple dissociation of memory system: Hippocampus, amygdala, and dorsal striatum. Behav. Neurosci. 107:3-22.

Madison, D.V. and Nicoll, R.A. (1982) Noradrenaline blocks accommodation of pyramidal cell discharge in the hippocampus. Nature 299:636-638.

Madison, D.V. and Nicoll, R.A. (1984) Control of repetitive discharge of rat CA1 pyramidal neurons *in vitro*. J. Physiol. 354:319-331.

Malenka, R.C.; Kauer, J.A.; Perkel, D.J.; Mauk, M.D. Kelly, P.T.; Nicoll, R.A.; and Waxham, M.N. (1989) An essential role for postsynaptic calmodulin and protein kinase activity in long-term potentiation. Nature 340:554-557.

Malenka, R.C.; Madison, D.V.; Nicoll, R.A. (1986) Potentiation of synaptic transmission in the hippocampus by phorbol esters. Nature 321:175-177.

Malinow, R.; Otmakhov, N.; Blum, K.I.; and Lisman, J. (1994) Visualizing hippocampal synaptic function by optical detection of Ca^{2+} entry through the N-methyl-D-aspartate channel. Proc. Natl. Acad. Sci. USA 91:8170-8174.

Malinow, R. and Tsien, R.W. (1990) Presynaptic enhancement shown by whole-cell recordings of long-term potentiation in hippocampal slices. Nature 346:177-180.

Malinow, R.; Schulman, H.; and Tsien, R.W. (1989) Inhibition of postsynaptic PKC or CaMKII blocks induction but not expression of LTP. Science 245:862-866.

Manabe, T. and Nicoll, R.A. (1994) Long-term potentiation: evidence against an increase in transmitter release probability in the CA1 region of the hippocampus. Science 265:1888-1892.

Manabe, T.; Renner, P.; and Nicoll, R.A. (1992) Postsynaptic contribution to long-term potentiation revealed by the analysis of miniature synaptic currents. Nature 355: 50-55.

Manabe,T.; Wyllie; D.J.A.; Perkel; D.J.; and Nicoll, R.A. (1993) Modulation of synaptic transmission and long-term potentiation: effects of paired pulse facilitation and

EPSC variance in the CA1 region of the hippocampus. J. Neurophysiol. 70:1451-1459.

Manzoni, O.J.; Weisskopf, M.G.; and Nicoll, R.A. (1994) MCPG antagonizes metabotropic glutamate receptors but not long-term potentiation in the hippocampus. Eur. J. Neurosci. 6:1050-1054.

Marks, G.S.; Brien, J.F.; Nakatsu, K.; and McLaughlin, B.E. (1991) Does carbon monoxide have a physiological function? TIPS 12:185-188.

Masu, M.; Tanabe, Y.; Tsuchida, K.; Shigemoto, R.; and Nakanishi, S. (1991) Sequence and expression of a metabotropic glutamate receptor. Nature 349:760-765.

McGlade-McCulloh, E.; Yamamoto, H.; Tan, S.-E.; Brickey, D.A.; and Soderling, T.R. (1993) Phosphorylation and regulation of glutamate receptors by calcium/calmodulin-dependent protein kinase II. Nature 362:640-642.

McLachlan, E.M. (1978) The statistics of transmitter release at chemical synapses. In International Review of Physiology. Neurophysiology III, Vol 17, R. Porter, ed. (Baltimore: University Park Press), pp. 49-117.

McLean, S.; Rothman, R.B.; Jacobson, A.E.; Rice, K.C.; and Herkenham, M. (1987) Distribution of opiate receptor subtypes and enkephalin and dynorphin immunoreactivity in the hippocampus of squirrel, guinea pig, rat, and hamster. J. Comp. Neurol. 255:497-510.

McNamara, R.K.; Kirkby, D.R.; dePape, G.E.; Skelton, R.W.; and Corcoran, M.E. (1993) Differential effects of kindling and kindled seizures on place learning in the Morris water maze. Hippocampus 3:149-152.

McNaughton, B.L. (1996) Cognitive cartography. Nature 381:368-369.

McNaughton, B.L. (1980) Evidence for two physiologically distinct perforant pathways to the fascia dentata. Brain Res. 199:1-19.

McNaughton, B.L. and Barnes, C.A. (1977) Physiological identification and analysis of dentate granule cell responses to stimulation of the medial and lateral perforant pathways in rat. J. Comp. Neurol. 175:439-454.

McNaughton, B.L.; Douglas R.M.; and Goddard G.V. (1978) Synaptic enhancement in fascia dentata: cooperativity among coactive afferent. Brain Res. 157:277-293.

McNaughton, B.L.; Barnes, C.A.; Rao, G.; Baldwin, J.; and Rasmussen, M. (1986) Long-term enhancement of hippocampal synaptic transmission and the acquisition of

spatial information. J. Neurosci. 6:563-571.

Milner, B.; Corkin, S.; Teuber, H.L. (1968) Further analysis of the hippocampal amnesic syndrome: Fourteen years follow-up study of H.M. Neuropsychologia 6:215-234.

Mitchell, S.J. and Ranck, J.B. JR. (1980) Generation of theta rhythm in medial entorhinal cortex of freely moving rat. Brian Res. 189:49-66.

Mody, I.; De Koninck, Y.; Otis, T.S.; and Soltesz, I. (1994) Bridging the cleft at GABA synapses in the brain. TINS 17:517-525.

Monaghan, D.T.; Holets, V.R.; Toy, D.W.; and Cotman, C.W. (1983) Anatomical distribution of four pharmacologically distinct ^{3}H-L-glutamate binding sites. Nature 306, 176-179.

Moore, R.Y. and Halaris, A.E. (1975) Hippocampal innervation by serotonin neurons of the midbrain raphe in the rat. J. Comp. Neurol. 164:171-183.

Moore, R.Y.; Ziegler, B.; and Bayer, S.A. (1978) Monoamine neuron innervation of the hippocampal formation: Alteration by neonatal irradiation. Exp. Neurol. 60:318-326.

Morris, R.G.M.; Garrund, P.; Rawlins, J.N.P.; and O'Keefe, J. (1982) Place navigation impaired in rats with hippocampal lesions. Nature 297:681-683.

Morris, R.G.M.; Anderson, E.; Lynch, G.S.; and Baudry, M. (1986) Selective impairment of learning and blockade of long-term potentiation by an N-methyl-D-aspartate receptor agonist, AP5. Nature 319:774-776.

Morris, R.G.M.; Schenk, F.; Tweedie, F.; and Jarrard, L.E. (1990) Ibotenate lesions of hippocampus and/or subiculum: Dissociating components of allocentric spatial learning. Eur. J. Neurosci. 2:1016-1028.

Mott, D. D. and Lewis, D.V. (1991) Facilitation of the induction of long-term potentiation by $GABA_B$ receptors. Science 252:1718-1720.

Mott, D.D. and Lewis, D.V. (1994) The pharmacology and function of central $GABA_B$ receptors. Int. Rev. Neurobiol. 36:97-223.

Muller, R.U.; Kubie, J.L.; and Ranck, Jr. J.B. (1987) Spatial firing patterns of hippocampal complex-spike cells in a fixed environment. J. Neurosci. 7:1935-1950.

Muller, R.U. and Kubie, J.L. (1978) The effects of changes in the environment on the

spatial firing of hippocampal complex-spike cells. J. Neurosci. 7:1951-1968.

Müller, W. and Misgeld, M. (1986) Slow cholinergic excitation of guinea pig hippocampal neurons is mediated by two muscarinic receptor subtypes. Neurosci. Lett. 67:107-112.

Muller, D.; Joly, M.; and Lynch, G. (1989) Contributions of quisqualate and NMDA receptors to the induction and expression of LTP. Science 242:1694-1697.

Nadler, J. V.; Vaca, K.W.; White, W.F.; Lynch, G.S.; and Cotman, C.W. (1976) Aspartate and glutamate as possible transmitters of excitatory hippocampal afferents. Nature 260:538-540.

Nafstad, P.H.J. (1967) An electron microscope study on the termination of the perforant path fibres in the hippocampus and the fascia dentata. Z. Zellforsch Mikrosk Anat. 76:532-542.

Neumaier, J.F.; Mailheau, S.; and Chavkin, C. (1988) Opioid receptor-mediated responses in the dentate gyrus and CA1 region of the rat hippocampus. J. Pharmacol. Exp. Ther. 244:564-570.

Neuman, R.S. and Harley, C.W. (1983) Long-lasting potentiation of the dentate gyrus population spike by norepinephrine. Brain Res. 273:162-165.

Newberry, N.R. and Nicoll, R.A. (1984) A bicuculline-resistant inhibitory post-synaptic potential in rat hippocampal pyramidal cells *in vitro*. J. Physiol. 348:239-254.

Nguyen, P.V.; Abel, T.; and Kandel, E.R. (1994) Requirement of a critical period of transcription for induction of a late phase LTP. Science 265:1104-1107.

Nicholls, D and Attwell, D. (1990) The release and uptake of excitatory amino acids. TIPS 11:462-468.

Nicoll, R.A. and Malenka, R.C. (1995) Contrasting properties of two forms of long-term potentiation in the hippocampus. Nature 377:115-118.

Nowak, L.; Bregestovski, P.; Ascher, P.; Herbet, A.; and Prochiantz, A. (1984) Magnesium gates glutamate-activated channels in mouse central neurons. Nature 307:462-465.

O'Dell, T.J.; Hawkins, R.D.; Kandel, E.R.; and Arancio, O. (1991) Tests of two diffusible substances in long-term potentation: evidence for nitric oxide as a possible early retrograde messenger. Proc. Natl. Acad. Sci. USA 88:11285-11289.

O'Dell, T.J.; Huang, P.L.; Dawson, T.M.; Dinerman, J.L.; Snyder, S.H.; Kandel, E.R.; and Fishman, C.M. (1994) Endothelial NOS and the blockade of LTP by NOS inhibitors in mice lacking neuronal NOS. Science 265:542-546.

O'Connor, J.J.; Rowan, M.J; and Anwyl, R.(1994) Long-lasting enhancement of NMDA receptor-mediated synaptic transmission by metabotropic glutamate receptor activation. Nature 367:557-559.

O'Keefe, J. (1976) Place units in the hippocampus of the freely moving rat. Exp. Neurol. 51:78-109.

O'Keefe, J. and Burgess, N. (1996) Geometric determinants of the place fields of hippocampal neurons. Nature 381:425-428.

O'Keefe, J. and Dostrovsky, J. (1971) The hippocampus as a spatial map. Preliminary evidence from unit activity in the freely-moving rat. Brain Res. 34:171-175.

Olpe, H.-R.; Steinmann, M.W.; Ferrat, T.; Pozza, M.F.; Greiner, K.; Brugger, F.; Froestl, W.; Mickel, S.J.; and Bittiger, H. (1993) The actions of orally active $GABA_B$ receptor antagonists on GABAergic transmission *in vivo* and *in vitro*. Eur. J. Pharmacol. 233:179-186.

Olton, D.S. (1986) Hippocampal function and memory for temporal context. In Isaacson, R.L. and Pribram, K.H. (Eds.), The hippocampus (Vol.4). New York: Plenum Press.

Olton, D.S.; Becker, J.T.; and Handlemann, G.E. (1979) Hippocampus, space, and memory. Brain and Behavioral Sciences 2:313-365.

Otis, T.S. and Mody, I. (1992) Differential activation of $GABA_A$ and $GABA_B$ receptors by spontaneously released transmitter. J. Neurophysiol. 67:227-235.

Otto, T.; Eichenbaum, H. (1992) Toward a comprehensive account of hippocampal function: Studies of olfactory learning permit an integration of data across multiple levels of neurobiological analysis. In Squire, L.R. and Butters, N. (Eds.), Neuropsychology of Memory (2nd ed., pp.415-428). New York: Guilford.

Otto, T.; Eichenbaum, H.; Wiener, S.I.; and Wible, C.G. (1991) Learning-related patterns of CA1 spike trains parallel stimulation parameters optimal for inducing hippocampal long-term potentiation. Hippocampus 1:181-192.

Parkinson, J.K.; Murray, E. and Mishkin, M. (1988) A selective mnemonic role for the hippocampus in monkeys: Memory for the location of objects. J. Neurosci. 8:4159-4167.

Patneau, D.K. and Mayer, M.L. (1990) Structure-activity relationship for amino acid transmitter candidates acting at NMDA and quisqualate receptors. J. Neurosci. 10:2385-2399.

Pekhletski, R.; Gerlai, R.; Overstreet, L.S.; Huang, X.-P.; Agopyan, N.; Slater, N.T.; Abramow-Newerly, W.; Roder, J.C.; and Hampson, D.R. (1996) Impaired cerebellar synaptic plasticity and motor performance in mice lacking the mGluR4 subtype of metabotropic glutamate receptor. J. Neurosci. 16:6364-6373.

Penfield, W. and Milner, B. (1958) Memory deficit produced by bilateral lesions of the hippocampal zone. Arch. Neurol. Psychiatry 79:475-497.

Penfield, W. and Mathieson, G. (1974) Memory: Autopsy findings and comments on the role of hippocampus in experiential recall. Arch. Neurol. 31:145-154.

Peralta, E.G., Ashkenazi, A., Winslow, J.W., Ramachandran, J. and Capon, D.J. (1988) Differential regulation of PI hydrolysis and adenylyl cyclase by muscarinic receptor subtypes. Nature 334:434-437.

Perkel, D.J. and Nicoll, R.A. (1993) Evidence for all-or-none regulation of neurotransmitter release: Implications for long-term potentiation. J. Physiol. (Lond.) 471:481-500.

Perkins, A.T.; Teyler, T.J. (1988) A critical period of long-term potentiation in the developing rat visual cortex. Brain Res. 439:222-229.

Petralia, R.S.; Yokotani, N.; and Wenthold, R.J. (1994) Light and electron microscope distribution of the NMDA receptor subunit NMDAR1 in the rat nervous system using a selective anti-peptide antibody. J. Neurosci. 14:667-696.

Pickel, V.M.; Segal, M.; and Bloom, F.E. (1974) A radioautographic study of the efferent pathways of the nucleus locus coeruleus. J. Comp. Neurol. 155:15-42.

Piguet, P. and North, R.A. (1993) Opioid actions at mu and delta receptors in the rat dentate gyrus in vitro. J. Pharmacol. Exp. Ther. 266:1139-1146.

Plager, M.D. and Vogt, B.A. (1988) μ- And δ-opioid receptor binding peaks and κ-homogeneity in the molecular layers of rat hippocampal formation. Brain Res. 460:150-154.

Pook, P.C.; Sunter, D.C.; Udvarhelyi, P.M.; and Watkins, J.C. (1992) Evidence for presynaptic depression of monosynaptic excitation in neonatal rat motoneurones by (1S,3S)-and (1S,3R)-ACPD. Exp. Physiol. 77:529-532.

Racine, R.J.; Milgram, S.W.; and Hafner, S. (1986) Long-term potentiation phenomenon in the rat limbic forebrain. Brain Res. 260:217-231.

Rainbow, T.C., Parsons, B., and Wolfe, B.B. (1984) Quantitative autoradiography of β1 and β2-adrenergic receptors in rat brain. Proc. Natl. Acad. Sci. USA 81:1585-1589.

Rasmusson, D.D. and Dykes, R.W. (1988) Long-term enhancement of evoked potential in cat somatosensory cortex produced by coactivation of the basal forebrain and cutaneous receptors. Exp. Brain Res. 70:276-286.

Regehr, W.; Kehoe, J.S.; Ascher, P.; and Armstrong, C. (1993) Synaptically triggered action potentials in dendrites. Neuron 11:145-151.

Reymann, K.G.; Davies, S.N.; Matthies, H.; Kase, H.; and Collingridge, G.L. (1990) Activation of a K-252b-sensitive protein kinase is necessary for a post-synaptic phase of long-term potentiation in area CA1 of rat hippocampus. Eur. J. Neurosci. 2:481-486.

Ribak, C.E. and Anderson, L. (1980) Ultrastructure of the pyramidal basket cells in the dentate gyrus of the rat. J. Comp. Neurol. 192:903-916.

Ribak, C.E. and Peterson, G.M. (1991) Intragranular mossy fibers in rats and gerbils form synapses with the somata and proximal dendrites of basket cells in the dentate gyrus. Hippocampus 1:355-364.

Ribak, C.E.; Seress, L.; Amaral, D.G. (1985) The development, ultrastructure and synaptic connections of the mossy cells of the dentate gyrus. J. Neurcytol. 14:835-857.

Richter-Levin, G.; Errington, M.L.; Maegawa, H.; and Bliss, T.P.V. (1994) Activation of metabotropic glutamate receptors is necessary for long-term potentiation in the dentate gyrus and for spatial learning. Neuropharmacol. 33:853-857.

Rickard, N.S. and Ng, K.T. (1995) Blockade of metabotropic glutamate receptors prevents long-term memory consolidation. Brain Res. Bulletin 36:355-359.

Riedel, G.; Wetzel, W.; and Reymann, K.G. (1994) (R,S)-alpha-methyl-4-carboxyphenylglycine (MCPG) blocks spatial learning in rats and long-term potentiation in the dentate gyrus in vivo. Neurosci. Letters 167:141-144.

Riedel, G.; Casabona, G.; and Reymann, K.G. (1995) Inhibition of long-term potentiation in the dentate gyrus of freely moving rats by the metabotropic glutamate receptor antagonist MCPG. J. Neurosci. 15:87-98.

Riveros, N.; Fiedler, J.; Lagos, N.; Munoz, C.; Orrego, F. (1986) Glutamate in rat brain cortex synaptic vesicles : influence of the vesicle isolation procedure. Brain Res. 386:405-408.

Robinson, J. (1976) Estimation of parameters for a model of transmitter release at synapses. Biometrics 32: 61-68.

Rolls, E.T.; Miyashita, Y.; Cahusac, P.M.; Kesner, R.P.; Niki, H.; Feigenbaum, J.D.; and Bach, L. (1989) Hippocampal neurons in the monkey with activity related to the place in which a stimulus is shown. J. Neurosci. 9:1835-1845.

Room, P.; Groenewegen, H.J.; and Lohman, A.H.M. (1984) Inputs from the olfactory bulb and olfactory cortex to the entorhinal cortex in the cat. I. Anatomical observations. Exp. Brain Res. 56:488-496.

Rosenmund, C.; Clements, J. D.; and Westbrook, G. L. (1993) Nonuniform probability of glutamate release at a hippocampal synapse. Science 262:754-757.

Ruth, R.E.; Collier, T.J.; and Routtenberg, A. (1982) Topography between the entorhinal cortex and the dentate septotemporal axis in rats: I. Medial and intermediate entorhinal projection cells. J. Comp. Neurol. 209:69-78.

Ruth, R.E.; Collier, T.J.; and Routtenberg, A. (1988) Topographical relationship between the entorhinal cortex and the dentate septotemporal axis in rats: II. Cells projecting from lateral entorhinal subdivisions. J. Comp. Neurol. 270:506-516.

Rye, D.B. Weiner, B.H.; Mesulam, M.-M.; Mufson, E.J.; and Saper, C.B. (1984) Cortical projections arising from the basal forebrain: a study of cholinergic and non-cholinergic components employing combined retrograde tracing and immunohistochemical localization of choline acetyltransferase. Neurosci. 13:627-643.

Sakamoto, T.; Porter, L.L.; and Asanuma, H. (1987) Long-lasting potentiation of synaptic potentials in the motor cortex produced by stimulation of the sensory cortex in the cat: a basis of motor learning. Brain Res. 413:360-364.

Sastry, B.R.; Goh, J.W.; and Auyeung, A. (1986) Associative induction of posttetanic and long-term potentiation in CA1 neurons of rat hippocampus. Science 232:988-990.

Saucier, D. and Cain, D.P. (1995) Spatial learning in the absence of NMDA receptor-dependent long-term potentiation. Nature 378:186-189.

Segal, M. (1990) A subset of local interneurons generate slow inhibitory postsynaptic potentials in hippocampal neurons. Brain Res. 511:163-164.

Selig, D.K.; Lee, H.; Bear, M.F.; and Malenka, R.C. (1995) Reexamination of the effects of MCPG on hippocampal LTP, LTD, and depotentiation. J. Neurophysiol. 74:1075-1082.

Schwartz, S.P. and Coleman, P.D. (1981) Neurons of origin of the perforant path. Exp. Neurol. 74:305-312.

Schoepp, D.D. and Conn, P.J. (1993) Metabotropic glutamate receptor in brain function and pathology. Trends Pharmacol. Sci. 14:13-20.

Schuman, E.M. and Madison, D.V. (1991) A requirement for the intercellular messenger nitric oxide in long-term potentiation. Science 254:1503-1506.

Schwartzkroin, P. and Wester, K. (1975) Long-lasting facilitation of a synaptic potential following tetanization in the *in vitro* hippocampal slice. Brain Res. 89:107-119.

Schwartzkroin, P.A.; Scharfman, H.E.; and Sloviter, R.S. (1990) Similarities in circuitry between Ammon's horn and dentate gyrus: local interneurons and parallel processing. Prog. Brain Res. 83:269-286.

Scoville, W.B. and Milner, B. (1957) Loss of recent memory after bilateral hippocampal lesions. J. Neurol. Neurosurg. Psychiatr. 20:11-21.

Segovia, G.; Porras, A.; and More, F. (1994) Effect of a nitric oxide donor on glutamate and GABA release in striatum and hippocampus of the conscious rat. Neuroreport 5:1937-1940.

Shupliakov, O; Brodin, L.; Cullheim, S.; Ottersen, O.P.; and Storm-Mathisen, J. (1992) Immunogold quantification of glutamate in two types of excitatory synapse with different firing patterns. J. Neurosci. 12:3789-3803.

Shupliakov, O.; Atwood, H.L.; Ottersen, O.P.; Storm-Mathisen, J.; and Brodin, L. (1995) Presynaptic glutamate levels in tonic and phasic motor axons correlate with properties of synaptic release. J. Neurosci. 15:7168-7180.

Silva, A.J.; Paylor, C.F.R.; Wehner, J. W.; and Tonegawa, S. (1992a) Impaired spatial learning in α-calcium-calmodulin kinase II mutant mice. Science 257:206-211.

Silva, A.J.; Stevens, C.F.; Tonegawa, S.; Wang, Y. (1992b) Deficient hippocampal long-term potentiation in alpha-calcium-calmodulin kinase II mutant mice. Science 257:201-206.

Sinton, C.M. (1988a) Cholecystokinin and an evoked response in the dentate gyrus. Neuropeptides 12:29-34.

Sinton, C.M. (1988b) Cholecystokinin and cholecystokinin antagonists enhance postsynaptic excitability in the dentate gyrus. Peptides 9:1094-1053.

Sloviter, R.S. (1991) Feedforward and feedback inhibition of hippocampal principal cell activity evoked by perforant path stimulation: GABA-mediated mechanisms that regulate excitability *in vivo*. Hippocampus 1:31-40.

Sloviter, R.S. and Brisman, J.L. (1995) Lateral inhibition and granule cell synchrony in the rat hippocampal dentate gyrus. J. Neurosci. 15:811-820.

Smith, B.R., Wojtowicz, J.M., and Atwood, H.L. (1991) Maximum likelihood estimation of non-uniform transmitter release probabilities at the crayfish neuromuscular junction. J. Theor. Biol. 150:457-472.

Smith, B.R. (1993) Mixture estimation and the neurophysiological quantal hypothesis. Biometrics 49:643-651.

Solís, J.M. and Nicoll, R.A. (1992) Postsynaptic action of endogenous GABA released by nipecotic acid in the hippocampus. Neurosci. Lett. 147,16-20.

Somogyi, P.; Hodgson, A.J.; Smith, A.D.; Nunzi, M.G.; Gorio, A.; and Wu, J.Y. (1984) Different populations of GABAergic neurons in the visual cortex and hippocampus of cat contain somatostatin- or cholecystokinin-immunoreactive material. J. Neruosci. 4:2590-2603.

Squire, L.R. (1992) Declarative and nondeclarative memory: Multiple brain systems supporting learning and memory. J. Cogn. Neurosci. 99:195-231.

Squire, L.R. and Zola-Morgan, S. (1991) The medial temporal lobe memory system. Science 253:1380-1386.

Staley, K. J.; Otis, T. S.; and Mody, I. (1992) Membrane properties of dentate gyrus granule cells: Comparison of sharp microelectrode and whole-cell recordings. J. Neurophysiol. 67:1346-1358.

Stanton, P.K. and Sarvey, J.M. (1984) Blockade of norepinephrine induced long-lasting potentiation in the hippocampal dentate gyrus by an inhibitor of protein synthesis. Brain Res. 361:276-283.

Stanton, P.K. and Sarvey, J.M. (1985) Depletion of norepinephrine, but not serotonin, reduces long-term potentiation in the dentate gyrus of rat hippocampal slices. J. Neurosci. 5:2169-2176.

Stanton, P.K. and Sarvey, J.M. (1987) Norepinephrine regulates long-term

potentiation of both the population spike and dendritic EPSP in hippocampal dentate gyrus. Brain Res. Bull. 18:115-119.

Stanton, P.K., Mody, I., and Heinemann, U. (1989) A role for N-methyl-D-aspartate receptors in norepinephrine-induced long-lasting potentiation in the dentate gyrus. Exp. Brain Res. 77:517-530.

Staubli, U.; Ivy, G. and Lynch, G. (1984) Hippocampal denervation causes rapid forgetting of olfactory information in rats. Proc. Netl. Acad. Sci. 81:5885-5887.

Staubli, U.; Le, T.-T.; and Lynch, G.(1995) Variants of olfactory memory and their dependencies on the hippocampal formation. J. Neurosci. 15:1162-1171.

Stevens, C.F. and Wang, Y. (1994) Changes in reliability of synaptic function as a mechanism for plasticity. Nature 371:704-707.

Steward, O. (1976) Topographic organization of the projections from the entorhinal area to the hippocampal formation of the rat. J. Comp. Neurol. 167:285-314.

Steward, O. and Scoville, S.A. (1976) Cells of origin of entorhinal cortical afferent to the hippocampus and fascia dentata of the rat. J. Comp. Neurol. 169:347-370.

Storm-Mathisen, J. (1970) Quantitative histochemistry of acetylcholinesterase in rat hippocampal region correlated to histochemical staining. J. Neurochem. 17:739-750.

Storm-Mathisen, J. (1977) Glutamic acid and excitatory nerve endings: Reduction of glutamic acid uptake after axotomy. Brain Res. 120:379-386.

Storm-Mathisen, J.; Leknes, A.K.; Bore, A.T.; Vaaland, J.L.; Edminson, P.; Haug, F.M.; and Ottersen, O.P. (1983) First visualization of glutamate and GABA in neurones by immunocytochemistry. Nature 301:517-520.

Stripling, J.S.; Patneau, D.K.; and Gramlich, C.A. (1988) Selective long-term potentiation in the pyriform cortex. Brain Res. 441:281-291.

Sugita, S.; Johnson, S.W.; and North, R.A. (1992) Synaptic inputs to $GABA_A$ and $GABA_B$ receptors originate from discrete afferent neurons. Neurosci. Lette. 134:207-211.

Sutherland, R.L. and Rudy, J. W. (1989) Configural association theory: The role of hippocampal formation in learning, memory and amnesia. Psychobiology 17:129-144.

Sutherland, R.L.; Dringenberg, H.C.; and Hoesing, J.M. (1993) Induction of long-term

potentiation at perforant path-dentate synapses does not affect place learning or memory. Hippocampus 3:141-148.

Swanson, L.W.; Sawchenko, P.E.; and Cowan, W.M. (1981) Evidence for collateral projections by neurons in ammon's horn, the dentate gyrus, and the subiculum: A multiple retrograde labelling study in the rat. J. Neurosci. 1:548-559.

Swanson, L.W. and Cowan, W.M. (1977) An autoradiographic study of the organization of the efferent connections of the hippocampal formation in the rat. J. Comp. Neurol. 172:49-84.

Swanson, L.W. and Hartman, B.K. (1975) The central adrenergic system: An immunofluorescence study of the location of cell bodies and their efferent connections in the rat utilizing dopamine-6-hydroxylase as a marker. J. Comp. Neruol. 163:467-506.

Swearengen, E. and Chavkin, C. (1989) Comparison of opioid and GABA receptor control of excitability and membrane conductance in hippocampal CA1 pyramidal cells in rat. Neuropharmacology 28:689-697.

Tamamaki, N. and Nojyo, Y. (1993) Projection of the entorhinal layer II neurons in the rat as revealed by intracellular pressure-injection of neurobiotin. Hippocampus 3:471-480.

Tan, S.-E.; Wenthold, R.; and Soderling, T.R. (1994) Phosphorylation of AMPA-type glutamate receptor by calcium/calmodulin-dependent protein kinase II and protein kinase C in cultured hippocampal neurons. J. Neurosci. 14:1123-1129.

Thomson, A.M.; Deuchars, J.; and West, D.C. (1993) Large, deep layer pyramid-pyramid single axon EPSPs in slices of rat motor cortex display paired pulse and frequency-dependent depression, mediated presynaptically and self-facilitation, mediated postsynaptically. J. Neurophysiol. 70:2354-2369.

Thomson, A.M., and Deuchars, J. (1994) Temporal and spatial properties of local circuits in neocortex. TINS 17:119-126.

Tielen, A.M.; Lopes Da Silva, F.H.; Mollevanger, W.J.; and De Jonge, F.J. (1981) Differential effects of enkephalin within hippocampal areas. Exp. Brain Res. 44:343-346.

Tomasulo, R.A.; Ramirez, J.J.; and Steward O. (1993) Synaptic inhibition regulates associative interactions between afferents during the induction of long-term potentiation and depression. Proc. Natl. Acad. Sci. USA 90:11578-11582.

Trombley, P.Q. and Westbrook, G.L. (1992) L-AP4 inhibits calcium current and synaptic transmission via a G-protein-coupled glutamate receptor. J. Neurosci. 12:2043-2050.

Tsien, R.W. and Malinow, R. (1990) Long-term potentiation: presynaptic enhancement following postsynaptic activation of Ca^{2+}-dependent protein kinases. Cold Spr. Harb. Symp. Quant. Biol. LV, 147-159.

Turner, R.W.; Baimbridge, K.G. and Miller, J.J. (1982) Calcium-induced long-term potentiation in the hippocampus. Neurosci. 7:1411-1416.

Van Hooff, C.O.M., De Graan, P.N.E., Oestreicher, A.B. and Gispen, W.H. (1989) Muscarinic receptor activation stimulates B-50/GAP43 phosphorylation in isolated nerve growth cones. J. Neurosci. 9:3753-3759.

Verma, A.; Hirsch, D.J.; Glatt, C.E.; Ronnett, G.V.; and Snyder, S.H. (1993) Carbon monoxide: a putative neural messenger. Science 259:381-384.

Vogt, B.A. and Miller, M.W. (1983) Cortical connections between rat cingulate cortex and visual, motor, and postsubicular cortices. J. Comp. Neurol. 216:192-210.

Vogt. B.A.; Sikes, R.W. Swadlow, H.A.; and Weyand, T.G. (1986) Rabbit cingulate cortex: Cytoarchitecture, physiological border with visual cortex, and afferent cortical connections of visual, motor, postsubicular, and intracingulate origin. J. Comp. Neurol. 248:74-94.

Voronin, L.L. (1993) On the quantal analysis of hippocampal long-term potentiation and related phenomena of synaptic plasticity. Neuroscience 56:275-304.

Wagner, J.J.; Caudle, R.M.; Neumaier, J.F.; and Chavkin, C. (1990) Stimulation of endogenous opioid release displaces mu receptor binding in rat hippocampus. Neurosci. 37:45-53.

Wagner, J.J.; Neumaier, J.F.; Caudle, R.M. and Chavkin, C. (1989) Stimulation-induced release of endogenous opioid peptides causes displacement of mu and kappa ligand binding in the hippocampus. Soc. Neurosci. Abst. 15:981.

Walrond, J.P.; Govind, C.K.; Huestis, S.E. (1993) Two structural adaptations for regulating transmitter release at lobster neuromuscular synapses. J. Neurosci. 13:4831-4845.

Wang, L.-Y.; Salter, M.W.; and MacDonald, J. F. (1991) Regulation of kainate receptors by cAMP-dependent protein kinase and phosphatases. Science 253:1132-1135.

Wang, S.; Wojtowicz, J.M.; and Atwood H.L. (1996) Synaptic recruitment during long-term potentiation at synapses of the medial perforant pathway in the dentate gyrus of the rat brain. Synapse 21:78-86.

Wang, S. and Wojtowicz, J.M (1996) Prolonged membrane depolarization and increased number of action potentials during induction of long-term potentiation in rat dentate gyrus. Neurosci. Soci. Abst. 22:1513.

Watkins, J. and Collingridge, G. (1994) Phenylglycine derivatives as antagonists of metabotropic glutamate receptors. TIPS 15:333-342.

Weisskopf, M.G.; Castillo, P.E.; Zalutsky, R.A.; and Nicoll, R.A. (1994) Mediation of hippocampal mossy fiber long-term potentiation by cyclic AMP. Science 265:1878-1882.

White, W.F.; Nadler, J.V.; Hamberger, A.; Cotman, C.W.; and Cummings, J.T. (1977) Glutamate as transmitter of hippocampal perforant path. Nature 270:356-357.

White, G.; Levy, W.B.; and Steward, O. (1988) Evidence that associative interactions between afferents during the induction of long-term potentiation occur within local dendritic domains. Proc. Natl. Acad. Sci. USA 85:2368-2372.

White, G.; Levy, W.B.; and Steward, O. (1990) Spatial overlap between populations of synapses determines the extent of their associative interaction during the induction of long-term potentiation and depression. J. Neurophysiol. 64:1186-1198.

Wiesner, J.B.; Henriksen, S.J.; and Bloom, F.E. (1986) Opioid enhancement of perforant path transmission: effect of an enkephalin analog on inhibition and facilitation in the dentate gyrus. Brain Res. 399:404-408.

Wiesner, J.B. and Henriksen, S.J. (1987) Enkephalin enhances responsiveness to perforant path input while decreasing spontaneous activity in the dentate gyrus. Neurosi. Lett. 74:95-101.

Wigström, H. and Gustafsson, B. (1983) Large long-lasting potentiation in the dentate gyrus in vitro during blockade of inhibition. Brain Res. 275:153-158.

Wigström, H. and Gustafsson, B. (1986) Postsynaptic control of hippocampal long-term potentiation. J. Physiol. (Lond.) 81:228-236.

Wigström, H.; Gustafsson, B.; Huang, Y.Y.; and Abraham, W.C. (1986) Hippocampal long-term potentiation is induced by pairing single afferent volleys with intracellularly injected depolarizing current pulses. Acta. Physiol. Scand. 126:317-319.

Williams, J.H.; Bliss, T.V.P. (1989) An in vitro study of the effects of lipoxygenase and cyclo-oxygenase inhibitors of arachidonic acid on the induction and maintenance of long-term potentiation in the hippocampus. Neurosci. Lett. 107:301-306.

Williams, J.H.; Errington, M.L.; Lynch, M.A.; and Bliss, T.V.P. (1989) Arachidonic acid induces a long-term activity-dependent enhancement of synaptic transmission in hippocampus. Nature 341:739-742.

Wilson, R.C. and Steward, O. (1978) Polysynaptic activation of the dentate gyrus of the hippocampal formation: An olfactory input via the lateral entorhinal cortex. Exp. Brain Res. 33:523-534.

Witter, M.P. (1993) Organization of the entorhinal-hippocampal system: a review of current anatomical data. Hippocampus 3:33-44.

Witter, M.P. and Groenewegen, H.J. (1984) Laminar origin and septotemporal distribution of entorhinal and perirhinal projections to the hippocampus in the cat. J. Comp. Neurol. 224:371-385.

Witter, M.P.; Groenewegen, H.J.; and Lopes DA Silva, F.H. (1989) Functional organization of the extrinsic and intrinsic circuitry of the parahippocampal region. Progr. Neurobiol. 33:161-253.

Woodson, W.; Nitecka, L.; and Ben-Ari, Y. (1989) Organization of the GABAergic system in the rat hippocampal formation: a quantitative immunocytochemical study. J. Comp. Neurol. 280:254-271.

Woolf, N.J.; Eckenstein, F. and Butcher, L. (1984) Cholinergic systems in the rat brain. I. Projections to the limbic telecephalon. Brain Res. Bull. 13:751-784.

Wojtowicz, J.M. and Atwood, H.L. (1986) Long-term facilitation alters transmitter releasing properties at the crayfish neuromuscular junction. J. Neurophysiol. 55:484-498.

Wojtowicz, J.M., Smith, B.R., and Atwood, H.L. (1991) Activity-dependent recruitment of silent synapses. Ann. NY Acad. Sci. 627:169-179.

Wyllie, D.J.A.; Manabe, T.; and Nicoll, R.A. (1994) A rise in postsynaptic Ca^{++} potentiates miniature excitatory postsynaptic currents and AMPA responses in hippocampal neurons. Neuron 12:127-138.

Wyss, J.M. (1981) An autoradiographic study of the efferent connections of the entorhinal cortex in the rat. J. Comp. Neurol. 199:495-512.

Xiang, Z., Greenwood, A.C., Kairiss, E.W., and Brown, T.H. (1994) Quantal mechanism of long-term potentiation in hippocampal mossy-fiber synapses. J. Neurophysiol. 71:2552-2556.

Xie, C.W. and Lewis, D.V. (1991) Opioid-mediated facilitation of long-term potentiation at the lateral perforant path-dentate granule cell synapse. J. Pharmacol. Exp. Ther. 256:289-296.

Xie, C.W. and Lewis, D.V. (1995) Endogenous opioids regulate long-term potentiation of synaptic inhibition in the dentate gyrus of rat hippocampus. J. Neurosci. 15:3788-3795.

Xie, C.W.; Morrisett, R.A.; and Lewis, D.V. (1992) Mu opioid receptor-mediated modulation of synaptic currents in dentate granule cells of rat hippocampus. J. Neurophysiol. 68:1113-1120.

Xie, X.; Barrionuevo, G.; and Berger, T.W. (1996) Differential expression of short-term potentiation by AMPA and NMDA receptors in dentate gyrus. Learning & Memory 3:115-123.

Xie, X.; Ji, A.; and Berger, T.W. (1995) Comparison of AMPA and NMDA receptors in the expression of short- and long-term potentiation. Soc. Neurosci. Abs. 21:82.

Xie, X.; Berger, T.W.; and Barrionuevo, G. (1992) Isolated NMDA receptor mediated synaptic responses express both LTP and LTD. J. Neurophysiol. 67:1009-1013.

Zheng, F. and Gallagher, J.P. (1992) Metabotropic glutamate receptors are required for the induction of long-term potentiation. Neuron 9:163-172.

Zimmer, J. (1971) Ipsilateral afferent to the commissural zone of the fascia dentata, demonstrated in decommissurated rats by silver impregnation. J. Comp. Neurol. 142:393-416.

Zola-Morgan, S.; Squire, L.R.; and Amaral, D.G. (1986) Human amnesia and the medial temporal region: Enduring memory impairment following a bilateral lesion limited to field CA1 of the hippocampus. J. Neurosci. 6:2950-2967.

Zola-Morgan, S.; Squire, L.R.; Rempel, N.L.; Clower, R.P.; and Amaral, D.G. (1992) Enduring memory impairment in monkeys after ischemic damage to the hippocampus. J. Neuorsci. 12:2582-2596.

Zalutsky, R.A. and Nicoll, R.A. (1990) Comparison of two forms of long-term potentiation in single hippocampal neurons. Science 248:1619-1624.

Zucker, R.S. (1989) Short-term synaptic plasticity. Ann. Rev. Neurosci. 12:13-31.

Appendix

Copyright agreement for the paper in "Synapse" (Chapter 5).

605 Third Avenue
New York, NY 10158-0012
212.850.6000
FAX 212. 850.6088

John Wiley & Sons, Inc.
Publishers Since 1807

June 17, 1997

Sabrina Wang
Dept. of Physiology
University of Toronto
Medical Science Building
Toronto, Ontario, CANADA M5S 1A8

Dear Ms. Wang:

Thank you for your request of June 2, 1997. Please be aware that although you assigned rights to this work to us *in your contributor agreement*, you retained the following non-exclusive print rights:

1. Proprietary rights, other than copyright, such as patent rights.
2. The right to make copies of all or part of the work for your use in classroom teaching.
3. The right to use, after publication, all or part of this material in a book by you or in a collection of your works.
4. The right to make copies of the work for internal distribution within the institution where you work.
5. The right to use figures and tables from the work, and up to 250 words of text, in print media only.
6. The right to make oral presentation of the material in any forum.

You must include a credit notice with the following information: Title, author(s), journal title, Copyright © (year and owner.).

If you have any questions please call (212) 850-8607.

Sincerely,

Christopher Sheridan
Senior Permissions Assistant
(212) 850-8607

VISIT OUR WEBSITE @ "HTTP://WWW.WILEY.COM" FOR PERMISSIONS INFORMATION AND REQUEST FORMS

ck617c1.doc

Reprint permission from "Neuroscience".

DEPARTMENT OF PHYSIOLOGY
FACULTY OF MEDICINE

Medical Sciences Building
Toronto, Ontario, Canada
M5S 1A8

Telephone: (416) 978-2674
Fax: (416) 978-4940

UNIVERSITY OF TORONTO

Elsevier Science Ltd.
The Boulevard, Langford Lane
Kidlington, Oxford
OX5 1GB
U.K.

March 13, 1997

To whom it may concern,

I am writing to request permission to reprint a paper that was accepted for publication in the Neuroscience, on which I am the first author, as part of my Ph.D. thesis.

The paper is : MS#: A96134RR MS NO 2160.
Wang, S. and Wojtowicz, J.M. (1997) Effect of $GABA_B$ receptors on synaptic interactions in dentate gyrus granule neurons of the rat. Neuroscience.

Thank you for your consideration,

Sabrina Wang

PLEASE TURN OVER

THIS IS.

18 MAR 1997

We hereby grant you permission to reprint the material specified in your letter (see recto) for the purpose you have indicated therein, at no charge, provided that:

1. The material to be used has appeared in our publication without credit or acknowledgement to another source.

2. Suitable acknowledgement to the source is given as follows:

For Books: "Reprinted from (Author/Title), Copyright (Year), Pages No., with kind permission from Elsevier Science Ltd, The Boulevard, Langford Lane, Kidlington 0X5 1GB, UK"

For Journals: "Reprinted from Journal title, Volume number, Author(s), Title of article, Pages No., Copyright (Year), with kind permission from Elsevier Science Ltd, The Boulevard, Langford Lane, Kidlington 0X5 1GB, UK"

3. Reproduction of this material is confined to the purpose for which permission is hereby given.

For future permissions, please contact:
Frances Rothwell (Mrs)
Subsidiary Rights Manager
Elsevier Science Ltd
The Boulevard, Langford Lane
Kidlington 0X5 1GB, U.K.

Should your thesis be published commercially, please reapply for permission.

IMAGE EVALUATION TEST TARGET (QA-3)

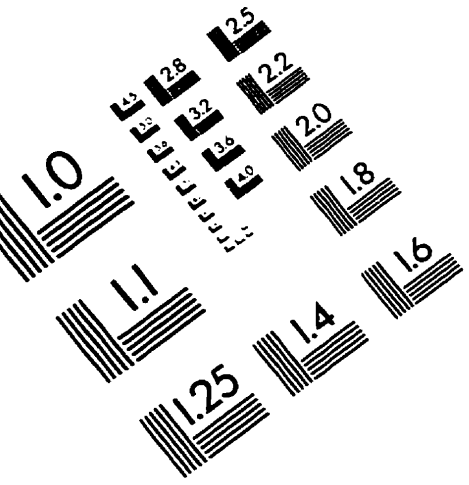

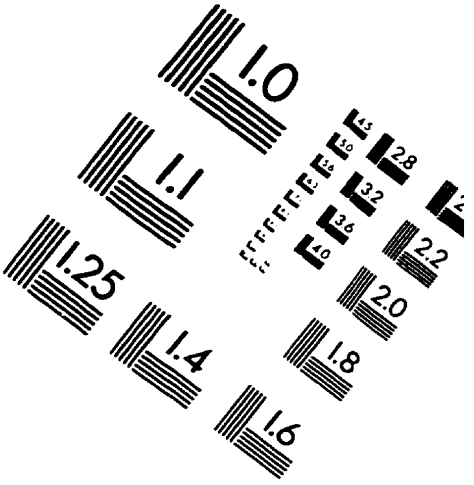

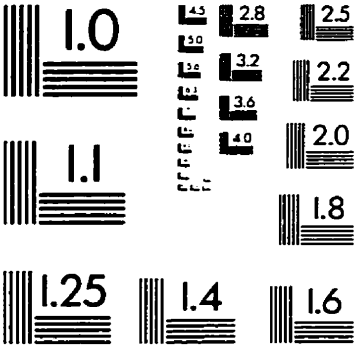

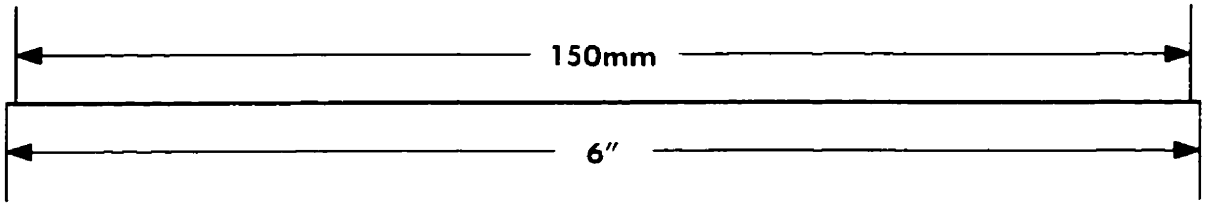

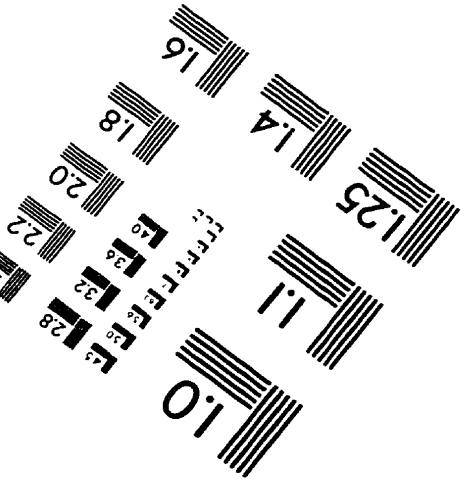

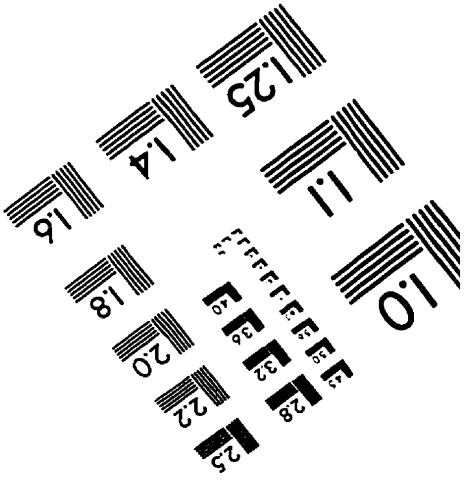

APPLIED IMAGE . Inc
1653 East Main Street
Rochester, NY 14609 USA
Phone: 716/482-0300
Fax: 716/288-5989